

**RADIOPHARMACEUTICALS FOR SCINTIGRAPHY OF  
SOMATOSTATIN RECEPTOR-POSITIVE TUMORS**



**RADIOPHARMACEUTICALS FOR SCINTIGRAPHY OF  
SOMATOSTATIN RECEPTOR-POSITIVE TUMORS**

**RADIOFARMACA VOOR SCINTIGRAFIE VAN  
SOMATOSTATINERECEPTOR-POSITIEVE TUMOREN**

**PROEFSCHRIFT**

ter verkrijging van de graad van doctor  
aan de Erasmus Universiteit Rotterdam  
op gezag van de Rector Magnificus  
Prof. Dr. C.J. Rijnvos  
en volgens besluit van het College van Dekanen.  
De openbare verdediging zal plaats vinden op  
woensdag 20 mei 1992 om 13.45 uur

door

**Willem Hendrik Bakker**

geboren te 's-Gravenhage

Promotiecommissie:

Promotor: Prof. Dr. E.P. Krenning

Overige leden: Prof. Dr. S.W.J. Lamberts  
Prof. Dr. Ir. T.J. Visser  
Prof. Dr. H.E. Schütte

The investigations described in this thesis were performed in the Departments of Nuclear Medicine (head: Prof. Dr. E.P. Krenning), Internal Medicine III and Clinical Endocrinology (head: Prof. Dr. J.C. Birkenhäger), University Hospital Rotterdam and Erasmus University, Rotterdam, The Netherlands, under the guidance of Prof. Dr. E.P. Krenning, Prof. Dr. S.W.J. Lamberts and Prof. Dr. Ir. T.J. Visser, and at Sandoz Research Institute (Dr. J.-C. Reubi), Berne, and Sandoz Pharma A.G. (Dr. J. Pless), Basel, Switzerland.

The co-operation in this project with Mallinckrodt Medical B.V. is gratefully acknowledged.

*NE IUPITER QUIDEM OMNIBUS*

*(zelfs Jupiter kan het niet iedereen naar de zin maken)*

Spreuk in het fries onder de kroonlijst van de topgevel  
van het Oude Stadhuis van 's-Gravenhage (1565).

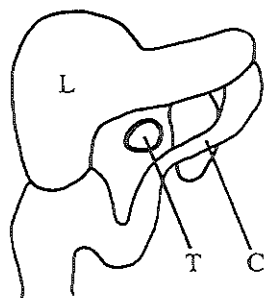
*voor mijn ouders,*

*aan Joan, Marjolein en Maarten*

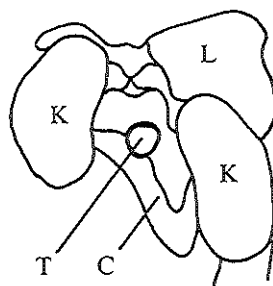


On the cover pages, three-dimensional images are presented of a patient with a somatostatin receptor-positive tumor. The images were generated using the reconstructed transversal slices of the patient study as collected with a three-head gamma camera (Prism 3000, Picker), 48 hours after intravenous injection of [ $^{111}\text{In}$ -DTPA-D-Phe $^1$ ]-octreotide (220 MBq).

The *front cover* shows an anterior view of the abdomen with the tumor (T) projected between the liver (L) and the colon (C).



On the *back cover* the same tumor (T) is visible from posterior between kidneys (K), colon (C), and liver (L).







## CONTENTS

LIST OF ABBREVIATIONS	1
CHAPTER 1	Introduction to somatostatin receptor scintigraphy. . . . . 3
CHAPTER 2	Receptor scintigraphy with a radioiodinated somatostatin analogue: Radiolabeling, purification, biological activity and in vivo application in animals. . . . . 17
CHAPTER 3	In vivo use of a radioiodinated somatostatin analogue: dynamics, metabolism and binding to somatostatin receptor-positive tumors in man. . . . . 35
CHAPTER 4	[ <sup>111</sup> In-DTPA-D-Phe <sup>1</sup> ]-octreotide, a potential radiopharmaceutical for imaging of somatostatin receptor-positive tumors: synthesis, radiolabeling and in vitro validation. . . . . 47
CHAPTER 5	In vivo application of [ <sup>111</sup> In-DTPA-D-Phe <sup>1</sup> ]-octreotide for detection of somatostatin receptor-positive tumors in rats. . . . . 59
CHAPTER 6	Somatostatin scintigraphy with [ <sup>111</sup> In-DTPA-D-Phe <sup>1</sup> ]-octreotide in man: metabolism, dosimetry and comparison with [ <sup>123</sup> I-Tyr <sup>3</sup> ]-octreotide. . . . . 71
CHAPTER 7	Kinetic handling of [ <sup>125</sup> I-Tyr <sup>3</sup> ]-octreotide and [ <sup>111</sup> In-DTPA-D-Phe <sup>1</sup> ]-octreotide by the isolated perfused rat liver. . . . . 89

<i>APPENDIX PAPERS</i> . . . . .	103
Appendix I      Localization of endocrine-related tumors with radioiodinated analogue of somatostatin. . . . .	105
Appendix II      Parallel in vivo and in vitro detection of functional somatostatin receptors in human endocrine pancreatic tumors: Consequences with regard to diagnosis, localization and therapy. . . . .	113
Appendix III     Somatostatin-receptor imaging in the localization of endocrine tumors. . . . .	123
Appendix IV     Treatment with Sandostatin and in vivo localization of tumors with radiolabeled somatostatin analogs. . . . .	127
 SUMMARY AND CONCLUSION . . . . .	 131
 SAMENVATTING EN CONCLUSIE . . . . .	 137
 NAWOORD . . . . .	 145
 CURRICULUM VITAE . . . . .	 147

## LIST OF ABBREVIATIONS

kD	Kilodalton
pK <sub>i</sub>	- log(inhibitory affinity constant)
rGH	Rat growth hormone
APUD	Amine precursor uptake and decarboxylation
ATPase	Adenosine triphosphatase
BSA	Bovine serum albumin
B <sub>max</sub>	Receptor concentration
Bq	Becquerel
CT	Computed tomography
DNA	Deoxyribonucleic acid
DMSA	Dimethyl succinic acid
DTPA	Diethylenetriaminopentaacetic acid
EGF	Epidermal growth factor
GH	Growth hormone
GI	Gastrointestinal
GRF	Growth hormone-releasing factor
GRIF	Growth hormone release-inhibiting factor
Gy	Gray
HIDA	Hepatobiliary imaging agent containing iminodiacetic acid
HPLC	High-performance liquid chromatography
HSA	Human serum albumin
IC <sub>50</sub>	Concentration, needed to achieve 50 % inhibition of binding
IGF-I	Insulin-like growth factor type I
ITLC	Instant thin layer chromatography
K <sub>i</sub>	Affinity constant
K <sub>d</sub>	Dissociation constant
LLI	Lower large intestine
MAG <sub>3</sub>	Mercaptoacetyltriglycine
MEN	Multiple endocrine neoplasia
MIBG	Metaiodobenzylguanidine
MRI	Magnetic resonance imaging
PET	Positron emission tomography
PRL	Prolactin

PTH	Parathyroid hormone
SMS	Sandoz mini somatostatin
SPECT	Single photon emission computed tomography
Sv	Sievert
SS-14	Somatostatin-14
SS-28	Somatostatin-28
TSH	Thyroid-stimulating hormone
ULI	Upper large intestine
VIP	Vasoactive intestinal polypeptide

## CHAPTER 1

### Introduction to somatostatin receptor scintigraphy

In this thesis tumor scintigraphy by means of new radiopharmaceuticals is described, based on the binding of a peptide hormone, *somatostatin*, to its receptors, which are often present in large numbers on various endocrine tumors. Consequently, these tumors can be visualized by gamma camera scintigraphy after in vivo administration of radiolabeled somatostatin analogues which have similar high affinities for the somatostatin receptor. Before discussing this in more detail, brief introductions are given about radioactivity, radiopharmaceuticals, somatostatin and somatostatin receptor-positive tumors.

The first section of this chapter briefly describes the history of radionuclides from the time of discovery of radioactivity via the general availability of artificial radionuclides to the first tumor-seeking applications of radionuclides.

In the second section the general biochemical principles of scintigraphic imaging are presented by a description of the three different types of current radiopharmaceuticals, according to their structure and biochemical behaviour, while special attention is paid to the developments in the field of tumor scintigraphy.

More specifically, this chapter will be concluded with a section about *somatostatin* and tumors containing receptors for somatostatin. This final section is intended as an introduction to the following chapters dealing with the preparation, the in vitro validation, the kinetic handling by the isolated perfused rat liver, and the in vivo application in rats and humans, of two radiolabeled somatostatin analogues for the scintigraphic imaging of *somatostatin receptor-containing tumors*.

### FROM DISCOVERY OF RADIOACTIVITY TO TUMOR SCINTIGRAPHY<sup>1</sup>

At the end of the 19<sup>th</sup> century Henry Becquerel was continuing his father's study on the luminous radiations emitted by the double sulfate of potassium and uranium. By accident he discovered that, long after the phosphorescent radiation had extinguished, these uranium salts still produced very sharp silhouettes in

---

<sup>1</sup>The data of this introductory section are mainly derived from references 1-3.

photographic emulsions. He demonstrated that this radiation had similar properties to the X-rays discovered by Roentgen at about the same time, namely passing through black paper and even through thin metal foils. Apparently this phenomenon was caused by certain properties of the uranium compound *itself*. This experiment marked the discovery of a new phenomenon, not related to the chemical state of the compound, for which Marie Curie (working in Henry Becquerel's laboratory) introduced the name *radioactivity*. Marie Curie successively discovered other radioactive elements, such as thorium, polonium and radium. The biological effect of radiation already had been demonstrated long before the first medical application of radionuclides (radioactive elements): a reddened area on Becquerel's abdominal skin due to a sample of radium in his vest pocket during a journey to England. The existence of *two different kinds of radiation*, both emerging from radium, was described by Villard in 1900. The first one is deviated by electric charge and stopped by less than 1 cm glass (*particle radiation*), and the second, more penetrating one, is not deviated by electric charge and is weakened only slightly by matter. Because the characteristics were similar to the penetrating radiation produced by electric discharge tubes which had been demonstrated by Roentgen in 1895, Villard at first named this also X-radiation. Later, however, this electromagnetic radiation, emanating from the atomic nuclei, was called *gamma radiation*. Further investigations of the types of radiation were undertaken by Rutherford, Curie, Bragg and Soddy. Three types of radiation emerging from nuclei of radionuclides were established:  $\alpha$ -particles (clusters of two neutrons with two protons:  ${}^4\text{He}$  nuclei),  $\beta$ -particles (electrons) and  $\gamma$ -radiation (electromagnetic radiation).

Application of radioactivity to living matter was introduced by Hevesy in 1923, who introduced the "tracer"-concept in the investigation of lead-metabolism in plants using the naturally occurring decay product of radium,  ${}^{212}\text{Pb}$ , and a sensitive radiation detection method. One of the first described human *in vivo* nuclear medicine studies, by Blumgart and Yens in 1926, concerns the investigations of the velocity of blood flow using Radium-C (or  ${}^{214}\text{Bi}$ , emanating from a radium solution) dissolved in saline, as the tracer administered in one arm and a cloud chamber (to visualize the path of ionizing particles through a gas) as the detection apparatus situated at the other arm. Until 1930, only naturally occurring radionuclides were available and detecting systems were insufficient. In the thirties, several important events took place which advanced nuclear science. In 1932 Chadwick suggested that capture of an  $\alpha$ -particle by a  ${}^9\text{Be}$  nucleus should result in an artificial  ${}^{12}\text{C}$ -nucleus together with the emission of a neutron. Artificial radionuclide production was subsequently presented by Joliot and Marie Curie's daughter Irène. They proposed the formation of the radioactive nucleus  ${}^{13}\text{N}$  after capture of an  $\alpha$ -particle by  ${}^{10}\text{B}$  and emanation of a neutron.  ${}^{13}\text{N}$  decays via emission of positrons (i.e., positively charged electrons). Also, they presented two other ( $\alpha, n$ ) nuclear reactions resulting in the formation of  ${}^{30}\text{P}$  and  ${}^{27}\text{Si}$ . Similarly, Joliot and Curie predicted at the same time the origin of artificial radioactivity on the

basis of neutron capture. Only three months later, in May 1934, Fermi presented his experiments concerning the production of fourteen different new radionuclides by neutron irradiation. Apart from radionuclide generation by charged particles originating from radioactive sources, the much more powerful cyclotron, first described by Lawrence in 1932, was used for the production of artificial radionuclides. The cyclotron is still used extensively nowadays. Livingood and Seaberg were the first to describe the cyclotron production of two isotopes of iodine ( $^{131}\text{I}$  and  $^{126}\text{I}$  with physical half-lives of 8 and 13 days, respectively) by 8 MeV deuteron bombardment of stable tellurium. However, the radioiodine which was firstly used as indicator for thyroid function by Hertz and coworkers, was still prepared by neutron irradiation of stable  $^{127}\text{I}$  by a radium-beryllium neutron source, resulting in  $^{128}\text{I}$  with a physical half-life of 25 minutes. Only after the discovery of nuclear fission by Hahn and Strassmann in 1939, radioactive isotopes became more readily available by application of high neutron fluxes in the nuclear reactor. The first announcement that radioactive isotopes were available for public distribution was published in the June 14, 1946, issue of Science. For quite a few years  $^{131}\text{I}$  was the most important radionuclide in nuclear medicine. The largest breakthrough, however, came with the ready availability of  $^{99\text{m}}\text{Tc}$ , a radionuclide with ideal physical characteristics, after the development of the  $^{99}\text{Mo}$ - $^{99\text{m}}\text{Tc}$ -generator in 1958 (4), long after the discovery of the  $^{99}\text{Mo}$ - $^{99\text{m}}\text{Tc}$  system by Segrè and Seaborg in 1938 (5). Also, in 1958 the scintillation camera was introduced by Anger (6). The combination of the general accessibility of  $^{99\text{m}}\text{Tc}$  and the scintillation camera marked a clear improvement for nuclear medicine. Nowadays still the majority of nuclear medicine in vivo investigations in The Netherlands (and probably also elsewhere) are performed with  $^{99\text{m}}\text{Tc}$  (7). However, the first successful investigations in the field of tumor scintigraphy concerned the use of  $^{203}\text{Hg}$ -neohydrin for brain tumor localization (8), reported in 1962, two years after the demonstration of accumulation of this radiopharmaceutical in brain tumor tissue after biopsy (9). Also, in 1962, a second radiopharmaceutical,  $^{57}\text{Co}$ -tetraphenylporphine sulfonate, was presented for the scintillation scanning of neoplasms (10). The use of  $^{99\text{m}}\text{Tc}$  in the form of the generator-eluted pertechnetate was firstly reported some years later in the scintigraphy of brain tumors (11, 12).

## RADIOPHARMACEUTICALS<sup>1</sup>

Before going any further into the matter of scintigraphic imaging of tumors containing somatostatin receptors, the general *biochemical* principles on which scintigraphic imaging is based, the various types of radiopharmaceuticals, and developments in tumor scintigraphy, will be discussed.

---

<sup>1</sup>Various data are derived from reference 13.

## *Biochemical principles of scintigraphic imaging*

Various processes, such as tumors, abscesses, hyperfunctioning glands, lung embolism, and reflux of urine from the bladder to the kidney, can be localized and imaged with the gamma camera by means of the biochemical properties of radiopharmaceuticals, roughly based on four general principles: (a) changes in flow, (b) changes in permeability of the capillary wall, (c) metabolic properties of the radiopharmaceutical, and (d) ligand-receptor binding.

### *Types of radiopharmaceuticals*

Radiopharmaceuticals can be divided into three different categories: (a) radionuclides in elementary and ionic state, (b) radionuclides, coupled to solid particles (including blood cells), and (c) radionuclides as part of dissolved compounds. Most radiopharmaceuticals are administered intravenously and use the blood circulation to reach their target. A minority of these substances is administered via other routes. In the following paragraphs examples of all types of radiopharmaceuticals will be discussed briefly, along with their specific biochemical behaviour.

#### *a) Ionic and elementary radionuclides.*

In its ionic and elementary state, a radionuclide acts according to the biochemical properties of its non-radioactive analogue. Examples of some radiopharmaceuticals, firstly in the form of radioactive ions and secondly as radioactive elements, will be given below.

Radioactive cations as well as anions are widely used for scintigraphic imaging.

Next to  $^{99m}\text{Tc}$ , radioactive iodine (in the form of  $^{123}\text{I}^-$  and  $^{131}\text{I}^-$ ) is probably the best well-known radionuclide in nuclear medicine. Anyway,  $^{131}\text{I}$  was the first radionuclide that achieved widespread use. Radioiodide, administered orally as well as intravenously, accumulates in one organ: the thyroid. Thyroid scintigraphy is possible not only because of radionuclide trapping by the plasma membrane of the thyroid follicle cells (this trapping mechanism can also be imaged with  $^{99m}\text{TcO}_4^-$ ), but also because of accumulation due to *organification* by the follicle cells of the thyroid, resulting in incorporation into thyroid hormone. Consequently, a higher concentration of radioiodine is measured in hyperfunctioning thyroid tissue (e.g., in a "hot" thyroid nodule), compared to the surrounding thyroid tissue. In contrast, a relatively lower uptake within the thyroid is observed in areas, where less functioning thyroid hormone-producing cells are situated (e.g., in cases of thyroid carcinoma and thyroiditis).

The radioactive cations of the alkali metals (e.g.,  $^{43}\text{K}^+$ ,  $^{81}\text{Rb}^+$ , and  $^{137}\text{Cs}^+$ ) and  $^{201}\text{Tl}^+$  behave *in vivo* like the stable potassium ion and can be used for scintigraphy of the myocardium (14). The accumulation is dependent on the regional blood



flow. Additionally, these cations accumulate in normal myocardial tissue by means of the  $\text{Na}^+\text{-K}^+\text{-ATPase}$  system, i.e., following the *metabolic* behaviour of potassium. Because of its nuclear properties  $^{201}\text{Tl}$ , in the form of thallium chloride, is used most often for myocardial scintigraphy. Absence of radioactivity means an ischaemic or an infarcted region.  $^{201}\text{Tl}^+$  is also used for scintigraphy of various malignancies, such as thyroid carcinoma (15) and lung cancer (16). Like myocardial scintigraphy, tumor imaging with thallium is probably due to increased blood supply of tumorous tissue together with an active hyperaccumulation of  $^{201}\text{Tl}$  via the  $\text{Na}^+\text{-K}^+\text{-pump}$  of the tumor cells.

$^{67}\text{Ga}^{3+}$  is an example of a non-specific radiopharmaceutical agent used in imaging of tumors and inflammatory processes (17). The exact mechanism of  $^{67}\text{Ga}$ -accumulation is still unknown (18), but it is probably a combination of a *partly iron-like metabolism* and *defects in capillary vessel walls* in tumorous and inflammatory processes (17). It has been suggested that gallium resembles iron in its metabolism, because after intravenous administration in the form of gallium citrate,  $^{67}\text{Ga}^{3+}$ , like iron, binds to the plasma proteins transferrin and lactoferrin. Although the radionuclide will not be incorporated into hemoglobin, transferrin and lactoferrin play a clear role in the mechanism that is responsible for tumor imaging with  $^{67}\text{Ga}$ . For instance, iron saturation of transferrin prevents accumulation of gallium in tumors and diminishes liver uptake in favour of a more rapid clearance via the kidneys. Accumulation of  $^{67}\text{Ga}$  in tumors will be favoured by increased blood supply and defects in the capillary endothelium in tumorous tissue. High ferritin concentrations in tumors (competing with transferrin and lactoferrin) will accumulate  $^{67}\text{Ga}$ , allowing the scintigraphic imaging of these processes. Likewise, as lactoferrin is a major protein constituent of neutrophilic leukocytes, it is not surprising that also abscesses can be visualized using  $^{67}\text{Ga}$ .

At last, radioactive *noble gasses* such as  $^{81\text{m}}\text{Kr}$ ,  $^{127}\text{Xe}$  and  $^{133}\text{Xe}$  are used in ventilation and perfusion studies of the lungs and the brain, respectively, on the basis of their *inert biochemical behaviour*. There is minimal retention of radionuclide in the body because of immediate exhalation. The widest use of these radiogasses is made in scintigraphy of the ventilation of the lungs, predominantly in combination with the perfusion scintigraphy in the detection of pulmonary embolism (see below). Dissolved in saline, radioactive noble gasses are used intravenously in investigations of the regional cerebral blood flow.

#### b) Radionuclides, coupled to *particles* and *aerosols*.

Visualization of organs or processes by means of radioactive particles (including blood cells) and aerosols is based on their dimensions or their specific physiological properties.

$^{99\text{m}}\text{Tc}$ -coupled microspheres and macroaggregates are used for the detection of obstructed blood vessels. Due to their dimensions (20 - 80  $\mu\text{m}$ ), these radiolabeled particles, which are injected intravenously, are trapped in capillaries. In lung

perfusion scintigraphy images are made of the capillary bed of the lungs. Absence of radioactivity can indicate the presence of lung embolism, especially if that particular area is well ventilated. The radiopharmaceutical is also used in radiophlebography, showing collateral venous blood flow, when a major vein of the leg is obstructed by thrombosis.

Radioactive particles of smaller dimensions (less than  $2\text{ }\mu\text{m}$ ) are the  $^{99\text{m}}\text{Tc}$ -colloids, such as tin-, sulphur- and albumin-colloids, which are used in liver and spleen scintigraphy on the basis of phagocytosis by the reticulo-endothelial cells in these organs. A second application of radioactive colloids is lymphoscintigraphy in which drainage of lymph vessels with small colloidal particles visualizes the lymph nodes and lymph vessels.

Radiolabeled aerosols are composed of  $^{99\text{m}}\text{Tc}$  solutions. Mostly a solution of  $^{99\text{m}}\text{Tc}$ -DTPA (diethylenetriaminopentaacetic acid) in saline is nebulized and administered via oral inhalation. Ventilation scintigraphy of the lung is mainly combined with lung perfusion scintigraphy in examining the presence of lung embolism. The use of a radiolabeled aerosol is an alternative for radiogasses.

Radiolabeled solid food (e.g.,  $^{99\text{m}}\text{Tc}$ -colloid in a pancake) or liquid food (e.g., a solution of radiolabeled DTPA) is used to image oesophageal transit and gastric emptying.

Finally, radiolabeled blood cells have to be mentioned. Without going into detail, it must be stated that these agents are used as blood pool markers in heart function scintigraphy (radiolabeled erythrocytes) and to visualize, for instance, gastrointestinal bleeding sites and locations of degradation (by radiolabeled erythrocytes), thrombosis (radiolabeled thrombocytes) and abscesses (by radiolabeled leucocytes).

#### c) Radionuclides in *dissolved compounds*.

Radioactive dissolved compounds, in which the radionuclide is a *part* of the molecule, form the largest group of radiopharmaceuticals. Usually these radiopharmaceuticals are also administered intravenously.

##### *Compounds with non-specific biochemical properties.*

$^{99\text{m}}\text{Tc}$ , in the form of sodium pertechnetate, is used in perfusion imaging and radionuclide angiography as a marker for the blood circulation. In this application, specific accumulation in the thyroid (see below) is prevented by a previous blocking dose of  $\text{KClO}_4$  or  $\text{KI}$ .

$^{131}\text{I}$ -albumin has been previously used in imaging of brain tumors which have a defective blood-brain barrier, and in cisternoscintigraphy after intrathecal administration of the radiopharmaceutical.

##### *Compounds with specific metabolic properties.*

$^{99\text{m}}\text{TcO}_4^-$ , which resembles iodide, is trapped by the follicle cells of the thyroid,

enabling thyroid scintigraphy.

$^{99m}\text{Tc}$ -phosphonates visualize bone metabolism scintigraphically due to their affinity for hydroxyapatite crystals.

$^{99m}\text{Tc}$ -mercaptoacetyltriglycine ( $\text{MAG}_3$ ) and  $^{99m}\text{Tc}$ -DTPA are used for renal studies, based on tubular excretion and glomerular filtration, respectively.

$^{99m}\text{Tc}$ -dimercaptosuccinic acid (DMSA) is used for scintigraphic imaging of the morphology of the kidney, because of its longer renal retention after glomerular filtration as compared to  $^{99m}\text{Tc}$ -DTPA.

$^{99m}\text{Tc}$ -etifenine (HIDA) and various other iminodiacetic acid derivatives are used for scintigraphy of the hepatobiliary function on the basis of uptake of these lipophilic compounds by hepatocytes, followed by excretion into the biliary system.

Ortho- $^{123}\text{I}$ -hippuric acid (Hippuran<sup>®</sup>) is excreted via the tubuli and, therefore, used for renal studies.

$6\beta$ - $^{131}\text{I}$ -iodomethyl-19-norcholest-5-(10)-en-3 $\beta$ -ol (NP-59), as a steroid precursor, accumulates in adrenocortical cells and is, therefore, used in scintigraphy of the adrenal cortex.

$^{123}\text{I}$ -meta-iodobenzylguanidine (MIBG), like the related norepinephrine, accumulates in the chromaffin granules of adrenergic tissue, present in pheochromocytoma and neuroblastoma (19), enabling scintigraphic imaging of these groups of tumors.

In some radiolabeled gasses, amino acids, sugars and catecholamines such as  $\text{CO}_2$ , glutamic acid, glucose and norepinephrine, the structure and consequently the metabolism is not affected at all by the radionuclide, because of replacement of a stable isotope by a radioisotope (e.g. by  $^{11}\text{C}$ ,  $^{13}\text{N}$  and  $^{15}\text{O}$ ). Such isotopic replacements make metabolic studies of these simple compounds by positron emission tomography (PET) possible, which however has gained limited use for economic reasons and is mostly limited to the brain and the heart.

#### *Compounds characterized by specific binding to tissue cells.*

These compounds are used in the detection of tissue-specific components.

Radiolabeled monoclonal antibodies and radiolabeled fragments of these antibodies are used to visualize various processes. Myocardial infarction and rejection after heart transplantation, thrombosis, and ovarian cancer can be localized with  $^{111}\text{In}$ -antimyosin (binding to myosin),  $^{111}\text{In}$ -antifibrin (binding to fibrin clots), and  $^{111}\text{In}$ -OV-TL 3 or  $^{111}\text{In}$ -OC 125 (binding to antigens present in ovarium carcinoma tissue), respectively.

Radiolabeled peptide hormones can be used for specific detection of receptor-positive tissues including tumors (see below).

#### *Developments in tumor scintigraphy*

It is surprising that in the past 30 years only two simple cationic materials,  $^{67}\text{Ga}$

and  $^{201}\text{Tl}$  have achieved significant and widespread clinical utility in tumor scintigraphy, while still little is known about their accumulation mechanism in tumor and normal tissue (18). Five hundred articles, published in The Journal of Nuclear Medicine since its first issue in 1960, are related to nearly 100 different radiopharmaceuticals for tumor-imaging (18). A vast majority of these radiopharmaceuticals, including gamma as well as positron emitters, turned out to have merely scientific merit; this holds especially for the last kind. Out of these developments the application of radiolabeled polyclonal (after 1970) and monoclonal (after 1980) antibodies seemed to be very promising, not only for imaging, but also for subsequent therapeutic purposes (e.g., labeled with a suitable  $\alpha$ - or  $\beta$ -emitting radionuclide). However, until now, real success or widespread use of radiolabeled antibodies has not yet been achieved, mostly due to low tumor accumulation combined with aspecific sequestration and slow clearance from the body. Perhaps not the high molecular weight radiolabeled antibodies, but *radiolabeled tumor-specific oligo/polypeptides*, with more suitable *in vivo* properties (e.g., a more rapid clearance), will turn out to be more successful tumor-imaging agents.

In the following section a new concept will be introduced with respect to the *in vivo* application of radiolabeled small peptides, based on their well-established *in vitro receptor binding*. It was intended to develop such a radiopharmaceutical based on the knowledge of the specific binding of native somatostatin to somatostatin receptor-positive tissues, including tumors. Therefore, some aspects of the native peptide somatostatin and the particular somatostatin receptor-positive tumors will be reviewed hereafter.

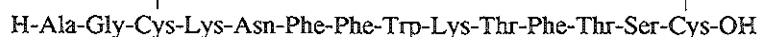
## SOMATOSTATIN AND SOMATOSTATIN RECEPTOR-POSITIVE TUMORS

This section deals with the physiological and biochemical aspects of somatostatin, especially with its receptors in normal and tumorous tissues.

### *The function of somatostatin.*

Experimental and clinical observations (20) have led to the concept that the hypothalamus controls and regulates the secretion of pituitary growth hormone. In 1968 Krulich (21) investigated the growth hormone (GH) production by anterior pituitaries in the presence of various concentrations of sheep and rat hypothalamic extracts. It appeared that *in vitro* GH production by rat pituitaries was stimulated by these extracts, while *in vivo* administration of hypothalamic extracts to rats led to a decrease of serum GH concentrations. The contrary was the case in sheep. These observations led to the discovery of two separate peptide-like substances in these hypothalamic extracts, one having a stimulating effect on GH production (hence called *GH-releasing factor*: GRF) and the second one inhibiting GH

secretion (*GH-release-inhibiting factor*: GRIF). In 1973 Brazeau and coworkers (22) reported the isolation and the primary structure of GRIF in the ovine hypothalamic gland which was later called *somatostatin* (23), because of its supposed specific function: inhibition of *somatotropin* (mostly called growth hormone, GH) secretion by the pituitary gland. In vitro GH release from both human and rat pituitary cells is inhibited at somatostatin levels above  $10^{-9}$  M. Similarly, GH inhibition was demonstrated in vivo in rats (22). Somatostatin was shown to be a polypeptide consisting of 14 amino acids (SS-14) including a disulfide bridge:



Nowadays, it is clear that the identical peptide structure is present not only in the hypothalamus, but also in various other organs (24) of mammalian species, indicating that inhibition of GH secretion is not its only function. Furthermore, somatostatin also exists as a somewhat larger peptide than the already mentioned tetradecapeptide: somatostatine-28 (SS-28). The same somatostatin molecule is also found as a part of still larger molecules in fish (25), pigeon (26), and even in protozoa (27). The tetradecapeptide somatostatin itself has also been identified in the porcine hypothalamus (28) and in the pancreas of the pigeon (26), and the catfish (29). It was therefore concluded that somatostatin was already present before the separate evolution of invertebrates and vertebrates, presumably more than 400 million years ago (24). After the laboratory synthesis of the linear tetradecapeptide, which was shown to have similar GH-inhibitory properties as the native somatostatin (22), Rivier reported the first synthetic somatostatin with cyclic structure, identical to the native tetradecapeptide (30). Thereafter, antisera were prepared, which led to the subsequent development of the radioimmunoassay for somatostatin (31) and immunohistochemical studies (32). These studies demonstrated the presence of somatostatin (and its derivatives) in a large number of tissues. High amounts of somatostatin and somatostatin-like peptides were found in the gastrointestinal tract, the cerebral cortex, the spinal cord, the brainstem, the hypothalamus and the pancreas, with the highest concentrations located in the D-cells of the pancreatic islets and the central nervous system (33).

Somatostatin has been shown to have many different biological activities, such as being a neurotransmitter (acting within the central nervous system), a neurohormone (inhibiting the release of the pituitary hormones GH and TSH), a classical hormone (secreted by the D-cells of the pancreatic islets into the portal vein) or a paracrine factor (mediating the influence of the D-cells on the A- and B-cells of the pancreatic islets) (33). The action of somatostatin is mainly characterized by its inhibitory function, which is not only restricted to the inhibition of the GH secretion. Somatostatin also has inhibitory effects on the secretion of hormones by the pancreatic islands (insulin, glucagon) and on the exocrine pancreatic function. Also, somatostatin inhibits normal gastrin production and consequently gastric acid and pepsin production.

The very rapid action of somatostatin (34, 35) suggests a mechanism of action via plasma membrane receptors in contrast to steroids and some actions of thyroid

**Figure 1**

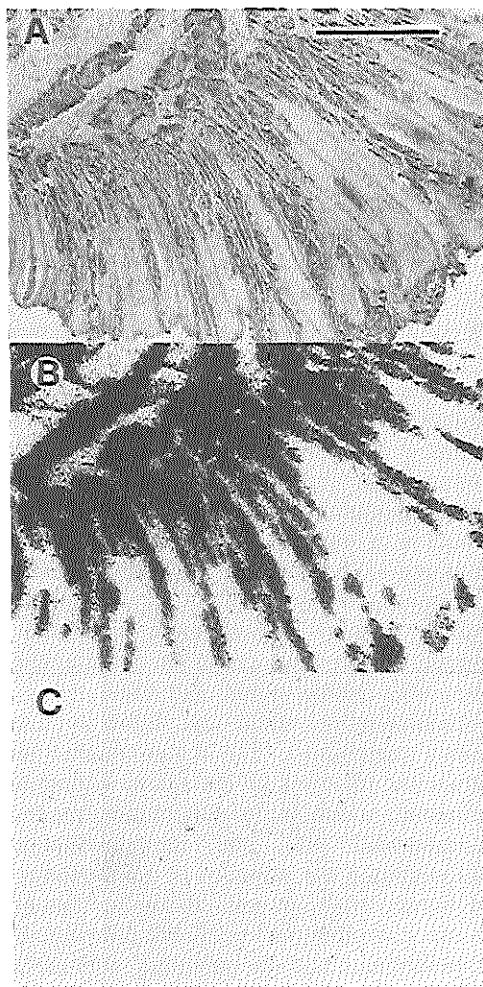
*Somatostatin receptors in a human carcinoid tumor (reproduced with kind permission of Dr. J.-C. Reubi)*

*A: Hematoxylin-eosin stained section.*

*B: Autoradiogram showing total binding of [<sup>125</sup>I-Tyr<sup>3</sup>]-octreotide.*

*C: Autoradiogram showing nearly no non-specific binding of [<sup>125</sup>I-Tyr<sup>3</sup>]-octreotide (in presence of 10<sup>-6</sup> M [Tyr<sup>3</sup>]-octreotide).*

*The receptors are exclusively located on the tumor strands and nests. Bar = 1 mm.*



hormones, which require intracellular translocation. High-affinity binding sites for somatostatin have been identified on cultured pituitary tumor cells (36) and on rat cortical membranes (37, 38). The binding affinity for somatostatin receptors on pituitary tumor cells is high ( $K_a \approx 1 \times 10^{10} \text{ M}^{-1}$ ) and a receptor number of  $0.11 \times 10^{12} \text{ mol/mg cell protein}$  (14000 binding sites per cell) have been reported (36). The affinity for neuronal membranes was also about  $1 \times 10^{10} \text{ M}^{-1}$  and the number of binding sites  $0.16 \times 10^{12} \text{ mol/mg}$  (38). The effects of somatostatin on the electrical activity of pancreatic B-cells (39) and on the activity of neuronal cells (40, 41) suggest that somatostatin acts at the membrane level. These binding sites are clearly seen on autoradiographic images of normal and pathological tissues. Autoradiography of normal pituitary tissue illustrates the location of somatostatin receptors within the anterior lobe of the gland (42).

### *Somatostatin receptor-positive tumors.*

The general inhibitory effect of somatostatin on hormone production by various glands led to the concept of possible beneficial effects of somatostatin in the treatment of diseases, based on gland hyperfunction and on overproduction of hormones by endocrine active tumors. However, some difficulties had to be overcome, for the tetradecapeptide somatostatin itself turned out to be unsuitable for routine treatment. After intravenous injection somatostatin has a half-life of less than 3 mins in man (43, 44) and is rapidly degraded enzymatically (45). Treatment with somatostatin has only a very short duration of 30-60 mins (33), when administered subcutaneously and no long-term studies with somatostatin have been undertaken. Short-term somatostatin treatment has been investigated in patients with diabetes (46), acromegaly (47, 48) and various pancreatic islet cell tumors (49, 50). In recent years successful efforts have been undertaken to prepare somatostatin derivatives that are more resistant to enzymatic degradation by modifying the molecule in various ways with preservation of the specific biological characteristics of the original compound. Firstly, the biologically active site of the somatostatin molecule was preserved as much as possible while making the somatostatin derivative as small as possible. Furthermore, D-aminoacids have been introduced to increase the resistance to enzymatic degradation. Many of these somatostatin analogues have been shown to inhibit the secretion of growth hormone, insulin and glucagon even better than somatostatin itself. The 8 amino acids-containing somatostatin analogue octreotide (Sandostatin® or SMS 201-995) is currently widely used successfully in the treatment of endocrine active tumors such as GH-producing pituitary adenomas and gastroenteropancreatic tumors (51, 52).

Apart from the presence of somatostatin receptors in normal tissues, it is obvious that hormone-secreting tumors that are treated successfully with somatostatin analogues might contain receptors for somatostatin. Indeed, on most endocrine active gastrointestinal tumors large numbers of high-affinity binding sites for somatostatin have been detected (53). In figure 1 the somatostatin receptors are clearly visualized in the autoradiographic image of a human carcinoid tumor, using [<sup>125</sup>I-Tyr<sup>3</sup>]-octreotide as radiolabeled somatostatin analogue.

Following the *in vitro* characterization of the somatostatin receptor status of tumors, the *in vivo* administration of radiolabeled somatostatin analogues as new radiopharmaceuticals was launched for the purpose of scintigraphic imaging of these tumors, which are often difficult to localize.

In the next chapters the preparation and *in vivo* behaviour of two different new radiopharmaceuticals (both radiolabeled somatostatin analogues) in animals and man with somatostatin receptor-positive tumors will be presented.

## REFERENCES

1. Friedlander G, Kennedy JW, Macias ES, and Miller JM. *Nuclear and Radiochemistry*. 3rd ed. New York: John Wiley & Sons; 1981: 1-16.
2. Brucer M, Harris CG, MacIntyre WJ, and Taplin GV, eds. *The Heritage of Nuclear Medicine*. New York: The Society of Nuclear Medicine; 1979.
3. Myers WG, and Wagner HN Jr. Nuclear Medicine: How it began. In:

- Wagner HN Jr ed. *Nuclear Medicine*. New York: HP Publishing Co., Inc.; 1975.
4. Tucker WD, Greene MW, Weiss AJ, et al: *Transactions of the 4th Annual Meeting of the American Nuclear Society*, vol 1, no 1, New York, Academic Press, 1958: 160-161.
  5. Segrè E, and Seaborg GT. Nuclear Isomerism in Element 43. *Phys Rev* 1938; 54: 772.
  6. Anger HO. Scintillation Camera. *Rev Scientif Instrum* 1958; 29: 27-33.
  7. Bakker WH. In vivo Nucleaire Geneeskunde in Nederland 1984-1988. *Nucl Geneesk Bull* 1990; 12: 88-98.
  8. Blau M, and Bender MA. Clinical evaluation of  $^{203}\text{Hg}$  neohydrin and  $^{131}\text{I}$  albumin in brain tumor localization. *J Nucl Med* 1960; 1: 106.
  9. Blau M, and Bender MA. Radiomercury( $^{203}\text{Hg}$ )-labeled neohydrin: a new agent for brain tumor localization. *J. Nucl Med* 1962; 3: 83-92.
  10. Winkelman J, McAfee JG, Wagner HN, and Long RG. The synthesis of  $^{57}\text{Co}$ -tetraphenylporphine sulfonate and its use in the scintillation scanning of neoplasms. *J Nucl Med* 1962; 3: 249-253.
  11. McAfee JG, Fueger CF, Stern HS, and Wagner HN Jr, Migita T. [ $^{99\text{m}}\text{Tc}$ ]pertechnetate for brain scanning. *J Nucl Med* 1964; 5: 811-827.
  12. Quinn JL III, Hauser W, and Ciric I. Analysis of 100 consecutive abnormal brain scans using  $^{99\text{m}}\text{Tc}$  as pertechnetate. *J Nucl Med* 1965; 6: 121-130.
  13. Alazraki NP, and Mishkin FS, eds. *Fundamentals of Nuclear Medicine*, 2nd edition. New York, The Society of Nuclear Medicine; 1991.
  14. Wackers FJT. Characteristics of radiopharmaceuticals in nuclear cardiology. Implications for practical imaging. In: Simoons ML and Reiber JHC, eds. *Nuclear imaging in clinical cardiology*. Boston: Martinus Nijhoff; 1984: 19-37.
  15. Hoefnagel CA, Delprat CC, Zanin D, and Van der Schoot JB. New radionuclide tracers for the diagnosis and therapy of medullary thyroid carcinoma. *Clin Nucl Med* 1988; 13: 159-165.
  16. Tonami N, Shuke N, Yokoyama K, Seki H, Takayama T, Kinuya S, Nakajama K, Aburano T, Hisada K, and Watanabe Y. Thallium-201 single photon emission computed tomography in the evaluation of suspected lung cancer. *J Nucl Med* 1989; 30: 997-1004.
  17. Hoffer PB. Mechanisms of localization. In: Hoffer PB, Bekermann C, and Henkin RE. *Gallium-67 Imaging*. New York: Wiley; 1978: 3-8.
  18. Davis M. The current and future use of tumor-localizing agents. *J Nucl Med* 1990; 30: 1658-1661.
  19. Beierwaltes WH. Endocrine imaging: Parathyroid, adrenal cortex and medulla, and other endocrine tumors. Part II. *J Nucl Med* 1991; 32: 1627-1639.
  20. Pecile A, and Muller E, Eds. Growth Hormone, *Excerpta Medica*, Amsterdam; 1968.
  21. Krulich L, Dhariwal APS, and McCann SM. Stimulatory and inhibitory effects of purified hypothalamic extracts on growth hormone release from rat pituitary in vitro. *Endocrinology* 1968; 83: 783-790.
  22. Brazeau P, Vale W, Burgus R, Ling N, Butcher M, Rivier J, and Guillemin R. Hypothalamic polypeptide that inhibits the secretion of immunoreactive



- pituitary growth hormone. *Science* 1973; 179: 77-79.
23. Burgus R, Ling N, Butcher M, and Guillemin R. Primary structure of somatostatin, a hypothalamic peptide that inhibits the secretion of pituitary growth hormone. *Proc Natl Acad Sci USA* 1973; 70: 684-688.
  24. Reichlin S. Somatostatin. *N Eng J Med* 1983; 309: 1495-1501.
  25. Hobart P, Crawford R, Shen LP, Pictet R, and Rutter WJ. Cloning and sequence analysis of cDNAs encoding two distinct somatostatin and precursors found in the endocrine pancreas of anglerfish. *Nature* 1980; 288: 137-141.
  26. Spiess J, Rivier JE, Rodkey JA, Bennet CD, and Vale W. Isolation and characterization of somatostatin from pigeon pancreas. *Proc Natl Acad Sci USA* 1979; 76: 2974-2978.
  27. Berelowitz M, LeRoith D, von Schenk H, Newgard C, Szabo M, Frohman LA, Shiloach J, and Roth J. Somatostatin-like immunoreactivity and biological activity is present in *Tetrahymena pyriformis*, a ciliated protozoan. *Endocrinology* 1982; 110: 1939-1944.
  28. Schally AV, Dupont A, Arimura A, Redding TW, Nishi N, Linthicum GL, and Schlesinger DH. Isolation and structure of somatostatin from porcine hypothalamus. *Biochemistry* 1976; 15: 509-514.
  29. Andrews PC, and Dixon JE. Isolation and structure of a peptide hormone predicted from a mRNA sequence. *J Biol Chem* 1981; 256: 8267-8270.
  30. Rivier JEF. Somatostatin. Total solid phase synthesis. *J Am Chem Soc* 1974; 96:2986-2992.
  31. Harris V, Conlon JM, Srikant CB, McCorkle K, Schusdziarra V, Ipp E, and Unger RH. Measurements of somatostatin-like immunoreactivity in plasma. *Clin Chim Acta* 1978; 87: 275-283.
  32. Hökfelt T, Efendic S, Hellerström C, Johansson O, Luft R, and Arimura A. Cellular localization of somatostatin in endocrine-like cells and neurons of the rat with special references to the A<sub>1</sub>-cells of the pancreatic islets and to the hypothalamus. *Acta Endocrinol Suppl* 1975; 200: 5-41.
  33. Gottesmann IS, Mandarino LJ, and Gerich JE. Somatostatin: Its role in health and disease. In: Cohen M and Foa P, eds. *Special topics in endocrinology and metabolism*. Vol. 4. New York: Alan R. Liss, 1982: 177-243.
  34. Lin BJ. Effects of somatostatin on insulin biosynthesis, glucose oxidation, and cyclic guanosine monophosphate level. *Metabolism* 1978; 27 (Suppl 1): 1295-1298.
  35. Vale W, Brazeau P, Rivier C, Brown M, Boss B, Rivier J, Burgus R, Ling N, and Guillemin R. Somatostatin. *Recent Prog Horm Res* 1975; 34: 365-397.
  36. Schonbrunn A, and Tashjian AH Jr. Characterization of functional receptors for somatostatin in rat pituitary cells in culture. *J Biol Chem* 1978; 253: 6473-6483.
  37. Reubi JC, Perrin MH, Rivier JE, and Vale W. High affinity binding sites for a somatostatin-28 analog in rat brain. *Life Sci* 1981; 28: 2191-2198.
  38. Srikant CB, and Patel YC. Somatostatin receptors: Identification and characterization in rat brain membranes. *Proc Natl Acad Sci USA* 1981; 78: 3930-3934.
  39. Pace CS, Murphy M, Conant S, and Lacy PE. Somatostatin inhibition of

- glucose-induced electrical activity in cultured rat islet cells. *Am J Physiol* 1977; 233: C164-C171.
40. Randic M, and Miletic V. Depressant actions of methionine-enkephalin and somatostatin in cat dorsal horn neurons activated by noxious stimuli. *Brain Res* 1978; 152: 196-202.
  41. Renaud LP, Martin JB, and Brazeau P. Depressant action of TRH, LH-RH, and somatostatin on activity of central neurones. *Nature* 1975; 255: 233-235.
  42. Reubi JC, and Maurer R. Autoradiographic mapping of somatostatin receptors in the rat central nervous system and pituitary. *Neurosci* 1985; 15: 1183-1193.
  43. Bethge N, Diel F, Rösick M, and Holz J. Somatostatin half-life: A case report in one healthy volunteer and a three-month followup. *Horm Metabol Res* 1981; 13: 709-710.
  44. Sheppard M, Shapiro B, Pimstone B, Kronheim S, Berelowitz M, and Gregory M. Metabolic clearance and plasma half disappearance time of exogenous somatostatin in man. *J Clin Endocrinol Metab* 1979; 48: 50-53.
  45. Pless J, Bauer W, Briner U, Doepfner W, Marbach P, Maurer R, Petcher TJ, Reubi J-C, Vonderscher J. Chemistry and pharmacology of SMS 201-995, a long-acting octapeptide analogue of somatostatin. *Scand J Gastroenterol* 1986; 21 (suppl 119): 54-64.
  46. Greco AV, Ghirlanda G, Altomonte L, Manna R, Rebuzzi AG, and Bertoli A. Somatostatin and insulin infusion in the management of diabetic ketoacidosis. *Horm Metab Res* 1981; 13: 310-314.
  47. Hall R, Besser GM, Schally AV, Coy DH, Evered D, Goldie DJ, Kastin AJ, McNeilly AS, Mortimer CH, Phenekos C, Tunbridge WMG, and Weightman D. Action of growth-hormone-release inhibitory hormone in healthy men and in acromegaly. *Lancet* 1973; 2: 581-584.
  48. Yen SSC, Siler TM, and DeVane GW. Effect of somatostatin in patients with acromegaly. *N Engl J Med* 1974; 290: 935-938.
  49. Galmiche JP, Colin R, DuBois PM, Chayville JA, Descos F, and Geffroy Y. Calcitonin secretion by a pancreatic somatostatinoma. *N Engl J Med* 1978; 299: 1252.
  50. Kahn CR, Bhathena SJ, Recant L, and Rivier J. Use of somatostatin and somatostatin analogs in a patient with a glucagonoma. *J Clin Endocrinol Metab* 1981; 53: 543-549.
  51. Lamberts SWJ, Uitterlinden P, Verschoor L, van Dongen KJ, and del Pozo E. Long-term treatment of acromegaly with the somatostatin analogue SMS 201-995. *N Engl J Med* 1985; 313: 1576-1580.
  52. Kvois LK, Moertel CG, O'Connell MJ, Schutt AJ, Rubin J, and Hahn RG. Treatment of malignant carcinoid syndrome. Evaluation of a long-acting somatostatin analogue. *N Engl J Med* 1986; 315: 663-666.
  53. Reubi JC, Häcki WH, and Lamberts SWJ. Hormone-producing gastrointestinal tumours contain high density of somatostatin receptors. *J Clin Endocrinol Metab* 1987; 65: 1127-1134.

## CHAPTER 2

### **Receptor scintigraphy with a radioiodinated somatostatin analogue: Radiolabeling, purification, biologic activity, and in vivo application in animals**

Willem H. Bakker, Eric P. Krenning, Wout A. Breeman, Jan W. Koper,  
Peter P. Kooij, Jean-Claude Reubi, Jan G. Klijn, Theo J. Visser,  
Roel Docter, and Steven W. Lamberts.

Departments of Nuclear Medicine and Internal Medicine III,  
University Hospital Dijkzigt and Erasmus University Medical School,  
Rotterdam, The Netherlands;  
Division of Endocrine Oncology, Dr. Daniël den Hoed Cancer Centre,  
Rotterdam, The Netherlands;  
and Sandoz Research Institute,  
Berne, Switzerland.

Radioiodinated [Tyr<sup>3</sup>]-octreotide, a somatostatin analogue, is a useful ligand for the in vitro detection of somatostatin receptors. In this study, we have investigated the possible in vivo application of this radioligand in the detection of somatostatin receptor-bearing tumors by scintigraphy. The specific somatostatin-like biologic activity of radioiodinated [Tyr<sup>3</sup>]-octreotide was confirmed in vitro: (a) radioiodinated [Tyr<sup>3</sup>]-octreotide competes in the nanomolar range with specific receptor binding of somatostatin to suspended human meningioma membranes and (b) the secretion of growth hormone by cultured rat pituitary cells was similarly inhibited by iodinated [Tyr<sup>3</sup>]-octreotide and somatostatin. In rats intravenously injected [<sup>125</sup>I-Tyr<sup>3</sup>]-octreotide is rapidly cleared from the circulation mainly by the liver. Although this rapid clearance limits the amount of tracer available for somatostatin receptor-bearing tumors, the advantage of this rapid clearance is that the background level is rapidly reduced in favor of scintigraphic imaging of these tumors. Pancreatic tumors in rats were localized by scintigraphy after intravenous injection of [<sup>125</sup>I-Tyr<sup>3</sup>]-octreotide.

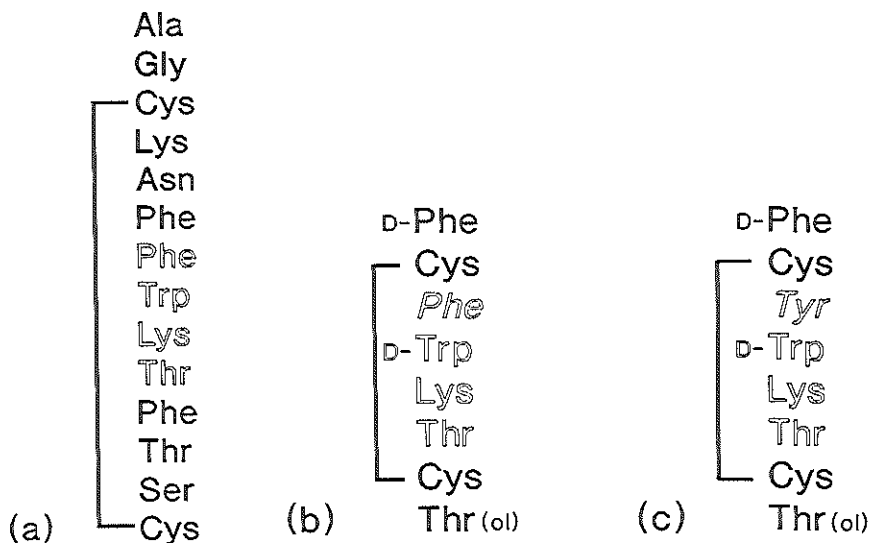


**Figure 1**

*Structural formulae of native somatostatin (a) with the Phe-Trp-Lys-Thr sequence which has been proposed to be the active site of the molecule (23, 24) and octreotide (b). In [Tyr<sup>3</sup>]-octreotide (c) Phe is replaced by Tyr to make radioiodination possible with preservation of biologic activity.*

Most endocrine active gastrointestinal tumors are usually slow-growing. They are often very small and therefore difficult to localize with conventional techniques (1). Hormone secretion by several of these tumors is inhibited by the tetradecapeptide somatostatin (Fig. 1a), which is endogenously produced, e.g., by the hypothalamus and pancreas (2). Somatostatin also inhibits the growth of some tumors (3). The native hormone, however, is susceptible to rapid enzymatic degradation (4); therefore, it is not suitable for long-term therapeutic use. For that reason, synthetic derivatives with a similar bioactive structure as somatostatin have been developed, which are not only less susceptible to biologic degradation but also have a stronger inhibitory effect on hormone release by the relevant tumors. The octapeptide octreotide (SMS 201-995 or Sandostatin<sup>®</sup>; Fig. 1b) fulfills these criteria (4). After subcutaneous injection, this peptide has a longer biologic half-life than somatostatin itself and, hence, prolonged inhibitory effects on normal growth hormone production (5), hormone release by endocrine pancreatic tumors (6) and on tumor growth (6-9). Octreotide is currently used in the treatment of gastroenteropancreatic tumors and acromegaly (6, 10).

Large numbers of high affinity binding sites for native somatostatin and synthetic octreotide have been detected on most endocrine active tumors (11). This opens the possibility for the scintigraphic localization of such tumors using a radiolabeled somatostatin derivative. Since octreotide cannot be radiolabeled easily with a gamma-emitting radionuclide, a synthetic analogue ([Tyr<sup>3</sup>]-octreotide) has been developed in which phenylalanine has been replaced by tyrosine, allowing radioiodination of the molecule (Fig. 1c). This compound has been used successfully as <sup>125</sup>I-radioligand for in vitro somatostatin receptor studies (12). Since its application for human scintigraphy needs methodologic changes (use of <sup>123</sup>I with different properties instead of <sup>125</sup>I and omitting toxic substances during purification), we report here the radiolabeling, the subsequent purification procedure and the confirmation of the specific biologic activity of radiolabeled [Tyr<sup>3</sup>]-octreotide. The distribution and metabolism of the radiolabeled somatostatin derivative have been studied following its intravenous administration to rats by gamma camera scintigraphy and measurements of radioactivity in isolated organs. Radioiodinated [Tyr<sup>3</sup>]-octreotide was shown to be an attractive new radiopharmaceutical for the in vivo detection of somatostatin receptors using a rat tumor model.

## MATERIALS AND METHODS

### *Radiopharmaceuticals*

Octreotide and [Tyr<sup>3</sup>]-octreotide were obtained from Sandoz (Basel, Switzerland). Radioiodination of [Tyr<sup>3</sup>]-octreotide was performed on the basis of the <sup>125</sup>I-iodination technique described by Reubi (12). Toxic substances were omitted during the purification steps in connection with the proposed i.v. administration. Two iodine isotopes (<sup>125</sup>I and <sup>123</sup>I) from different manufacturers were used. Radioactivity concentrations (and specific activities) amounted to 1.85 GBq <sup>125</sup>I/ml (0.62 TBq <sup>125</sup>I/mg) and 3.7 GBq <sup>123</sup>I/ml (3.7 TBq <sup>123</sup>I/mg). To the solution of radioiodide (in 40 µl 0.01 M NaOH) in the manufacturer's vial were added successively 20 µl 0.05 M phosphate (pH 7.5) and 1.4 µg [Tyr<sup>3</sup>]-octreotide in 20 µl 0.05 M acetic acid. The solution was vortexed. The iodination was started by adding 1.6 µg chloramine-T in (20 µl 0.05 M phosphate), representing only a 5-fold excess over peptide in order to prevent oxidation of the disulfide bridge of the [Tyr<sup>3</sup>]-octreotide. The mixture was then vortexed for 1 min. The iodination was stopped by the addition of 0.1 ml 10 % human serum albumin (Merieux, Lyon, France). After vortexing for 30 sec, 1.85 ml 5 mM ammonium acetate was added. Purification was performed by using a SEP-PAK C<sub>18</sub> reversed-phase extraction cartridge (Waters Associates, Milford, MA), which was prewashed with 5 ml 70 % ethanol and subsequently activated with 5 ml 2-propanol. After application of the sample, the cartridge was washed successively with 5 ml distilled

water and 5 ml 0.5 M acetic acid. Radioiodinated [Tyr<sup>3</sup>]-octreotide was eluted with 5 ml 96 % ethanol. The solvent was evaporated at 40 °C under a gentle stream of nitrogen. The dry residue was dissolved in 2 - 10 ml 154 mM NaCl and 0.05 M acetic acid (pH 3). After passing through a low protein-binding 0.22-micron Millex-GV filter (Millipore, Milford, MA) the solution was ready for i.v. administration. The labeling procedure was scaled up at least 30-fold when larger amounts of radiolabeled peptide were necessary for (human) scintigraphic purposes. In those cases, 10-fold higher peptide- and chloramine-T concentrations were used in order to keep the reaction volume below 1 ml. For labeling with <sup>125</sup>I and <sup>123</sup>I, 1.5 and 30-fold excess of peptide over iodide were used, respectively.

### *Quality control*

The radioactivities in the fractions eluted from SEP-PAK C<sub>18</sub> were measured in a dose calibrator (VDC-202, Veenstra, Joure, The Netherlands) under similar geometric conditions (5 ml liquid). Also, the SEP-PAK C<sub>18</sub> cartridge itself was measured after the elutions, taking into account the different geometric conditions.

The ammonium acetate, water, and acetic acid fractions eluted from SEP-PAK C<sub>18</sub> were examined for low molecular weight (< 1.5 kD) iodine (i.e., free iodide and peptide-bound radioiodine) and high molecular weight (> 1.5 kD) protein-bound iodine (i.e., radioiodinated human serum albumin) using Sephadex G-25 gel filtration chromatography (PD-10 column, Pharmacia, Sweden) with 154 mM NaCl as the eluent. The low molecular weight PD-10 fractions were analyzed by reversed-phase, high-performance liquid chromatography (HPLC), described hereafter.

The acetic acid and ethanol fractions eluted from SEP-PAK C<sub>18</sub> were analyzed by HPLC with a Waters 600 E multisolvent delivery system connected to a  $\mu$ -Bondapak-C<sub>18</sub> reversed-phase column (300 x 3.9 mm, particle size 10  $\mu$ m). Elution was carried out at a flow of 1 ml/min with a linear gradient of 40 % to 80 % methanol in 154 mM NaCl in 20 min and the latter composition was maintained for another 5 min. Eluted radioactivity was monitored on-line using a NaI probe connected to a Canberra single-channel analyzer with a recorder. Collected fractions were measured by routine scintillation counting.

The receptor-binding affinity of the radioiodinated [Tyr<sup>3</sup>]-octreotide was measured using suspensions of human meningioma membranes, which are reported to contain somatostatin receptors (13). A similar procedure as described previously (12) was used. Meningioma membranes (280  $\mu$ g protein) were incubated in a total volume of 100  $\mu$ l (triplicate tubes) at 20°C for 1 hr with five different concentrations of [<sup>125</sup>I-Tyr<sup>3</sup>]-octreotide between 0.2 and 8 nM in the absence or presence of 10  $\mu$ M somatostatin. The incubation contained 10 mM HEPES buffer (pH 7.6), 0.5 % BSA, 5 mM MgCl<sub>2</sub>, and bacitracin (20  $\mu$ g/ml). The incubation was stopped by the addition of 1 ml ice-cold HEPES buffer followed by centrifugation (2 min at 14,000 rpm in an Eppendorf microcentrifuge). The

membrane pellet was washed twice with 1 ml ice-cold HEPES buffer and the final pellet was counted in a LKB-1282-Compugamma system. Specific receptor binding was calculated to be the difference between binding in the absence and in the presence of 10  $\mu$ M somatostatin. The data were analysed using the method of Scatchard (14), giving the dissociation constant ( $K_d$ ) and the number of binding sites ( $B_{max}$ ) for the meningioma preparation.

The biologic activity of HPLC-purified mono-iodinated [ $^{125}$ I-Tyr $^3$ ]-octreotide (i.e., free from unlabeled [Tyr $^3$ ]-octreotide) was assessed by measuring its potency to inhibit the secretion of rat growth hormone (rGH) by cultured rat pituitary cells as described previously (15). Iodine-125 was used instead of  $^{123}$ I because we were only able to establish the exact specific radioactivity of the [ $^{125}$ I-Tyr $^3$ ]-octreotide (see Discussion).

### *Animals and tumors*

A transplantable rat pancreatic tumor model (CA 20948) with somatostatin receptors, as demonstrated with in vitro assays (16), was used. Inhibition of the growth of this tumor by 40 % - 70 % compared to controls under chronic treatment with the somatostatin analogue octreotide during 6 wk had been demonstrated previously (17, 18). Eight male Lewis rats were inoculated with a suspension of pancreatic tumor cells as described before (17). Two weeks after tumor transplantation 95 % of the rats showed a detectable tumor mass. When the tumors had reached a solid palpable mass, the animals were used for the experiments. Nine male Lewis rats without tumor were used as controls. (18.5 - 37 MBq (1 - 3  $\mu$ g) [ $^{125}$ I-Tyr $^3$ ]-octreotide in 0.5 - 0.8 ml 154 mM NaCl and 0.05 M acetic acid were injected intravenously in tumor-bearing and control rats. The thyroids of the animals were not blocked. The radiopharmakon was injected in the dorsal vein of the penis. Two out of eight tumor-bearing rats received 1 mg octreotide subcutaneously 30 min before injection of [ $^{125}$ I-Tyr $^3$ ]-octreotide in order to saturate somatostatin receptors on the tumors.

### *Data acquisition and analysis*

Images were acquired with a large field of view gamma camera (Counterbalance 37 ZLC, Siemens Gammasonics) equipped with a 190-keV parallel-hole collimator. The animals were in a supine position on the collimator in such a way that overprojection of the tumor and the intestines was avoided. The analyzer was set to 159 keV with a 20% window. Data were stored in a dedicated computer (Gamma-11, Nuclear Diagnostics). In all animals (9 controls, 6 tumor-bearing animals without and 2 with octreotide pretreatment), acquisition took place for 40 intervals of 3 sec and 18 intervals of 60 sec (matrix 64 x 64) during the first 20 min of the study. After 30 min, static images were made containing 500K counts for a good quality image. Of four control animals and two tumor-bearing

animals, additional static images (500K counts) were made 3 and 5 hr after injection; 24 hr after injection of the radiopharmakon another static image was made during 15 min. Static images were acquired in a 128 x 128 matrix and on X-ray film. In order to investigate the organ distribution of radioactivity, animals were killed 30 min (5 control and 2 tumor-bearing animals) and 24 hr (4 control and 2 tumor-bearing animals) after injection of the radiopharmakon and the radioactivity in the various tissues was measured with a GeLi-detector equipped with a multichannel analyzer (Series 40, Canberra). Tissues were not isolated from octreotide-pretreated animals.

One urine sample, collected from a tumor-bearing animal 30 min after injection, was used to investigate the radiochemical composition by HPLC (after 1:10 dilution in 40 % methanol in 154 mM NaCl). Urine samples obtained 24 hr after injection from 2 tumor-bearing animals were analyzed on a SEP-PAK C<sub>18</sub> cartridge.

## RESULTS

### *Radiolabeling.*

In Figure 2, a typical elution pattern is presented of the purification of <sup>123</sup>I-[Tyr<sup>3</sup>]-octreotide over a SEP-PAK C<sub>18</sub> reversed-phase extraction cartridge. The radioactivity eluted with the ammonium acetate and water fractions appeared to be free radioiodide. The acetic acid fraction contained some peptide-bound radioiodine. The ethanol fraction contained 40 % - 60 % of the applied radioactivity when <sup>125</sup>I was used for the labeling and 70 % - 80 % when <sup>123</sup>I was used. Usually the specific activity of the SEP-PAK C<sub>18</sub>-purified [<sup>123</sup>I-Tyr<sup>3</sup>]-octreotide reached a value of 30 - 37 MBq/μg peptide. Occasionally, labeling yields of less than 5 % were observed after labeling with <sup>123</sup>I (see Discussion). With high labeling yields the SEP-PAK C<sub>18</sub> separations resulted in > 99 % peptide-bound radioiodine. HPLC analysis of the material in the ethanol fraction is shown in Figure 3a-b. After labeling with <sup>125</sup>I, two major peaks (at 19 and 21 min) were seen (Fig. 3a), of which the first one represents the mono-iodinated peptide (12) and the second probably the di-iodinated compound (see Discussion). With <sup>123</sup>I, usually over 99 % of the labeled product consisted of mono-iodinated [Tyr<sup>3</sup>]-octreotide (Fig. 3b), whereas in cases of low labeling yields, mentioned above, radioactivity was clearly present as di-iodinated peptide as well (up to 70 % of total peptide-bound activity). For all further experiments, at least 99 % radiochemically pure mono-iodinated [Tyr<sup>3</sup>]-octreotide was used.

It was not possible to detect the low peptide mass of radioiodinated [Tyr<sup>3</sup>]-octreotide along with the radioactivity in the elution profiles presented in Figure 3 (using either <sup>123</sup>I or <sup>125</sup>I). Furthermore, "cold" mono-iodinated [<sup>127</sup>I-Tyr<sup>3</sup>]-octreotide and di-iodinated [<sup>127</sup>I-Tyr<sup>3</sup>]-octreotide were not available. However, a clear



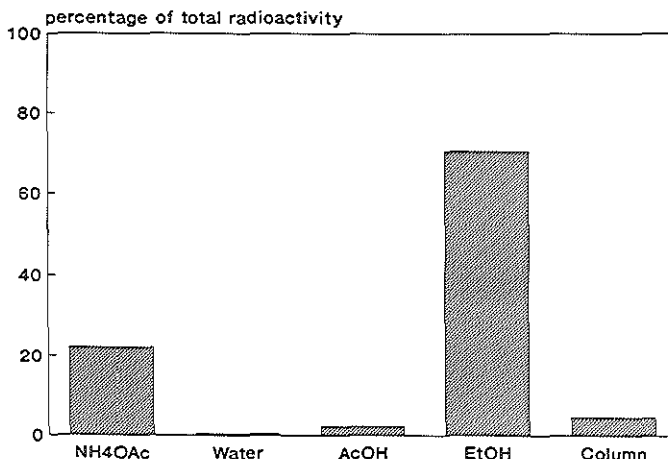


**Figure 2**

*SEP-PAK  $C_{18}$  elution pattern after radioiodination of [Tyr<sup>3</sup>]-octreotide.*

separation between mono-radioiodinated (retention time 19 min) and unlabeled [Tyr<sup>3</sup>]-octreotide (retention time 15 min) by HPLC was demonstrated.

In an attempt to increase the labeling efficiency with <sup>125</sup>I, a range of higher chloramine-T concentrations was tested. These radiolabeling procedures led not only to a substantial lowering of the labeling efficiency but also to a lower specific biologic somatostatin response measured as inhibition of the growth hormone secretion in rat pituitary cell cultures (data not shown). This is probably due to oxidative damage of [Tyr<sup>3</sup>]-octreotide at high chloramine-T concentrations.

#### ***Receptor binding and specific biologic activity.***

In Figure 4, the binding characteristics of radiolabeled [Tyr<sup>3</sup>]-octreotide to human meningioma membranes are illustrated. Scatchard analysis of the data (inset Fig. 4) showed a dissociation constant  $K_d$  of 1.50 nM ( $r = 0.96$ ) and a receptor concentration ( $B_{max}$ ) of 98 fmol/mg of membrane protein, values similar to those reported for [<sup>125</sup>I-Tyr<sup>11</sup>]-somatostatin (13).

Radiolabeled [Tyr<sup>3</sup>]-octreotide showed the same biologic activity as octreotide, and somatostatin. In Table 1 the secretion of rat growth hormone (rGH) by cultured rat pituitary cells is shown as a function of added [Tyr<sup>3</sup>]-octreotide, HPLC-purified mono-iodinated [<sup>125</sup>I-Tyr<sup>3</sup>]-octreotide and somatostatin. The inhibition of rGH secretion by all three peptides was very similar. The presence of the radionuclide <sup>125</sup>I in the peptide did not disturb the results of the rGH radioimmunoassay.

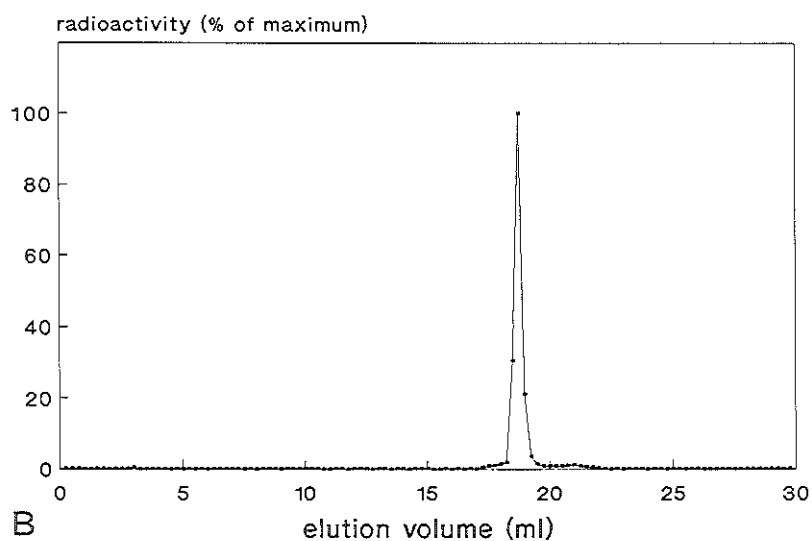
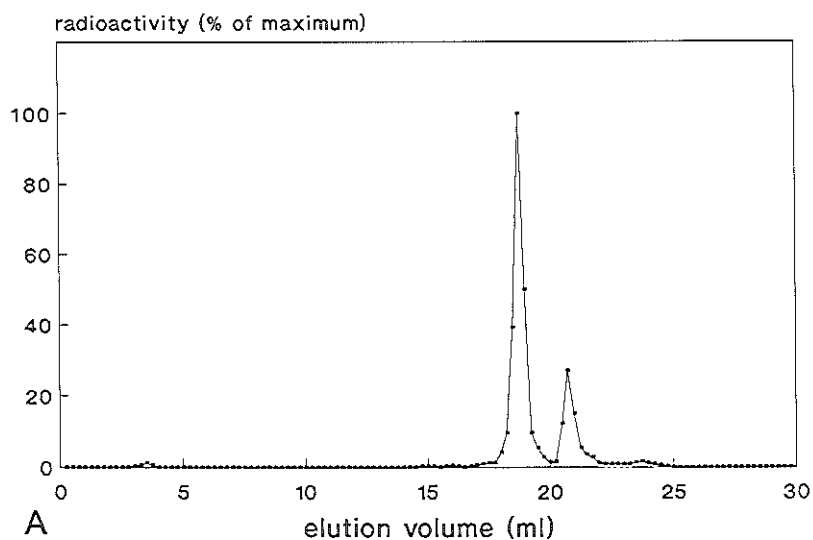


**Figure 3**

*HPLC elution patterns after labeling [Tyr<sup>3</sup>]-octreotide with <sup>125</sup>I (A) and [Tyr<sup>3</sup>]-octreotide with <sup>123</sup>I (B).*

### *Animal studies.*

Dynamic scintigraphy of control rats after i.v. administration of [ $^{125}$ I-Tyr $^3$ ]-octreotide showed a fast disappearance of the radioactivity from the blood circulation. Measurements with the gamma camera above the heart region showed that the time required to reach 50 % of the highest radioactivity in the blood circulation was less than 2 min. Thirty minutes after injection static images showed clear appearance of radioactivity in the liver and intestines. The left kidney was seen as well as excreted activity in the bladder. The right kidney was not visible because of overprojection of the intestines. The accumulation of the radiolabeled [Tyr $^3$ ]-octreotide in the liver was immediately followed by hepatobiliary excretion. Thirty minutes after injection no further radioactivity accumulation was seen elsewhere. Two hours after injection the thyroid was visible. The main radioactivity at that time was situated in the intestines, while activity in the bladder was also seen. Five and 24 hr after injection the radioactivity in the thyroid was further increased. Although after 24 hr the highest activity was found in the thyroid, a similar amount was spread diffusely over the intestines, but little radioactivity was seen in other tissues at that time.

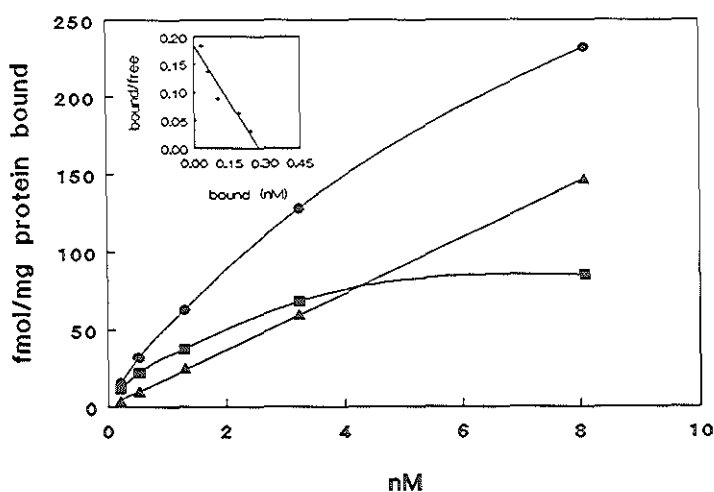


*Figure 4*

*Saturation curve of radiolabeled [Tyr $^3$ ]-octreotide binding to human meningioma membranes: (●) total binding in absence of 10  $\mu$ M somatostatin, (▲) non-specific binding in presence of 10  $\mu$ M somatostatin and (■) specific binding. Points are average of triplicates. Inset: Scatchard plot.*

*Table 1*

*Biologic activity of (HPLC-purified) [<sup>125</sup>I-Tyr<sup>3</sup>]-octreotide\*.*

Peptide	Concentration (nM)	Rat growth hormone (ng/ml ± s.d.) (%)	
[ <sup>125</sup> I-Tyr <sup>3</sup> ]-octreotide	0	296 ± 11	100
	0.05	299 ± 6	101
	0.1	220 ± 7	74
	0.5	188 ± 21	64
	1.0	184 ± 22	62
[Tyr <sup>3</sup> ]-octreotide	0	303 ± 11	100
	0.05	282 ± 11	93
	0.1	285 ± 13	94
	0.5	204 ± 13	67
	1.0	172 ± 19	57
Somatostatin	0	344 ± 18	100
	0.05	290 ± 27	84
	0.1	267 ± 24	77
	0.5	185 ± 18	54
	1.0	158 ± 8	46

\**Secretion of rat growth hormone from cultured rat pituitary cells (n = 4); by radiolabeled [Tyr<sup>3</sup>]-octreotide, [Tyr<sup>3</sup>]-octreotide and somatostatin.*

The tissue radioactivity distributions in control rats, 30 min and 24 hr after i.v. injection of [<sup>125</sup>I-Tyr<sup>3</sup>]-octreotide, were analyzed by radioactivity measurements of the various organs with a GeLi-detector. Thirty minutes after injection most of the administered radionuclide was located in the intestines, the liver, and the kidneys, while the highest radioactivity concentrations (% dose/g tissue) were found in the intestines, the adrenals, the kidneys and the liver (Table 2). However, even much

*Table 2*

*Tissue distribution in five rats 30 min after intravenous administration of [<sup>125</sup>I-Tyr<sup>3</sup>]-octreotide*

Tissue	% dose (mean $\pm$ s.d.)	% dose/g (mean $\pm$ s.d.)
Intestines	50 $\pm$ 10	2.7 $\pm$ 0.5
Liver	12 $\pm$ 2	1.3 $\pm$ 0.2
Kidneys	3.5 $\pm$ 0.5	1.5 $\pm$ 0.2
Lungs	0.44 $\pm$ 0.12	0.37 $\pm$ 0.07
Spleen	0.10 $\pm$ 0.07	0.20 $\pm$ 0.12
Heart	0.10 $\pm$ 0.02	0.11 $\pm$ 0.01
Adrenals	0.06 $\pm$ 0.01	1.6 $\pm$ 0.3
Parotis	0.06 $\pm$ 0.03	0.11 $\pm$ 0.04
Thymus	0.048 $\pm$ 0.008	0.11 $\pm$ 0.02
Thyroid	0.004 $\pm$ 0.006	0.15 $\pm$ 0.06
Rest	26 $\pm$ 5	0.13 $\pm$ 0.02
Blood		0.24 $\pm$ 0.05
Urine		16 $\pm$ 13

higher concentrations of radioactivity were found in the collected urine specimens 30 min after injection. Twenty-four hours after injection the highest activities were measured in the thyroid and the intestines, with the thyroid having the highest concentration of radioactivity (Table 3). Urine samples were not collected 24 hr after injection.

In tumor-bearing rats, accumulation of the radioiodinated [Tyr<sup>3</sup>]-octreotide at tumor sites could be demonstrated with the gamma camera. The scintigrams demonstrate a clear visualization of tumors at 30 min, 3 and 5 h after injection. However, 24 hr after injection the previously accumulated radioactivity at the tumor sites had disappeared, which was confirmed by counting the isolated tumors 30 min and 24 hr after injection (data not shown).

Figure 5 shows a posterior view of a rat with somatostatin receptor-positive tumors to the left (320 mm<sup>2</sup>) and to the right (144 mm<sup>2</sup>) 30 min after injection, whereas at the same time point in a rat pretreated with 1 mg octreotide subcutaneously 30 min before injection of [<sup>125</sup>I-Tyr<sup>3</sup>]-octreotide an even larger tumor at the left (640 mm<sup>2</sup>) was only visible as vascular tissue radioactivity (Fig. 6).

A significant increase in radioactivity was demonstrated above nine tumors in six

**Table 3**

*Tissue distribution in four rats 24 hr after intravenous administration of [<sup>125</sup>I-Tyr<sup>3</sup>]-octreotide*

Tissue	% dose (mean ± s.d.)	% dose/g (mean ± s.d.)
Intestines	9 ± 10	0.6 ± 0.7
Liver	0.31 ± 0.03	0.027 ± 0.005
Kidneys	0.26 ± 0.04	0.10 ± 0.01
Lungs	0.040 ± 0.011	0.033 ± 0.006
Spleen	0.011 ± 0.010	0.028 ± 0.021
Heart	0.007 ± 0.002	0.009 ± 0.002
Adrenals	0.0028 ± 0.0007	0.07 ± 0.02
Parotis	0.0045 ± 0.0020	0.009 ± 0.004
Thymus	0.006 ± 0.003	0.016 ± 0.007
Thyroid	7 ± 2	180 ± 50
Rest	3.0 ± 0.6	0.016 ± 0.004
Blood		0.020 ± 0.006

animals immediately after i.v. injection. Because of different sizes of tumors (and normal tissues) in various animals normalization of data was necessary. The measured radioactivity during the first minute after injection was taken as a reference. Figure 7 shows the radioactivity as a function of time measured above nine tumors in six animals, expressed as percentage of the 1-min value. In Figure 7 is also shown that the above tumors in two rats (of which one is depicted in Fig. 6), which were pretreated subcutaneously with 1 mg octreotide 30 min before injection of the radiopharmakon, a decrease of radioactivity with time was measured similar to control tissues in eight animals reflecting the decreasing vascular tissue radioactivity.

Compared to the uptake in the liver the initial increase of radioactivity above the tumors was clearly higher in six tumors, equal in two tumors, and less in one tumor.

The tissue radioactivity distribution in tumor-bearing rats was similar to that in control rats both 30 min and 24 hr after [<sup>125</sup>I-Tyr<sup>3</sup>]-octreotide injection (data not shown).

The biodistribution of the radiopharmakon in octreotide-pretreated animals showed a similar pattern as in the animals not pretreated with octreotide (including the controls), according to gamma camera measurements.

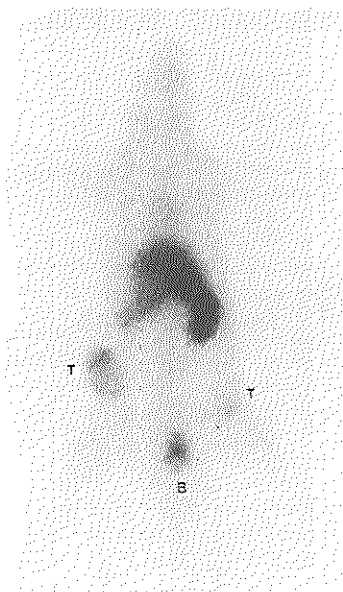


**Figure 5**

*Scintigraphy of a rat with one somatostatin receptor-positive tumor at the left (surface: 320 mm<sup>2</sup>) and one at the right (144 mm<sup>2</sup>), 20 min after i.v. injection of radiolabeled [Tyr<sup>3</sup>]-octreotide. Apart from tumors (T) and bladder (B) activity is seen in heart, liver, intestines (including right kidney), and the left kidney.*

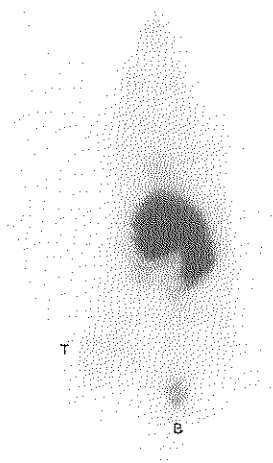


**Figure 6**

*Scintigraphy of a rat pretreated with 1 mg octreotide with one somatostatin receptor-positive tumor at the left (surface: 640 mm<sup>2</sup>) 20 min after i.v. injection of radiolabeled [Tyr<sup>3</sup>]-octreotide. (See also Fig. 5 legend)*

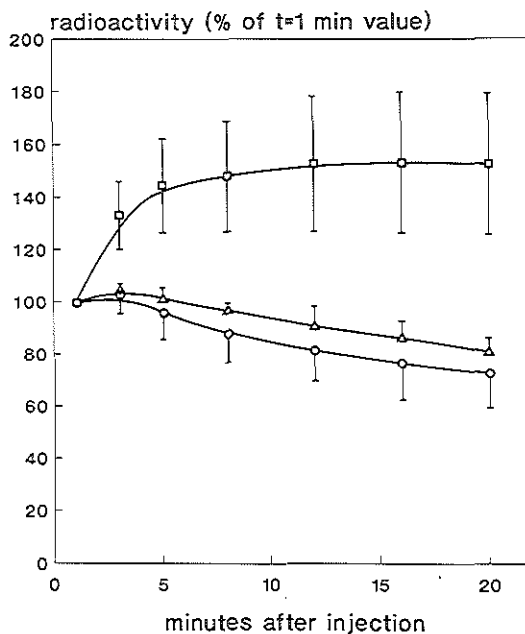
A 30-min urine sample was obtained from one tumor-bearing animal. HPLC-analysis of that sample showed, that [<sup>125</sup>I-Tyr<sup>3</sup>]-octreotide was excreted in unchanged form. Extraction of urine samples obtained 24 hr after injection from two tumor-bearing animals with a SEP-PAK C<sub>18</sub> cartridge showed that more than 95 % of the radioactivity was free radioiodide.

## DISCUSSION

[Tyr<sup>3</sup>]-octreotide is a stable analogue of somatostatin that can be easily radioiodinated (12). In this study, the postulate is tested that radioiodinated [Tyr<sup>3</sup>]-

**Figure 7**

*Radioactivity as a function of time, expressed as percentage ( $\pm$  s.d.) of the 1-min value, measured above nine tumors in six rats ( $\blacksquare$ ), two tumors in two rats, which were pretreated with 1 mg octreotide ( $\blacktriangle$ ) and control tissues in eight animals ( $\bullet$ ).*



octreotide, which has been used successfully in detecting somatostatin receptors in isolated tissues (12, 19, 20), is also suitable for in vivo imaging of tumors containing somatostatin receptors with  $^{123}\text{I}$  as a radiolabel. For this, we investigated the radiolabeling of  $[\text{Tyr}^3]\text{-octreotide}$  ( $^{123}\text{I}$  compared with  $^{125}\text{I}$ ), the purification of the radiolabeled product, its specific biologic characteristics, in vivo metabolism, and application for imaging somatostatin receptor-positive tumors in the rat.

With  $^{125}\text{I}$ , always consistent labeling yields of 40 % - 60 % are obtained at a peptide : iodide ratio of 3 : 2. Because of the very high specific activity of  $^{123}\text{I}$  a large excess of  $[\text{Tyr}^3]\text{-octreotide}$  over total iodide can be used while keeping the absolute amount of peptide low (peptide : iodide = 100 : 3). In general, very high labeling yields (70 % - 80 %) with high specific activities are obtained using  $^{123}\text{I}$ . Occasionally, however, very low radiolabeling yields (below 5 %) are observed with  $^{123}\text{I}$ . These difficulties are never seen when completely carrier-free  $^{125}\text{I}$  (Amersham, England) is used. In the case of  $^{123}\text{I}$ , other iodine isotopes (e.g.,  $^{125}\text{I}$  and stable  $^{127}\text{I}$ ) are contaminating the  $^{123}\text{I}$ -preparation (maximal seven other iodine atoms versus one  $^{123}\text{I}$  atom at the time of labeling) as a consequence of the radionuclide production method. The occasionally observed labeling yields below 5 % are caused by production problems by which the product specifications ( $> 3.7 \text{ TBq } ^{123}\text{I}/\text{mg iodine}$ ) are not met (see also below). The best and constant results are finally obtained with  $^{123}\text{I}$  obtained from Medgenix (Fleurus, Belgium).

The high peptide-to-iodide ratio (100 : 3) favors not only a high labeling yield but also the formation of mono-iodinated over di-iodinated  $[\text{Tyr}^3]\text{-octreotide}$ . Radioactivity in the first HPLC-eluted peptide peak representing the mono-



iodinated  $^{125}\text{I}$ -compound usually was more than 99 % of the total peptide radioactivity. This is in contrast to the  $^{125}\text{I}$ -labeling (with a much lower peptide : iodide ratio of 3 : 2), where the second HPLC-eluted di-iodinated product always represents at least 30 % of the total peptide-bound radioactivity, and HPLC is necessary to isolate the mono-iodinated peptide. A similar separation of radioiodinated  $[\text{Tyr}^3]$ -octreotide in two components has been reported previously (12) using  $^{125}\text{I}$  as radiolabel and a different HPLC system. The occasionally low labeling yields with  $^{125}\text{I}$  are always associated with formation of relatively much di-iodinated  $[\text{Tyr}^3]$ -octreotide (up to 70 % of all peptide bound radioactivity) because of the unexpectedly high amount of stable  $^{127}\text{I}$  in the radionuclide preparation, which was afterwards confirmed by the manufacturer. Clearly a large excess of  $[\text{Tyr}^3]$ -octreotide compared to total iodide guarantees a high labeling yield and the formation of mainly mono-iodinated  $[\text{Tyr}^3]$ -octreotide, of which high binding to somatostatin receptors was reported (12). Thus, it appears that the SEP-PAK  $\text{C}_{18}$  separation technique is adequate to prepare high activities (e.g., more than 2 GBq) of mono-iodinated  $[\text{Tyr}^3]$ -octreotide.

The specific radioactivity of the  $^{125}\text{I}$ -labeled peptide isolated on SEP-PAK  $\text{C}_{18}$  is proven to be high enough to demonstrate specific binding to human meningioma membranes. This suggests that additional HPLC purification is not necessary for the large amounts of radioactivity required for routine i.v. administration.

To demonstrate the specific biologic activity of the radiolabeled compound, the latter has been isolated by HPLC; it inhibits growth hormone release to a similar extent as  $[\text{Tyr}^3]$ -octreotide and somatostatin. This indicates that the radiolabeling procedure is not deleterious to the biologic activity of the peptide. In this case, mono-iodinated  $[\text{Tyr}^3]$ -octreotide has been isolated, of which the specific radioactivity can be exactly calculated. This is not possible with  $^{125}\text{I}$  because of the contamination with variable and unknown amounts of other iodine isotopes (see above).

In vivo disposal of circulating radioiodinated  $[\text{Tyr}^3]$ -octreotide in both control and tumor-bearing rats occurs predominantly by rapid hepatic clearance and biliary excretion as demonstrated with the scintigraphic studies and analyses of radioactivity in isolated tissues. This finding is in accordance with studies with octreotide itself (21) and another somatostatin analogue in the rat model (22).

A second route of clearance via the kidneys is demonstrated at 30 min on the scintigrams (left kidney and bladder) and organ distributions (Table 2). Note the very high radioactivity concentration in the urine samples collected at that time. The identification of urinary radioactivity in the form of unchanged radioiodinated  $[\text{Tyr}^3]$ -octreotide in a 30-min sample demonstrates that the compound is cleared intact by the kidneys. Of the low radioactivity in the 24-hr samples at least 95 % is in the form of free radioiodide. The appearance of radioiodide in the urine is explained by complete hydrolysis of the labeled peptide followed by deiodination of iodotyrosine. A relatively high amount (7 % - 11 %) of injected radioiodine is trapped in the thyroid after 24 hr, since the thyroids of the animals were not

blocked.

The relatively high adrenal radioactivity concentration found 30 min after injection in control and tumor-bearing animals is in accordance with reported autoradiographic experiments (20), demonstrating the existence of somatostatin receptors in the rat adrenal.

The observed rapid decrease in circulating radioactivity of the radiopharmaceutical may benefit the sensitivity of the scintigraphic detection technique, especially as the receptor-bound radioactivity is stable once binding has taken place. This will result in a higher tumor/background ratio. For *in vivo* experiments, radioiodinated [Tyr<sup>3</sup>]-octreotide is injected intravenously in rats with transplantable rat pancreatic tumors (CA 20948), which are known to contain somatostatin receptors *in vitro* (16 - 18). The increasing radioactivity measured above the tumor sites immediately after injection contrasts with the decreasing blood-pool radioactivity, which excludes imaging of the tumors solely on the basis of blood-pool radioactivity. This increase is usually more pronounced than that above the liver, which is an indication of a very rapid binding process. Obviously, the total maximum radioactivity above the liver is higher due to its greater size.

The specificity of the binding of [<sup>125</sup>I-Tyr<sup>3</sup>]-octreotide to the tumors is most firmly established by the observation that pretreatment of the tumor-bearing rats with a high dose (1 mg) of octreotide (without changing the biodistribution of the radiopharmaceutical as observed with the gammacamera) results in a complete inhibition of the binding of label to the tumors. Consequently, immediately after injection decreasing radioactivity is measured over the blocked tumors, reflecting the radioactivity in the vascular pool, in contrast to the increasing radioactivity measured over the unblocked tumors (Fig. 7).

## CONCLUSION

The radioiodination of [Tyr<sup>3</sup>]-octreotide and the described purification procedure do not alter the specific somatostatin characteristics of the original compound, which means that this radiopharmaceutical is suitable for scintigraphic imaging of somatostatin receptors *in vivo*.

The fast disappearance from plasma of radioiodinated [Tyr<sup>3</sup>]-octreotide after *i.v.* administration rapidly reduces the background level in the circulation, enhancing the possibility of scintigraphic imaging of somatostatin receptor-bearing tumors.

Because of the successful scintigraphic demonstration of somatostatin receptor-bearing tumors in the rat model using radioiodinated [Tyr<sup>3</sup>]-octreotide, application of this new radiopharmaceutical in humans is promising since it is known that various human tumors possess large numbers of high-affinity somatostatin receptors, as demonstrated with [<sup>125</sup>I-Tyr<sup>3</sup>]-octreotide *in vitro* (11, 13).

## ACKNOWLEDGEMENTS

The authors thank Fred den Holder, Marion de Jong, Ina Loeve, Marcel van der Pluijm, Buddy Setyono-Han, and Frank van der Spek for their technical assistance.

## REFERENCES

1. Hodgson HJF, Maton PN. Carcinoid and neuroendocrine tumours of the liver. *Baillière's Clinical Gastroenterology* 1987; 1: 35-61.
2. Reichlin S. Somatostatin. *N Engl J Med* 1983; 309: 1495-1501 and 1556-1563.
3. Schally AV. Oncological applications of somatostatin analogues. *Cancer Res* 1988; 48: 6977-6985.
4. Pless J, Bauer W, Briner U, et al. Chemistry and pharmacology of SMS 201-995, a long-acting analogue of somatostatin. *Scand J Gastroenterol* 1986; 21 (suppl 119): 54-64.
5. Del Pozo E, Neufeld M, Schlutter K, et al. Endocrine profile of a long-acting somatostatin derivative SMS 201-995. Study in normal volunteers following subcutaneous administration. *Acta Endocrinol* (Copenhagen) 1986; 111: 433.
6. Kvoils LK, Moertel CG, O'Connell MJ, Schut AJ, Rubin J, Hahn RG. Treatment of the malignant carcinoid syndrome: evaluation of a long-acting somatostatin analogue. *N Engl J Med* 1986; 315: 663-666.
7. Reubi JC. A somatostatin analogue inhibits chondrosarcoma and insulinoma tumor growth. *Acta Endocrinol* 1985; 109: 108-114.
8. Lamberts SWJ, Reubi JC, Uitterlinden P, Zuiderwijk J, van der Werf P, van Hal P. Studies on the mechanism of action of the inhibitory effect of the somatostatin analog SMS 201-995 on the growth of the prolactin/adrenocorticotropin-secreting pituitary tumour 7315a. *Endocrinology* 1986; 118: 2188-2194.
9. Lamberts SWJ, Koper JW, Reubi JC. The potential role of somatostatin analogs in the treatment of cancer. *Eur J Clin Invest* 1987; 17: 281-287.
10. Lamberts SWJ, Uitterlinden P, Verschoor L, van Dongen KJ, del Pozo E. Long-term treatment of acromegaly with the somatostatin analogue SMS 201-995. *N Engl J Med* 1985; 313: 1576-1580.
11. Reubi JC, Häcki WH, Lamberts SWJ. Hormone-producing gastrointestinal tumours contain high density of somatostatin receptors. *J Clin Endocrinol Metab* 1987; 65: 1127-1134.
12. Reubi JC. New specific radioligand for one subpopulation of brain somatostatin receptors. *Life Sci* 1985; 36: 1829-1836.
13. Reubi JC, Maurer R, Klijn JG, et al. High incidence of somatostatin receptors in human meningiomas: biochemical characterization. *J Clin Endocrinol Metab* 1986; 63: 433-438.

14. Scatchard G. The attractions of proteins for small molecules and ions. *Ann NY Acad Sci* 1949; 51: 660-672.
15. Oosterom R, Verleun T, Zuiderwijk J, Lamberts S. Growth hormone secretion by cultured rat anterior pituitary cells. Effects of culture conditions and dexamethasone. *Endocrinology* 1983; 113: 735-741.
16. Reubi JC, Horisberger U, Essed CE, Jeekel J, Klijn JGM, Lamberts SWJ. Absence of somatostatin receptors in human exocrine pancreatic adenocarcinomas. *Gastroenterology* 1988; 95: 760-763.
17. Klijn JGM, Setyono-Han B, Bakker GH, Henkelman MS, Portengen H, Foekens JA. Effects of somatostatin analog (Sandostatin) treatment in experimental and human cancer. In: Klijn JGM, Paridaens R, Foekens JA, eds. *Hormonal Manipulation of Cancer: peptides, growth factors and new (anti) steroidal agents, EORTC Monograph Series, Volume 18*. New York, Raven Press; 1987: 459-468.
18. Klijn JGM, Setyono-Han B, Bakker GH, Portengen H, Foekens JA. Prophylactic neuropeptide-analog treatment of a transplantable pancreatic tumor in rats. In: Bresciani F, King RJB, Lippman ME, Raynaud JP, eds. *Progress in cancer research and therapy, Volume 35, Hormones and Cancer 3*. New York, Raven Press; 1988: 550-553.
19. Reubi JC, Maurer R. Autoradiographic mapping of somatostatin receptors in the rat central nervous system and pituitary. *Neuroscience* 1985; 15: 1183-1193.
20. Maurer R, Reubi JC. Somatostatin receptors in the adrenal. *Molec Cell Endocrinol* 1986; 45: 81-90.
21. Lemaire M, Andres H, Marbach P. Disposition of Sandostatin (SMS 201-995) in the rat. *Pharmaceut Weekbl* (Scientific Edition) 1988; 10: 52.
22. Baker JR, Kemmenoe BH, McMartin C, Peters GE. Pharmacokinetics, distribution and elimination of a synthetic analogue of somatostatin in the rat. *Regul Pept* 1984; 9: 213-226.
23. Veber DF, Holly FW, Nutt RF, et al. Highly active cyclic and bicyclic somatostatin analogues of reduced size. *Nature* 1979; 280: 512-514.
24. Veber DF, Freidinger RM, Schwenk-Perlow D, et al. A potent cyclic hexapeptide analogue of somatostatin. *Nature* 1981; 292: 55-58.

### CHAPTER 3

#### **In vivo use of a radioiodinated somatostatin analogue: dynamics, metabolism and binding to somatostatin receptor-positive tumors in man**

Willem H. Bakker, Eric P. Krenning, Wout A. P. Breeman, Peter P. M. Kooij, Jean-Claude Reubi, Jan W. Koper, Marion de Jong, Johannes S. Laméris, Theo J. Visser, Steven W. Lamberts.

Departments of Nuclear Medicine, Internal Medicine III and Radiology,  
University Hospital Dijkzigt and Erasmus University Medical School,  
Rotterdam, The Netherlands and  
Sandoz Research Institute, Berne, Switzerland.

Somatostatin analogues, labeled with gamma-emitting radionuclides, are of potential value in the localization of somatostatin receptor-positive tumors with gamma camera imaging. We investigated the application in man of a radioiodinated analogue of somatostatin, [ $^{123}\text{I}$ -Tyr $^3$ ]-octreotide, which has similar biologic characteristics as the native peptide.

The radiopharmaceutical is cleared rapidly from the circulation (up to 85 % of the dose after 10 minutes) mainly by the liver. Liver radioactivity is rapidly excreted into the biliary system. Until 3 hr after injection, radioactivity in the circulation is mainly in the form of [ $^{123}\text{I}$ -Tyr $^3$ ]-octreotide. Thereafter, plasma samples contain increasing proportions of free iodide. Similarly, during the first hours after injection, radioactivity in the urine exists mainly in the form of the unchanged peptide. Thereafter, a progressive increase in radioiodide excretion is observed, indicating degradation of the radiopharmaceutical in vivo. Fecal excretion of radioactivity amounts to only a few percent of the dose.

The calculated median effective dose equivalent is comparable with values for applications of other  $^{123}\text{I}$ -radiopharmaceuticals (0.021 mSv/MBq).

[ $^{123}\text{I}$ -Tyr $^3$ ]-octreotide can be used for the visualization of a variety of somatostatin receptor-positive cancers. One patient with an endocrine pancreatic tumor and a meningioma is presented.

Somatostatin is a peptide hormone which exerts a wide variety of actions throughout the body. It plays an inhibitory role in the normal regulation of several organ systems, including the central nervous system, the hypothalamus, the pituitary gland, the gastrointestinal tract and the endocrine and exocrine pancreas (1, 2). Large numbers of binding sites with a high affinity for somatostatin have been detected with in vitro techniques in many tumors arising from these organ systems; these include pituitary tumors (3), brain tumors like meningiomas and low-grade astrocytomas (4, 5), and hormone-producing tumors in the gastrointestinal tract including the pancreas (6, 7). It has previously been shown in animal studies that it is possible to detect somatostatin receptors in vivo after administration of [ $^{125}\text{I}$ -Tyr $^3$ ]-octreotide to somatostatin receptor-positive tumor-bearing rats (8).

It has also been shown in a preliminary study that the in vivo application of the same radiopharmaceutical in man results in scintigraphic imaging of somatostatin receptor-positive tumors (9). In this study we present data on the metabolism of intravenously administered [ $^{125}\text{I}$ -Tyr $^3$ ]-octreotide in man and estimates of the radiation dose. Also scintigraphy is shown of a patient with two different somatostatin receptor-positive tumors.

## MATERIALS AND METHODS

### *Radiopharmaceuticals*

Radioiodination of [Tyr $^3$ ]-octreotide was performed with the chloramine-T method as described previously (8). Specific activities ranged from 18.5 to 37 MBq/ $\mu\text{g}$  (0.5 - 1 mCi/ $\mu\text{g}$ ) of [ $^{125}\text{I}$ -Tyr $^3$ ]-octreotide. Images were obtained after intravenous injection of 370 - 555 MBq (10 - 15 mCi; 15 - 25  $\mu\text{g}$ )  $^{125}\text{I}$ -labeled somatostatin analogue. To prevent accumulation of radioiodine in the thyroid, patients were given daily 3 x 50 mg potassium iodide and 4 x 250 mg potassium perchlorate for 3 days, starting 1 day before injection of [ $^{125}\text{I}$ -Tyr $^3$ ]-octreotide.

### *Imaging*

Planar and SPECT images were obtained with a large field of view gamma camera (Counterbalance 3700 and ROTA-II, Siemens) equipped with a 190 keV parallel-hole collimator. The analyzer was set to 159 keV with a 20 % window. Data were stored in a dedicated computer (Gamma-11, Nuclear Diagnostics, Hägersten, Sweden). During the first 30 minutes of the study, computer images (matrix 64 x 64) were acquired in 40 intervals of 3 sec each and 28 intervals of 1 min each. Analogue images were made at regular intervals during the first 30 min. Anterior and posterior whole-body scintigraphy were performed 30 min after injection. Images (both analogue and digital, matrix 128 x 128) were also obtained

at approximately 4 and 24 hr after injection. In a few cases, scintigraphy was also performed after 2 and 48 hr. SPECT was always performed for localization of primary tumors in the head/neck region as well as in case of overprojection of tumor with normal tissue (e.g., liver and kidneys). SPECT reconstruction images were made at 60 angles for 360°. Acquisition time per angle was always 30 sec. The original data were prefiltered with a Wiener filter. The filtered data were reconstructed with a Ramp filter. The reconstruction program (SPETS version 6.01) was obtained from Nuclear Diagnostics.

### *Measurements of radioactivity in blood, urine and feces.*

The radioactivity in blood, urine, and feces was measured with a LKB-1282-Compugamma system or a GeLi-detector equipped with a multichannel analyzer (Series 40, Canberra). Blood samples were collected directly before the injection and after 2, 5, 10, 20, 40, 60, 90 min and 2, 3, 5, 8 and 20 hr. Urine was collected in 5-hr intervals until 50 hours after injection. If feasible, feces were collected until 48 hours after injection.

The chemical status of the radionuclide in blood and urine was analyzed as function of time by using the SEP-PAK C<sub>18</sub>, HPLC and gel filtration techniques described previously (8). The nature of peptide-bound radioactivity in blood and urine was tested by investigation of specific binding to human meningioma membranes as described previously (4).

### *Patients*

Kinetic studies with [<sup>125</sup>I-Tyr<sup>3</sup>]-octreotide by means of gamma camera scintigraphy were performed in 13 patients with several types of tumors, including endocrine pancreatic tumors, metastatic carcinoids, and meningiomas. Additionally plasma, urine, and feces samples were obtained from seven, eight and seven patients, respectively.

### *Dosimetry*

For the estimation of the radiation dose the MIRDOSE version 2 program (10) and ICRP publication 53 (11) were used. The dose estimates were calculated on the basis of the following. The uptakes in the most important source organs, the gallbladder, the liver, the urinary bladder, and the total body, were determined as a function of time. Radioactivity in liver and the gallbladder was calculated using the geometric mean of anterior and posterior counts. Patient overall thickness, for attenuation correction, was determined from a lateral view and was assumed to be constant over the abdomen. An anatomic liver phantom contained in a waterbath was used to calculate the effects of the object geometry (12). The water thickness was varied from 15 to 20 centimeters, a typical patient range.

Calibrated amounts of radioactivity were placed in the liver phantom and in a standard bottle. The standard bottle was placed on top of the collimator and counts were determined from one view. From calculated counts in the liver phantom and measured counts in the standard bottle a geometry factor was determined as a function of the water thickness. Because of the observed small variations in the geometry factor, as a function of water thickness, a constant was used to calculate the absolute uptake of the radionuclide in the liver (13). The gallbladder was regarded to have the same geometry as the standard bottle. A geometry factor for the intestines could not be determined but was taken to be the same as for the liver. In order to quantitate the percentage uptake in the various organs a standard bottle containing an aliquot of the injected dose was measured just before each patient study. Background correction for the liver was performed on the basis of an area just outside the liver region. Background correction for the gallbladder was performed on the basis of a region within the liver next to the gallbladder.

For dosimetry the biological half-life of the liver activity was calculated by analysis of the computer images 4 and 24 hours after injection. The biologic half-life in the gallbladder could not be measured, but was estimated to be 2.5 hr based upon experimental circumstances and literature (11). No predominant accumulation of radioactivity was seen in organs other than liver and gallbladder during patient studies. With further exception of the urinary bladder contents and the total body other organs therefore were disregarded as source organs. Since urine data were not available for all patients, it was assumed for dose calculations (including calculations of the urinary bladder content) that the activity in the urine for these patients was equal to the mean activity in the urine for the eight patients with correct urine collection. Total body radioactivity was assumed to be 100 % minus that in liver, gallbladder, urinary bladder and collected urine together. Furthermore, dosimetry calculations were performed on an individual basis.

## RESULTS

In seven consecutive patients injected with [ $^{125}\text{I-Tyr}^3$ ]-octreotide, the average plasma radioactivity decreased rapidly after injection. Assuming a plasma volume of 3 liters, the radioactivity in the circulation was calculated to decrease within 10 minutes to less than 15 % (s.d. 5 %) of the dose. In two patients the chemical status of the radionuclide in the plasma was investigated as a function of time. During the first hours, plasma radioactivity was mostly peptide-bound. After 3 hr, the peptide-bound fraction of total radioiodide was still about 70 %. In Figure 1, the time course of total and peptide-bound radioactivity are presented during the first 5 hr after injection of [ $^{125}\text{I-Tyr}^3$ ]-octreotide.

The urinary excretion of radioactivity in eight patients was measured by collecting samples at 5-hr intervals. Figure 1 (inset) shows that about 45 % of the administered dose was excreted in the urine within 30 hr after injection. The



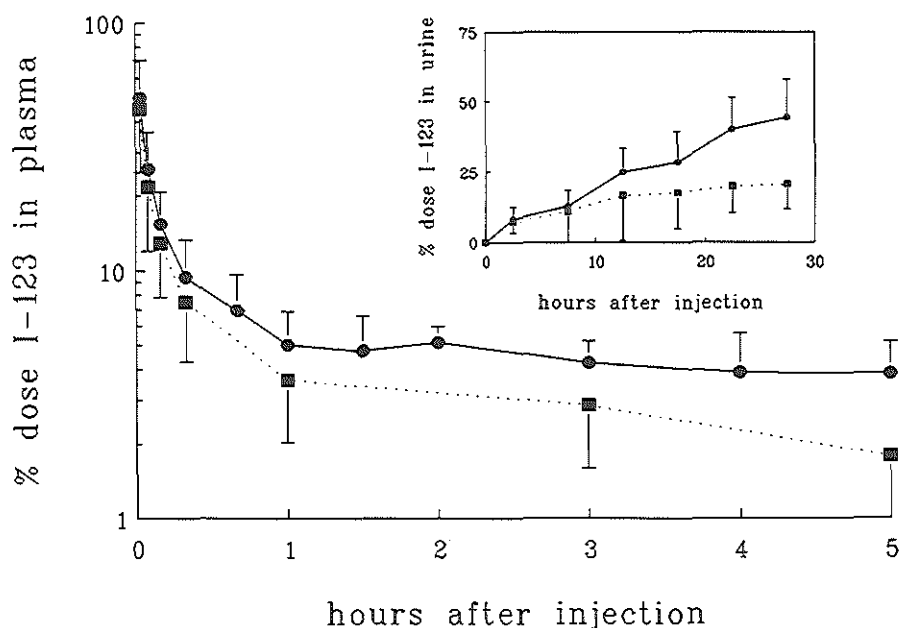


**Figure 1**

Total plasma radioactivity (●) after administration of [ $^{123}\text{I-Tyr}^3$ ]-octreotide in seven patients. Peptide-bound (■) radioactivity was calculated on the basis of data from two patients. Data are expressed as percentage (mean  $\pm$  s.d.) of the dose. (Inset) Cumulative total  $^{123}\text{I}$ -excretion (●) in the urine after intravenous injection of [ $^{123}\text{I-Tyr}^3$ ]-octreotide in eight patients. Cumulative peptide-bound radioactivity (■) was calculated on the basis of data obtained from four patients. Data are expressed as percentage (mean  $\pm$  s.d.) of the dose.

chemical status of the radionuclide in the urine was investigated as a function of time. Figure 1 (inset) also shows that in four of the patients mainly peptide-bound activity was excreted during the first 10 hr after injection. Thereafter, a progressive increase in radioiodide excretion was observed.

In four patients with a normal intestinal function, feces collected until 48 hr after injection of [ $^{123}\text{I-Tyr}^3$ ]-octreotide, contained less than 2 % of the administered radioactivity. However, in another 3 patients with abnormal intestinal function (e.g., due to previous intestinal surgery), 20 % - 45 % of the administered radioactivity was excreted in the feces within 48 hr after injection. This difference in fecal excretion was in accordance with scintigraphy, showing more radioactivity in the colon of the patients with abnormal intestinal function compared with

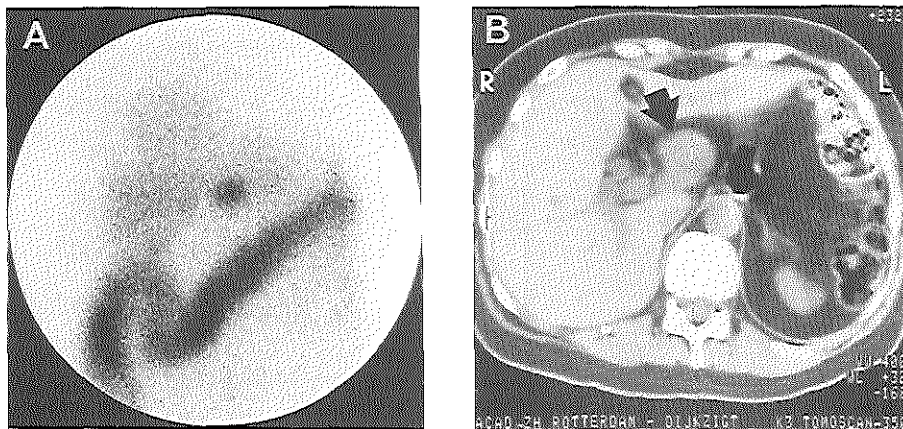


**Figure 2**

*(A) Anterior abdominal image of somatostatin receptor-positive gastrinoma, taken 28 hours after injection of [ $^{123}\text{I}$ -Tyr $^3$ ]-octreotide in a patient after gastrectomy and intestinal surgery. (B) CT scan of the abdomen with a slice at the level of the hot spot in Figure 2A showing an enlarged lymph node containing a gastrinoma metastasis (see arrow).*

patients with normal intestinal function. Figure 2A is an example of a patient with a disturbed intestinal function (after total gastrectomy and partial removal of the duodenum), which clearly shows the presence of radioactivity in the colon.

The SEP-PAK  $\text{C}_{18}$  and HPLC-purified radiolabeled-peptide component in plasma and urine showed the same biologic activity as the radiopharmaceutical itself as indicated by its specific binding to human meningioma membranes (data not shown).

After the intravenous administration of [ $^{123}\text{I}$ -Tyr $^3$ ]-octreotide scintigraphy demonstrated that radioactivity was rapidly cleared from the circulation, as measured by a decreasing blood-pool activity over the cardiac region. Gamma camera images showed that at the same time the radiopharmaceutical accumulates rapidly in the liver, immediately followed by appearance in the biliary system and eventually in the small intestines, confirming the data of our animal experiments (8).

The calculated uptakes in liver and gallbladder, which varied strongly between patients, reached their highest values between 0.5 and 1.5 hours after injection of [ $^{123}\text{I}$ -Tyr $^3$ ]-octreotide. After an initial rapid passage through the liver the median radioactivity in the liver decreased to 28 % of the dose (range 13 % - 41 %) 4 hr after injection, and 6 % of the dose (range 2 % - 17 %) after 24 hr. Radioactivity in the gallbladder could already be observed after 5 min. After 4 hr, the ac-

*Table 1*

*Dose estimates after intravenous administration of [ $^{123}\text{I}$ -Tyr $^3$ ]-octreotide in man on the basis of gamma camera measurements ( $n = 13$ ) and measurements of urinary excretion ( $n = 8$ ).*

Target organ	median absorbed dose (mGy/MBq)	range (mGy/MBq)
Gallbladder wall	0.119	0.043 - 0.222
Liver	0.048	0.024 - 0.081
Urinary bladder wall	0.041	0.040 - 0.045

Median effective dose equivalent (mSv/MBq)	range (mSv/MBq)
0.021	0.018 - 0.031

cumulation in the gallbladder was 18 % of the dose (range 3 % - 35 %). Radioactivity in the gallbladder had disappeared after 24 hr. After 4 hr less than 2 % of the dose was measured in the intestines. In patients without tumors in the intestinal region and in patients who did not undergo intestinal surgery, some activity was measured in this area (median 6 %, range 2 % - 9 %) after 24 hr. Because of the short physical half-life of  $^{123}\text{I}$  and the low intestinal residence time, the intestines were disregarded as source organ in dosimetry. The calculated uptake in the total body in individual patients did not show a significant decrease from 4 to 24 hr after injection. For this reason, in the dose calculations the effective half-life for the total body was the same as the physical half-life of  $^{123}\text{I}$ . Patients were investigated under maximum thyroid-blocking conditions to prevent accumulation of the radionuclide in the thyroid. Therefore, the circulating free radioiodide, released from the radiolabeled analogue, was largely cleared by the kidneys. Indeed, only very low thyroïdal accumulation was seen. Consequently, the radiation dose to the thyroid was negligible and was not considered in the calculations. The kidneys and the intestines were sometimes seen on the gamma camera images but treated as negligible source organs because of the short residence time of the radionuclide in these organs. The results of the dosimetry are shown in Table 1.

### *Case history*

As an example, the detection of two different somatostatin receptor-positive tumors in one patient is presented. The patient, a 40 year old woman, underwent a total gastrectomy, subtotal pancreatectomy, and partial removal of the duodenum because of a large gastrin-secreting tumor in the cauda and corpus of the pancreas as well as in the wall of the duodenum at age 34. In the last 4 yr, serum gastrin

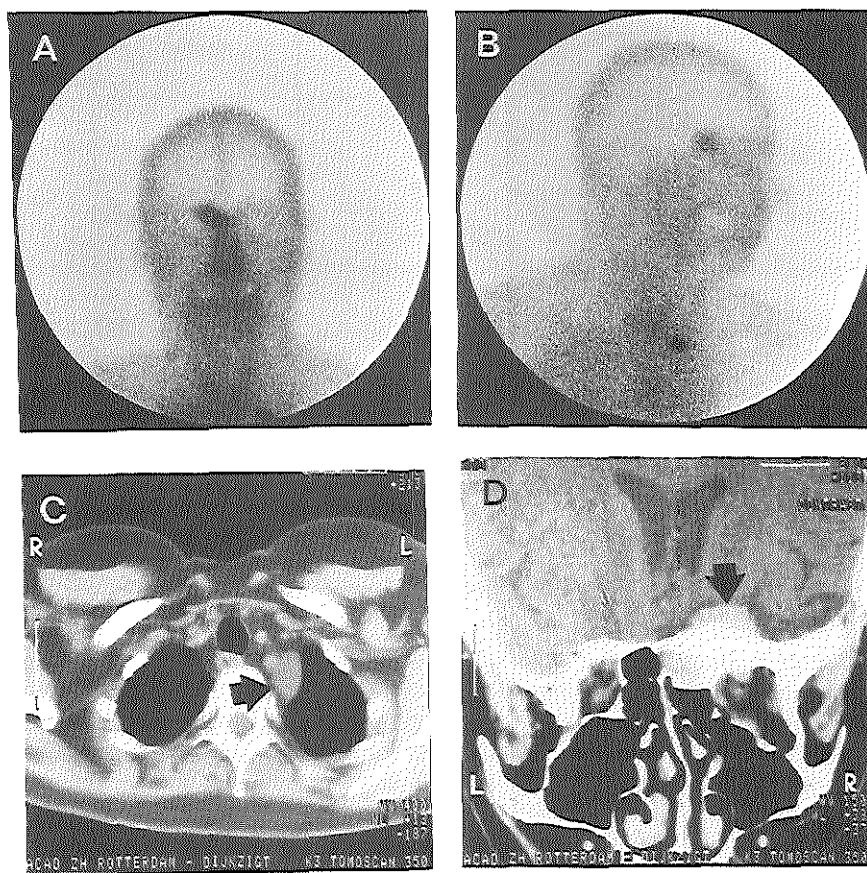


**Figure 3**

(A) Anterior scintigraphy of a lymph node metastasis of the gastrinoma (on the left side of the mediastinum) and a meningioma 24 hr after injection of [ $^{125}$ I-Tyr $^3$ ]-octreotide. (B) Right lateral scintigraphy of the lymph node metastasis and the meningioma. (C) CT-scan of a lymph node metastasis of the gastrinoma in the mediastinum (see arrow). (D) CT-scan of the somatostatin receptor-positive meningioma (see arrow).

levels increased steadily to levels 20 times above the upper limit of normal. This suggested the recurrence of gastrin-secreting tumor tissue, but its location could not be established immediately. In addition, this patient had a meningioma located parasellarly on the right side, which was removed at age 36. This tumor recurred, causing loss of vision of the right eye.

The presence of a somatostatin receptor-positive tumor (diameter 5 cm), which was subsequently shown to be a single gastrinoma-containing lymph node, was seen 3 min after injection of [ $^{123}\text{I-Tyr}^3$ ]-octreotide (not shown here) and was still clearly visible after 28 hr. Figure 2A shows the gastrinoma together with colon radioactivity and decreased liver activity on an anterior abdominal image 28 hr after injection of [ $^{123}\text{I-Tyr}^3$ ]-octreotide. Figure 2B shows this gastrinoma on the CT scan. At abdominal surgery, no other gastrinoma metastases were found in the abdomen or in the liver.

Figures 3A-B (24 hr after administration of [ $^{123}\text{I-Tyr}^3$ ]-octreotide) indicate the existence of another lymph node metastasis of the gastrinoma on the left side of the mediastinum, while the somatostatin receptor-positive meningioma is also clearly visualized. Figures 3C-D present CT-images of the lymph node metastasis and the meningioma, respectively.

## DISCUSSION

[ $\text{Tyr}^3$ ]-octreotide, labeled with  $^{125}\text{I}$ , which is successfully applied to *in vitro* somatostatin receptor studies, is not suitable for *in vivo* imaging because of the low-energy gamma emissions of  $^{125}\text{I}$ . Although the radiation emitted by  $^{131}\text{I}$  is more favourable for scintigraphy, the disadvantage that this isotope shares with  $^{125}\text{I}$  is its low specific activity (14), which necessitates purification of the radioiodination products by HPLC and lowers the yield of monoiodinated [ $\text{Tyr}^3$ ]-octreotide especially when the usual, low amounts of peptide are labeled. However, with the availability of cyclotron-produced  $^{123}\text{I}$  (half-life 13.2 hours, gamma energy 159 keV), efficient radiolabeling of [ $\text{Tyr}^3$ ]-octreotide is possible (8), enabling excellent imaging, including SPECT. Because of its short half-life it is possible to administer high doses (maximal 555 MBq  $^{123}\text{I}$  was used), while the dose equivalent to the patient can be kept within regular limits of common nuclear medicine studies.

The metabolism of intravenously administered radio-iodinated [ $\text{Tyr}^3$ ]-octreotide in man is primarily characterized by a rapid clearance by the liver, immediately followed by biliary excretion into the small intestine. On the basis of preliminary rat liver perfusion experiments (Bakker WH et al, unpublished data), it is presumed that [ $^{123}\text{I-Tyr}^3$ ]-octreotide is excreted intact through the bile in man. The degradation of [ $^{123}\text{I-Tyr}^3$ ]-octreotide in the intestines is uncertain, but presumably the compound is hydrolyzed and its degradation products are enterally absorbed like those of octreotide (15). Thereafter, deiodination happens in tissues after which free radioiodide is ultimately cleared via the kidneys. This is supported by the observations in our patients that nearly all excreted radioactivity is present in the urine and normally only a very small amount is found in the feces, despite considerable biliary excretion. Exceptions are patients with previous intestinal operations leading to a short bowel syndrome as in the case presented in Fig. 2A.

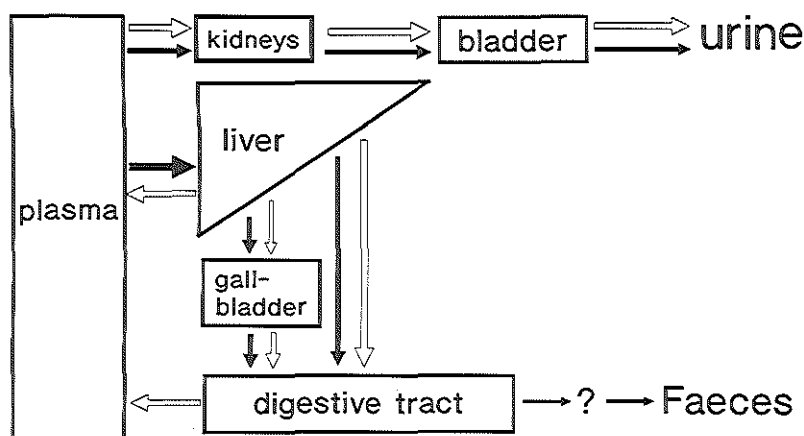


*Figure 4*

*Hypothetical model of the metabolism of [ $^{123}\text{I-Tyr}^3$ ]-octreotide. (Closed arrows)  $^{123}\text{I-Tyr-3-octreotide}$  and (open arrows) degradation products of [ $^{123}\text{I-Tyr}^3$ ]-octreotide including free iodide.*

Analysis of the chemical status of plasma radioactivity in the samples of the first 3 hr after injection mainly shows peptide-bound radioiodine in the form of the original [ $^{123}\text{I-Tyr}^3$ ]-octreotide. Analysis of radioactivity in the urine as a function of time shows predominantly intact [ $^{123}\text{I-Tyr}^3$ ]-octreotide during the first 10 hr after injection. In the subsequent samples, more and more free radioiodide is found. This free iodide is excreted over a long time course. These observations clearly indicate an effective deiodination of the injected compound and/or its degradation products in vivo. On the basis of these data a metabolic model is presented in Figure 4.

In order to visualize a tumor by receptor binding of [ $^{123}\text{I-Tyr}^3$ ]-octreotide, the specific activity expressed in counts per unit of area must exceed the local background radiation. For instance, in the hepatic region tumor receptor accumulation is more difficult to visualize during the period of normal hepatic uptake of the radioligand. The rapidly decreasing background activity (also in the liver area due to biliary excretion) facilitates the detection and localization of somatostatin receptor-positive tumors, which is further improved by the use of SPECT.

We previously reported successful imaging with this procedure of various somatostatin receptor-positive tumors, including endocrine pancreatic tumors, carcinoids, meningiomas, small cell cancers of the lung, neuroblastomas, paragangliomas, pheochromocytomas, astrocytomas, and some hormone-producing pituitary tumors (9, 16-19).

The advantage of this technique compared with currently available diagnostic radiological procedures is evident. [ $^{123}\text{I-Tyr}^3$ ]-octreotide scintigraphy is a convenient, painless, and harmless technique without side effects and with an acceptable effective dose equivalent, comparable with values for other  $^{123}\text{I}$ -labeled

radiopharmaceuticals (11). Apart from the detection of previously often unknown metastases or multiple-tumor localizations with whole-body scintigraphy, the visualization of somatostatin receptor-positive tumors may predict the possible success of octreotide radiotherapy. Although  $^{131}\text{I}$  is an attractive radionuclide for this purpose, its low specific activity would necessitate the administration of very high amounts (milligrams) of  $[\text{Tyr}^3]\text{-octreotide}$  required for binding of therapeutic amounts of  $^{131}\text{I}$ . However, somatostatin analogues radiolabeled with an ultra pure short-lived alpha or beta emitter are potential, new therapeutic radiopharmaceuticals in the treatment of somatostatin receptor-positive cancer.

## ACKNOWLEDGEMENTS

We thank Ina Loeve, Marcel van der Pluijm, Yolanda de Graaf, and René Rijsdijk for expert technical assistance.

## REFERENCES

1. Reichlin S. Somatostatin, *N Engl J Med* 1983; 309: 1495-1501 and 1556-1563.
2. Lamberts SWJ. Therapeutic effects of somatostatin analogs. *ISI Atlas of Science: Pharmacology* 1988: 179-184.
3. Reubi JC and Landolt AM. High density of somatostatin receptors in pituitary tumors from acromegalic patients. *J Clin Endocrinol Metab* 1984; 59: 1148-1151.
4. Reubi JC, Maurer R, Klijn JGM, Stefanko SZ, Foekens JA, Blaauw G, et al. High incidence of somatostatin receptors in human meningiomas: biochemical characterization. *J Clin Endocrinol Metab* 1986; 63: 433-438.
5. Reubi JC, Horisberger U, Lang W, et al. Coincidence of EGF receptors and somatostatin receptors in meningiomas but inverse, differentiation-dependant relationship in glial tumors. *Am J Pathol* 1989; 134: 337-344.
6. Reubi JC, Häcki WH and Lamberts SWJ. Hormone-producing gastrointestinal tumors contain a high density of somatostatin receptors, *J Clin Endocrinol Metab* 1987; 65: 1127-1134.
7. Reubi JC, Kvols L, Charboneau W, Reading C and Moertel C. Carcinoid tumors have a high density of somatostatin receptors that may be assessed by percutaneous needle biopsy. *Proc Am An Cancer Res* 1989; 30: 308.
8. Bakker WH, Krenning EP, Breeman WAP, et al. Receptor scintigraphy with a radioiodinated somatostatin analogue: Radiolabeling, purification, biological activity and in vivo application in animals. *J Nucl Med* 1990; 31: 1501 - 1509.
9. Krenning EP, Bakker WH, Breeman WAP, et al. Localisation of endocrine-related tumours with radioiodinated analogue of somatostatin. *Lancet* 1989; 1: 242-244.
10. Watson EE, Stabin M and Bolch WE, *Documentation package for MIRDOSE (version 2)* 1988; Oak Ridge Associated Universities.

11. International Commission on Radiological Protection. Radiation dose to patients from radiopharmaceuticals. *ICRP-publication 53*, Pergamon Press, Oxford, 1988.
12. Fleming JS. A technique for the absolute measurement of activity using a gamma camera and computer. *Phys Med Biol* 1979; 24: 176-180.
13. Myers MJ, Lavender JP, de Oliveira JB and Maseri. A simplified method of quantitating organ uptake using a gamma camera. *Brit J Radiol* 1981: 1062-1067.
14. Bale WF, Helmkamp RW, Davis TP, Izzo MJ, Goodland RL, Contreras MA and Spar IL. High specific activity labeling of protein with  $^{131}\text{I}$  by the iodine monochloride method. *Proc Soc Exper Biol & Med* 1966; 122: 407-414.
15. Lemaire M, Azria M, Dannecker R, Marbach P, Schweitzer A and Maurer G. Disposition of sandostatin, a new synthetic somatostatin analogue, in rats. *Drug Metab Dispos* 1989; 17: 699-703.
16. Krenning EP, Bakker WH, Kooij PPM, Lameris JS, Reubi JC and Lamberts SWJ. Scintigraphy of various tumours with  $^{123}\text{I}$ -labeled Tyr-3-octreotide (T-3-O), A synthetic somatostatin (SMS) analogue. Abstract. 50th Anniversary of Jules Bordet Institute Symposium on Tumour Targeting, Brussels, 1989.
17. Lamberts SWJ, Krenning EP and Klijn JGM. Clinical applications of somatostatin analogs. *Trends in Endocrinol and Metab* 1990; 3: 139-144.
18. Lamberts SWJ, Hofland LJ, van Koetsveld PM, et al. Parallel *in vivo* and *in vitro* detection of functional somatostatin receptors in human endocrine pancreatic tumors: Consequences with regard to diagnosis, localization and therapy. *J Clin Endocrinol Metab* 1990; 71: 566-574.
19. Pauw KH, Krenning EP, van Urk H, et al. Scintigraphy of glomus tumors with  $^{123}\text{I}$ -labeled Tyr-3-octreotide, a synthetic somatostatin (SMS) analogue. Abstract 63, Int Congress Otorhinology, Las Palmas, 1989.

(Dosimetry data mentioned in the original article were extended by taking into account the urinary bladder as additional source organ)



## CHAPTER 4

### **[<sup>111</sup>In-DTPA-D-Phe<sup>1</sup>]-octreotide, a potential radiopharmaceutical for imaging of somatostatin receptor-positive tumors: Synthesis, radiolabeling and in vitro validation**

W.H. Bakker, R. Albert, C. Bruns, W.A.P. Breeman,  
L.J. Hofland, P. Marbach, J. Pless, D. Pralet, B. Stolz, J.W. Koper,  
S.W.J. Lamberts, T.J. Visser, and E.P. Krenning.

Departments of Nuclear Medicine and Internal Medicine III,  
University Hospital Dijkzigt and Erasmus University, Rotterdam, The Netherlands,  
Department of Endocrinology, Sandoz Pharma AG, Basel, Switzerland.

### **Summary**

Somatostatin receptor-positive human tumors can be detected using radioiodinated analogues of somatostatin, both in vitro and in vivo. [<sup>123</sup>I-Tyr<sup>3</sup>]-octreotide has been successfully used in the visualization of somatostatin receptor-positive tumors by gamma camera scintigraphy, but this radiopharmaceutical has some major drawbacks, which can be overcome with other radionuclides such as <sup>111</sup>In. As starting material for a potentially convenient radiopharmaceutical, a diethylenetriaminopentaacetic acid (DTPA) conjugated derivative of octreotide (SMS 201-995) was prepared. This peptide, [DTPA-D-Phe<sup>1</sup>]-octreotide (SDZ 215-811) binds more than 95 % of added <sup>111</sup>In in an easy, single-step labeling procedure without necessity of further purification. The specific somatostatin-like biologic effect of these analogues was proven by the inhibition of growth hormone secretion by cultured rat pituitary cells in a dose-dependent fashion by octreotide, [DTPA-D-Phe<sup>1</sup>]-octreotide and non-radioactive [<sup>115</sup>In-DTPA-D-Phe<sup>1</sup>]-octreotide. The binding of [<sup>111</sup>In-DTPA-D-Phe<sup>1</sup>]-octreotide to rat brain cortex membranes proved to be displaced similarly by natural somatostatin as well as by octreotide, suggesting specific binding of [<sup>111</sup>In-DTPA-D-Phe<sup>1</sup>]-octreotide to somatostatin receptors. The binding of the indium-labeled compound showed a somewhat lower affinity when compared with the iodinated [Tyr<sup>3</sup>]-octreo-

tide, but indium-labeled [DTPA-D-Phe<sup>1</sup>]-octreotide still binds with nanomolar affinity. In conjunction with in vivo studies, these results suggest that [<sup>111</sup>In-DTPA-D-Phe<sup>1</sup>]-octreotide is a promising radiopharmaceutical for scintigraphic imaging of somatostatin receptor-positive tumors.

Many endocrine tumors are small and difficult to localize with the usual radiological techniques (1, 2). Most endocrine pancreatic tumors and carcinoids contain receptors for the native peptide somatostatin (3). It has been previously shown that a <sup>125</sup>I-labeled somatostatin analogue with similar biologic activity as native somatostatin specifically binds to receptors on cell membranes of these tumors (3). Subsequently, we showed with the use of the same somatostatin analogue, labeled with <sup>125</sup>I ([<sup>125</sup>I-Tyr<sup>3</sup>]-octreotide or <sup>125</sup>I-SDZ 204-090), that somatostatin receptor-positive tumors can be visualized in vivo by means of gamma camera scintigraphy both in animals (4) and man (5).

[<sup>125</sup>I-Tyr<sup>3</sup>]-octreotide, however, has the following major drawbacks (4). (a) The cyclotron-produced radionuclide <sup>125</sup>I, with the very high-quality specifications required, is not readily available world-wide. (b) The radiolabeling and consecutive purification steps are time-consuming and make the application of this label unsuitable for routine investigations. (c) Although favourable in terms of the radiation dose to the patient, the physical half-life of the radionuclide is so short that scintigraphy later than 24 hours after administration of the radiopharmaceutical is difficult. (d) After intravenous injection [<sup>125</sup>I-Tyr<sup>3</sup>]-octreotide is cleared very rapidly from the blood with a consequent relatively low effective residence time that limits its accumulation in tumor tissue, although this has the advantage of a very low interfering background radioactivity already shortly after injection. (e) The potential accumulation of radioactivity in endocrine tumors in or around the liver, bile ducts, gallbladder and gastro-intestinal tract is difficult to interpret because of the extensive hepatic clearance of [<sup>125</sup>I-Tyr<sup>3</sup>]-octreotide followed by rapid biliary excretion in the intestinal tract.

In recent years many radiopharmaceuticals, mostly larger proteins (e.g. albumin and antibodies) have been conjugated successfully with the strong metal-chelating group diethylenetriaminopentaacetic acid (DTPA) with the purpose of labeling the molecule in a simple, one-step procedure with <sup>111</sup>In (6). In contrast to <sup>125</sup>I, this isotope is readily available and has attractive physical characteristics (half-life, gamma energy). To cope with at least some of the drawbacks of [<sup>125</sup>I-Tyr<sup>3</sup>]-octreotide mentioned above, introduction of DTPA in a somatostatin derivative was proposed. Conjugation of proteins with DTPA-dianhydride as described by Hnatowich (6) occurs especially at ε-NH<sub>2</sub> groups of lysine residues. However, this method did not seem appropriate in the case of somatostatin derivatives, because of the location of the lysine residue within the bioactive site of the molecule. A synthetic method was used, therefore, in which the lysine residue in the active site of octreotide was protected before reaction with DTPA-dianhydride and de-protected afterwards. In this way only the α-NH<sub>2</sub> group was coupled with DTPA.

In the present manuscript we describe the synthesis of [DTPA-D-Phe<sup>1</sup>]-octreotide, the preparation and the quality control of the radiopharmaceutical, as well as the biologic activity and binding characteristics of the <sup>111</sup>In-coupled compound.

## MATERIALS AND METHODS

### *Synthesis of [DTPA-D-Phe<sup>1</sup>]-octreotide (Fig. 1)*

The N<sup>ε</sup>-diethylenetriaminepentaacetic acid (DTPA, Fluka) derivative of octreotide (Sandostatin<sup>®</sup>) was synthesized using the protected [ $\epsilon$ -t-butyloxy-carbonyl-Lys<sup>5</sup>]-octreotide as starting material which was available by the reaction of octreotide (7) with di-t-butyl-dicarbonate [(Boc)<sub>2</sub>O, Fluka] in dimethylformamide (unpublished results). DTPA was coupled to the selectively protected octreotide in form of its dianhydride (6). The starting material was dissolved in dioxane/water (1/1) and after addition of 20 equivalents sodiumhydrogencarbonate 1.1 equivalents of the DTPA-dianhydride were added. After 5 min dioxane was removed under diminished pressure and the remaining aqueous solution was lyophilized. Purification of the product was achieved by silicagel chromatography (Silica Gel 60, Merck) with chloroform/methanol/acetic acid<sub>30%</sub> (7/3/1) in order to separate the wanted [DTPA-D-Phe<sup>1</sup>- $\epsilon$ -Boc-Lys<sup>5</sup>]-octreotide from the contaminating double substituted DTPA-derivative and unreacted starting material. Deprotection with trifluoroacetic acid and subsequent sequential purification on Silica Gel 60, Duolite<sup>®</sup> ES-861 (Diaprosim) and a weak basic anionic exchanger AG4-X4 (BioRad) yielded homogeneous [DTPA-D-Phe<sup>1</sup>]-octreotide as lyophilisate. The purity was checked by reverse phase HPLC [mobile phase: solvent A = H<sub>2</sub>O/CH<sub>3</sub>CN/H<sub>3</sub>PO<sub>4</sub>(85%)/TMAH (tetramethylammonium-hydroxide, 10 % in water, Merck), 90/10/0.2/4 (pH 2.9) and solvent B, 30/70/0.4/4 (pH 4.0); gradient 5 - 95 % B in 20 min; column temperature: 45°C; flow rate: 1.5 ml/min; wavelength 205 nm] and on Silica Gel 60 HPTLC plates (Merck). Structure and amino acid composition were proven by means of nuclear magnetic resonance, fast atom bombardment mass spectrometry and by amino acid analysis.

### *Preparation and purification of [<sup>111</sup>In-DTPA-D-Phe<sup>1</sup>]-octreotide*

In order to label [DTPA-D-Phe<sup>1</sup>]-octreotide efficiently with <sup>111</sup>In, a 40- to 70-fold molar excess of peptide over radionuclide was used. [DTPA-D-Phe<sup>1</sup>]-octreotide was labeled with <sup>111</sup>In by reaction (10 min at room temperature) of 2  $\mu$ g peptide in 20  $\mu$ l 0.1 M acetic acid with 37 MBq <sup>111</sup>In in 20  $\mu$ l 0.04 M HCl ("INS.1P", Amersham, England), preparation A, or by reaction of 60  $\mu$ g peptide in 300  $\mu$ l 0.01 M acetic acid with 1000 - 1500 MBq "ultrapure" <sup>111</sup>InCl<sub>3</sub> in 2 ml 0.05 M HCl (Mallinckrodt, The Netherlands), preparation B. The resulting

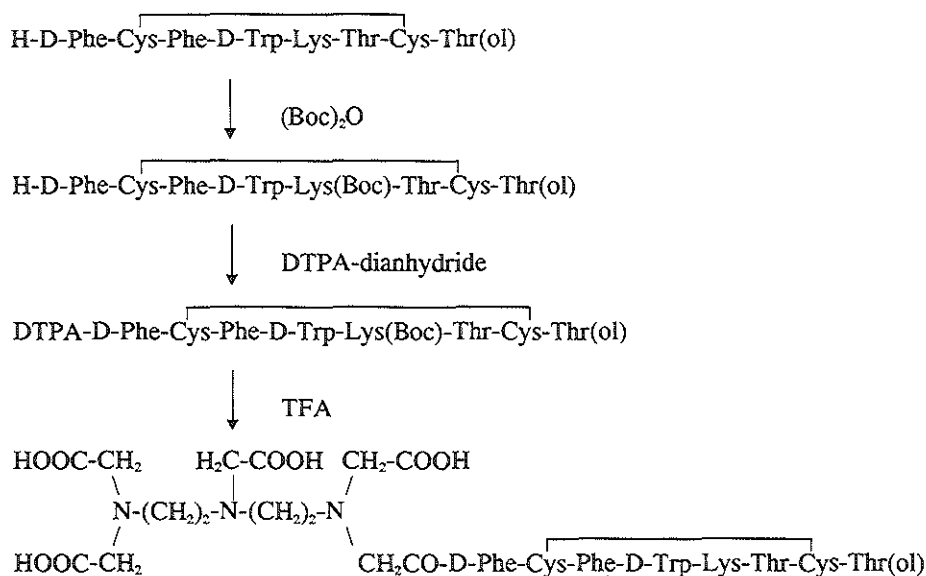


**Figure 1**

*Reaction scheme for the synthesis of [DTPA-D-Phe<sup>1</sup>]-octreotide*

specific radioactivity (radioactivity/mass labeled and unlabeled [DTPA-D-Phe<sup>1</sup>]-octreotide) amounted from 17 to 25 MBq <sup>111</sup>In/μg peptide. Nonradioactive [<sup>115</sup>In-DTPA-D-Phe<sup>1</sup>]-octreotide was prepared by mixing [DTPA-D-Phe<sup>1</sup>]-octreotide (10<sup>-4</sup> M) with a large excess of <sup>115</sup>InCl<sub>3</sub> (0.2 M; Aldrich) in 0.01 M acetic acid.

The efficiency of the labeling was tested using Instant Thin Layer Chromatography (ITLC-SG, Gelman, Ann Arbor, MI) with 0.1 M Na-citrate (pH 5) as solvent. Under these conditions indium citrate and indium chloride migrate along with the solvent front, whereas peptide-bound <sup>111</sup>In stays near the origin. Further quality control was performed by reversed-phase HPLC using a μBondapak-C<sub>18</sub> column (300 x 3.9 mm, particle size 10 μm; Waters, Milford, MA) with a linear gradient of 40 % to 80 % methanol in 0.05 M acetate (pH 5.5) in 20 min. The final solvent composition was maintained another 5 min.

### ***Radioligand binding studies***

The binding assay for [<sup>111</sup>In-DTPA-D-Phe<sup>1</sup>]-octreotide was carried out using rat brain cortex membranes according to Reubi et al (8). Briefly, cerebral cortex was dissected on ice and homogenized in 10 mM HEPES buffer, pH 7.6, centrifuged and washed two times with ten volumes of the same buffer. Cortex membranes corresponding to 50 μg protein/tube were incubated for 30 min at room

temperature with approximately  $2 \times 10^5$  cpm of [ $^{111}\text{In}$ -DTPA-D-Phe<sup>1</sup>]-octreotide and increasing concentrations of somatostatin analogues in a final volume of 300  $\mu\text{l}$ . Incubation was stopped by rapid filtration through Whatman GF/C filters. Specific radioligand binding was defined as total binding minus binding in the presence of 0.1  $\mu\text{M}$  octreotide (non-specific binding). Binding curves were calculated from 3 experiments (triplicate determinations) using the computer fitting program of De Lean (9).

To compare the affinities of (mono)-iodinated [Tyr<sup>3</sup>]-octreotide with indium-labeled [DTPA-D-Phe<sup>1</sup>]-octreotide the same displacement studies as described above have been performed using [ $^{125}\text{I}$ -Tyr<sup>3</sup>]-octreotide as radioligand and [ $^{127}\text{I}$ -Tyr<sup>3</sup>]-octreotide and [ $^{111}\text{In}$ -DTPA-D-Phe<sup>1</sup>]-octreotide as competing peptides.

### ***Biologic activity of [DTPA-D-Phe<sup>1</sup>]-octreotide***

To test its specific biologic activity, [DTPA-D-Phe<sup>1</sup>]-octreotide was compared with octreotide with regard to its growth hormone (GH) release-inhibitory effect on cultured rat pituitary cells. The preparation of dispersed female rat anterior pituitary cells and cell culture conditions have been described previously (10). Briefly, the pituitary cells were cultured at a density of  $10^5$  cells per well per ml in 48-well plates (Costar, Cambridge, MA). On day 4 the culture medium was changed and after another medium change on day 7 of culture, 4 hr incubations without or with drugs were performed in quadruplicate. The culture medium consisted of minimal essential medium, supplemented with non-essential amino acids, sodium pyruvate (1 mM), penicillin ( $10^5$  U/l), streptomycin (100 mg/l), fungizone (0.5 mg/l), L-glutamine (2 mmol/l), sodium bicarbonate (2.2 g/l) and 10 % fetal calf serum. Rat GH concentrations in the culture media were determined by a double-antibody RIA as described previously (11).

## **RESULTS**

### ***Synthesis***

[DTPA-D-Phe<sup>1</sup>]-octreotide was synthesized according to the protocol given above by a two step synthesis. The DTPA conjugation products consisted for more than 60 % of the protected [DTPA-D-Phe<sup>1</sup>]-octreotide and for about 30 % of the also formed double substituted analogue (two peptide molecules linked to the DTPA-group). The protected [DTPA-D-Phe<sup>1</sup>]-octreotide was well separated from this bis-derivative as well as from unreacted starting material by silicagel chromatography. The pure end product (overall yield 10 %) had a purity higher than 95 % which was determined by reversed phase HPLC [retention time 8.9 min (octreotide: 8.1 min)] and with silica gel HPTLC plates [ $R_f$  0.3 (octreotide 0.8)]. Amino acid analysis yielded a peptide content of 95 % and an amino acid com-

position in the correct ratio and in addition a molecular weight of 1395 was detected by fast atom bombardment mass spectroscopy.

### *Preparation and quality control of the radiopharmaceutical*

A 40- to 70-fold molar excess of peptide over  $^{111}\text{In}$  was used to assure efficient labeling of [DTPA-D-Phe<sup>1</sup>]-octreotide in the presence of (variable) amounts of other trace metals in the radionuclide solution. ITLC and HPLC analyses of the product revealed that the labeling efficiency was more than 95 %. A typical HPLC elution profile is presented in Fig. 2. With ITLC nearly all activity remained near the origin while with HPLC it eluted predominantly as a single peak with a retention time of 19.5 min. Within 1.5 hr after labeling less than 5 % of the activity was found to be bound to other compounds. Some minor peaks eluting before [ $^{111}\text{In}$ -DTPA-D-Phe<sup>1</sup>]-octreotide (between 17 and 19 min) increased with time of storage up to 24 or more hours. Formation of these contaminants was observed to be inhibited by either dilution or addition of a quencher, such as ascorbic acid or even [DTPA-D-Phe<sup>1</sup>]-octreotide itself (data not shown). Otherwise, if used within 1 hr after radiolabeling, further purification on HPLC did not improve the binding properties of the tracer. No purification was, therefore, performed after the labeling procedure except that aliquots were checked by HPLC for quality control.

### *Receptor binding studies*

To characterize the binding properties of the indium-labeled somatostatin analogue, the pharmacological profile of somatostatin binding sites labeled by [ $^{111}\text{In}$ -DTPA-D-Phe<sup>1</sup>]-octreotide was determined. Therefore, the inhibitory effects of various somatostatin analogues were tested in competition experiments using rat brain cortex membranes as a source of somatostatin receptors as described above. Representative competition experiments with the various analogues are shown in Fig. 3. The rank order of potency of different somatostatin analogues corresponded to that obtained with other well characterized ligands, such as [ $^{125}\text{I}$ -Tyr<sup>3</sup>]-octreotide (12). The analogues [Lys(ol)<sup>8</sup>]-octreotide (SDZ 203-304) and [Orn<sup>5</sup>]-octreotide (SDZ 204-354), which are relatively ineffective in inhibiting growth hormone release, also exhibited weak affinities for the [ $^{111}\text{In}$ -DTPA-D-Phe<sup>1</sup>]-octreotide recognition site. In contrast, somatostatin and octreotide showed the expected high affinities with  $\text{IC}_{50}$  values in the sub-nanomolar range, while [ $^{111}\text{In}$ -DTPA-D-Phe<sup>1</sup>]-octreotide and unlabeled [DTPA-D-Phe<sup>1</sup>]-octreotide showed intermediate affinities with  $\text{IC}_{50}$ 's in the nanomolar range. Under these conditions total binding was 2-5 % of total radioactivity and non-specific binding was less than 10 % of total binding. Stable  $^{115}\text{In}^{3+}$  alone did not inhibit receptor binding (data not shown).

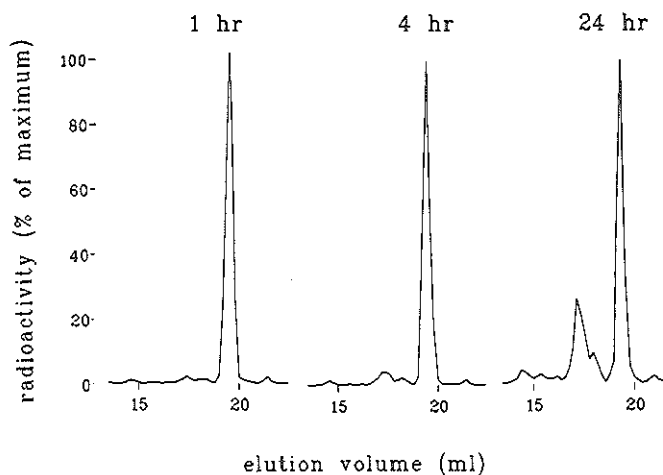


Figure 2

HPLC elution profiles 1, 4 and 24 hr after labeling of [DTPA-D-Phe<sup>1</sup>]-octreotide with <sup>111</sup>In.

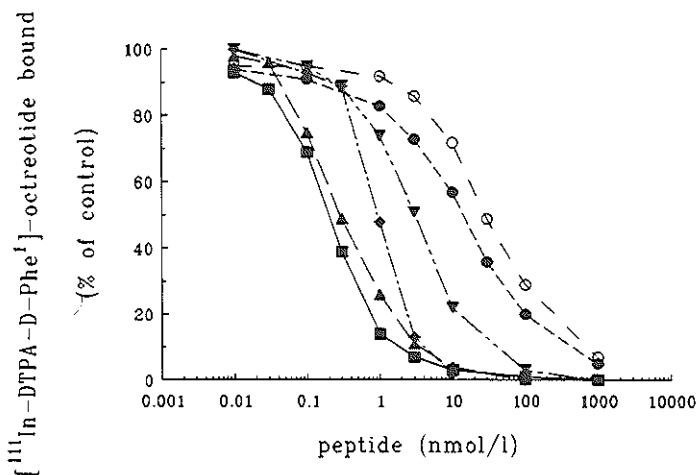
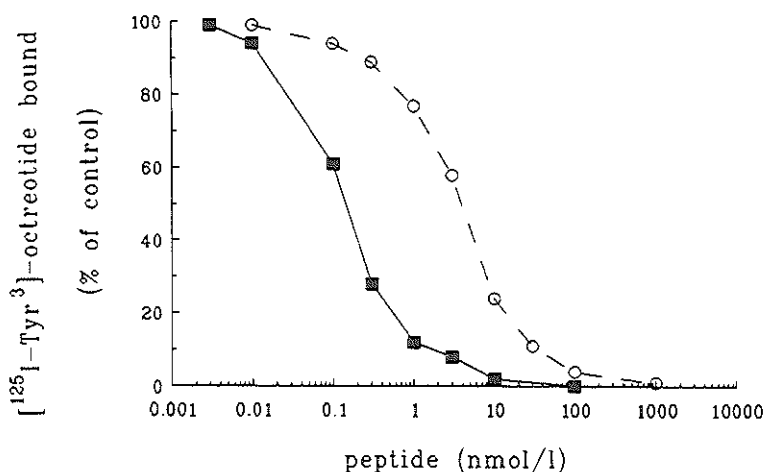


Figure 3

Binding of [<sup>111</sup>In-DTPA-D-Phe<sup>1</sup>]-octreotide to rat brain cortex membranes in the presence of increasing concentrations of somatostatin-14 (■), octreotide (▲), [<sup>115</sup>In-DTPA-D-Phe<sup>1</sup>]-octreotide (◆), [DTPA-D-Phe<sup>1</sup>]-octreotide (▼), [Orn<sup>5</sup>]-octreotide (●) and [Lys(ol)<sup>8</sup>]-octreotide (○), expressed as percentage of binding in the absence of competing compounds (n = 3, maximal SEM < 5 %).



**Figure 4**

*Binding of [<sup>125</sup>I-Tyr<sup>3</sup>]-octreotide to rat brain cortex membranes in the presence of increasing concentrations of [<sup>127</sup>I-Tyr<sup>3</sup>]-octreotide (■) and [<sup>115</sup>In-DTPA-D-Phe<sup>1</sup>]-octreotide (○), expressed as percentage of binding in the absence of competing compounds (n = 3, maximal SEM < 5 %).*

In Figure 4 the difference in affinity of the <sup>115</sup>In-labeled [DTPA-D-Phe<sup>1</sup>]-octreotide and <sup>127</sup>I-labeled [Tyr<sup>3</sup>]-octreotide for the somatostatin receptors in rat brain cortex membranes is shown with pK<sub>i</sub>-values of  $8.4 \pm 0.2$  and  $9.9 \pm 0.3$  (mean  $\pm$  SEM, n=3), respectively, indicating a somewhat lower affinity for the <sup>115</sup>In-labeled compound. Total binding was 15 % to 20 % of total radioactivity and non-specific binding was less than 10 % of total binding.

#### ***Biologic activity of [DTPA-D-Phe<sup>1</sup>]-octreotide***

Figure 5 shows results from a representative experiment on the effects of unlabeled [DTPA-D-Phe<sup>1</sup>]-octreotide and octreotide on GH release by female rat anterior pituitary cells. Both peptides inhibited GH release in a dose-dependent manner, with octreotide being about 10 times more potent than [DTPA-D-Phe<sup>1</sup>]-octreotide. Similar results were obtained with unlabeled and <sup>115</sup>In-labeled [DTPA-D-Phe<sup>1</sup>]-octreotide (data not shown). Stable <sup>115</sup>In<sup>3+</sup> alone did not inhibit GH release (data not shown).



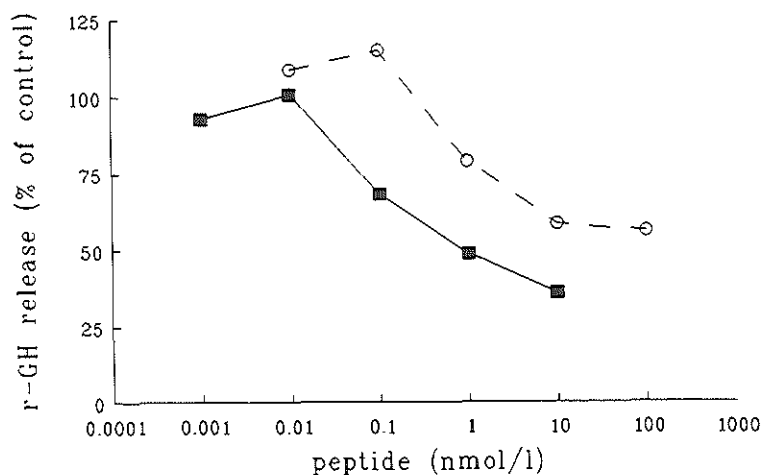


**Figure 5**

*Effects of unlabeled octreotide (■) and [DTPA-D-Phe¹]-octreotide (○) on the secretion of rat growth hormone by cultured rat pituitary cells (maximal SEM < 10%).*

## DISCUSSION

The radiolabeling of [DTPA-D-Phe¹]-octreotide with  $^{111}\text{In}$  is an easy single-step procedure with high yields (> 95 %) which does not require special equipment. However, ultrapure  $^{111}\text{InCl}_3$  is required for an efficient labeling, since contaminating metals, which might be present in some preparations in unknown quantities, compete with  $^{111}\text{In}$ . The use of the highest possible specific activity is therefore recommended. It is not surprising that the disulfide-containing peptide, if radiolabeled to high specific radioactivity, is susceptible to radiation damage. This results in the generation of compounds with shorter retention times on HPLC, which may represent degradation products of [ $^{111}\text{In}$ -DTPA-D-Phe¹]-octreotide. Effective prevention of radiolytic deterioration by dilution or by addition of scavengers allow the use of [ $^{111}\text{In}$ -DTPA-D-Phe¹]-octreotide up to several hours after labeling without further purification. Because of the fact, that somatostatin binding sites are very well characterized in rat brain cortex membranes (13), this system was used for binding studies. The results of the binding studies demonstrate that [ $^{111}\text{In}$ -DTPA-D-Phe¹]-octreotide is a high affinity, selective radioligand for somatostatin receptors, although its affinity is less than that of [ $^{125}\text{I}$ -Tyr³]-octreotide. Complexing of [DTPA-D-Phe¹]-octreotide with indium increased the affinity for the somatostatin receptor compared with the unlabeled compound. Rat

growth hormone inhibition experiments showed a similar biologic effect with unlabeled [DTPA-D-Phe<sup>1</sup>]-octreotide and <sup>111</sup>In-labeled [DTPA-D-Phe<sup>1</sup>]-octreotide, although it was less than with octreotide. However, in the accompanying paper it will be shown, that this new radiopharmaceutical has a completely different, but more suitable metabolic and pharmacokinetic behaviour. Its renal clearance without degradation in vivo contrasts to the hepato-biliary clearance of [<sup>123</sup>I-Tyr<sup>3</sup>]-octreotide and subsequent degradation in vivo (4, 14, 15). Because of the longer physical half-life of <sup>111</sup>In (2.8 days) and consequent easy availability [<sup>111</sup>In-DTPA-D-Phe<sup>1</sup>]-octreotide can be used everywhere. This also contrasts with the previously used <sup>123</sup>I, which has a half-life of 13.2 hr. An additional advantage of the longer physical half-life of <sup>111</sup>In is that gamma camera imaging will be improved later than 24 hr after injection. In the presence of an appropriate quencher [<sup>111</sup>In-DTPA-D-Phe<sup>1</sup>]-octreotide is very well suited for preparation in a "kit" procedure and may be used several hours after the labeling procedure. [<sup>111</sup>In-DTPA-D-Phe<sup>1</sup>]-octreotide, therefore, is a promising radiopharmaceutical for routine in vivo imaging of somatostatin receptor-positive tumors in animals and man.

## ACKNOWLEDGEMENTS

We wish to thank Christine Bourquin, Peter van Koetsveld, Marcel van der Pluijm, Michiel de Roo and Joke Zuyderwijk for their excellent technical help.

## REFERENCES

1. Lamberts SWJ, Krenning EP, Klijn JGM, and Reubi JC. The clinical use of somatostatin analogues in the treatment of cancer. *Baillière's Clinical Endocrinology and Metabolism* 1987, vol 4, no. 1: 29-49.
2. Lamberts SWJ, Hofland LJ, Van Koetsveld PM, Reubi JC, Bruining HA, Bakker WH, and Krenning EP. Parallel in vivo and in vitro detection of functional somatostatin receptors in human endocrine pancreatic tumors: consequences with regard to diagnosis, localization, and therapy. *J Clin Endocrinol Metab* 1990; 71: 566-574.
3. Reubi JC, Häcki WH, and Lamberts SWJ. Hormone-producing gastrointestinal tumours contain high density of somatostatin receptors. *J Clin Endocrinol Metab* 1987; 65: 1127-1134.
4. Bakker WH, Krenning EP, Breeman WAP, Koper JW, Kooij PP, Reubi JC, Klijn JG, Visser TJ, Docter R, and Lamberts SW. Receptor scintigraphy with a radioiodinated somatostatin analogue: Radiolabeling, purification, biological activity and in vivo application in animals. *J Nucl Med* 1990; 31: 1501 - 1509.

5. Krenning EP, Bakker WH, Breeman WAP, Koper JW, Kooij PPM, Ausema L, Laméris JS, Reubi JC, and Lamberts SWJ. Localisation of endocrine-related tumours with radioiodinated analogue of somatostatin. *Lancet* 1989; 1: 242-244.
6. Hnatowich DJ, Layne WW, Childs RL, Lanteigne D, Davis MA, Griffin TW, and Doherty PW. Radiolabeling of antibody: a simple and efficient method. *Science* 1983; 220: 613-615.
7. Bauer W, Briner U, Doeppner W, Haller R, Huguenin R, Marbach P, Petcher TJ, and Pless J. SMS 201-995: A very potent and selective octapeptide analogue of somatostatin with prolonged action. *Life Sci* 1982; 31: 1133-1140.
8. Reubi JC, Perrin MH, Rivier JE, and Vale W. High affinity binding sites for a somatostatin-28 analog in rat brain. *Life Sci* 1981; 28: 2191-2198.
9. De Lean A. Ph.D. Thesis, Howard Hughes Medical Institute, Duke University, NC U.S.A. (1979).
10. Hofland LJ, Van Koetsveld PM, Verleun TM, and Lamberts SWJ. Long-term culture of rat mammotrope and somatotrope subpopulations separated on continuous Percoll density gradients: Effects of dopamine, TRH, GHRH and somatostatin. *Acta Endocrinol* 1990; 122: 127-136.
11. Oosterom R, Verleun T, Zuijderwijk J, and Lamberts SWJ. Growth hormone secretion by cultured rat anterior pituitary cells. Effects of culture conditions and dexamethazone. *Endocrinology* 1983; 113: 735-741.
12. Bruns C, Dietl MM, Palacios JM, and Pless J. Identification and characterization of somatostatin receptors in neonatal rat long bones. *Biochem J* 1990; 265: 39-44 (1990).
13. Reubi JC. New specific radioligand for one subpopulation of brain somatostatin receptors. *Life Sci* 1985; 36: 1829-1836.
14. Bakker WH, Krenning EP, Breeman WA, Kooij PPM, Reubi JC, Koper JW, De Jong M, Laméris JS, Visser TJ, and Lamberts SW. In vivo use of a radioiodinated somatostatin analogue: Dynamics, Metabolism, and binding to somatostatin receptor-positive tumors in man. *J Nucl Med* 1991; 32: 1184-1189.
15. Bakker WH, Krenning EP, Reubi JC, Breeman WAP, Setyono-Han B, De Jong M, Kooij PPM, Bruns C, Van Hagen PM, Marbach P, Visser TJ, Pless J, and Lamberts SWJ. *Life Sci* 1991; 49: 1593-1601.



## CHAPTER 5

### **In vivo application of [<sup>111</sup>In-DTPA-D-Phe<sup>1</sup>]-octreotide for detection of somatostatin receptor-positive tumors in rats**

W.H. Bakker, E.P. Krenning, J.-C. Reubi, W.A.P. Breeman, B. Setyono-Han,  
M. de Jong, P.P.M. Kooij, C. Bruns, P.M. van Hagen, P. Marbach,  
T.J. Visser, J. Pless, and S.W.J. Lamberts.

Departments of Nuclear Medicine and Internal Medicine III,  
University Hospital Dijkzigt and Erasmus University, Rotterdam,  
The Netherlands;

Sandoz Research Institute, Berne, Switzerland;

Division of Endocrine Oncology, Dr Daniel den Hoed Cancer Centre,  
Rotterdam, The Netherlands;

Department of Endocrinology, Sandoz Pharma AG, Basel, Switzerland

### **Summary**

Radioiodinated somatostatin analogues are useful ligands for the in vitro and in vivo detection of somatostatin receptors. [<sup>111</sup>In-DTPA-D-Phe<sup>1</sup>]-octreotide, a somatostatin analogue labeled with a different radionuclide, also binds specifically to somatostatin receptors in vitro. In this study we investigated its in vivo application in the visualization of somatostatin receptor-positive tumors in rats. The distribution of the radiopharmaceutical was investigated after intravenous injection in normal rats and in rats bearing the somatostatin receptor-positive rat pancreatic carcinoma CA 20948. After injection the radiopharmaceutical was rapidly cleared (50 % decrease in maximal blood radioactivity in 4 min), predominantly by the kidneys. Excreted radioactivity was mainly in the form of the intact radiopharmaceutical. Ex vivo autoradiographic studies showed that specific accumulation of radioactivity occurred in somatostatin receptor-containing tissue (anterior pituitary gland). However, in contrast to the adrenals and pituitary, the tracer accumulation in the kidneys was not mediated by somatostatin receptors. Increasing radioactivity over the somatostatin

receptor-positive tumors was measured rapidly after injection and the tumors were clearly visualized by gamma camera scintigraphy. In rats pretreated with 1 mg octreotide accumulation of [ $^{111}\text{In}$ -DTPA-D-Phe $^1$ ]-octreotide in the tumors was prevented. Because of its relatively long effective half-life, [ $^{111}\text{In}$ -DTPA-D-Phe $^1$ ]-octreotide is a radionuclide-coupled somatostatin analogue which can be used to visualize somatostatin receptor-bearing tumors efficiently after 24 hr, when interfering background radioactivity is minimized by renal clearance. This is an advantage over the previously used [ $^{125}\text{I}$ -Tyr $^3$ ]-octreotide which has a shorter effective half-life and shows high abdominal interference due to its hepato-biliary clearance. Therefore, [ $^{111}\text{In}$ -DTPA-D-Phe $^1$ ]-octreotide seems a better alternative for scintigraphic imaging of somatostatin receptor-bearing tumors.

Radioiodinated analogues have been used extensively in the detection of somatostatin receptors in vitro (1). Recently one of these analogues, [ $^{125}\text{I}$ -Tyr $^3$ ]-octreotide, intravenously administered, was shown to visualize somatostatin receptor-positive tumors in vivo by means of gamma camera scintigraphy (2, 3, 4). However, because of a number of drawbacks of this radioiodinated compound, such as its short effective half-life in the blood circulation and high background radiation in the abdominal region, a search was made for an alternative somatostatin analogue, which could be labeled with a different radionuclide,  $^{111}\text{In}$ . Predominant advantages of  $^{111}\text{In}$  over  $^{125}\text{I}$  (half-life 13.2 hr) are its ready availability as well as its attractive physical properties, such as 173 keV and 246 keV gamma radiation, appropriate for scintigraphy, and half-life of 2.8 d, enabling scintigraphy at longer intervals after injection. Therefore, the somatostatin analogue [DTPA-D-Phe $^1$ ]-octreotide has been synthesized and the specific binding properties of this peptide, labeled with  $^{111}\text{In}$ , to somatostatin receptors have been demonstrated (5).

## MATERIALS AND METHODS

### *Somatostatin analogues*

Somatostatin analogues [DTPA-D-Phe $^1$ ]-octreotide (SDZ 215-811), [Tyr $^3$ ]-octreotide (SDZ 204-090) and octreotide (SMS 201-995) were obtained from Sandoz (Basle, Switzerland). Radiolabeling of [Tyr $^3$ ]-octreotide and [DTPA-D-Phe $^1$ ]-octreotide with respectively  $^{125}\text{I}$  and  $^{111}\text{In}$  and consecutive quality control were performed as described before (3, 5). The radiochemical purity of the radiolabeled somatostatin analogues [ $^{125}\text{I}$ -Tyr $^3$ ]-octreotide and [ $^{111}\text{In}$ -DTPA-D-Phe $^1$ ]-octreotide was greater than 95 %.

## *Animals and tumors*

Nine male Lewis rats were inoculated in both upper left- and right hindlegs with the transplantable rat pancreatic tumor CA 20948, which was previously shown to possess somatostatin receptors (6). The growth of this tumor is inhibited by octreotide treatment (7). All conditions were as described before (3). Twelve control animals were studied in parallel. The tumor-bearing animals were divided into two groups: (a) 4 animals without pretreatment and (b) 5 animals which were pretreated subcutaneously with 1 mg octreotide, 30 min before injection of the radiopharmaceutical. All tumor-bearing animals and 10 control animals, used for gamma camera scintigraphy and tissue radioactivity measurements, received 18.5 MBq (0.5 - 1  $\mu$ g) [ $^{111}\text{In}$ -DTPA-D-Phe $^1$ ]-octreotide in 0.5 - 0.8 ml 154 mM NaCl intravenously via the dorsal vein of the penis. Two control animals used for ex vivo autoradiography received 74 MBq (1  $\mu$ g) [ $^{111}\text{In}$ -DTPA-D-Phe $^1$ ]-octreotide. For injection and scintigraphy the animals were anaesthetized with ether.

## *Data acquisition and analysis*

The gamma camera and computer system were as described before (3). A medium-energy parallel-hole collimator was used. The analyzer was set to both  $^{111}\text{In}$  peaks: 173 keV and 246 keV, window 20 %. Dynamic acquisition took place in 1 min intervals during the first 30 min after injection of [ $^{111}\text{In}$ -DTPA-D-Phe $^1$ ]-octreotide. For the disappearance of radioactivity from the blood the percentage of the injected dose measured over the heart area was calculated. The renal excretion during the first 30 min after injection, measured over the kidneys together with the bladder, was also calculated as percentage of the injected dose. Over less well-defined regions such as tumor, head and lower right hindleg fixed areas were chosen in which the time course of radioactivity was expressed relative to that measured during the first min immediately after injection. Static images were obtained 30 min, 4 hr and 24 hr after injection. On the basis of the static digital images of the animals and proper standards, estimates were made of whole body, kidney and tumor retentions. The 24-hr results of the gamma camera measurements were compared with determinations of radioactivity in isolated tissues using a semi-conductor (GeLi) detector connected to a multichannel analyzer (Series 40, Canberra). The distance to the detector was 20 cm. The uptake of the radionuclide was calculated as a percentage of the dose and as a percentage of the dose/gram tissue. Urine samples of four different control rats were obtained 30 min, 2 hr and 24 hr after injection of [ $^{111}\text{In}$ -DTPA-D-Phe $^1$ ]-octreotide for analysis by high performance liquid chromatography (HPLC) as previously described (5). For this purpose urine samples were diluted 1:10 in HPLC solvent, i.e. 40 % methanol in 0.05 M acetate buffer, pH 5.5, and applied to the  $\text{C}_{18}$  column.

Two control animals were perfused with 100 ml 2.5 % glutaraldehyde solution 2 hr, respectively 24 hr after injection of the radiopharmaceutical. Kidneys and

pituitaries were isolated and cut with a cryostat (Leitz, Wetzlar, Germany) or a freezing microtome (Jung, Heidelberg, Germany) into 10 - 15  $\mu\text{m}$  thick sections. The sections were then apposed to [ $^3\text{H}$ ]-LKB ultrafilm as described previously (8). Kidneys of control rats were tested for the presence of somatostatin receptors by means of in vitro receptor autoradiography using [ $^{125}\text{I}$ -Tyr $^3$ ]-octreotide as ligand (1).

The statistical significance of differences was determined with Student's t-test or by analysis of variance. Differences were considered significant if  $p < 0.05$ . All data are reported as mean  $\pm$  SD.

## RESULTS

[ $^{111}\text{In}$ -DTPA-D-Phe $^1$ ]-octreotide is rapidly cleared from the blood as is indicated by the decreasing radioactivity above the heart area (Fig. 1). During the fifth min after injection radioactivity over the heart had decreased to 50 % of that during the first min. Dynamic gamma camera observations show that the radionuclide is cleared almost exclusively via the kidneys. Already 4 min after injection radioactivity appears in the bladder. Also in Fig. 1 the renal activity together with the excretion of the radionuclide in the bladder, is presented as a function of time. In control rats about 50 % of the injected dose had already been cleared within 30 min via the kidneys, whereas in tumor-bearing rats this clearance was significantly slower ( $p < 0.05$ ).

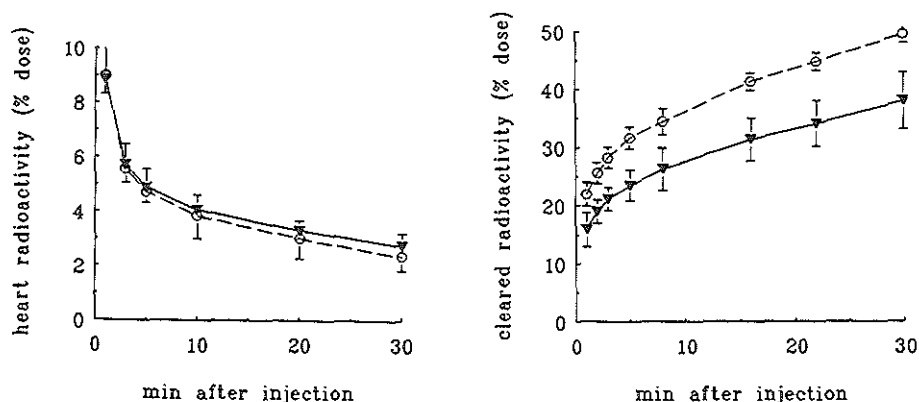


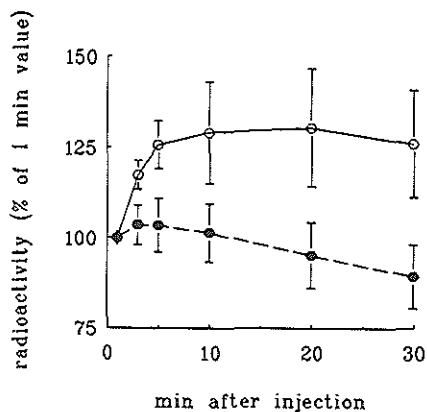
**Figure 1**

*Disappearance of [ $^{111}\text{In}$ -DTPA-D-Phe $^1$ ]-octreotide from the blood (left) expressed as mean  $\pm$  SD percentage of the administered dose measured over the heart area and renal clearance (right) expressed as mean  $\pm$  SD percentage of the administered dose measured over the kidneys and the bladder together in 4 control rats (○) and 9 tumor-bearing rats (▼).*



**Figure 2**

*Radioactivity as function of time, expressed as mean  $\pm$  SD percentage of the 1-min value, measured above 8 tumors in 4 untreated rats (  $\circ$  ) and 10 tumors in 5 rats, which were pretreated with 1 mg octreotide (  $\bullet$  ).*



Pretreatment with 1 mg octreotide did not influence blood clearance or renal clearance (data not shown). During the first 30 min after injection radioactivity measured above the head and lower right hindleg (without tumor) of all investigated animals showed decreasing blood pool radioactivity (data not shown). Increasing radioactivity was observed over the tumors of the animals immediately after injection, whereas this was not the case in the octreotide-pretreated group ( $p < 0.001$ , Fig. 2). Figure 3 presents static analogue images, 30 min and 24 hr after injection, of one untreated and one octreotide-pretreated animal. It is evident that the clear visualization of this transplantable pancreatic carcinoma (notably after 24 hr) was prevented by pretreatment with the high dose of unlabeled somatostatin analogue.

From digital static images obtained 24 hr after injection, whole body retention of radioactivity appeared to be about 10 % (Table I), which was mainly localized in the kidneys (7 %). This quantity closely parallels measurements in isolated kidneys using the semi-conductor detector (Table I). Radioactivity measured over the kidneys remained constant between 4 and 24 hr after injection. The presence of tumors did not significantly influence 24-hr kidney accumulation of radioactivity. Table I also gives the results of the measurements of radioactivity in the tumors with the gamma camera and the semi-conductor detector. In the tumors of the untreated animals significantly higher percentages of the injected dose were found in comparison with the tumors of the octreotide-pretreated group.

Results of radioactivity measurements in a number of tissues (of animals which were not pretreated with octreotide), isolated 24 hr after injection, are reported in Table II. The highest tissue radioactivity concentrations were found in the kidneys and the adrenals. There was no significant difference between radioactivity concentrations in most tissues of control and octreotide-pretreated animals. However, after pretreatment with octreotide the radioactivity concentrations were much lower in the adrenals and in the tumors.

30 min

24 hours

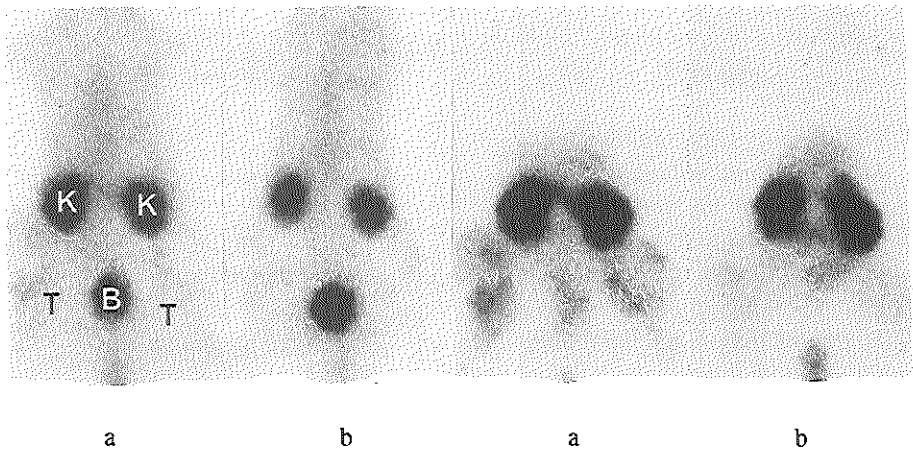


**Figure 3**

*Static images, 30 min and 24 hr after injection, of one untreated (a) and one octreotide-pretreated animal (b), showing accumulation in the kidneys (K) and/or urinary bladder (B). Accumulation of radioactivity in tumors (T) in both hindlegs is noted in a, not in b.*

Ex vivo autoradiography of the pituitary glands of control rats, obtained 2 and 24 hr after in vivo administration of [ $^{111}\text{In}$ -DTPA-D-Phe $^1$ ]-octreotide demonstrated accumulation of radioactivity in the anterior lobe but not in the posterior lobe (Fig. 4), confirming previous studies using in vitro or ex vivo autoradiography (9, 10). Interestingly, ex vivo autoradiography of kidney tissue of the same animals clearly showed the presence of radioactivity in the proximal tubules but not in the glomeruli (Fig. 5). However, with in vitro autoradiography using [ $^{125}\text{I}$ -Tyr $^{23}$ ]-octreotide as ligand, no specific somatostatin receptors were detected in the kidney (data not shown).

HPLC of a 30-min and a 2-hr urine sample of two different control rats showed that the excreted radioactivity was in the form of the intact [ $^{111}\text{In}$ -DTPA-D-Phe $^1$ ]-octreotide. Of two late urine samples obtained from control rats 24 hr after injection of the radiopharmaceutical (when most radioactivity already had been excreted, see Table I) more than 90 % of the radioactivity was not peptide-bound and eluted in the void volume, probably representing  $^{111}\text{In}$ -DTPA.

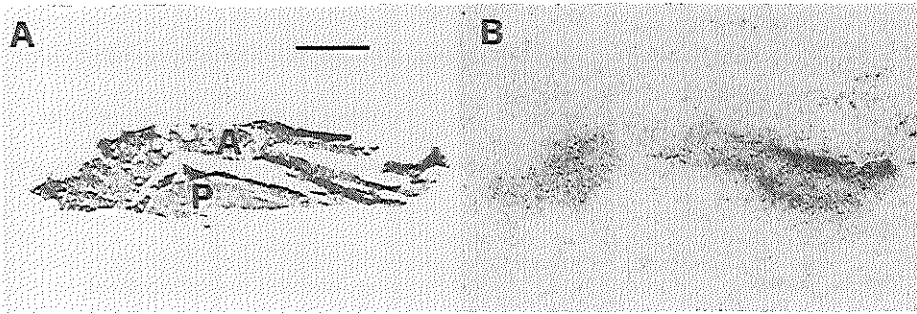


**Figure 4**

*Ex vivo autoradiography 24 hr after injection, showing the somatostatin receptors in the rat pituitary gland: A) hematoxylin-eosin stained section showing anterior (A) and posterior (P) pituitary gland. B) autoradiogram showing binding in the anterior pituitary but not in the posterior lobe. Bar=1 mm.*

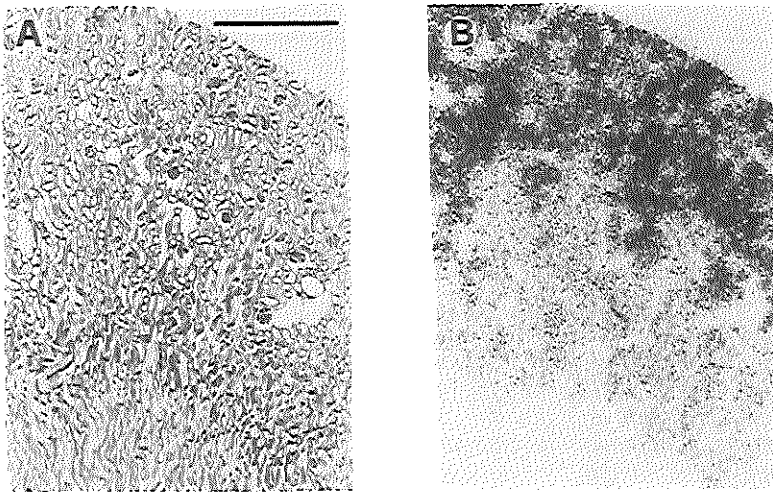


**Figure 5**

*Ex vivo autoradiography showing accumulation of [ $^{111}$ In-DTPA-D-Phe<sup>1</sup>]octreotide by the proximal tubules of the rat kidney (same animal and procedure as Fig. 4). A) Hematoxylin-eosin stained section. B) Autoradiogram showing dense labeling of the proximal tubules with sparing of the glomeruli. As discussed in the text the labeling does not represent receptor-bound ligand. Bar=1 mm.*

TABLE I

	Method	n	% dose at 4 hr	% dose at 24 hr
<u>Whole body</u>				
Control animals	A	2	15 ± 3	10 ± 1
Tumor-bearing animals	A	4	21 ± 2	13 ± 2
<u>Kidneys</u>				
Control animals	A	2	9 ± 1	7 ± 1
	B	6		6 ± 2
Tumor-bearing animals	A	4	8 ± 1	7 ± 1
	B	4		8 ± 1
<u>Tumor</u>				
Not pretreated <sup>a</sup>	A	8	1.6 ± 0.5	0.8 ± 0.3
	B	8		0.9 ± 0.4
Pretreated with octreotide <sup>b</sup>	A	10	0.6 ± 0.3 <sup>c</sup>	0.25 ± 0.28 <sup>c</sup>
	B	10		0.25 ± 0.08 <sup>c</sup>

Mean ± SD retention in the whole body, kidneys and tumor after the intravenous administration of [<sup>111</sup>In-DTPA-D-Phe<sup>1</sup>]-octreotide to control and tumor-bearing rats expressed as percentage of the dose, based on A) digital gamma camera images, and B) semi-conductor measurements of isolated tissues. <sup>a</sup>) Tumor mass (mean ± SD) 12 ± 5 gram; <sup>b</sup>) tumor mass 11 ± 4 gram. <sup>c</sup>) Significantly different (p < 0.001) from untreated rats).

## DISCUSSION

After injection of [<sup>111</sup>In-DTPA-D-Phe<sup>1</sup>]-octreotide the radionuclide disappears rapidly from the circulation. Blood clearance (measured over the heart) during the first 30 min was not noticeably influenced by octreotide-pretreatment nor by the presence of tumors. Gamma camera images indicate that radioactivity is mainly cleared by the kidneys and excreted with the urine into the bladder (Fig. 3). Total

TABLE II

Tissue	Control animals		Tumor-bearing animals	
	n=4		n=4	+ octreotide n=5
	% dose	% dose/gram	% dose/gram	% dose/gram
kidneys	6 ± 2	2.2 ± 0.6	2.5 ± 0.4	2.4 ± 0.7
liver	0.48 ± 0.05	0.041 ± 0.012	0.038 ± 0.003	0.039 ± 0.011
heart	0.011 ± 0.002	0.012 ± 0.002	0.012 ± 0.004	0.011 ± 0.001
intestines <sup>a</sup>	2.1 ± 0.4	0.13 ± 0.03	0.09 ± 0.02	0.09 ± 0.06
spleen	0.032 ± 0.010	0.06 ± 0.02	0.05 ± 0.03	0.06 ± 0.02
adrenals	0.08 ± 0.02	2.0 ± 0.4	2.2 ± 0.6	0.19 ± 0.04 <sup>b</sup>
lungs	0.028 ± 0.004	0.019 ± 0.003	0.015 ± 0.003	0.015 ± 0.003
thymus	< 0.01			
thyroid	< 0.01			
pituitary	< 0.01			
rest	1.1 ± 0.3	0.0049 ± 0.0010	0.005 ± 0.002	0.003 ± 0.001
blood		0.008 ± 0.001	0.030 ± 0.016	0.018 ± 0.007
urine		0.14 ± 0.04	0.18 ± 0.13	0.34 ± 0.58
tumors			0.09 ± 0.04	0.025 ± 0.008 <sup>b</sup>

Mean ± SD tissue distribution in rats 24 hr after intravenous administration of [<sup>111</sup>In-DTPA-D-Phe<sup>1</sup>]-octreotide, based on semi-conductor measurements of isolated tissues.

<sup>a</sup>) including pancreas

<sup>b</sup>) p < 0.001 vs untreated rats

renal excretion during the first 30 min after injection appeared to be lower in tumor-bearing rats than in control animals (Fig. 1), while the whole body retention at 24 hr after injection showed no significant difference (Table I). This suggests a decreased kidney function in tumor-bearing rats. The predominantly renal clearance of [<sup>111</sup>In-DTPA-D-Phe<sup>1</sup>]-octreotide contrasts with the (more rapid) hepatobiliary clearance of [<sup>123</sup>I-Tyr<sup>3</sup>]-octreotide as shown previously (3). With [<sup>111</sup>In-DTPA-D-Phe<sup>1</sup>]-octreotide 4 min are required to reduce blood radioactivity to 50 %, while [<sup>123</sup>I-Tyr<sup>3</sup>]-octreotide was cleared already by 50 % within 2 min. If it is presumed that this clearance already starts during the first min after injection, the difference in clearance rate between these radiopharmaceuticals might be even greater. Furthermore, in contrast to the <sup>123</sup>I-labeled somatostatin analogue, [<sup>111</sup>In-DTPA-D-Phe<sup>1</sup>]-octreotide is hardly metabolized and thus excreted intact.

Additionally, high radioactivity background levels interfering with scintigraphic detection in the abdominal region are not seen using [ $^{111}\text{In}$ -DTPA-D-Phe $^1$ ]-octreotide. Although initial renal clearance (during the first 30 min, Fig. 1) is higher in control animals, whole body retention of radioactivity after 24 hr is not significantly different between control and tumor-bearing rats, demonstrating that the presence of tumors does not noticeably influence the cumulative excretion. Renal retention after 24 hr was also not influenced by octreotide-pretreatment, suggesting that this process is not mediated via specific somatostatin receptors. Although the proximal tubules of the kidney showed accumulation of  $^{111}\text{In}$  as demonstrated by ex vivo autoradiography of kidneys from untreated control rats which were injected with [ $^{111}\text{In}$ -DTPA-D-Phe $^1$ ]-octreotide 2 and 24 hr before sacrifice, no somatostatin receptors were detected with in vitro autoradiography of the kidney with the somatostatin analogue [ $^{125}\text{I}$ -Tyr $^3$ ]-octreotide. We hypothesize therefore, that accumulation of [ $^{111}\text{In}$ -DTPA-D-Phe $^1$ ]-octreotide in the kidney occurs by fixation in the proximal tubules during reabsorption after glomerular filtration or during tubular excretion via the proximal tubules.

During the first 30 min studied, decreasing radioactivity was measured over the heads and lower hindlegs of all animals, reflecting the disappearance of radionuclide from the blood pool. However, over the tumors of the untreated animals radioactivity increased significantly, while the tumors of the octreotide-pretreated animals only showed decreasing blood pool activity. It should be realized that the increasing radioactivity over the tumors in the untreated animals is the sum of increasing receptor binding and decreasing blood pool radioactivity. The latter component masks the increase in specific tumor accumulation. Therefore, specific tumor accumulation increases even more sharply than depicted in Fig. 2. Measurements after 4 and 24 hr demonstrated significantly higher accumulation of  $^{111}\text{In}$  in tumors of untreated animals than in the octreotide-pretreated rats, suggesting binding to the somatostatin receptors of these tumors (Table I). These findings are confirmed by gamma camera scintigraphy after 24 hr (Fig. 3).

Furthermore, specific accumulation of [ $^{111}\text{In}$ -DTPA-D-Phe $^1$ ]-octreotide is shown in somatostatin receptor-positive tissues, such as the adrenals (8) and the anterior lobe of the pituitary gland (9), by counting of isolated organs and/or autoradiography, confirming the specificity of [ $^{111}\text{In}$ -DTPA-D-Phe $^1$ ]-octreotide as a radioligand for somatostatin receptors. Their high numbers in the brain (9) however are not visualized, probably because the radioligand does not cross the blood-brain barrier.

## CONCLUSION

[ $^{111}\text{In}$ -DTPA-D-Phe $^1$ ]-octreotide which has been shown to bind to somatostatin receptors in vitro, accumulates in vivo specifically in somatostatin receptor-positive

normal tissues such as the adrenal and anterior pituitary gland. Similarly, somatostatin receptor-positive tumors accumulate the radiopharmaceutical specifically and can be visualized by gamma camera scintigraphy.

Compared with the previously used somatostatin analogue [ $^{125}\text{I}$ -Tyr $^3$ ]-octreotide, the combination of the longer residence of [ $^{111}\text{In}$ -DTPA-D-Phe $^1$ ]-octreotide in the circulation, its longer physical half-life (2.8 d versus of 13 hr) and the absence of hepato-biliary metabolism (with consequent interfering radioactivity in this region) makes this compound very suitable for imaging of somatostatin receptor-positive tumors in rats. Tumor/background ratios were highest 24 hr after administration when interfering blood pool radiation was minimal. These properties suggest that [ $^{111}\text{In}$ -DTPA-D-Phe $^1$ ]-octreotide is also a very useful radiopharmaceutical for scintigraphic imaging of somatostatin receptor-positive tumors in man.

## ACKNOWLEDGEMENTS

The authors wish to thank Fred Bonthuis, Ursula Horisberger, Ina Loeve, Marcel van der Pluijm and Beatrice Waser for their expert assistance during the experiments.

## REFERENCES

1. Reubi JC, Häcki WH, and Lamberts SWJ. Hormone-producing gastrointestinal tumours contain high density of somatostatin receptors. *J Clin Endocrinol Metab* 1987; 65: 1127-1134.
2. Krenning EP, Bakker WH, Breeman WAP, et al. Localisation of endocrine-related tumours with radioiodinated analogue of somatostatin. *Lancet* 1989; 1: 242-244.
3. Bakker WH, Krenning EP, Breeman WAP, Koper JW, Kooij PP, Reubi JC, Klijn JG, Visser TJ, Docter R, and Lamberts SW. Receptor scintigraphy with a radioiodinated somatostatin analogue: Radiolabeling, purification, biological activity and in vivo application in animals. *J Nucl Med* 1990; 31: 1501 - 1509.
4. Bakker WH, Krenning EP, Breeman WA, Kooij PPM, Reubi JC, Koper JW, De Jong M, Laméris JS, Visser TJ, and Lamberts SW. In vivo use of a radioiodinated somatostatin analogue: Dynamics, Metabolism, and binding to somatostatin receptor-positive tumors in man. *J Nucl Med* 1991; 32: 1184-1189.
5. Bakker WH, Albert R, Bruns C, Breeman WAP, Hofland LJ, Marbach P, Pless J, Pralet D, Stolz B, Koper JW, Lamberts SWJ, Visser TJ, and Krenning EP. [ $^{111}\text{In}$ -DTPA-D-Phe $^1$ ]-octreotide, a potential radiopharmaceutical for imaging of somatostatin receptor-positive tumors: Synthesis, radiolabeling

- and in vitro validation. *Life Sci* 1991; 49: 1583-1591.
6. Reubi JC, Horisberger U, Essed CE, Jeekel J, Klijn JGM, Lamberts SWJ. Absence of somatostatin receptors in human exocrine pancreatic adenocarcinomas. *Gastroenterology* 1988; 95: 760-763.
  7. Klijn JGM, Setyono-Han B, Bakker GH, Portengen H, Foekens JA. Prophylactic neuropeptide-analog treatment of a transplantable pancreatic tumor in rats. In: Bresciani F, King RJB, Lippman ME, Raynaud JP, eds. *Progress in cancer research and therapy, Volume 35. Hormones and Cancer 3*. New York, Raven Press; 1988: 550-553.
  8. Maurer R, Reubi JC. Somatostatin receptors in the adrenal. *Molec Cell Endocrinol* 1986; 45: 81-90.
  9. Reubi JC, Maurer R. Autoradiographic mapping of somatostatin receptors in the rat central nervous system and pituitary. *Neuroscience* 1985; 15: 1183-1193.
  10. Reubi JC, Kvols L, Krenning E, and Lamberts SWJ. Distribution of somatostatin receptors in normal and tumor tissue. *Metabolism* 1990; 39 (Suppl 2): 78-81.



## CHAPTER 6

### **Somatostatin receptor scintigraphy with [<sup>111</sup>In-DTPA-D-Phe<sup>1</sup>]-octreotide in man: metabolism, dosimetry and comparison with [<sup>123</sup>I-Tyr<sup>3</sup>]-octreotide**

E.P. Krenning, W.H. Bakker, P.P.M. Kooij, W.A.P. Breeman, H.Y. Oei,  
M. de Jong, J.C. Reubi, T.J. Visser, C. Bruns, D.J. Kwekkeboom,  
A.E.M. Reijs, P.M. van Hagen, J.W. Koper, and S.W.J. Lamberts.

Departments of Nuclear Medicine and Internal Medicine III, University Hospital  
Dijkzigt, Rotterdam, The Netherlands; Sandoz Research Institute, Berne and  
Department of Endocrinology, Sandoz Pharma AG, Basel, Switzerland.

Scintigraphy with [<sup>123</sup>I-Tyr<sup>3</sup>]-octreotide has several major drawbacks as regards its metabolic behaviour, its cumbersome preparation and the short physical half-life of the radionuclide. The use of another radiolabeled analogue of somatostatin, [<sup>111</sup>In-DTPA-D-Phe<sup>1</sup>]-octreotide, has consequently been proposed. [DTPA-D-Phe<sup>1</sup>]-octreotide can be radiolabeled with <sup>111</sup>In in an easy single-step procedure. [<sup>111</sup>In-DTPA-D-Phe<sup>1</sup>]-octreotide is cleared predominantly via the kidneys. Fecal excretion of radioactivity amounts to only a few percent of the administered radioactivity. With regard to the radiation dose of normal tissues, the most important organs are the kidneys, the spleen, the urinary bladder, the liver and the remainder of the body. The calculated effective dose equivalent is 0.08 mSv/MBq. Optimal [<sup>111</sup>In-DTPA-D-Phe<sup>1</sup>]-octreotide scintigraphic imaging of various somatostatin receptor-positive tumors was obtained 24 hr after injection. In the six patients studied, tumor localization with [<sup>123</sup>I-Tyr<sup>3</sup>]-octreotide and with [<sup>111</sup>In-DTPA-D-Phe<sup>1</sup>]-octreotide were found to be similar. However, the normal pituitary is more frequently visualized with the latter radiopharmaceutical. In conclusion, [<sup>111</sup>In-DTPA-D-Phe<sup>1</sup>]-octreotide appears to be a sensitive somatostatin receptor-positive tissue-seeking radiopharmaceutical with some remarkable advantages: easy preparation, general availability, appropriate half-life and absence of major interference in the upper abdominal region, because of its renal clearance. Therefore [<sup>111</sup>In-DTPA-D-Phe<sup>1</sup>]-octreotide is very suitable for use in SPECT of the abdomen, which is especially of importance in the localization of small endocrine gastroenteropancreatic tumors.

Recently we introduced the somatostatin analogue [Tyr<sup>3</sup>]-octreotide labeled with <sup>123</sup>I for the localization of primary and metastatic somatostatin receptor-rich tumors, such as carcinoids, islet cell tumors of the pancreas, paragangliomas and small cell carcinomas of the lungs (1-4). Our experience points to several drawbacks of [<sup>123</sup>I-Tyr<sup>3</sup>]-octreotide in its use for *in vivo* scintigraphy. First, the labeling of [Tyr<sup>3</sup>]-octreotide with <sup>123</sup>I is cumbersome and requires special skills. Second, Na<sup>123</sup>I of high specific activity (5,6) is expensive and hardly available world-wide. Third, the moment of the labeling and scanning procedures is dependent on the logistics of the production and delivery of Na<sup>123</sup>I. Finally, substantial accumulation of radioactivity is seen in the intestines, since a major part of [<sup>123</sup>I-Tyr<sup>3</sup>]-octreotide is rapidly cleared via the liver and biliary system. This makes the interpretation of planar and single photon emission computed tomographic (SPECT) images of the upper abdomen difficult.

Part of these problems can be solved by replacing <sup>123</sup>I with <sup>111</sup>In, which also improves scintigraphy 24 to 48 hr after application by virtue of its longer half-life. Binding of <sup>111</sup>In to the somatostatin analogue octreotide has been carried out by complexing with a diethylenetriaminepentaacetic acid (DTPA) group coupled to the αNH<sub>2</sub>-group of the N-terminal D-Phe residue (7). In rats, it appeared that [<sup>111</sup>In-DTPA-D-Phe<sup>1</sup>]-octreotide 1) is excreted via the kidneys, 2) shows only minor accumulation in the liver, and 3) has an initial plasma half-life in the order of minutes (8).

In this study we report data concerning the metabolism of intravenously administered [<sup>111</sup>In-DTPA-D-Phe<sup>1</sup>]-octreotide in man, as well as estimates of its radiation dose in principal organs and the effective dose equivalent. Also, scintigraphic images of various somatostatin receptor-positive tumors have been compared using both [<sup>123</sup>I-Tyr<sup>3</sup>]-octreotide and [<sup>111</sup>In-DTPA-D-Phe<sup>1</sup>]-octreotide as radiopharmaceuticals in the same patients.

## MATERIALS AND METHODS

### *Radiopharmaceuticals*

The somatostatin derivatives [DTPA-D-Phe<sup>1</sup>]-octreotide (SDZ 215-811) and [Tyr<sup>3</sup>]-octreotide (SDZ 204-090) were prepared by Sandoz (Basel, Switzerland). <sup>111</sup>InCl<sub>3</sub> ("ultra-pure") and Na<sup>123</sup>I were obtained from Mallinckrodt Diagnostica (Petten, The Netherlands) and Medgenix (Fleurus, Belgium), respectively. <sup>111</sup>InCl<sub>3</sub> contained <sup>114m</sup>In to a limited extent (0.5 kBq <sup>114m</sup>In/MBq <sup>111</sup>In at calibration time). Radiolabeling of [DTPA-D-Phe<sup>1</sup>]-octreotide with <sup>111</sup>In and of [Tyr<sup>3</sup>]-octreotide with <sup>123</sup>I and quality control of the products were performed as described before (5-8). Depending on the interval between injection and scintigraphy, and whether SPECT was required, the administered radioactivity of [<sup>111</sup>In-DTPA-D-Phe<sup>1</sup>]-octreotide and of [<sup>123</sup>I-Tyr<sup>3</sup>]-octreotide ranged from 185 to 259 MBq and from 370

to 555 MBq, respectively, given as an intravenous bolus. The dose of the somatostatin analogues administered varied from 7 to 20  $\mu\text{g}$  per injection.

### *Imaging*

Planar and SPECT images were obtained with a large field of view gamma camera (Counterbalance 3700 and ROTA II, Siemens, Hoffman Estates, Ill), equipped with a medium-energy parallel-hole collimator. The pulse height analyzer windows were centered over both  $^{111}\text{In}$  photon peaks (172 keV and 245 keV) with a window width of 20 %. Data from both windows were added to the acquisition frames. The camera was connected to a dedicated PDP 11/73 computer (Digital Equipment Corp., Maynard, Ma.) using the Gamma 11 and SPETS V 6.1 software (Nuclear Diagnostics, Stockholm, Sweden). The acquisition parameters were for planar images 1) 128 x 128 word matrix, 2) images of head/neck: 300,000 preset counts (or max. 15 min) at 24 hr and 15 min preset time ( $\approx$ 200,000 counts) at 48 hr after injection, 3) images of the rest of the body: 500,000 counts (or max. 15 min), and for SPECT 1) 60 projections, 2) 64 x 64 word matrix, 3) 60 second acquisition time per projection. SPECT analysis was performed with a Wiener filter on original data. The filtered data were reconstructed with a Ramp filter. If indicated, SPECT studies were performed 4 hr (head and neck) or 24 hr (remainder of the body) after injection of the radiopharmaceutical. Planar studies were carried out both after 24 hr and 48 hr (vide supra) and in a few cases also after 0.5 hr and 4 hr with the same protocol as for the 24 hr studies. Total body scintigraphy (scintigraphy of extremities only if indicated) of every patient was performed at least once, in general 24 hr after injection.

### *Measurement of $^{111}\text{In}$ radioactivity in blood, urine and feces*

Radioactivity in blood, urine and feces was measured with an LKB-1282-Compugamma system or a GeLi-detector equipped with a multi-channel analyser (Series 40, Canberra).

Blood samples were collected directly before the injection and 2, 5, 10, 20 and 40 min and 1, 4, 20 and 48 hr after injection. Urine was collected from the time of injection in two 3-hr intervals and thereafter in intervals of 6 hr until 48 hr after injection. If feasible, feces was collected until 72 hr after injection.

The chemical status of the radionuclide in blood and urine was analysed as a function of time by using the SEP-PAK  $\text{C}_{18}$ , HPLC and gel filtration techniques as described previously (5).

The nature of peptide-bound radioactivity in blood and urine was tested by investigation of specific binding to somatostatin receptors on rat brain cortex cell membranes as described previously (9).

## *Patients*

The data described in this paper were derived from patients which had been referred for a variety of potentially somatostatin receptor-positive tumors. All patients gave informed consent to participate in the study, which had been approved by the ethics committee of our hospital. Kinetic studies with [ $^{111}\text{In}$ -DTPA-D-Phe $^1$ ]-octreotide by means of gamma camera scintigraphy were performed in 26 patients. Additionally, plasma, urine and feces samples were obtained from 9, 10 and 4 patients, respectively. In another six patients we were able to perform somatostatin-analogue scintigraphy with [ $^{125}\text{I}$ -Tyr $^3$ ]-octreotide as well as with [ $^{111}\text{In}$ -DTPA-D-Phe $^1$ ]-octreotide with a maximum interval of three months.

## *Dosimetry*

For the estimation of the radiation dose the MIRDose version 2 program (10) and ICRP publication 53 (11) were used. The uptakes in the most important source organs, the kidneys, the spleen, the liver, the urinary bladder and the remainder of the body, were determined as a function of time. Radioactivity in the kidneys, liver and spleen was calculated as described before (6). Radioactivity in the urinary bladder was calculated using the measured radioactivity excreted in the urine and assuming a bladder voiding interval of 3.5 hr (11). Radioactivity in the remainder of the body (expressed as percentage of the administered radioactivity) as a function of time was determined as 100 % minus the % uptake in kidneys, liver, spleen, urinary bladder and excreted radioactivity in urine and feces.

In 8 patients the uptake in the kidneys, spleen and liver was measured with the gamma camera 0.5, 4, 24 and 48 hr after injection of [ $^{111}\text{In}$ -DTPA-D-Phe $^1$ ]-octreotide. The results obtained in two patients could not be used because of an extensive overlap of the right kidney and the liver. In the 6 remaining patients the excreted radioactivity in the urine (until 48 hr after [ $^{111}\text{In}$ -DTPA-D-Phe $^1$ ]-octreotide injection) was measured as well. In 4 patients the fecal excretion was also determined until 72 hr after injection. The calculation of the radiation dose in the GI tract was performed using the mean radioactivity detected in the feces of these 4 patients. The dose estimates of the various organs and the effective dose equivalent were calculated for each of the 6 patients individually.

In order to perform dosimetry when only gamma camera measurements were available 24 and 48 hr after [ $^{111}\text{In}$ -DTPA-D-Phe $^1$ ]-octreotide injection, a model was developed. In this model the residence times for the kidneys, spleen and liver were calculated for each individual patient on the basis of the organ uptakes after 24 and 48 hr. For the urinary bladder contents and the remainder of the body measurements, mean residence times were used. Using this model it was possible to calculate the dose estimates and the effective dose equivalent in another 18 patients. Apart from the organs mentioned above, radioactivity was seen in most patients in the thyroid gland and the pituitary as well.

## RESULTS

### Metabolism

The average plasma radioactivity decreased rapidly after injection of [ $^{111}\text{In}$ -DTPA-D-Phe $^1$ ]-octreotide in 9 patients. Assuming a plasma volume of 3 l, the mean radioactivity in the blood circulation was calculated to decrease within 10 min to  $33 \pm 7\%$  (s.d.) of the injected amount. In 5 patients the chemical status of the radionuclide in the plasma was investigated as a function of time. In Figure 1 the time courses of total and peptide-bound radioactivity in plasma of these 5 patients are presented until 20 hr after injection of [ $^{111}\text{In}$ -DTPA-D-Phe $^1$ ]-octreotide.

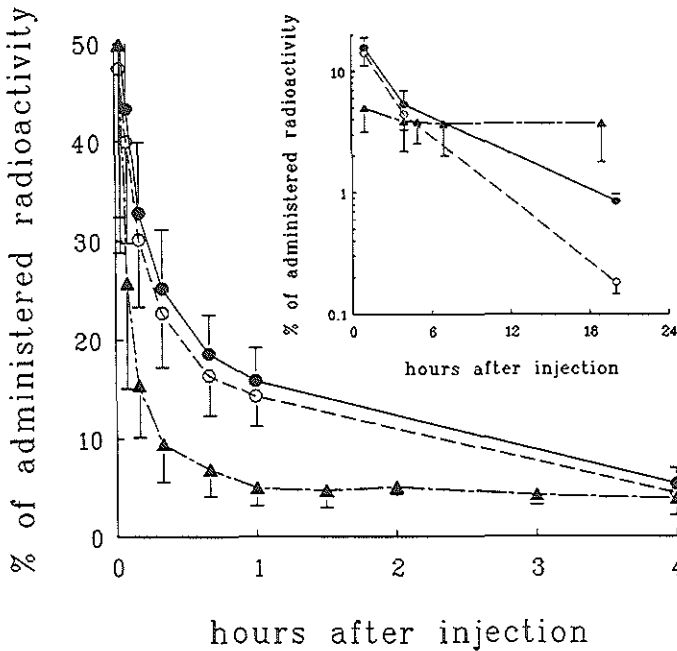


**Figure 1**

Total plasma ( $\bullet$ ) and peptide-bound ( $\circ$ ) radioactivity after administration of [ $^{111}\text{In}$ -DTPA-D-Phe $^1$ ]-octreotide in 5 patients. Results are compared with total plasma ( $\blacktriangle$ ) radioactivity after administration of [ $^{125}\text{I}$ -Tyr $^2$ ]-octreotide in 7 patients taken from ref. 6. Data are expressed as mean  $\pm$  s.d. percentage of the administered radioactivity. Note the logarithmic scale of values in the ordinate of the inset.

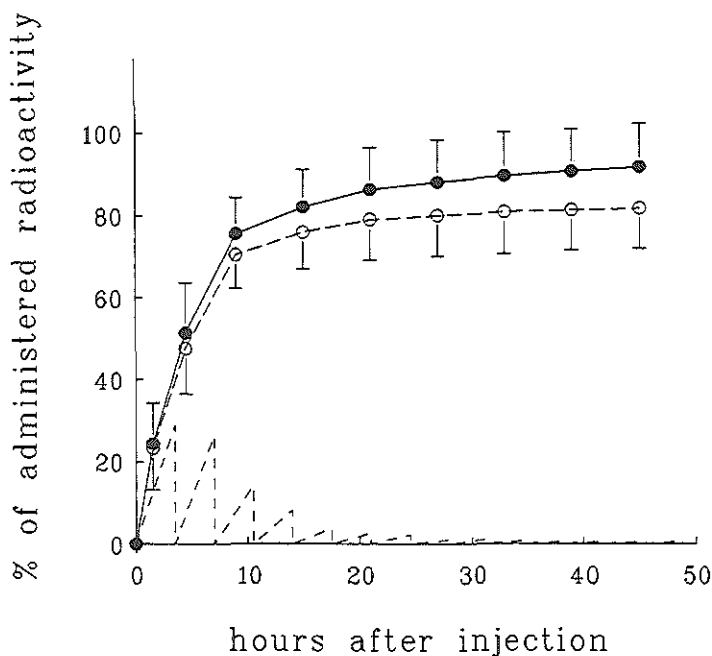


**Figure 2**

*Cumulative total (●) and peptide-bound (○)  $^{111}\text{In}$  urinary excretion ( $n=5$ ) and mean urinary bladder radioactivity voiding (----) ( $n=5$ ) after intravenous injection of [ $^{111}\text{In}$ -DTPA-D-Phe $^1$ ]-octreotide. Data are expressed as mean  $\pm$  s.d. percentage of the administered radioactivity.*

During the first 4 hr plasma radioactivity was mainly peptide-bound in the form of the intact [ $^{111}\text{In}$ -DTPA-D-Phe $^1$ ]-octreotide as demonstrated by HPLC. Only the last two points of the observation period showed proportionally increasing amounts of non-peptide-bound radioactivity, eluting in the void volume.

Urinary excretion of radioactivity was measured in 10 patients. In 5 of these patients the chemical status of the radionuclide in the urine was also investigated. Figure 2 shows in this group of 5 patients the rapid excretion of the administered radioactivity via the urine from about 25 % after 3 hr, 50 % after 6 hr, 85 % after 24 hr to over 90 % after 48 hr. Figure 2 also shows that in the 5 patients studied, excreted radioactivity was mainly peptide-bound. SEP-PAK and HPLC analyses of urine and plasma samples as functions of time after injection demonstrated that peptide-bound radioactivity predominantly consisted of [ $^{111}\text{In}$ -DTPA-D-Phe $^1$ ]-octreotide during the first hours after injection. Twenty-four hr after injection, in addition to [ $^{111}\text{In}$ -D-Phe $^1$ ]-octreotide and peptide-bound degradation products, a

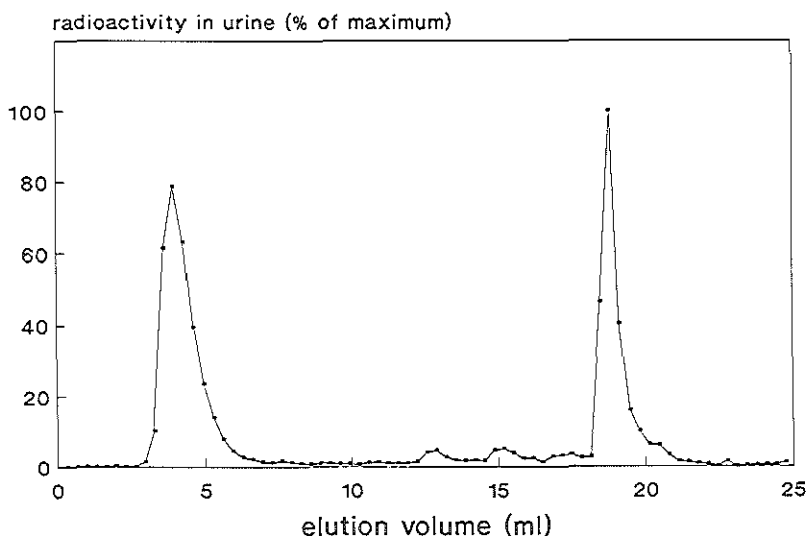


**Figure 3**

*Typical HPLC-elution profile of human urine, collected 24 hr after i.v. injection of [ $^{111}\text{In}$ -DTPA-D-Phe $^1$ ]-octreotide. At a retention volume of about 4 ml not peptide-bound  $^{111}\text{In}$ , such as  $^{111}\text{In}$ -DTPA is eluted, at 12-18 ml  $^{111}\text{In}$ -containing degradation products, and at about 19 ml the original radioligand.*

major part of urinary radioactivity eluted from the HPLC in the void volume (Figure 3).

Feces, collected until 72 hr after injection of [ $^{111}\text{In}$ -DTPA-D-Phe $^1$ ]-octreotide from 4 patients with a normal intestinal function, contained less than 2 % of the administered radioactivity.

The SEP-PAK  $\text{C}_{18}$  and HPLC-purified radiolabeled peptide component in plasma and urine showed the same biological activity as the radiopharmaceutical itself, as indicated by its specific binding to somatostatin receptors on rat brain cortex cell membranes (data not shown).

### **Dosimetry**

The uptake of radioactivity in the liver, spleen and kidneys was measured with the gamma camera in 6 patients. If the thyroid gland or the pituitary, or both, were clearly distinguishable from the surrounding tissue, the uptake in these organs was measured as well. Other organs (e.g. the intestines) showed low accumulations of radioactivity and were, therefore, disregarded in the gamma camera measure-

**Table 1**

*Radioactivity in selected organs and remainder of the body (mean  $\pm$  s.d.) as a function of time after intravenous administration of [ $^{111}\text{In}$ -DTPA-D-Phe<sup>1</sup>]-octreotide in man on the basis of gamma camera measurements and calculations respectively (see text) expressed as percentage of the administered radioactivity.*

Time (hr)	% Uptake				
	n	Liver	Spleen	Kidneys	Remainder of the body <sup>1</sup>
0.5	6	2.8 $\pm$ 1.2	2.0 $\pm$ 0.9	6.8 $\pm$ 1.3	84.2 $\pm$ 7.7
4	6	1.9 $\pm$ 0.4	2.4 $\pm$ 0.9	7.2 $\pm$ 1.8	46.7 $\pm$ 17.9
24	6	2.2 $\pm$ 0.6	2.6 $\pm$ 1.1	6.3 $\pm$ 2.1	8.7 $\pm$ 9.7
48	6	1.8 $\pm$ 0.4	1.8 $\pm$ 0.6	5.0 $\pm$ 2.0	7.2 $\pm$ 8.8
24	18	3.0 $\pm$ 1.3	2.9 $\pm$ 1.6	4.8 $\pm$ 1.7	
48	18	2.5 $\pm$ 1.0	2.1 $\pm$ 1.2	3.5 $\pm$ 1.3	

<sup>1</sup>The radioactivity in the remainder of the body is the administered radioactivity (100 %) minus the % radioactivity in liver, spleen, kidneys, urinary bladder, urine and feces.

ments. The time courses of radioactivity in the liver, spleen and kidneys showed close similarities between individual patients (data not shown). The results of the uptake measurements are given in Table 1. Five thyroid glands and two pituitaries in the group of 6 patients could be completely distinguished from the surrounding background (vide infra). The radioactivity in the thyroid gland (maximal 0.03 %) and the pituitary (maximal 0.003 %) varied strongly between individual patients. Frequently these organs were only visible on the 24 hr images. Therefore the residence time was calculated assuming that the effective half-life equals the physical half-life. The absorbed doses for the thyroid gland and the pituitary (12,13), corresponding to the maximum uptake measured in the group of 6 patients, are given in Table 2. Radioactivity excreted in the urine was used for the calculation of the residence time of the urinary bladder contents and showed for all patients the same course as the mean depicted in Figure 2. For all patients the radioactivity in the feces was taken to be the mean of the radioactivity measured in the 4 patients (0.5 % and 1.7 % after 24 and 48 hr, respectively). Even assuming that these maximum values occurred in the same patient, the contribution of the



thyroid gland, the pituitary and the feces to the effective dose equivalent was less than 5 % and could therefore be neglected. The dose estimates of the various organs and the effective dose equivalent were calculated for these 6 patients (data not shown).

The contribution to the absorbed dose caused by the  $^{114m}\text{In}$  contamination was calculated on the basis of the information obtained from the manufacturer and was found to be less than 0.5 % of the dose from  $^{111}\text{In}$ . In practice the radionuclide was administered before calibration time, thus even lowering the contribution of the  $^{114m}\text{In}$  to the radiation dose.

On the basis of the data obtained in the 6 patients, it appears that more than 70 % of the effective dose equivalent results from the radioactivity accumulated in the kidneys, spleen and liver. The uptake of radioactivity in these organs showed much greater individual variation in the 6 patients than the radioactivity excreted in the urine and the calculated uptake in the remainder of the body. Therefore, in the model employed, the uptake of radioactivity in the liver, kidneys and spleen is based on individual gamma camera measurements. Table 1 shows that in the group of 6 patients radioactivity in the spleen increases slightly from 0.5 to 24 hr and decreases afterwards in all patients. In the liver the radioactivity decreases rapidly during the first hour, thereafter an increase is measured until 24 hr, followed by a decrease. For the calculation of the residence time in the model, the radioactivity in the liver and the spleen was assumed to remain constant from 0 to 24 hr and to decrease after 24 hr mono-exponentially with time. Radioactivity in the kidneys shows a steady decrease (Table 1) starting shortly after the injection of the radiopharmaceutical. For this reason the calculation of the kidney residence time was based on a monoexponential curve. The initial uptake in the kidneys was calculated by extrapolating the uptakes at 24 and 48 hr to  $t=0$ . The periodic accumulation and discharge of radioactivity in the urinary bladder was calculated from the mean collected urinary radioactivity in 10 patients. There is no significant difference in the cumulative urinary radioactivity between these 10 and the 5 patients presented in Figure 2. The radioactivity in the remainder of the body was calculated by subtraction of the mean uptakes in the kidneys ( $n = 6$ ), spleen ( $n = 6$ ), liver ( $n = 6$ ), urinary bladder contents ( $n = 10$ ) and mean excreted radioactivity in urine ( $n = 10$ ) and feces ( $n = 4$ ) from the administered amount. The residence time in the remainder of the body could be determined by fitting a monoexponential curve to the radioactivity course after injection. The 6 patients were recalculated using the model described. There were statistically no significant differences in the dose estimates of the various organs and in the effective dose equivalent in comparison to the direct estimates for each individual (data not shown). Therefore, application of the model appeared to be valid.

In 18 patients the uptake in the kidneys, spleen and liver was measured after 24 and 48 hr. The results are given in Table 1. These data did not differ significantly from the values obtained at the same time points in the 6 patients. Consequently, the model was applied to the additional 18 patients. The final dosimetric results for

the complete group of 24 patients are shown in Table 2.

**Table 2**

*Dose estimates after intravenous administration of [ $^{111}\text{In}$ -DTPA-D-Phe $^1$ ]-octreotide in man on the basis of gamma camera measurements ( $n = 24$ ), measurements of urinary excretion ( $n = 10$ ) and measurements of fecal excretion ( $n = 4$ ). The input to the Small Intestines is taken to be the same as the fecal excretion during 72 hr ( $n=4$ ), viz 1.7 %. For the thyroid gland and the pituitary ( $n=6$ ) the radiation dose corresponds to the maximum organ uptake measured in these patients.*

Target organ	Absorbed dose (mGy/MBq)	Range (mGy/MBq)
Kidneys	0.45 <sup>MD</sup>	0.19 - 0.80
Liver	0.07 <sup>MD</sup>	0.04 - 0.15
Spleen	0.32 <sup>MD</sup>	0.10 - 0.66
Gonads	0.019 <sup>MD</sup>	0.015 - 0.026
Red Marrow	0.020 <sup>MD</sup>	0.016 - 0.026
Urinary bladder wall	0.18 <sup>MN</sup>	n.a. <sup>†</sup>
GI tract		
Small Intest. wall	0.03 <sup>MN,§</sup>	n.a. <sup>†</sup>
ULI wall	0.04 <sup>MN,§</sup>	n.a. <sup>†</sup>
LLI wall	0.06 <sup>MN,§</sup>	n.a. <sup>†</sup>
Thyroid gland	0.04 <sup>MX</sup>	
Pituitary	0.11 <sup>MX</sup>	
Median effective dose equivalent (mSv/MBq)		Range (mSv/MBq)
0.08		0.05 - 0.12

<sup>MD</sup> = median

<sup>MN</sup> = mean

<sup>MX</sup> = calculated for the maximum uptake

<sup>§</sup> ICRP 30 GI model used

<sup>†</sup> not applicable due to the model

*[<sup>123</sup>I-Tyr<sup>3</sup>]-octreotide and [<sup>111</sup>In-DTPA-D-Phe<sup>1</sup>]-octreotide scintigraphy: comparison in localization of tumor tissue*

A comparison between scintigraphy with [<sup>123</sup>I-Tyr<sup>3</sup>]-octreotide and scintigraphy with [<sup>111</sup>In-DTPA-D-Phe<sup>1</sup>]-octreotide, performed with an interval of less than 3 months in the same patients, is given in Table 3. In 4 out of 6 patients (patients 1-3, and 6) the results of the subsequent scintigrams were identical. In patient 2, [<sup>123</sup>I-Tyr<sup>3</sup>]-octreotide scintigraphy showed accumulation of radioactivity in the region of the gallbladder, which is not unusual for this radiopharmaceutical, consi-

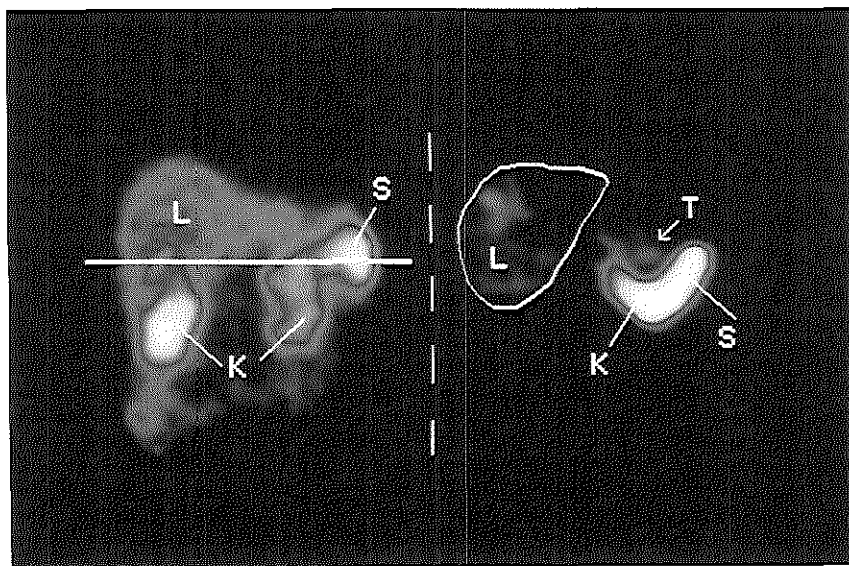


**Figure 4**

*[<sup>111</sup>In-DTPA-D-Phe<sup>1</sup>]-octreotide 24 hr SPECT image of a patient (no 3) with a solitary insulinoma in the tail of the pancreas, which is shown medial and anterior to the spleen and left kidney. The line on the reference image (left sided panel) indicates the position of the transversal slice (right sided panel). K = kidney, S = spleen, T = tumor and L = liver.*

dering its extensive biliary clearance. However, the same was observed with [<sup>111</sup>In-DTPA-D-Phe<sup>1</sup>]-octreotide, which is unusual, since this radiopharmaceutical is largely excreted by the kidneys. SPECT with [<sup>111</sup>In-DTPA-D-Phe<sup>1</sup>]-octreotide demonstrated a tumor located ventral to the gallbladder. In patient 3, SPECT images after [<sup>111</sup>In-DTPA-D-Phe<sup>1</sup>]-octreotide injection revealed the localization of the insulinoma, medial and anterior to the spleen and left kidney respectively (Figure 4). However, this localization had not been recognized on planar images

**Table 3**

*Patient data and results of somatostatin receptor scintigraphy, using the analogues [<sup>123</sup>I-Tyr<sup>3</sup>]-octreotide and [<sup>111</sup>In-DTPA-D-Phe<sup>1</sup>]-octreotide.*

Patient	Sex	Age	Tumor type	Interval between scans	Abnormal sites of radioactive accumulation	
					<sup>123</sup> I-octreotide	<sup>111</sup> In-octreotide
1	F	66	Small cell lung cancer	5 weeks	Right lung, lower lobe	Right lung, lower lobe
2	M	65	Gastrinoma	7 weeks	Gallbladder region	Gallbladder region (see text)
3	F	59	Insulinoma	1 week	None (SPECT not done)	None (SPECT positive, Fig. 4)
4	F	50	Carcinoid	10 weeks	Left supraclavicular lymph node, liver	Left + right supraclavicular lymph node, abdomen, chest, liver
5	F	64	Carcinoid	5 weeks	3 caudal abdominal sites, 1 cranial abdominal site	3 caudal abdominal sites, liver (gallbladder removed; see text)
6	F	28	Pheochromocytoma	4 weeks	Lower left abdomen	Lower left abdomen

with both radiopharmaceuticals. In patient 4, presumed carcinoid deposits were more numerous using [ $^{111}\text{In}$ -DTPA-D-Phe $^1$ ]-octreotide scintigraphy. Tumor progression in the relatively long interval between the two scintigrams cannot be excluded, however. In patient 5, the liver showed an irregular uptake pattern of [ $^{111}\text{In}$ -DTPA-D-Phe $^1$ ]-octreotide, whereas a homogeneous distribution was seen with [ $^{123}\text{I}$ -Tyr $^3$ ]-octreotide scintigraphy. The cranial abdominal site of radionuclide accumulation observed with [ $^{123}\text{I}$ -Tyr $^3$ ]-octreotide was not seen on the subsequent [ $^{111}\text{In}$ -DTPA-D-Phe $^1$ ]-octreotide scintigram. This site very likely represented abnormal uptake in the gallbladder and the hepatoduodenal ligament, which had been surgically removed between the two scintigrams and were proven to be massively infiltrated by a carcinoid tumor.

Apart from the marked differences in hepatic and renal clearances (Figure 5), tissue accumulation of both radiopharmaceuticals was similar except for the pituitary, which was nearly always visible with [ $^{111}\text{In}$ -DTPA-D-Phe $^1$ ]-octreotide in contrast to [ $^{123}\text{I}$ -Tyr $^3$ ]-octreotide scintigraphy. However, discrimination between accumulation of [ $^{111}\text{In}$ -DTPA-D-Phe $^1$ ]-octreotide in the pituitary and in the surrounding tissues is often impossible, especially caudally. Consequently, only the contour of the cranial part of the pituitary can be distinguished since in the region of the brain the (background) radioactivity is relatively very low because of the blood-brain barrier. With both radiopharmaceuticals radioactivity was always observed in the thyroid gland, liver, spleen and kidneys, the urinary bladder, and in the intestinal tract, although in the last organ [ $^{111}\text{In}$ -DTPA-D-Phe $^1$ ]-octreotide was much less visible.

## DISCUSSION

In spite of a lower affinity of [ $^{111}\text{In}$ -DTPA-D-Phe $^1$ ]-octreotide for the rat brain somatostatin receptor compared to that of [ $^{123}\text{I}$ -Tyr $^3$ ]-octreotide (7), the indium-labeled compound visualized somatostatin receptor-positive animal tumors more efficiently *in vivo*, probably due to its different metabolic behaviour (8). These metabolic properties turned out to be similar in man; our study shows that after intravenous administration [ $^{111}\text{In}$ -DTPA-D-Phe $^1$ ]-octreotide is rapidly cleared from the circulation via the kidneys. However, its initial disappearance from the circulation is considerably slower compared to that of [ $^{123}\text{I}$ -Tyr $^3$ ]-octreotide (Figure 1)(6). This slower initial clearance, combined with the longer physical half-life of  $^{111}\text{In}$  ( $t_{1/2} = 2.8$  days for  $^{111}\text{In}$  versus 13.2 hr for  $^{123}\text{I}$ ) results in a longer residence time of the radiopharmaceutical in the tissues. The presence of a lower radioactivity in the remainder of the body 24 hr after injection of [ $^{111}\text{In}$ -DTPA-D-Phe $^1$ ]-octreotide leads to a lower background radioactivity (Figure 1)(6). The higher background radioactivity with [ $^{123}\text{I}$ -Tyr $^3$ ]-octreotide is due to its much higher circulating levels of degradation products than is the case with [ $^{111}\text{In}$ -DTPA-D-Phe $^1$ ]-octreotide. Therefore, [ $^{111}\text{In}$ -DTPA-D-Phe $^1$ ]-octreotide is a more suitable

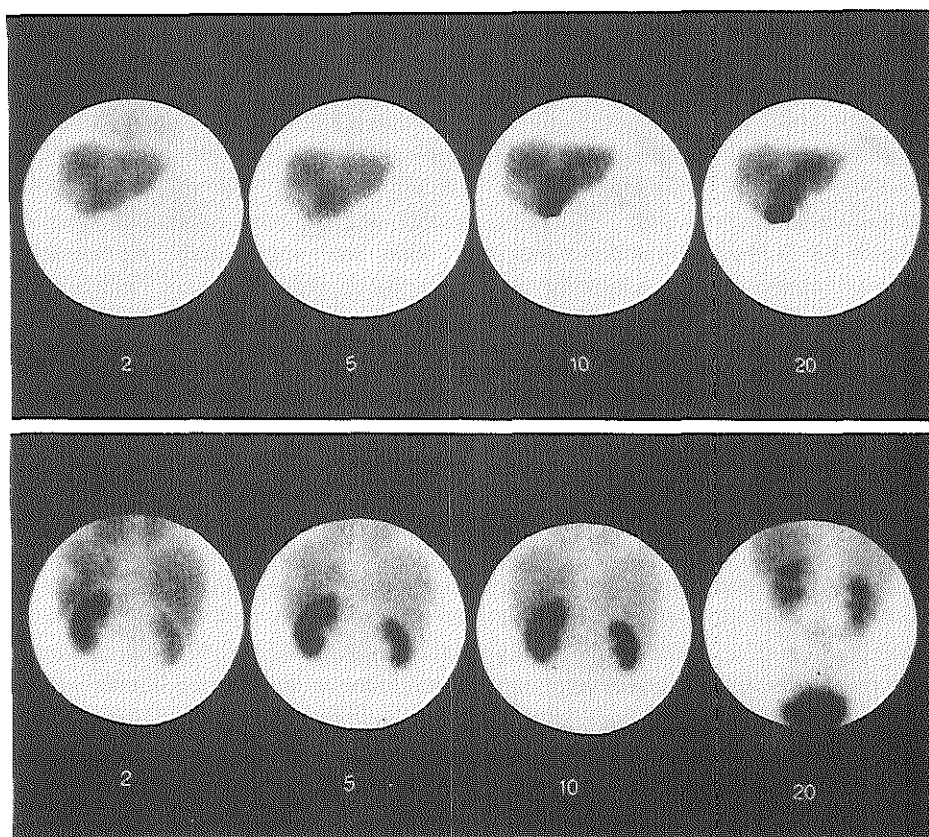


**Figure 5**

*Sequential anterior abdominal views of  $[^{123}\text{I-Tyr}^3]$ -octreotide scintigraphy (upper panel) showing the rapid hepato-biliary clearance, and posterior abdominal views of  $[^{111}\text{In-DTPA-D-Phe}^1]$ -octreotide scintigraphy (lower panel) showing the rapid renal clearance. Note the rapidly decreasing bloodpool radioactivity over the heart with both radiopharmaceuticals. The 20 min image of the latter scintigrams also shows a low grade accumulation of radioactivity in the lower part of the vertebral column, due to a chondrosarcoma.*

radioligand to localize somatostatin receptor-rich tissues (vide infra). Furthermore, using  $[^{111}\text{In-DTPA-D-Phe}^1]$ -octreotide, interpretation of scintigrams of the abdominal region is less affected by intestinal background radioactivity. This contrasts remarkably with  $[^{123}\text{I-Tyr}^3]$ -octreotide scintigraphy, because the hepato-biliary clearance of this compound results in a high hepatic and intestinal accumulation of radioactivity, which is hardly overcome with laxatives.

Analysis of the chemical status of plasma radioactivity during the first 4 hr after injection shows mainly peptide-bound  $^{111}\text{In}$  in the form of the original [ $^{111}\text{In}$ -DTPA-D-Phe<sup>1</sup>]-octreotide. Similarly, analysis of radioactivity in the urine shows predominantly intact [ $^{111}\text{In}$ -DTPA-D-Phe<sup>1</sup>]-octreotide during the first hours after injection. Furthermore, peptide-bound radioactivity in plasma and urine has somatostatin receptor-binding properties as demonstrated by specific binding to rat brain cortex cell membranes. Degradation of [ $^{111}\text{In}$ -DTPA-D-Phe<sup>1</sup>]-octreotide was observed only in plasma and urine samples obtained more than 4 hr after intravenous injection of the radiopharmaceutical, when circulating radioactivity amounted to less than 10 % of the administered radioactivity. Ultimately, degradation to  $^{111}\text{In}$  labeled products such as  $^{111}\text{In}$ -DTPA is suggested by the appearance of the peak in the void volume of HPLC analysis.

Accumulation of radioactivity after intravenous administration of [ $^{111}\text{In}$ -DTPA-D-Phe<sup>1</sup>]-octreotide in man is observed in the pituitary and thyroid gland, the spleen, liver, kidneys and the urinary bladder. Imaging of the gallbladder is occasionally seen, whereas the presence of intestinal radioactivity (mainly in the colon at 24 hr) depends on the simultaneous use of laxatives. The relatively low clearance of the radioligand via the hepato-biliary system favors its use in SPECT of the abdomen, which is strongly indicated in the localization of small endocrine pancreatic tumors. At present the mechanism of the thyroid gland imaging is still unclear. With radiolabeled somatostatin analogue autoradiography we could not find somatostatin receptors in normal thyroid gland and differentiated thyroid carcinoma (papillary cancer) tissue slices (14,15). However, a high percentage of malignant parafollicular thyroid tumors are somatostatin receptor-positive by both autoradiography and scintigraphy (14,15). It is remarkable that in the two cases with Graves' hyperthyroidism investigated so far, accumulation of radioactivity in the thyroid gland was increased (unpublished). The presence of lymphocytes (which can be somatostatin receptor-positive, 16) in the thyroid gland could explain this observation. Autoradiography of normal spleen tissue revealed the presence of somatostatin receptors (unpublished); however, the exact cell-type bearing the somatostatin receptor has not been identified yet. Patients on octreotide treatment show a diminished accumulation of radioligand in the spleen (unpublished), compatible with occupancy of spleen somatostatin receptors by the unlabeled octreotide.

The rapid appearance of intact [ $^{111}\text{In}$ -DTPA-D-Phe<sup>1</sup>]-octreotide in the urine indicates an effective renal clearance of this radiopharmaceutical. By contrast, [ $^{125}\text{I}$ -Tyr<sup>3</sup>]-octreotide is rapidly cleared by the liver and little of it is excreted intact into the urine. The different metabolism of [ $^{111}\text{In}$ -DTPA-D-Phe<sup>1</sup>]-octreotide compared with [ $^{125}\text{I}$ -Tyr<sup>3</sup>]-octreotide indicates that the modification of octreotide with the  $^{111}\text{In}$ -DTPA group inhibits hepatic clearance and/or facilitates renal clearance. Rat liver perfusion studies have indeed shown that [ $^{111}\text{In}$ -DTPA-D-Phe<sup>1</sup>]-octreotide is cleared much more slowly by the liver than [ $^{125}\text{I}$ -Tyr<sup>3</sup>]-octreotide (unpublished). It is unknown whether the effect of the  $^{111}\text{In}$ -DTPA group on the metabolic routing of

peptides is a general phenomenon. The relatively long residence time of [ $^{111}\text{In}$ -DTPA-D-Phe<sup>1</sup>]-octreotide in the kidneys suggests that following glomerular filtration part of the label is reabsorbed in the tubules (8).

Remarkable is the higher sensitivity of [ $^{111}\text{In}$ -DTPA-D-Phe<sup>1</sup>]-octreotide compared to [ $^{125}\text{I}$ -Tyr<sup>3</sup>]-octreotide in localizing the pituitary, since in vitro studies have shown a higher affinity of the radioiodinated ligand for somatostatin receptors in rat brain (7). However, its actual affinity for somatostatin receptors on the pituitary is at present unknown.

For several somatostatin receptor-positive tumors, [ $^{111}\text{In}$ -DTPA-D-Phe<sup>1</sup>]-octreotide shares with [ $^{125}\text{I}$ -Tyr<sup>3</sup>]-octreotide the advantage of providing a more sensitive imaging technique compared with currently available diagnostic procedures, e.g. CT, ultrasound and MRI. Furthermore, the future availability of both [DTPA-D-Phe<sup>1</sup>]-octreotide and pure  $^{111}\text{InCl}_3$  will make an easy single-step labeling procedure possible and, hence, scintigraphy of somatostatin receptor-positive tumors generally available. The effective dose equivalent, although higher than that of [ $^{125}\text{I}$ -Tyr<sup>3</sup>]-octreotide, is comparable with values for other  $^{111}\text{In}$ -labeled radiopharmaceuticals (11) and is acceptable in view of the clinical indications.

## ACKNOWLEDGEMENTS

We thank Ina Loeve, Marianne Goemaat-Visser, Marcel van der Pluijm and Michiel de Roo for their expert technical assistance and Michael Stabin for providing the S-value tables for the  $^{114\text{m}}\text{In}$ .

## REFERENCES

- 1 Krenning EP, Bakker WH, Breeman WAP, et al. Localisation of endocrine-related tumours with radioiodinated analogue of somatostatin. *Lancet* 1989; 1: 242-244.
- 2 Lamberts SWJ, Bakker WH, Reubi J-C and Krenning EP. Somatostatin-receptor imaging in the localization of endocrine tumors. *N Engl J Med* 1990; 323: 1246-1249.
- 3 Lamberts SWJ, Hofland LJ, van Koetsveld PM, et al. Parallel in vivo and in vitro detection of functional somatostatin receptors in human endocrine pancreatic tumors: consequences with regard to diagnosis, localization, and therapy. *J Clin Endocrinol Metab* 1990; 71: 566-574.
- 4 Kwekkeboom DJ, Krenning EP, Bakker WH, et al. Radioiodinated somatostatin analog scintigraphy in small cell lung cancer. *J Nucl Med* 1991; 32: 1845-1848.
- 5 Bakker WH, Krenning EP, Breeman WAP, et al. Receptor scintigraphy with a radioiodinated somatostatin analogue: Radiolabeling, purification, biologic



- activity and in vivo application in animals. *J Nucl Med* 1990; 31: 1501-1509.
- 6 Bakker WH, Krenning EP, Breeman WAP, et al. In vivo use of a radioiodinated somatostatin analogue: dynamics, metabolism and binding to somatostatin receptor positive tumors in man. *J Nucl Med* 1991; 32: 1184-1189.
  - 7 Bakker WH, Albert R, Bruns C, et al. [<sup>111</sup>In-DTPA-D-Phe<sup>1</sup>]-octreotide, a potential radiopharmaceutical for imaging of somatostatin receptor-positive tumors: Synthesis, radiolabeling and in vitro validation. *Life Sci* 1991; 49: 1583-1591.
  - 8 Bakker WH, Krenning EP, Reubi JC, et al. In vivo application of [<sup>111</sup>In-DTPA-D-Phe<sup>1</sup>]-octreotide for detection of somatostatin receptor-positive tumors in rats. *Life Sci* 1991; 49: 1593-1601.
  - 9 Reubi JC, Maurer R, Klijn JGM, et al. High incidence of somatostatin receptors in human meningiomas: biochemical characterization. *J Clin Endocrinol Metab* 1986; 63: 433-438.
  - 10 Watson EE, Stabin M, and Bolch WE, *Documentation package for MIRDOSE (version 2)* 1988; Oak Ridge Associated Universities.
  - 11 International Commission on Radiological Protection. Radiation dose to patients from radiopharmaceuticals. *ICRP-publication 53*, Pergamon Press, Oxford, 1988.
  - 12 Siegel JA, and Stabin MG. Absorbed fractions for electrons and beta particles in small spheres. *J Nucl Med* 1988; 29(5): 803
  - 13 Ellett WH, and Humes RM. Absorbed fractions for small volumes containing photon-emitting radioactivity. MIRD Pamphlet No. 8, *J Nucl Med* 1971; 12(suppl 5): 25-32
  - 14 Reubi JC, Modigliani E, Calmettes C, et al. In vitro and in vivo identification of somatostatin receptors in medullary thyroid carcinomas, pheochromocytomas and paragangliomas. In: *Medullary thyroid carcinoma* (eds. C. Calmettes, J.M. Guliana). Colloque INSERM/ John Libbey Eurotext Ltd. 1991; 211: 85-87.
  - 15 Reubi JC, Chayvialle JA, Franc B, et al. Somatostatin receptors and somatostatin content in medullary thyroid carcinomas. *Lab Invest* 1991; 64 (4): 567-573.
  - 16 Sreedharan SP, Kodama KT, Peterson KE, and Goetzl EJ. Distinct subsets of somatostatin receptors on cultured human lymphocytes. *J Biol Chem* 1989; 264: 949-953.



## CHAPTER 7

### Kinetic handling of [ $^{125}$ I-Tyr $^3$ ]-octreotide and [ $^{111}$ In-DTPA-D-Phe $^1$ ]-octreotide by the isolated perfused rat liver

Marion de Jong, Willem H. Bakker, Wout A.P. Breeman, Marcel van der Pluijm, Peter P.M. Kooij, Theo J. Visser, Roelof Docter, and Eric P. Krenning.

Departments of Nuclear Medicine and Internal Medicine III,  
University Hospital Dijkzigt and Erasmus University Medical School,  
Rotterdam, The Netherlands.

#### Abstract

Certain radiolabeled bioactive peptides show receptor-mediated binding to tumors, making them suitable for scintigraphic imaging of these tumors. The liver is an important organ for the clearance of many of these peptides. Therefore, we compared the hepatobiliary handling of [ $^{125}$ I-Tyr $^3$ ]-octreotide and [ $^{111}$ In-DTPA-D-Phe $^1$ ]-octreotide, which are successfully used in imaging of somatostatin receptor-positive tumors in vivo. This investigation was done in isolated recirculating perfused rat livers to gain insight into the uptake and intracellular processing of these somatostatin analogues. During 60 min following administration of the radiolabeled peptides, medium and biliary radioactivity was analyzed at regular intervals. Radioiodinated [Tyr $^3$ ]-octreotide appeared to be rapidly cleared by the liver and to be excreted intact into the bile. After 60 min 60 % of the administered dose was excreted into the bile. In contrast, [ $^{111}$ In-DTPA-D-Phe $^1$ ]-octreotide, was not cleared by the liver: radioactivity levels remained about constant in the circulating medium and little radioactivity was found in the bile (2 % of the dose after 60 min). These findings show that whereas [ $^{125}$ I-Tyr $^3$ ]-octreotide is rapidly cleared by the liver and excreted intact into the bile, [ $^{111}$ In-DTPA-D-Phe $^1$ ]-octreotide is not handled by the liver. The results obtained here are in excellent agreement with in vivo findings in rats and humans. From this study, it can be concluded that the isolated rat liver perfusion is a rapid method to investigate the hepatic handling of radiopharmaceuticals. As the liver, besides the

kidneys, is an important organ in the removal of many bioactive peptides from the body, such investigations may also have a predictable value for the *in vivo* metabolism.

Tumor receptor-binding radiopharmaceuticals are among the interesting recent developments in nuclear medicine, as these substances can be used for *in vivo* scintigraphic imaging of such tumors. An example is somatostatin (Fig. 1A), which binds to its receptors on tumors of neuro-endocrine origin (1).

This native peptide, however, is susceptible to very rapid enzymatic degradation (2), and therefore not very useful for *in vivo* application. For that reason, more stable synthetic somatostatin analogues have been developed. The octapeptide octreotide (SMS 201-995 or Sandostatin<sup>®</sup>, Fig. 1B) fulfils this criterium (3). Large numbers of high affinity binding sites for native somatostatin and synthetic octreotide have been detected on most endocrine-active tumors (4). Since octreotide cannot be radiolabeled easily with a gamma-emitting radionuclide, a synthetic analogue ([Tyr<sup>3</sup>]-octreotide) has been developed in which a phenylalanine has been replaced by tyrosine, allowing radioiodination of the molecule (Fig. 1C). This compound, radiolabeled with <sup>125</sup>I or <sup>123</sup>I, has been used successfully for *in vitro* somatostatin receptor studies (4-7) and tumor scintigraphy in animals (6,8) as well as in man (1,9,10). Another radioactive analogue of somatostatin is [<sup>111</sup>In-DTPA-D-Phe<sup>1</sup>]-octreotide (Fig. 1D), which is also used for *in vivo* scintigraphy. Furthermore, it lacks some drawbacks of [<sup>123</sup>I-Tyr<sup>3</sup>]-octreotide (7,8; see also Discussion).

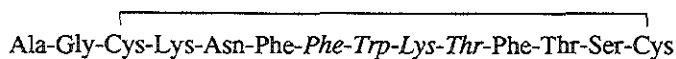
The liver is an important organ in the degradation of many circulating peptides. However, as far as we know, the uptake and intracellular handling of the octreotide analogues has not been previously investigated in an isolated rat liver perfusion system and our understanding of the pharmacokinetic behaviour of these compounds is only limited. Therefore, we compared the liver handling and excretion into the bile of [<sup>125</sup>I-Tyr<sup>3</sup>]-octreotide and [<sup>111</sup>In-DTPA-D-Phe<sup>1</sup>]-octreotide by means of the isolated recirculating perfused rat liver.

## MATERIALS AND METHODS

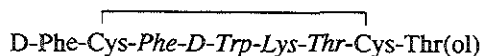
### *Materials*

Na<sup>125</sup>I (IMS.30) was obtained from Amersham International, UK. <sup>111</sup>InCl<sub>3</sub> (DRN 4901) was obtained from Mallinckrodt Medical BV, Petten, The Netherlands. [Tyr<sup>3</sup>]-octreotide and [DTPA-D-Phe<sup>1</sup>]-octreotide were obtained from Sandoz Pharma AG, Basle, Switzerland. <sup>131</sup>I-Human serum albumin (HSA) was purchased from Sorin Biomedica, Italy. Bovine serum albumin (BSA; Boserol) was a product

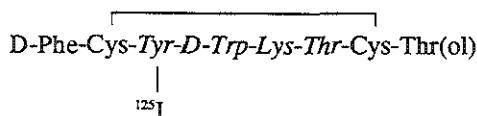
A. *Somatostatin*



B. *Octreotide*



C. [<sup>125</sup>I-Tyr<sup>3</sup>]-*octreotide*



D. [<sup>111</sup>In-DTPA-D-Phe<sup>1</sup>]-*octreotide*

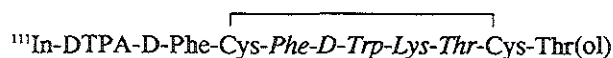


**Figure 1**

*Somatostatin and analogues with the supposed bioactive site printed in italics.*

of Organon Teknika (Oss, The Netherlands). All other reagents were of the highest purity commercially available.

**Radiolabeling**

Radioiodination of [Tyr<sup>3</sup>]-octreotide with <sup>125</sup>I was performed with the chloramine-T method as described previously (6). Labeling of [<sup>111</sup>In-DTPA-D-Phe<sup>1</sup>]-octreotide with <sup>111</sup>In was carried out as described (7).

### *Isolated perfused rat liver*

Livers of male Wistar rats, 200-250 g body weight, were isolated and perfused in a recirculating system at 37 °C as described previously (11), using 150 ml Krebs-Ringer buffer supplemented with 10 mM glucose and 1 % BSA. The pH of the medium was maintained at 7.43 by gassing with carbogen (95 % CO<sub>2</sub> and 5 % O<sub>2</sub>, 400 ml/min). The function of the liver was monitored by its outer appearance, measurement of hydrostatic pressure necessary to maintain a medium flow of 40 ml/min, bile flow, and pH of the medium. Livers were preperfused for 30 min. The experiment was started by addition of 370 kBq of tracer (10<sup>-9</sup> mol) to the medium. Subsequently, 0.5 ml medium samples were taken at 1, 2, 3, 4, 5, 6, 7, 8, 9, 10, 15, 20, 25, 30, 40, 50 and 60 min. For the determination of a correct curve fitting more samples were taken in the first minutes of some experiments. Bile samples were collected during 10 min intervals. The samples were stored at -20 °C until analysis.

### *Analysis of medium and bile samples*

The chemical status of the radionuclide in medium and bile samples was analysed as a function of time using SEP-PAK C<sub>18</sub> chromatography. Medium and bile samples were applied to SEP-PAK C<sub>18</sub> columns, which had been activated with 5 ml 2-propanol. Elution of the different fractions was performed with 5 ml distilled water and 5 ml 0.5 M acetic acid to remove free <sup>125</sup>I<sup>-</sup>, and 5 ml 96 % ethanol to elute peptide-bound radioactivity. Fractions were collected and counted for radioactivity. Radiochemical composition of the different samples was confirmed by HPLC-analysis with a Waters 600 E multisolvent delivery system connected to a  $\mu$ -Bondapak-C<sub>18</sub> reversed-phase column (300 x 3.9 mm, particle size 10  $\mu$ m). Before HPLC, bile samples were diluted 1:10 with 40 % methanol in 154 mM NaCl. Elution was carried out at a flow of 1 ml/min with a linear gradient of 40 % to 80 % methanol in 154 mM NaCl in 20 min. The latter composition was maintained for another 5 min. Collected fractions were measured by routine scintillation counting.

### *Calculations*

Curve-fitting of the two-exponential medium tracer disappearance curve was done as described previously (11). All data are reported as mean  $\pm$  SD (n  $\geq$  4).

## RESULTS

### *[<sup>125</sup>I-Tyr<sup>3</sup>]-octreotide*

Fig. 2A and 2B show typical time courses in medium and bile of total radioactivity, peptide-bound radioactivity and liberated <sup>125</sup>I, after administration of [<sup>125</sup>I-Tyr<sup>3</sup>]-octreotide to the medium. Results are expressed as percentage of the administered dose. After administration of the tracer, radioactivity shows a very rapid disappearance from the medium, followed by a rapid excretion into the bile. In Table 1A, it is shown that of the administered radioactivity 27 % peptide-bound

**Figure 2A**

*Rat liver perfusion: typical example of disappearance of total (○) and peptide-bound (●) radioactivity from the medium and appearance of <sup>125</sup>I- (▲) in medium after administration of [<sup>125</sup>I-Tyr<sup>3</sup>]-octreotide.*

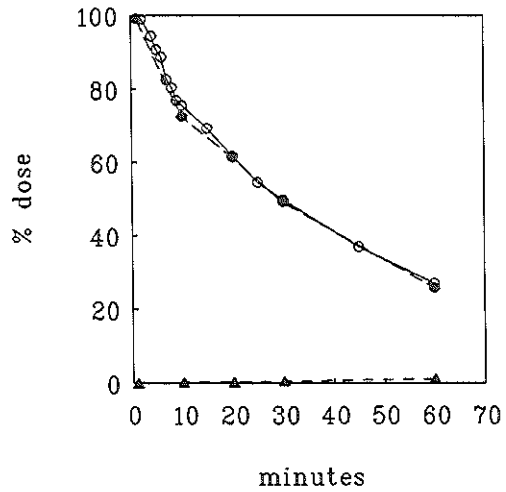


**Figure 2B**

*Typical example of cumulative excretion by the perfused rat liver of total radioactivity (●), divided in peptide-bound radioactivity (open bar) and <sup>125</sup>I- (solid bar), into the bile after administration of [<sup>125</sup>I-Tyr<sup>3</sup>]-octreotide.*

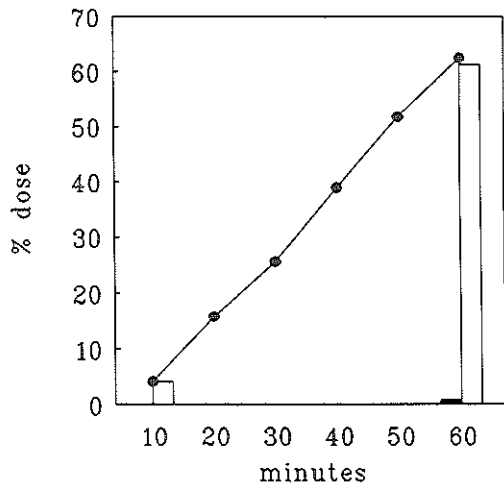


**Table 1A**

*Original peptides and break-down products expressed as peptide-bound radioactivity (PBR) and non-peptide-bound radioactivity (NPBR), e.g.,  $^{125}\text{I}^-$  and  $^{111}\text{In-DTPA}$ , in medium and bile after 60 min of perfusion with  $^{125}\text{I-Tyr}^3$ -octreotide or  $^{111}\text{In-DTPA-D-Phe}^1$ -octreotide. Results are given as mean (SD) % dose ( $n \geq 4$ ).*

	PBR (medium)	NPBR (medium)	PBR (bile)	NPBR (bile)
$^{125}\text{I-Tyr}^3$ -octreotide	26.9 (1.9)	1.2 (0.0)	60.4 (3.7)	1.0 (0.1)
$^{111}\text{In-DTPA-D-Phe}^1$ -octreotide	94.9 (0.8)	0.9 (0.1)	2.2 (0.2)	0.2 (0.0)

**Table 1B**

*Half-lives of the fast and slow components of medium disappearance of  $^{131}\text{I-HSA}$ ,  $^{125}\text{I-Tyr}^3$ -octreotide and  $^{111}\text{In-DTPA-D-Phe}^1$ -octreotide. Results are given in mean (SD) minutes ( $n \geq 4$ ).*

	fast component	slow component
$^{131}\text{I-HSA}$	0.29 (0.02)	$\infty$
$^{125}\text{I-Tyr}^3$ -octreotide	0.28 (0.04)	36.2 (3.9)
$^{111}\text{In-DTPA-D-Phe}^1$ -octreotide	0.25 (0.08)	$\infty$

radioactivity is left in the medium after 60 min, while about 1 % consists of free iodide. Concerning the bile, free iodide accounts for only 1 % of the administered radioactivity; most radioactivity (60 % dose) is excreted in peptide-bound form. HPLC-analysis revealed that the peptide-bound radioactivity in the bile is intact  $^{125}\text{I-Tyr}^3$ -octreotide (Fig. 3). In all experiments the disappearance of tracer  $^{125}\text{I-Tyr}^3$ -octreotide could be fitted to the sum of two exponentials. In Fig. 4, this two-exponential medium disappearance curve is shown and the half-lives of the fast and slow component were calculated.

The distribution time through the system was estimated by perfusion of livers with  $^{131}\text{I-HSA}$ , a substance that is not taken up into the liver. The half-life of the fast component of medium  $^{131}\text{I-HSA}$  disappearance was 0.3 min, whereas that of



the slow component was very long as almost no radioactivity disappeared from the medium. In the case of [ $^{125}\text{I}$ -Tyr $^3$ ]-octreotide the half-life of the fast component is 0.3 min (representing distribution through the perfusion system) and of the slow component 36 min (representing uptake and metabolism, Table 1B).

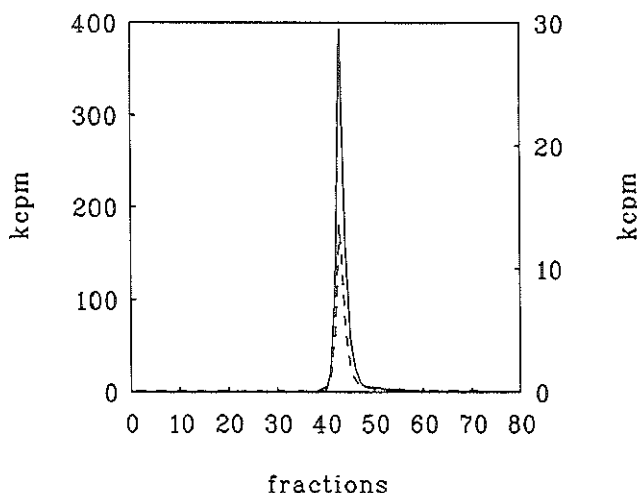


**Figure 3**

*Typical examples of HPLC elution patterns (expressed in kcpm per 0.3 ml fraction) of [ $^{125}\text{I}$ -Tyr $^3$ ]-octreotide, as added to the medium (solid line, left ordinate), and of protein-bound fraction excreted into the bile (dashed line, right ordinate).*

### **[ $^{111}\text{In}$ -DTPA-D-Phe $^1$ ]-octreotide**

Figs. 5A and 5B show typical time courses in medium and bile, respectively, of total radioactivity, peptide-bound radioactivity and non-peptide bound breakdown products after administration of [ $^{111}\text{In}$ -DTPA-D-Phe $^1$ ]-octreotide to the medium. In Table 1A, it is shown that after 60 min, 95 % of the administered radioactivity still consists of peptide-bound tracer in the medium, which is identical to intact [ $^{111}\text{In}$ -DTPA-D-Phe $^1$ ]-octreotide as demonstrated by HPLC (not shown). Concerning the bile, only a small portion (2 %) of the administered radioactivity is excreted. Furthermore, it was calculated that the half-lives of the fast and slow component of the biphasic medium disappearance (which is described as the sum of two exponentials) are 0.3 min (distribution) and unmeasurably long, respectively (Table 1B).

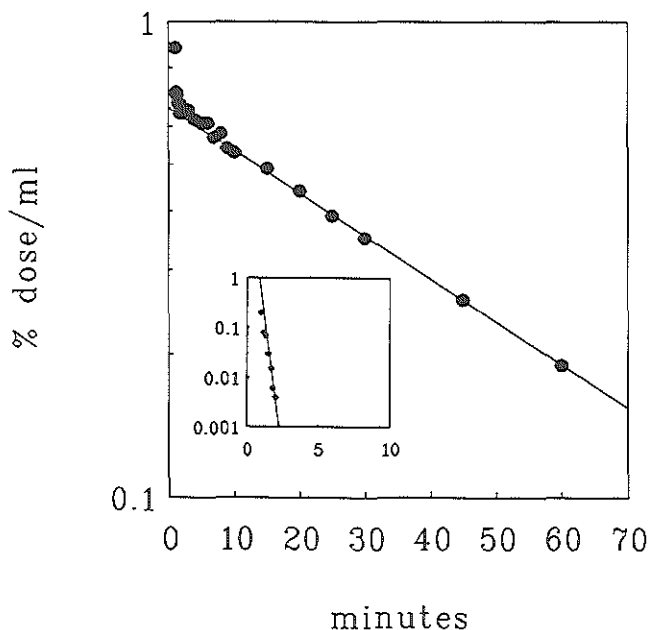


**Figure 4**

*Typical example of the curve fitting of a [ $^{125}$ I-Tyr $^3$ ]-octreotide disappearance curve by a two-exponential model. Plot of % dose per ml against time, with the least squares regression line on the final straight part of the curve (slow component). Inset: plot of the fast component, with the least squares regression line.*

## DISCUSSION

Radiolabeled octreotide analogues bind to the somatostatin receptors on neuroendocrine tumor cells, and are therefore suitable for scintigraphic imaging of these tumors. Although these radiopharmaceuticals have been investigated in vitro (binding studies and autoradiography of somatostatin receptor-positive tissues; Refs. 4-7) and in vivo (tumor scintigraphy; Refs. 1,6,8-10), little is known about the metabolism of these radioligands, especially in the liver. This is in contrast to the knowledge of the hepatic metabolism of the native peptides somatostatin-14 and somatostatin-28. They are degraded through the action of hepatic aminopeptidases and endopeptidases as studied in the perfused rat liver (12,13).

**Figure 5A**

*Rat liver perfusion: typical example of disappearance of total (○) and peptide-bound (●) radioactivity from the medium and appearance of non-peptide-bound breakdown products (▲) in medium after administration of [<sup>111</sup>In-DTPA-D-Phe<sup>1</sup>]-octreotide.*

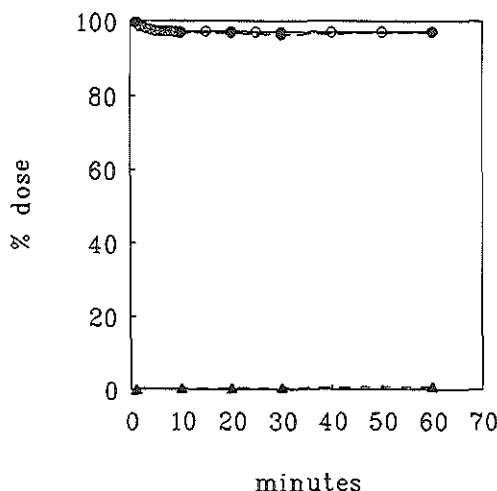
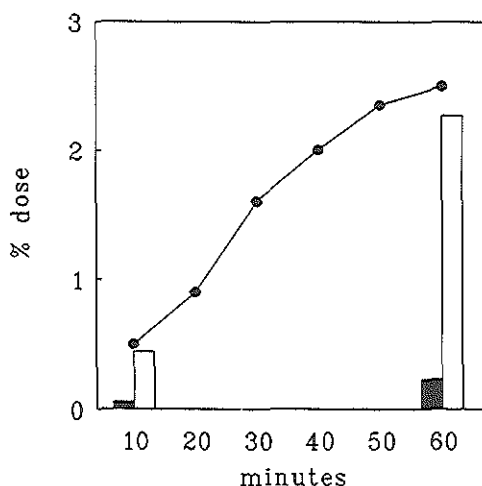


**Figure 5B**

*Typical example of cumulative excretion by the perfused rat liver of total radioactivity (●), divided in peptide-bound radioactivity (open bar) and non-peptide-bound breakdown products (solid bar) into the bile after administration of [<sup>111</sup>In-DTPA-D-Phe<sup>1</sup>]-octreotide.*



The perfused rat liver is very suitable to investigate several parameters of liver metabolism, such as the disappearance from the medium, appearance of degradation products and biliary excretion. Therefore, in this study we compared the liver handling of [<sup>125</sup>I-Tyr<sup>3</sup>]-octreotide and [<sup>111</sup>In-DTPA-D-Phe<sup>1</sup>]-octreotide in this system.

[<sup>125</sup>I-Tyr<sup>3</sup>]-octreotide is rapidly taken up into the liver, immediately followed by intact excretion into the bile (Fig. 4). As the half-life of the fast component of the medium disappearance is the same as that of <sup>131</sup>I-HSA, a substance that is not

transported into the hepatocytes but passively distributes into the liver interstitium, it is shown that this component is predominantly determined by distribution of the tracer through the system and the extracellular liver compartment. The half-life of the second component is mainly determined by handling in the liver. We recently reported transport and metabolism of thyroid hormone in the perfused rat liver; in that case an uptake and a metabolism component could be distinguished clearly in the biphasic medium disappearance curve after the distribution phase (11). In the case of [ $^{125}$ I-Tyr $^3$ ]-octreotide, uptake is immediately followed by excretion into the bile and therefore not seen as a distinct component. Chromatography of medium and bile showed that hardly any free radioactive iodide is found in medium and bile, while the majority of the administered dose is already excreted intact into the bile within 60 min. Only little of the administered radioactivity accumulates in the liver.

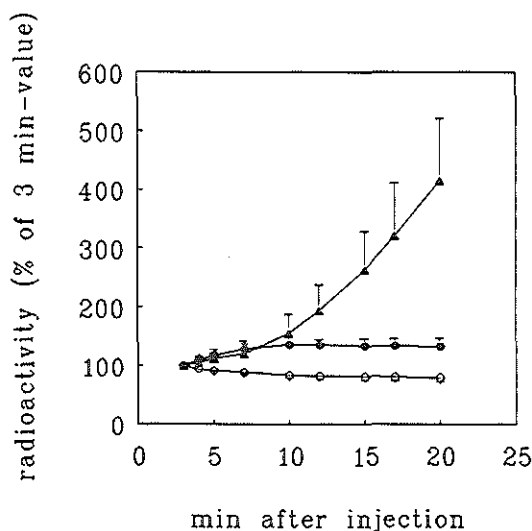


**Figure 6**

*Radioactivity, expressed as mean  $\pm$  SD percentage of the 3-min value, measured above regions of interest in humans, i.e. liver tissue without major bile ducts (after [ $^{125}$ I-Tyr $^3$ ]-octreotide [●,  $n=5$ ] and [ $^{111}$ In-DTPA-D-Phe $^1$ ]-octreotide [○,  $n=3$ ]) and gallbladder (after [ $^{125}$ I-Tyr $^3$ ]-octreotide [▲,  $n=5$ ]). After injection of [ $^{111}$ In-DTPA-D-Phe $^1$ ]-octreotide no bile-related radioactivity was measured neither in major bile-ducts nor in the gallbladder.*

An internalized peptide can reach bile by two pathways: (a) a lysosomal, or indirect pathway; and (b) a non-lysosomal, or direct pathway (14). In general, molecules processed by the first pathway are not excreted intact into the bile. Compounds that utilize the second pathway are generally excreted into bile as intact molecules and appear in bile sooner than those excreted by the lysosomal pathway. Our results show that [ $^{125}\text{I}$ -Tyr $^3$ ]-octreotide is translocated across the hepatocytes into the bile by the direct pathway, thereby bypassing the lysosomes, because the radiopharmaceutical is excreted intact into the bile and because there exists no lag time before excretion into the bile takes place. These findings are in accordance with the fact that [ $^{125}\text{I}$ -Tyr $^3$ ]-octreotide is very stable against (hepatic) enzymatic degradation, in contrast to the native peptides somatostatin-14 and somatostatin-28 (12,13), probably due to the introduction of a D-amino acid at the N-terminal and an amino-alcohol substituent at the C-terminal end of the peptide chain (3).

Recently, it has been reported for several types of cyclosomatostatins that uptake into isolated rat hepatocytes is a carrier-mediated process which is related to the multispecific bile acid transporter (15). Further transcellular bile-acid transport to the bile after uptake into the cells has been elucidated by electron microscope autoradiography, showing that these substances are excreted rapidly into the bile in a chemically unchanged form (for review, Ref. 16). We did not investigate possible carrier-mediated transport properties of our somatostatin analogues, but intact excretion into the bile after a rapid transcellular transport is in accordance with our findings in the perfused rat liver.

The results of our study in the perfused rat liver are in agreement with rat and human *in vivo* investigations with [ $^{125}\text{I}$ -Tyr $^3$ ]-octreotide, which show that disposal occurs predominantly by rapid uptake into the liver and excretion via the bile into the intestines (6,9). In Fig. 6 metabolism in the *human* liver is shown. Data are derived from studies, described in Ref. 9. [ $^{125}\text{I}$ -Tyr $^3$ ]-octreotide is rapidly cleared from the circulation by the liver, immediately followed by hepatobiliary excretion; radioactivity in a non-major bile duct-containing part of the liver does not increase above 150 % of the 3 min-value, but a sharp increase of radioactivity is seen above the gallbladder during the first 20 min after administration.

[ $^{111}\text{In}$ -DTPA-D-Phe $^1$ ]-octreotide is not taken up by the isolated perfused rat liver, as almost no tracer disappears from the medium. The half-life of the fast component is again determined by distribution through the system, whereas the half-life of the slow component is very long, indicating a very slow handling in the liver. Furthermore, hardly any radioactivity is found in the liver, and excretion into the bile is negligible. This may be due to the addition of the relatively large and very hydrophylic DTPA-group to the octapeptide-molecule, favouring renal excretion of the latter, like the radiolabeled chelate itself (for instance  $^{99\text{m}}\text{Tc}$ -DTPA), which is excreted exclusively by glomerular filtration (17). These findings are in excellent accordance with *in vivo* studies (8,10). In Fig. 6 metabolism in the human liver is shown using data derived from studies described in Ref. 10. After

administration of [ $^{111}\text{In}$ -DTPA-D-Phe $^1$ ]-octreotide the radioactivity, measured above the liver does not increase, but rather decreases, which can be explained by the fact that this radiopharmaceutical is not cleared by the liver but by the kidneys (8,10). Scintigraphically no radioactivity could be measured above the gallbladder.

[ $^{111}\text{In}$ -DTPA-D-Phe $^1$ ]-octreotide is the preferred analogue for in vivo scintigraphy, as it has several advantages compared to [ $^{125}\text{I}$ -Tyr $^3$ ]-octreotide: general availability, simple one-step method of radiolabeling, longer physiological half-life in plasma, and a more suitable metabolism. In order to visualize a tumor by receptor binding in vivo, the specific activity expressed in counts per unit of area must exceed the local background radiation. As - in contrast to radioiodinated [Tyr $^3$ ]-octreotide - [ $^{111}\text{In}$ -DTPA-D-Phe $^1$ ]-octreotide is not cleared via the liver and causes no accumulation of radioactivity in biliary and digestive tract, the latter radiopharmaceutical is more suitable for visualization of tumor receptor accumulation in the upper abdominal region, where the small endocrine gastro-entero-pancreatic target tumors are located.

From this study, it can be concluded that the investigation of the handling of radiopharmaceuticals by the isolated rat liver perfusion is a rapid method to study kinetics of these substances in this organ. As the liver, besides the kidneys, is an important organ in the removal of many bioactive peptides from the body, such investigations may also have a predictable value for the in vivo metabolism.

## REFERENCES

1. Krenning EP, Bakker WH, Breeman WAP, Koper JW, Kooij PPM, Aulsebrook L, Laméris JS, Reubi JC, and Lamberts SWJ. Localisation of endocrine-related tumours with radioiodinated analogue of somatostatin. *Lancet* 1989; 1: 242-244.
2. Patel YC, and Wheatley T. In vivo and in vitro plasma disappearance and metabolism of somatostatin-28 and somatostatin-14 in the rat. *Endocrinology* 1983; 112: 220.
3. Pless J, Bauer W, Briner U, Doepfner W, Marbach P, Maurer R, Petcher TJ, Reubi JC, and Vonderscher J. Chemistry and pharmacology of SMS 201-995, a long-acting analogue of somatostatin. *Scand J Gastroenterol* 1986; 21 (Suppl 119): 54-64.
4. Reubi JC, Häcki WH, and Lamberts SWL. Hormone-producing gastrointestinal tumours contain high density of somatostatin receptors. *J Clin Endocrinol Metab* 1987; 65: 1127-1134.
5. Reubi JC. New specific radioligand for one subpopulation of brain somatostatin receptors. *Life Sci* 1985; 36: 1829-1836.
6. Bakker WH, Krenning EP, Breeman WA, Koper JW, Kooij PP, Reubi JC, Klijn JG, Visser TJ, Docter R, and Lamberts SW. Receptor scintigraphy with a radioiodinated somatostatin analogue: Radiolabeling, purification, biologic

- activity and in vivo application in animals. *J Nucl Med* 1990; 31: 1501-1509.
7. Bakker WH, Albert R, Bruns C, Breeman WAP, Hofland LJ, Marbach P, Pless J, Pralet Stolz B, Koper JW, Lamberts SWJ, Visser TJ, and Krenning EP. [<sup>111</sup>In-DTPA-D-Phe<sup>1</sup>]-octreotide, a potential radiopharmaceutical for imaging of somatostatin receptor-positive tumors: Synthesis, Radiolabeling and in vitro validation. *Life Sci* 1991; 49: 1583-1591.
  8. Bakker WH, Krenning EP, Reubi JC, Breeman WAP, Setyono-Han B, de Jong M, Kooij PPM, Bruns C, van Hagen PM, Marbach P, Visser TJ, Pless J, and Lamberts SWJ. In vivo application of [<sup>111</sup>In-DTPA-D-Phe<sup>1</sup>]-octreotide for the detection of somatostatin receptor-positive tumors in rats. *Life Sci* 1991; 49: 1593-1601.
  9. Bakker WH, Krenning EP, Breeman WA, Kooij PPM, Reubi JC, Koper JW, de Jong M, Laméris JS, Visser TJ, and Lamberts SW. In vivo use of a radioiodinated somatostatin analogue: Dynamics, metabolism, and binding to somatostatin receptor-positive tumors in man. *J Nucl Med* 1991; 32: 1184-1189.
  10. Krenning EP, Bakker WH, Kooij PPM, Breeman WAP, Oei HY, De Jong M, Reubi JC, Visser TJ, Bruns C, Kwekkeboom DJ, Reijs AEM, Van Hagen PM, Koper JW, and Lamberts SWJ. Somatostatin receptor scintigraphy with [<sup>111</sup>In-DTPA-D-Phe<sup>1</sup>]-octreotide in man: metabolism, dosimetry and comparison with [<sup>123</sup>I-Tyr<sup>3</sup>]-octreotide. Accepted for publication in *J Nucl Med* (appearance: May 1992).
  11. Docter R, De Jong M, Van der Hoek HJ, Krenning EP, and Hennemann G. Development and use of a mathematical two-pool model of distribution and metabolism of 3,3',5-triiodothyronine in a recirculating rat liver perfusion system: albumin does not play a role in cellular transport. *Endocrinology* 1990; 126: 461-459.
  12. Sacks H, and Terry LC. Clearance of immunoreactive somatostatin by perfused rat liver. *J Clin Invest* 1981; 67: 419-425.
  13. Ruggere MD, and Patel Y. Hepatic metabolism of somatostatin-14 and somatostatin-28: immunochemical characterization of the metabolic fragments and comparison of cleavage sites. *Endocrinology* 1985; 117: 88-96.
  14. Coleman R. Biochemistry of bile secretion. *Biochem J* 1987; 244: 249-261.
  15. Ziegler K, Lins W, and Frimmer M. Hepatocellular transport of cyclosomatostatins: evidence for a carrier related to the multispecific bile acid transporter. *Biochim Biophys Acta* 1991; 1061: 287-296.
  16. Frimmer M, and Ziegler K. The transport of bile acids in liver cells. *Biochim Biophys Acta* 1988; 947: 75-99.
  17. Kloppper JF, Hauser W, Atkins HL, Eckelman WC, and Richards P. Evaluation of <sup>99m</sup>Tc-DTPA for measurement of glomerular filtration rate. *J Nucl Med* 1972; 13: 107-110.





## APPENDIX PAPERS



### **Localization of endocrine-related tumors with radioiodinated analogue of somatostatin**

E.P. Krenning, W.H. Bakker, W.A.P. Breeman, J.W. Koper, P.P.M. Kooij,  
L. Ausema, L.S. Laméris, J.C. Reubi, and S.W.J. Lamberts.

Departments of Internal Medicine III, Nuclear Medicine, and  
Radiology, University Hospital Dijkzigt, Erasmus University,  
Rotterdam, The Netherlands;  
and Sandoz Research Institute, Berne, Switzerland.

#### **Summary**

Various endocrine-related tumors contain large numbers of high-affinity somatostatin receptors. <sup>123</sup>I-labeled [Tyr<sup>3</sup>]-octreotide ([Tyr<sup>3</sup>]-SMS 201-995, a synthetic derivative of somatostatin) was used to localize such tumors in vivo with a gamma camera. Positive scans were obtained for two meningiomas, two gastrinomas, and one carcinoid; negative scans were obtained for one insulinoma (in which unlabeled octreotide had no effect on insulin levels), one pheochromocytoma, one adrenal carcinoma (octreotide had no effect on cortisol levels), and three medullary thyroid carcinomas (octreotide had no effect on calcitonin levels). Thus radioiodinated [Tyr<sup>3</sup>]-octreotide can label somatostatin receptors in endocrine-related tumors in vivo and can therefore be used for tumor localization.

#### **INTRODUCTION**

Large numbers of binding sites with high affinity for somatostatin have been reported in tumors such as growth-hormone-producing pituitary adenomas (1), meningiomas (2), malignant breast tumors (3), astrocytomas and oligodendrogliomas (4), medulloblastomas (3), neuroblastomas (3), and oat cell carcinomas of the lung (5). As well as inhibiting the secretion of specific hormones by some of these tumors (6-9), somatostatin may inhibit tumor growth (9-12). 204-090 ([Tyr<sup>3</sup>]-octreotide {[Tyr<sup>3</sup>]-SMS 201-995}, a synthetic derivative of somatostatin) and somatostatin have a common active site. We have studied the in-vivo

binding of radioiodinated 204-090 to several endocrine-related tumors. Information on the labeling procedure, bioassay, pharmacology, and dosimetry in rats and man will be reported elsewhere.

## PATIENTS AND METHODS

The somatostatin derivatives octreotide and 204-090 were prepared by Sandoz (Basel, Switzerland) (13,14). Radioiodination of octreotide was done with chloramine (13).

Depending on the labeling procedure, the interval between injection and scintigraphy, and whether single photon emission computed tomography (SPECT) was required, the doses of  $^{123}\text{I}$ -204-090 ranged from 37 to 555 MBq, given as an intravenous bolus. Planar and SPECT images were obtained with a large field of view gamma-camera ('Counterbalance 3700', Siemens Gammasonics), equipped with a 190 keV parallel-hole collimator. Generally the field of view at the time of injection of  $^{123}\text{I}$ -204-090 covered the abdomen and some of the lung and heart area. From the time of injection digital images were recorded with a 'Gamma-11' computer (Nuclear Diagnostics, Sweden) every 3 s for 2 min then every 60 s for 28 min. In this 30 min period analogue images were also obtained regularly. 30 min after injection, anterior and posterior whole-body static scintigraphy and, when indicated, SPECT were done. Static images, both analogue and digital, were obtained at about 0.5, 2, 4, 24, and sometimes 48 h after injection.  $^{99\text{m}}\text{Tc}$ -albumin microcolloid (56 MBq; Albu-Res, Solco, Switzerland) scintigraphy was used for subtraction of radioactivity in normal liver tissue.

All patients gave informed consent to participate. Clinical details are shown in the table.

## RESULTS

After the injection of  $^{123}\text{I}$ -204-090 no side-effects were noted. As well as distribution of activity in the blood, radioactivity accumulated rapidly in the liver. About half the activity was cleared from the blood within 2 min after injection. The table summarises our results. In all patients who showed significant inhibition of tumor hormone release in response to subcutaneous administration of 50 or 100  $\mu\text{g}$  octreotide, scintigraphy revealed rapid accumulation of  $^{123}\text{I}$ -204-090 at tumor sites, which were verified by computerised tomographic (CT) scanning. Tumors that were seen on the 24 and 48 h scans were also visible on the 4 h whole-body scans.

Both in patient 1 (gastrinoma) and 4 (carcinoid), metastases that had not been known about before the investigation were detected outside the abdomen. The primary tumor in the jejunum of patient 4 was also detected after the injection of

## CLINICAL DETAILS AND RESPONSES OF PATIENTS

Patient (sex/age [yr])	Diagnosis	Acute endocrine response to 50-100 µg octreotide <sup>§</sup>	Scintigraphy with <sup>123</sup> I-204-090 <sup>¶</sup>
1 (F/46)	Gastrinoma (MEN I syndrome); meningioma	+	+
2 (F/68)	Meningioma	NA	+
3 (M/37)	Gastrinoma	+	+
4 (M/75)	Carcinoid	+	+
5 (F/80)	Insulinoma	-	-
6 (F/57)	Pheochromocytoma	NT	-
7 (M/49)	Medullary thyroid carcinoma	-	-
8 (M/67)	Medullary thyroid carcinoma	-	-
9 (F/66)	Medullary thyroid carcinoma	-	-
10 (M/44)	Adrenal (cortex) carcinoma	-	-

<sup>§</sup>+ = decrease and - = no decrease in level of specific tumor-marker (patients 1 and 3, serum gastrin; 4, urinary 5-hydroxyindole acetic acid; 5, serum insulin; 7, 8, and 9, serum calcitonin; and 10, serum cortisol).

<sup>¶</sup>+ = correct localization of primary tumor and, if present, metastases, compared with CT scanning; - = no accumulation of label in tumor.

NA = not applicable and NT = not tested.

<sup>123</sup>I-204-090. Fig 1 shows images from patient 4. Despite metastases in the liver, the initial images (not shown) of the liver obtained with <sup>123</sup>I-204-090 revealed a diffuse pattern of radioactivity, which showed the capacity of these metastases to accumulate this radiopharmaceutical. Fig 2 shows localization of a gastrinoma (patient 3). Interestingly, two patients with meningioma (no 1 and 2) also showed accumulation of <sup>123</sup>I-204-090 at the site of this tumor. An image from patient 2 is shown in fig 3; brain tissue was not labeled in any patient by this technique. The timecourse of the distribution of radioactivity in all these tumors was distinct from that in blood (fig 1, centre, and 2).

## DISCUSSION

Using 204-090 in an in-vitro assay with tumor homogenates and in receptor autoradiography, Reubi et al (2,15) demonstrated high levels of somatostatin

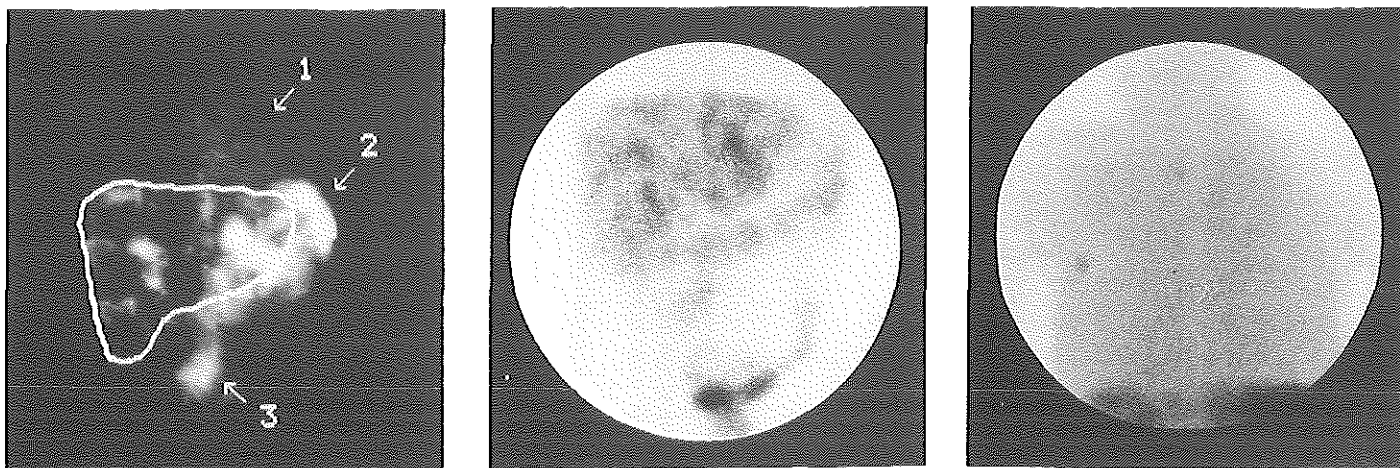


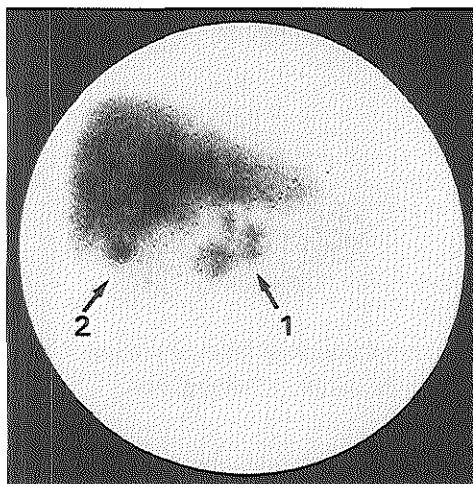
*Figure 1*

*Anterior abdominal images of patient 4 (carcinoid) after intravenous injection of  $^{123}\text{I}$ -204-090.*

*Left = subtraction image of  $^{123}\text{I}$ -204-090 and  $^{99\text{m}}\text{Tc}$ -microcolloid images at 20 min; 1 = heart, 2 = spleen, and 3 = primary tumor. Centre = 48 h  $^{123}\text{I}$ -204-090 image. Note the resemblance of these two images; at 48 h, in addition to radioactivity in digestive tract and bladder, only primary tumor and metastases in liver and mesenteric lymph nodes are seen. Metastases in thorax (e.g., left scapula, vertebra, and rib)(right = posterior view of thorax), neck, and supraclavicular region (not shown) were also found.*

**Figure 2**

*Anterior abdominal image of patient 3 at 30 min. 1 = primary site of gastrinoma. 2 = gallbladder. Note absence of spleen activity, because of splenectomy.*

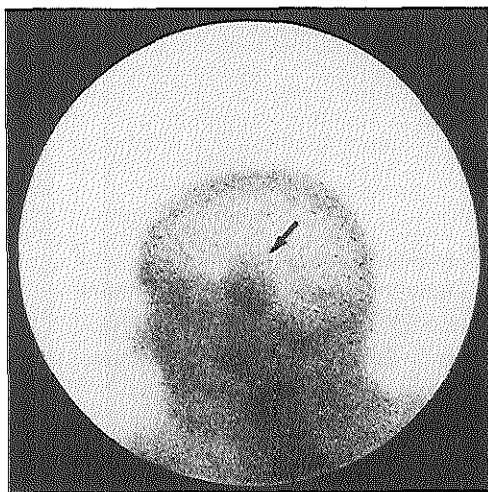


receptors in four of four gastrinomas, two of five insulinomas, and thirteen of thirteen meningiomas. A high proportion of carcinoids were also found to contain somatostatin receptors (J.C.R. and L.K. Kvols, unpublished). However, three pheochromocytomas and two medullary thyroid carcinomas tested in vitro did not contain somatostatin receptors (3). Our in-vivo findings agree with these in-vitro results and with the acute endocrine response to intravenously administered octreotide. Tumors were not detected by our technique in three cases of medullary thyroid carcinoma, one pheochromocytoma, and one insulinoma. Furthermore no acute endocrine response to octreotide was observed in these patients. Localization of the primary tumor and metastases with  $^{123}\text{I}$ -204-090 was possible in both cases of gastrinoma, in both cases of meningioma, and in one carcinoid case. The demonstration of previously unknown metastases in some of these patients shows the powerful discrimination of this technique. The detection also confirms in-vitro data which showed that metastases of somatostatin-receptor-positive primary tumors are themselves receptor-positive (3,15). The observed accumulation of radioactivity at the site of the tumor after intravenous injection was instantaneous and prolonged in contrast to activity in blood, which rapidly decreased. This excludes the possibility that the tumors were detected because of accumulation of blood in the tumor.

The results of our study and in-vitro data (2-4,15) suggest that tumors are labeled in vivo by binding of the radiopharmaceutical to membrane-bound receptors (1-4). In addition to tumor localization, scintigraphy with  $^{123}\text{I}$ -204-090 may demonstrate in vivo somatostatin receptors in tumors if an acute endocrine response to octreotide cannot be measured (e.g., when a specific hormonal tumor-marker is not available). This detection will especially apply if these receptors are involved in tumor growth, because octreotide affects the growth of endocrine-related tumors (9-12). If somatostatin is directly antiproliferative (12), the presence or absence of somatostatin receptors on tumors might be expected to determine the response to

*Figure 3*

*Lateral image of head of patient 2  
at 3 h. Arrow = meningioma.*



therapy with somatostatin analogues. In view of this, the potential role of  $^{123}\text{I}$ -204-090 scintigraphy and of beta-emitting radiolabeled analogues in radiotherapy needs further investigation. Whole-body scintigraphy with  $^{123}\text{I}$ -204-090 is feasible - images can be interpreted several minutes after injection because of the rapid decrease in background radioactivity.

Our study demonstrates tumor localization in patients by targeting receptor-rich tumors with relevant radioligands. The technique may not be limited to somatostatin receptor-rich tumors, but may be extended to other receptor-containing tumors (i.e., receptors for epidermal growth factor). The method may be a powerful alternative to tumor labeling with monoclonal antibodies.

We thank Dr J.W.F. Elte who contributed a patient to the study, Paula C. Schuijff and her staff for help with patients' management, Ina Loeve and Sjaak van Peski for technical assistance, and Joke M. Nijse for secretarial help.

## REFERENCES

1. Reubi JC, Landolt AM. High density of somatostatin receptors in pituitary tumours from acromegalic patients. *J Clin Endocrinol Metab* 1984; 59: 1148-1153.
2. Reubi JC, Maurer R, Klijn JGM, et al. High incidence of somatostatin receptors in human meningiomas: biochemical characterization. *J Clin Endocrinol Metab* 1986; 63: 433-438.
3. Reubi JC, Maurer R, von Werder K, Torhorst J, Klijn JGM, Lamberts SWJ. Somatostatin receptors in human endocrine tumors. *Cancer Res* 1987; 47: 551-558.



4. Reubi JC, Lang W, Maurer R, Koper JW, Lamberts SWJ. Distribution and biochemical characterization of somatostatin receptors in tumors of the human central nervous system. *Cancer Res* 1987; 47: 5758-5764.
5. Taylor JE, Bogden AE, Moreau J-P, Coy DH. In vitro and in vivo inhibition of human small cell lung carcinoma (NCI-H 69) growth by a somatostatin analogue. *Biochem Biophys Res Comm* 1988; 153: 81-86.
6. Lamberts SWJ, Oosterom R, Neufeld M, del Pozo E. The somatostatin analog SMS 201-995 induces long-acting inhibition of growth hormone secretion without rebound hypersecretion in acromegalic patients. *J Clin Endocrinol Metab* 1985; 60: 1161-1165.
7. Lamberts SWJ, Uitterlinden P, Verschoor L, van Dongen KJ, del Pozo E. Long-term treatment of acromegaly with the somatostatin analogue SMS 201-995. *N Engl J Med* 1985; 313: 1576-1580.
8. Maton MP, O'Dorisio TM, Howe BA, et al. Effect of a long-acting somatostatin analogue (SMS 201-995) in a patient with pancreatic cholera. *N Engl J Med* 1985; 312: 17-21.
9. Kvols LK, Moertel CG, O'Connell MJ, Schutt AJ, Rubin J, Hahn RG. Treatment of the malignant carcinoid syndrome: evaluation of a long-acting somatostatin analogue. *N Engl J Med* 1986; 315: 663-666.
10. Reubi JC. A somatostatin analogue inhibits chondrosarcoma and insulinoma tumor growth. *Acta Endocrinol* 1985; 109: 108-114.
11. Lamberts SWJ, Reubi JC, Uitterlinden P, Zuiderwijk J, van den Werf P, van Hal P. Studies on the mechanism of action of the inhibitory effect of the somatostatin analog SMS 201-995 on the growth of the prolactin adrenocorticotropin-secreting pituitary tumor 7315a. *Endocrinology* 1986; 118: 2188-2194.
12. Lamberts SWJ, Koper JW, Reubi JC. The potential role of somatostatin analogs in the treatment of cancer. *Eur J Clin Invest* 1987; 17: 281-287.
13. Reubi JC. New specific radioligand for one subpopulation of brain somatostatin receptors. *Life Sci* 1985; 36: 1829-1836.
14. Bauer W, Briner U, Doepfner WS, et al. SMS 201-995: a very potent and selective octapeptide analogue of somatostatin with prolonged action. *Life Sci* 1982; 31: 1133-1141.
15. Reubi JC, Häcki T, Lamberts SWJ. Hormone-producing gastro-intestinal tumours contain a high density of somatostatin receptors. *J Clin Endocrinol Metab* 1987; 65: 1127-1143.



## Parallel *in Vivo* and *in Vitro* Detection of Functional Somatostatin Receptors in Human Endocrine Pancreatic Tumors: Consequences with Regard to Diagnosis, Localization, and Therapy

STEVEN W. J. LAMBERTS, LEO J. HOFLAND, PETER M. VAN KOETSVELD, JEAN-CLAUDE REUBI, HAJO A. BRUINING, WILLEM H. BAKKER, AND ERIC P. KRENNING

Departments of Medicine (S.W.J.L., L.J.H., P.M.v.K., E.P.K.), Nuclear Medicine (W.H.B., E.P.K.), and Surgery (H.A.B.), Erasmus University, Rotterdam, The Netherlands; and Sandoz Research Institute (J.-C.R.), Berne, Switzerland

**ABSTRACT.** The effects of octreotide *in vivo* and *in vitro* on hormone release, *in vivo* [ $^{125}$ I]Tyr<sup>3</sup>-octreotide scanning, and *in vitro* [ $^{125}$ I]Tyr<sup>3</sup>-octreotide autoradiography were compared in five patients with endocrine pancreatic tumors.

[ $^{125}$ I]Tyr<sup>3</sup>-octreotide scanning localized the primary tumor and/or previously unknown metastases in four of the five patients. The patient with a negative scan had an insulinoma that did not respond to octreotide *in vivo*. No Tyr<sup>3</sup>-octreotide-binding sites were subsequently found at autoradiography of the tumor, whereas somatostatin-14 receptors were present at a high density. In parallel, culture studies with the cells prepared from this adenoma showed that insulin release was not affected by octreotide, while both somatostatin-14 and -28 significantly suppressed hormone release.

Culture studies of the tumor cells from two gastrinomas showed a dose-dependent inhibition of gastrin release by octreotide. Octreotide exerted direct antiproliferative effects in one of these gastrinomas, which had been shown to be rapidly growing

*in vivo*. Both gastrinomas had specific somatostatin receptors, as measured by *in vitro* receptor autoradiography. Somatostatin release by the cultured somatostatinoma cells from one of these patients was suppressed by octreotide.

In conclusion, 1) the [ $^{125}$ I]Tyr<sup>3</sup>-octreotide scanning procedure is valuable in the localization of primary endocrine pancreatic tumors as well their often clinically not yet recognized metastases; 2) the *in vitro* detection of somatostatin receptors in those tumors that were also visualized *in vivo* after injection of [ $^{125}$ I]Tyr<sup>3</sup>-octreotide indicates that the ligand binding to the tumor *in vivo* indeed represents binding to specific somatostatin receptors; and 3) the parallel between the presence of somatostatin receptors on tumors and *in vivo* and *in vitro* effects of octreotide on hormonal release from these tumors indicate that a positive scan predicts a good suppressive effect of octreotide on hormonal hypersecretion by these tumors. (*J Clin Endocrinol Metab* 71: 566-574, 1990)

**E**NDOCRINE pancreatic tumors in man are often difficult to localize, while metastases are in most cases already present at the time of their diagnosis (1, 2). Most previously used therapies are in the majority of patients of only temporary benefit (3-5). The clinical introduction of the somatostatin analog octreotide was reported to be especially successful in the control of the clinical signs and symptoms related to the hormonal hypersecretion of vasoactive intestinal polypeptide (VIP), gastrin, and glucagon (6-14). The possible tumor growth inhibitory effects of octreotide in endocrine pancreatic tumors seem to occur less frequently (15).

Previously, we demonstrated the presence of large

numbers of high affinity binding sites for the somatostatin analog [ $^{125}$ I]Tyr<sup>3</sup>-octreotide in 10 of 14 hormone-producing endocrine pancreatic tumors (16). Thereafter, we showed in a preliminary study that these receptors can also be visualized *in vivo* in patients harboring these tumors by a new nuclear medical procedure involving the iv administration of [ $^{125}$ I]Tyr<sup>3</sup>-octreotide (17). In the present study we compared, in a group of 5 patients with endocrine pancreatic tumors, the preoperative reaction of circulating hormone levels to the iv administration of a single dose of octreotide, the *in vivo* detection of somatostatin (analog) receptors after the injection of [ $^{125}$ I]Tyr<sup>3</sup>-octreotide, and the subsequent presence of these receptors on the tumor tissue investigated *in vitro*. Finally, the parallel *in vivo* and *in vitro* investigations were in a few cases completed by studies on the effects of octreotide on hormone secretion by the cultured cells prepared from these tumors.

Received November 17, 1989.

Address all correspondence and requests for reprints to: S. W. J. Lamberts, M.D., Department of Medicine, University Hospital Dijkzigt, 40 Doctor Molewaterplein, 3015 GD Rotterdam, The Netherlands.

## Materials and Methods

### Culture studies

Specimens of surgically removed tumor tissue (two gastrinomas, one parathyroid adenoma, one insulinoma, and one somatostatinoma) were dispersed into single cell suspensions using a mixture of dispase and collagenase, as described previously (18). The cells were cultured in Minimum Essential Medium supplemented with 10% fetal calf serum, sodium pyruvate (1 mmol/L), nonessential amino acids, L-glutamine (2 mmol/L), sodium bicarbonate (2.2 g/L), and antibiotics. Media and supplements were purchased from Flow (Irvine, Ayrshire, Scotland). The cells were cultured at a density of  $1-1.5 \times 10^5$  cells/well, except for the somatostatinoma cells, which were seeded at  $10^5$  cells/wells. All incubations (with or without drugs) were carried out in quadruplicate. At the end of the incubation period the media were collected. Cell extracts were prepared by lysis of the cells in distilled water containing 0.1% BSA (19). Media and cell extracts were stored at  $-20^\circ\text{C}$  until analysis.

### Assays

The DNA content of the tumor cells was determined according to the method described by Downs and Wilfinger (20) and has been described previously in detail (21).

Gastrin and insulin concentrations in the culture media, cell extracts, and sera were determined by double antibody RIAs, using kits purchased from Cambridge Medical Diagnostics (Billerica, MA) and MedGenix Diagnostics (Brussels, Belgium), respectively. PTH concentrations were determined by a immunoradiometric assay (IRMA) using a kit from Incstar Corp. (Stillwater, MN). Intra- and interassay variations were less than 8% for the gastrin RIA, less than 8% and less than 6% for the insulin RIA, and less than 5% and less than 10% for the PTH IRMA, respectively. Gastrin, insulin and PTH in the media and cell extracts diluted parallel to the respective standards supplied with kits. PRL was determined by RIA as described previously (22). Somatostatin concentrations were measured with standard RIA techniques with an antiserum supplied by Dr. R. Guillemin (Salk Institute, La Jolla, CA). The intraassay variation was 6%. Somatostatin in the medium of the cultured tumor cells diluted parallel to the standard, while octreotide up to a concentration of  $1 \mu\text{M}$  interfered less than 3% in the assay.

### In vitro determination of somatostatin receptors

Immediately after resection, a piece of tissue for receptor autoradiographic analysis was cooled on ice and frozen at  $-70^\circ\text{C}$ . The storage time of the tumors before autoradiographic processing ranged from 1-3 months. Tumor sample diameters were between 5-15 mm.

Somatostatin receptors were measured by autoradiography on cryostat sections of the tumor tissue, as described previously in detail for various endocrine tumors (16, 23). Two iodinated somatostatin analogs were used as radioligands, the Tyr<sup>3</sup> analog of octreotide, code named 204-090, [H-D-Phe-Cys-Tyr-D-Trp-Lys-Thr-Cys-Thr(ol)] (24), as well as the somatostatin-14 derivative [Tyr]somatostatin-14 (25). Both ligands were previ-

ously shown to specifically label somatostatin receptors (26). For autoradiography the tumors were cut on a cryostat (Leitz 1720, Rockleigh, NJ) in  $10\text{-}\mu\text{m}$  sections, mounted on precleaned microscope slides, and stored at  $-20^\circ\text{C}$  for at least 3 days to improve adhesion of the tissue to the slide. Sections were then incubated for 2 h at ambient temperature in 170 mM Tris-HCl buffer (pH 7.4) containing 1% BSA, bacitracin ( $40 \mu\text{g/mL}$ ), and  $\text{MgCl}_2$  (5 mM) to inhibit endogenous proteases in the presence of iodinated ligand ( $0.16 \times 10^6 \text{ dpm/mL}$ ;  $\sim 80 \text{ pM}$ ). Nonspecific binding was determined by adding unlabeled somatostatin-14 or 204-090 at a concentration of  $1 \mu\text{M}$ . Incubated sections were washed twice for 5 min in cold incubation buffer containing 0.25% BSA. Sections were washed in distilled water and dried quickly, apposed to  $^3\text{H}$  LKB films, and exposed for 1 week in x-ray cassettes.

Selected tumors in which somatostatin receptors were visualized with autoradiographical methods were also characterized biochemically in a homogenate binding assay in saturation and competition experiments, as described previously (25, 26).

### In vivo somatostatin receptor imaging

Tyr<sup>3</sup>-octreotide (204-090) was obtained from Sandoz (Basel, Switzerland). The preparation of [ $^{125}\text{I}$ ]Tyr<sup>3</sup>-octreotide, the dose administered ( $37-555 \text{ MBq}$ ), and the technique of scintigraphy with  $\gamma$ -camera pictures as well as with single photon emission computed tomography have been described previously (17).

All patients have informed consent to participate in the study, which was approved by the ethical committee of our hospital.

## Results

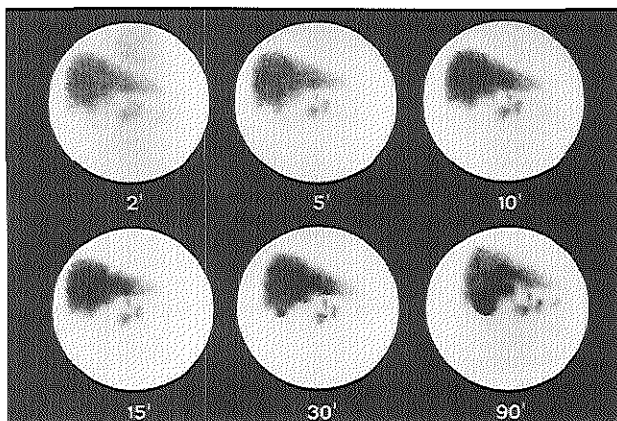
### Patient 1

This 38-yr-old man patient underwent two stomach operations in recent years because of bleeding from several duodenal ulcers, which could not be controlled by therapy with histamine<sub>2</sub>-receptor-blocking agents. Eventually, serum gastrin levels were found to be elevated ( $7200$  and  $8200 \text{ ng/L}$ , respectively), and at arteriography a tumor with a diameter of  $2.5 \text{ cm}$  was found in the corpus of the pancreas. Fifty micrograms of octreotide suppressed gastrin levels by 70% from 1-8 h after administration.

An [ $^{125}\text{I}$ ]Tyr<sup>3</sup>-octreotide scan was carried out (Fig. 1). Two minutes after injection of the isotope-coupled somatostatin analog a normal liver was visualized, while there was still some radioactivity in the heart. In the center of the abdomen under the left lobe of the liver a somatostatin receptor-positive tumor mass was seen, which became more clear in the subsequent pictures. After 30 and 90 min the gallbladder and bile duct contained high amounts of radioactivity. Throughout the scanning period it became clear that the positive picture in the region of the pancreas consisted of three more or less independent tumor deposits.

At subsequent laparotomy two tumors were found in

FIG. 1. [ $^{125}$ I]Tyr<sup>3</sup>-octreotide scan in patient 1 with a gastrinoma.  $\gamma$ -Camera pictures of the abdomen were taken 2, 5, 10, 15, 30, and 90 min after the iv injection of 15 mCi [ $^{125}$ I]Tyr<sup>3</sup>-octreotide. Note the normal liver, and the filling of the gallbladder and the bile ducts after 30 and 90 min. In the center of all pictures two gastrin-secreting tumors are visible in the pancreas, as well as a gastrinoma-containing lymph node in the retroperitoneum.



the corpus of the pancreas ( $4 \times 4$  and  $5 \times 6$  cm in diameter) as well as a tumor-containing lymph node. All tumor tissue stained immunohistochemically strongly positive with antigastrin. Autoradiographic studies with [ $^{125}$ I]Tyr<sup>3</sup>-octreotide revealed that both the two pancreatic tumors and the lymph node metastasis contained large numbers of somatostatin analog-binding sites, which were diffusely distributed over the tumor tissue. Biochemical analysis showed the presence of high affinity binding sites for Tyr<sup>3</sup>-octreotide, with a  $K_d$  of 0.16 nM and a binding capacity of 683 fmol/mg protein (Fig. 2). Similar results were obtained in the metastatic tumor tissue (data not shown).

From the primary tumors in the pancreas 3.6 g tissue were dispersed; this resulted in a total of  $800 \times 10^6$  viable tumor cells, which were seeded in the culture wells at a density of  $1.5 \times 10^5$  cells/well. During a period of 2 weeks the control cells continued to secrete large amounts of gastrin. Both 0.1 and 10 nM octreotide effectively controlled gastrin release by the cultured tumor cells; from day 8 on, gastrin secretion was completely blocked by the drug.

The possibility of a direct antimitotic effect of octreotide on these cultured tumor cells was evaluated and compared with that exerted by two cytostatic drugs (Table 1). Octreotide (10 nM), vincristin (10 nM), and adriamycin (10 nM) suppressed hormone release, the intracellular gastrin content, and the DNA content of these tumor cells. In Fig. 3 the close correlation between the gastrin content and the DNA content of those tumor cells exposed to octreotide and the cytostatic drugs is shown ( $P < 0.01$ ).

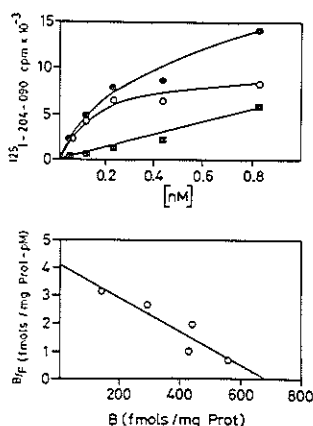


FIG. 2. Binding of [ $^{125}$ I]Tyr<sup>3</sup>-octreotide (204-090) to the membranes of the primary gastrinoma of patient 1. Top, Saturation curve using a gastrinoma membrane preparation incubated for 60 min with increasing concentrations of [ $^{125}$ I]Tyr<sup>3</sup>-octreotide. Specific binding minus binding persisting in the presence of 100 nM Tyr<sup>3</sup>-octreotide (nonspecific) is shown. Points are the average of triplicate tubes. Bottom, Scatchard plot from the data shown in the top figure ( $K_d$ , 0.16 nM; binding capacity, 683 fmol/mg protein). B/F, Bound to free ratio.

#### Patient 2

This 48-yr-old woman has multiple endocrine adenomatosis type I. In the past she had Cushing's syndrome

TABLE 1. The effects of octreotide, vincristin, and adriamycin on gastrin release and on the gastrin and DNA contents of the cultured tumor cells of two patients with malignant gastrinoma

	Gastrin			DNA ng/well
	Medium ( $\mu\text{g}/\text{well} \cdot 96 \text{ h}$ )	Content ( $\mu\text{g}$ )	Total ( $\mu\text{g}$ )	
Patient 1				
Control	$1.33 \pm 0.04$	$0.69 \pm 0.11$	$2.02 \pm 0.06$	$527 \pm 67$
Octreotide (10 nM)	$0.21 \pm 0.04^*$	$0.34 \pm 0.01^*$	$0.55 \pm 0.05^*$	$298 \pm 36^*$
Vincristin (10 nM)	$0.34 \pm 0.06^*$	$0.27 \pm 0.03^*$	$0.61 \pm 0.06^*$	$361 \pm 7^*$
Adriamycin (10 nM)	$0.43 \pm 0.03^*$	$0.49 \pm 0.05^*$	$0.92 \pm 0.04^*$	$344 \pm 26^*$
Patient 2				
Control	$37.0 \pm 2.5$	$6.5 \pm 0.3$	$43.5 \pm 1.7$	$1695 \pm 17$
Octreotide (10 nM)	$8.1 \pm 1.5^*$	$13.1 \pm 0.2^*$	$21.2 \pm 0.9^*$	$1332 \pm 135$
Vincristin (10 nM)	$32.0 \pm 4.0$	$3.7 \pm 0.4^*$	$35.7 \pm 3.3$	$1677 \pm 14$
Adriamycin (10 nM)	$21.3 \pm 0.7^*$	$4.8 \pm 0.1^*$	$26.1 \pm 0.5^*$	$1661 \pm 53$

The tumor cells had been preincubated for 96 h. Thereafter, the effects of the drugs were investigated for another 96 h (mean  $\pm$  SEM;  $n = 4$  wells/group).

\*  $P < 0.01$  vs. control.

<sup>a</sup>  $P < 0.05$  vs. control.

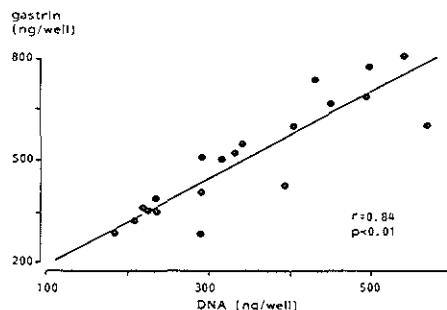


Fig. 3. The relation between the gastrin content and the DNA content of the cultured tumor cells prepared from the primary gastrinoma of patient 1 after a 96-h exposure to octreotide (10 nM), vincristin (10 nM), and adriamycin (10 nM;  $r = 0.84$ ;  $P < 0.01$ ).

caused by a unilateral adrenal adenoma, primary hyperparathyroidism which was unresolved despite the removal of two parathyroid adenomas (serum calcium at present, 3.2 mmol/L), a glucagonoma in the tail of the pancreas (removed), and subsequently, a gastrinoma in the corpus of the pancreas (removed). In addition, she had a microprolactinoma. In the past 5 yr her serum gastrin levels had slowly increased to 70,000 ng/L. Computed tomographic (CT) scanning of the abdomen and repeated ultrasound examinations did not reveal the localization of a metastasis of the gastrin-secreting tumor. Fifty micrograms of octreotide suppressed gastrin levels for more than 14 h to a low level of 6400 ng/L. The increased circulating concentrations of PTH and PRL were not affected by octreotide.

An [ $^{125}\text{I}$ ]Tyr<sup>3</sup>-octreotide scan (Fig. 4) 2 min after injection

of the isotope coupled to the somatostatin analog showed a somatostatin receptor-positive tumor in the middle of the abdomen. Subsequently, the liver and gallbladder started to absorb radioactivity (Fig. 4). The pituitary microadenoma and the parathyroid adenoma(s) could not be visualized (data not shown). Reexamination of the CT scan and ultrasounds showed one single enlarged lymph node in the hilus of the liver with a diameter of 6 cm, which was subsequently removed. Pathological examination showed in the lymph node a metastasis of an endocrine pancreatic tumor resembling the primary tumor, which had been removed in the past. Immunohistochemistry showed positive staining with antigastrin. The tumor-containing lymph node was shown in *in vitro* autoradiography to contain large numbers of somatostatin analog-binding sites which were homogeneously distributed over the tumor tissue. Competition experiments with membranes prepared from this tumor showed that increasing concentrations of 204-090 and somatostatin-28 displaced [ $^{125}\text{I}$ ]Tyr<sup>3</sup>-octreotide, while the biologically inactive derivative somatostatin-28 (1-12) was unable to displace the radioligand.

From 8.5 g tumor tissue  $250 \times 10^6$  tumor cells were prepared, which were cultured at a density of  $1.5 \times 10^6$  cell/well. In Table 2, short and long term effects of octreotide on hormone release, intracellular hormone content, and DNA content of the tumor cells are shown. In the 4- and 24-h incubations 10 nM octreotide inhibited gastrin release by 55% and 76%, respectively (Table 2). Octreotide (1  $\mu\text{M}$ ) maximally suppressed gastrin release after 8 days by 83%. The intracellular hormone content at the end of a 24-h incubation had increased from  $20.3 \pm 3.1$   $\mu\text{g}/\text{well}$  (control) to  $40.2 \pm 2.6$  to  $56.3 \pm 3.4$   $\mu\text{g}/\text{well}$  after octreotide at different concentrations. After an 8-day exposure to octreotide the intracellular gastrin

FIG. 4. The [ $^{125}$ I]Tyr<sup>3</sup>-octreotide scan in patient 2 with a metastasized gastrinoma.  $\gamma$ -Camera pictures of the abdomen taken 2, 5, 10, 15, 20, and 25 min after isotope administration show a normal liver and a slowly increasing amount of radioactivity in the gallbladder. At 2 min a gastrinoma-containing lymph node is visible in the middle of the abdomen.

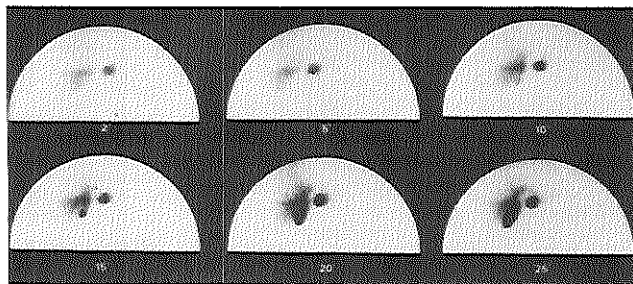


TABLE 2. The effect of octreotide on gastrin release and on the gastrin and DNA contents of the cultured tumor cells of the malignant gastrinoma of patient 2

	Gastrin ( $\mu$ g/well)				DNA after 8 days (ng/well)	
	4 h (medium)	24 h (medium)	8 days (medium)	Content	Total	
Control	18.3 $\pm$ 0.3	72.0 $\pm$ 3.6	134.9 $\pm$ 8.9	6.0 $\pm$ 0.7	140.9 $\pm$ 7.8	1146 $\pm$ 52
Octreotide (0.1 nM)	9.6 $\pm$ 0.3* (52)	20.9 $\pm$ 1.0* (29)	54.1 $\pm$ 4.1* (40)	16.5 $\pm$ 1.2*	70.6 $\pm$ 3.6*	1050 $\pm$ 38
Octreotide (10 nM)	8.2 $\pm$ 0.4* (45)	17.2 $\pm$ 0.5* (24)	38.8 $\pm$ 3.1* (29)	17.3 $\pm$ 0.7*	56.1 $\pm$ 4.1*	937 $\pm$ 36
Octreotide (1 $\mu$ M)	7.4 $\pm$ 0.2* (40)	14.5 $\pm$ 0.3** (20)	23.4 $\pm$ 2.6** (17)	17.9 $\pm$ 0.9*	41.3 $\pm$ 3.0**	964 $\pm$ 50

The tumor cells had not been preincubated. The effects of octreotide were measured for 4 and 24 h and for 8 days (mean  $\pm$  SEM; n = 4 wells/group). Percentages are given in parentheses.

\*  $P < 0.01$  vs. control.

\*\*  $P < 0.01$  vs. octreotide (0.1 nM).

content was also significantly higher than that in the control cells, while the DNA content of the cells had not changed (Table 2). In this case there was no significant correlation between the intracellular gastrin content and the DNA content of the tumor cells. In Table 1 the effects of octreotide, vincristin, and adriamycin are compared. Octreotide suppressed hormone release more effectively than both cytostatic drugs. However, octreotide-mediated inhibition of gastrin release was accompanied by an increase in the intracellular hormone content, which contrasts with the effects of vincristin and adriamycin.

Thereafter, patient 2 underwent a reexploration of the neck in order to remove the remaining parathyroid adenoma(s). One adenoma (3 g) was found and removed. Postoperatively, serum calcium concentrations normalized (2.38 mmol/L). No somatostatin receptors could be detected on this adenoma in the *in vitro* autoradiography. Dispersion of 0.9 g of the adenoma yielded a single cell suspension of  $13 \times 10^6$  adenoma cells. The cells were plated at  $10^4$  cells/well. Basal PTH release by these cells amounted to  $49.1 \pm 1.3$  ng/well  $\cdot$  24 h and was not affected by 1 nM, 10 nM, and 1  $\mu$ M octreotide (data not shown).

Patient 2 currently has slightly elevated gastrin levels (460 ng/L) and is free of complaints.

### Patient 3

This 36-yr-old woman developed psychiatric symptoms over the past 6 months which occurred in attacks.

She lost consciousness frequently and became aggressive afterward. During one incident a serum glucose level of 1.6 mmol/L was detected with an inappropriately elevated plasma insulin concentration of 136 pmol/L.

A tumor with a diameter of 2 cm was detected in the head of the pancreas at arteriography. The administration of 50  $\mu$ g octreotide, sc, suppressed fasting glucose levels from 2.7 to 2.4 mmol/L, without altering circulating insulin levels, which varied between 129–180 pmol/L. However, serum GH levels were suppressed for 2 h from 5.6  $\mu$ g/L to less than 1  $\mu$ g/L. The patient did not experience side-effects after the administration of octreotide. An [ $^{125}$ I]Tyr<sup>3</sup>-octreotide scan did not reveal evidence for the presence of a somatostatin receptor-positive tumor in the region of the pancreas or elsewhere (data not shown). At laparotomy a 2-cm adenoma was removed from the pancreas. Postoperatively this patient was well and did not experience hypoglycemic attacks in the follow-up period of 8 months.

Pathological examination revealed an endocrine pancreatic tumor which stained only with insulin in the immunohistochemical examination. *In vitro* autoradiography showed that the tumor had a low density of somatostatin analog [ $^{125}$ I]Tyr<sup>3</sup>-octreotide-binding sites. Only part of the tumor sample showed a low density of Tyr<sup>3</sup>-octreotide receptors, whereas the major part was devoid of them. Interestingly however, a very high den-

sity of [ $^{125}$ I]Tyr<sup>11</sup>-somatostatin-14-binding sites was found homogeneously distributed over the whole tumor sample in an adjacent section. From 0.8 g adenoma tissue  $13.5 \times 10^6$  dispersed tumor cells were prepared. These were plated at a density of  $5 \times 10^4$  cells/well. In addition, 0.8 g surrounding normal pancreatic tissue were dispersed. This resulted in a total of  $1 \times 10^6$  cells, which were also plated at a density of  $5 \times 10^4$  cells/well. The effects of octreotide, somatostatin-14, and somatostatin-28 on basal hormone release by the cultured insulinoma cells showed that octreotide did not suppress, while both 10 and 500 nM somatostatin-14 and -28 effectively suppressed tumorous insulin release effectively in a similar fashion by about 50%. Interestingly, insulin release from the cells prepared from the normal surrounding pancreatic tissue was effectively suppressed by octreotide as well as by somatostatin-14 and -28.

#### Patient 4

This 46-yr-old woman was referred to us 5 yr ago because of an infiltrating carcinoma of the pancreas. At laparotomy a  $12 \times 14$ -cm infiltrating tumor was found in the head of the pancreas, with several local metastases in lymph nodes. The surgeon (H.A.B.) was struck by the strange texture of the tumor, and pathological examination during operation of a tumor-containing lymph node was suggestive of apudoma. Therefore, a Whipple procedure was carried out, removing the complete pancreas and leaving several deposits of tumor infiltration in the surrounding tissue *in situ*. After 5 yr the patient is well and virtually without complaints. Retrospectively, she was known to have mild type II diabetes mellitus, which was well controlled with a sugar-free diet, and periods of loose stools, while asymptomatic gall stones were present.

Part of the tumor was dispersed and a total of  $900 \times 10^6$  tumor cells were plated at  $10^6$  cells/well. The tumor cells secreted  $18 \pm 2$  ng somatostatin/well  $\cdot 24$  h; 5 mM dibutyl cAMP stimulated hormone release to  $33 \pm 2$  ng ( $P < 0.01$  vs. control), while 3 mM calcium stimulated hormone release to  $27 \pm 2$  ng ( $P < 0.05$  vs. control). Low concentrations of 1 and 10 nM octreotide did not suppress, but 100 nM octreotide effectively suppressed somatostatin release by these tumor cells by 78% ( $P < 0.01$  vs. control; Table 3).

It was decided to ask the patient to undergo a somatostatin analog scan 5 yr after operation. This scan revealed the presence of somatostatin receptor-positive tumor tissue in the liver hilus, the peritoneum, a lymph node on the left side of the neck, and two ribs. Because the patient is asymptomatic, it was decided not to treat her at present.

TABLE 3. Somatostatin release by the cultured tumor cells prepared from the endocrine pancreatic tumor of patient 4

	Somatostatin (ng/well $\cdot 24$ h)
Control	$17.9 \pm 0.7$
Octreotide (1 nM)	$15.8 \pm 0.4$
Octreotide (10 nM)	$14.7 \pm 0.3$
Octreotide (100 nM)	$3.1 \pm 0.4^*$

Incubation time was 24 h. Values are the mean  $\pm$  SEM; four wells per group. The studies were carried out on day 4 of culture.

\*  $P < 0.01$  vs. control.

#### Patient 5

This 64-yr-old man underwent laparotomy 5 yr ago. At operation a carcinoma ( $12 \times 17$  cm) was found in the head of the pancreas which infiltrated into the surrounding tissue. It was decided that this tumor was inoperable. Pathological examination of a biopsy showed an undifferentiated carcinoma. No specific treatment seemed available for the patient, and only palliative therapy directed to alleviate pain was given. Over the next 5 yr, however, no obvious deterioration of the clinical condition occurred, although the pain in the abdomen was often excruciating requiring opiate drugs.

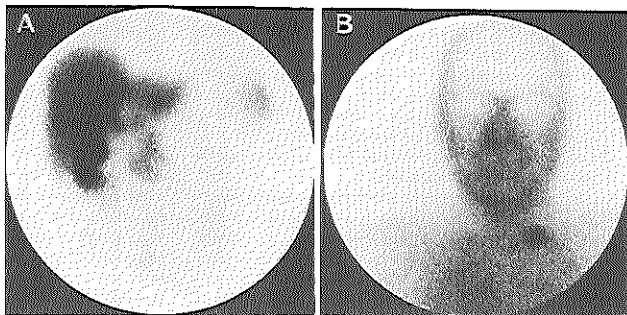
Because of the discrepancy between the actual clinical course and what had been expected, this patient underwent an [ $^{125}$ I]Tyr<sup>11</sup>-octreotide scan. Immediately after injection of the isotope labeled to the somatostatin analog a tumor was visualized in the region of the head of the pancreas. In Fig. 5A, the picture after 25 min is shown; both the liver and gallbladder can be clearly seen, as well as the spleen and, in the center, the tumor. The tumor remained visible 48 h after isotope administration. In Fig. 5B it is seen that a somatostatin receptor-positive tumor is also present on the left side of the neck. A needle biopsy in this just palpable, slightly enlarged lymph node in the neck revealed an undifferentiated carcinoma which was histologically similar to that found 5 yr previously. Further examinations proved that both tumor deposits were in fact apudomas (chromogranin positive and Grimelius positive), but immunohistochemistry was negative for 6 endocrine pancreatic hormones. Further clinical examination of the patient did also not reveal signs of symptoms of hypersecretion of hormones. This patient was treated thereafter with octreotide (three doses of 100  $\mu$ g/day, sc). This resulted in a considerable decrease in pain, enabling a decrease in the use of opiate drugs. After 6 months of therapy, reevaluation of tumor size by CT scanning did not reveal a change in the size of the pancreatic tumor.

#### Discussion

With the exception of insulinomas, most endocrine pancreatic tumors are malignant and have already metastasized at the time of diagnosis (1, 2). Surgery is



FIG. 5. A, the [ $^{125}$ I]Tyr<sup>3</sup>-octreotide scan in patient 5, 25 min after isotope administration. The normal liver, the gallbladder, the bile ducts, and a normal spleen are visible as well as a somatostatin receptor-positive tumor in the region of the head of the pancreas. B,  $\gamma$ -Camera picture of the head of the same patient 90 min after isotope administration. Note the somatostatin receptor-positive lymph node on the left side of the neck.



generally considered to be the primary treatment, but debulking of the tumor is often the only option when metastases are discovered during operation (2). Palliative treatment with cytostatic drugs and/or interferon and hepatic arterial embolization have been shown to be of temporary benefit in varying numbers of patients (3-5). Octreotide effectively controls the clinical syndromes related to hypersecretion of hormones by these tumors: invalidating diarrhea, dehydration and hypokalemia, peptic ulceration, life-threatening attacks of hypoglycemia, and necrolytic skin lesions were reported to improve during chronic therapy with 100-600  $\mu$ g octreotide daily in most patients (6-15). In parallel, we previously showed that 10 of 14 hormone-producing endocrine pancreatic tumors contained large numbers of high affinity binding sites for the somatostatin analog [ $^{125}$ I]Tyr<sup>3</sup>-octreotide (16). In the present study we extended in both gastrinoma patients the concept of a close relation between the inhibitory effects of octreotide on hormone secretion by this type of tumor *in vivo* and the presence of high numbers of high affinity somatostatin analog-binding sites on the tumor tissue *in vitro*. In the insulinoma patient, however, no suppressive effect of octreotide on tumorous insulin release was noted, while serum glucose levels even slightly decreased further in response to the drug. In parallel, several *in vitro* investigations underlined the virtual absence of somatostatin analog receptors on this tumor and the insensitivity of the cultured tumor cells to the analog.

The *in vitro* studies carried out with the cultured cells prepared from the two patients harboring a gastrinoma and the patient with the somatostatinoma might aid in understanding the mechanism of action of octreotide on endocrine pancreatic tumors. Octreotide directly inhibited hormone release by the cultured gastrinoma cells in a dose- and time-dependent fashion. In a 24-h incubation the maximal inhibitory concentrations of the drug ranged to 0.1-10 nM. Apart from an inhibitory effect on hormone

secretion, the total amount of gastrin (as reflected by the amount of hormone released plus the intercellular content) was suppressed by the exposure to octreotide. It is interesting to note that somatostatin release by the tumor cells prepared from the tumor of patient 4 was also inhibited during incubation with octreotide, albeit at a higher concentration of 100 nM. This suggests that in this particular tumor basal hormone release was already under the influence of an autocrine-mediated inhibitory control of somatostatin, requiring a higher exogenous concentration of somatostatin analog to further suppress hormone release.

Somatostatin analogs have been shown to suppress tumor growth in some patients with endocrine pancreatic tumors. Maton (15) recently summarized the literature concerning the possible effects on tumor size of chronic octreotide therapy in 46 patients with malignant endocrine pancreatic tumors. These patients received between 200-1500  $\mu$ g octreotide/day for over 2 months; the size of the metastases increased during therapy in 20 (44%), remained unchanged in 18 (39%), and decreased in 8 (17%) patients. Reduction of tumor size was noted in 3 patients with gastrinoma, 3 with a VIPoma, and 1 with a GH-releasing hormone-producing tumor. Our study shows an antiproliferative effect of octreotide on the cultured cells prepared from the tumor of patient 1. The mechanism of action of octreotide on hormone release and hormone synthesis by these tumor cells seemed to differ from that of the cytostatic compounds vincristin and adriamycin, in that octreotide more potently inhibited hormone release. The absence of an antiproliferative effect of octreotide and the two cytostatic drugs on the cultured tumor cells of patient 2 might reflect the slow growth of this tumor; one tumor-containing lymph node was found 7 yr after removal of the primary tumor. Probably, the cells of this tumor did not grow in culture, also explaining the absence of an effect of vincristin and adriamycin. The clinical history of patient 1 suggested

rapid tumor growth in the period preceding the operation. Our studies might, therefore, explain in part the often rather unconvincing observations of tumor growth inhibitory effects of octreotide in patients with metastatic endocrine pancreatic tumors. Most of these tumors are (very) slow growing cancers, and possible tumor growth inhibitory effects of octreotide in this category of patients might only be detected during extensive long term prospective placebo-controlled trials.

A new aspect of our present study is the application of the technique of *in vivo* imaging of somatostatin receptor-positive tumors (17). In this technique [ $^{125}$ I]-labeled Tyr<sup>3</sup>-octreotide, a somatostatin analog similar to octreotide in its biological actions, is injected iv. It is an easy, relatively cheap, and harmless technique, which in four of the five patients with endocrine pancreatic tumors investigated visualized both the primary and, in three cases (patients 1, 4, and 5), previously unknown metastases. There was a close relationship between the *in vitro* detection of somatostatin receptors in the tumors using autoradiography and the  $\gamma$ -camera pictures obtained after injection of [ $^{125}$ I]-Tyr<sup>3</sup>-octreotide. This indicates, therefore, that the ligand binding to the tumor *in vivo* indeed represents binding to specific somatostatin receptors. Furthermore, the close correlation between the presence of somatostatin receptors on tumors and the *in vivo* or *in vitro* effects of octreotide on hormonal release from these tumors clearly indicates that these receptors are functional. This indeed points to a high specificity of this new technique of tumor imaging. It is presently not known how sensitive this technique is in the detection of very small endocrine pancreatic tumors. Nevertheless, we already know that carcinoids can be visualized even when less than 1 cm in diameter. Our data showing that metastases of these tumors often retain a similar number and affinity of somatostatin receptors as the primary tumors are of importance with regard to both the future role of the *in vivo* imaging technique and therapy with octreotide. In the scanning procedure a small amount of Tyr<sup>3</sup>-octreotide (<10  $\mu$ g) is injected iv. Therefore, this scanning might be a safe alternative to *in vivo* octreotide administration in the selection of insulinoma patients for chronic treatment with the drug.

There is a wide variation in the clinical presentation of endocrine pancreatic tumors in man. Most tumors present with signs and symptoms related to the hormonal hypersecretion from these tumors, but less frequently symptomatology is related to the tumor mass itself (2). In these latter cases the often undifferentiated tumors do not secrete considerable amounts of biologically active hormones, or the clinical syndrome is rather inconspicuous (1-3, 27). The five patients described in our study seem to represent this spectrum of clinical presentation well, as patients 1-3 presented with signs and symptoms

related to hypersecretion of gastrin and/or insulin, while in patients 4 and 5 the tumors had been detected only by signs and symptoms related to the local infiltration of tumor in the surrounding tissue. Interestingly, the clinical symptomatology of patient 4 with a somatostatinoma (mild diabetes mellitus, gallstones, and loose stools) had not been recognized before the operation, while the actual diagnosis in patient 5 was made only 5 yr after the operation. In this category of patients especially the use of the [ $^{125}$ I]-Tyr<sup>3</sup>-octreotide scan might be successful. We previously showed that exocrine adenocarcinomas of the pancreas do not contain somatostatin receptors (28). In none of three patients with ductal adenocarcinomas of the pancreas were the tumor or its metastases visualized with the somatostatin analog scan (data not shown). The use of this visualization method of somatostatin receptor-positive tumors might gain a place in the differential diagnosis of ductal adenocarcinomas and undifferentiated endocrine pancreatic cancers, especially among the small group of long term survivors with the former diagnosis.

## References

1. Stefanini P, Carboni M, Patrassi N, Basoli A. Beta-islet tumors of the pancreas: results in 1,067 cases. *Surgery*. 1974;75:597-609.
2. Bloom SR, Polak JM. Chiechogenomas, VIPomas and somatostatinomas. *Clin Endocrinol Metab*. 1980;9:285-97.
3. Moertel CG, Hanley JA, Johnson LA. Streptozocin alone compared with streptozocin plus fluorouracil in the treatment of advanced islet-cell carcinoma. *N Engl J Med*. 1980;303:1189-94.
4. Eriksson E, Oberg K, Alon G, et al. Treatment of malignant endocrine pancreatic tumours with human leucocyte interferon. *Lancet*. 1986;2:1307-8.
5. Alison DM. Therapeutic embolisation. *Br J Hosp Med*. 1978;20:707-15.
6. Wood SM, Kraenzlin ME, Adrian TE, Bloom SR. Treatment of patients with pancreatic endocrine tumours using a new long-acting somatostatin analogue SMS 201-995: symptomatic and peptide responses. *Gut*. 1985;26:438-44.
7. Maton PM, O'Dorisio TM, Howe BA, et al. Effect of a long-acting somatostatin analogue (SMS 201-995) in patients with pancreatic cholera. *N Engl J Med*. 1985;312:17-21.
8. Bonfils S. New somatostatin molecule for management of endocrine tumours. *Gut*. 1985;26:433-7.
9. Anderson JV, Bloom SR. Neuroendocrine tumours of the gut: long-term therapy with the somatostatin analogue SMS 201-995. *Scand J Gastroenterol*. 1986;21:115-28.
10. Kvols LK, Buck M, Moertel CG, et al. Treatment of metastatic islet cell carcinoma with a somatostatin analogue (SMS 201-995). *Ann Intern Med*. 1987;107:162-8.
11. O'Dorisio TM. Neuroendocrine disorders of the gastroenteropancreatic system. Clinical applications of the somatostatin analogue SMS 201-995. *Am J Med*. 1986;81(Suppl 6B):1-101.
12. Vinik AI, Tsai ST, Moturi AR, et al. Somatostatin analogue (SMS 201-995) in the management of gastroenteropancreatic tumors and diarrhea syndrome. *Am J Med*. 1986;81(Suppl 6B):23-41.
13. Eriksson E, Oberg K, Anderson T, et al. Treatment of malignant endocrine pancreatic tumors with a new long-acting somatostatin analogue, SMS 201-995. *Scand J Gastroenterol*. 1988;23:508-12.
14. Woltering EA, Mezell EJ, O'Dorisio TM, Fletcher WS, Howe B. Suppression of primary and secondary peptides with somatostatin analog in the therapy of functional endocrine tumors. *Surg Gynecol Obstet*. 1988;167:453-62.
15. Maton PN, moderator. Somatostatin and somatostatin analogue

- (SMS 201-995) in treatment of hormone-secreting tumors of the pituitary and gastrointestinal tract and non-neoplastic diseases of the gut. *Ann Intern Med.* 1989;110:353-56.
16. Reubi J-C, Hacki WH, Lamberts SWJ. Hormone-producing gastrointestinal tumors contain a high density of somatostatin receptors. *J Clin Endocrinol Metab.* 1987;65:1127-34.
  17. Krenning EP, Bakker WH, Breeman WAP, et al. Localisation of endocrine-related tumours with radioiodinated analogue of somatostatin. *Lancet.* 1989;1:242-244.
  18. Oosterom R, Verleun P, Uitterlinden P, et al. Studies on insulin secretion by monolayer cultures of normal and tumorous human pancreatic cells. Effects of glucose, somatostatin and SMS 201-995. *J Endocrinol Invest.* 1987;10:547-52.
  19. Oosterom R, Verleun T, Lamberts SWJ. Basal and dopamine-inhibited prolactin secretion by rat anterior pituitary cells effects of culture conditions. *Mol Cell Endocrinol.* 1983;29:197-212.
  20. Downs TR, Wilfinger WW. Fluorometric quantification of DNA in cells and tissue. *Anal Biochem.* 1983;131:538-47.
  21. Hofland LJ, van Koetsveld PM, Lamberts SWJ. Percoll density gradient centrifugation of rat pituitary tumor cells: a study of functional heterogeneity within and between tumors with respect to growth rates, prolactin production and responsiveness to the somatostatin analog SMS 201-995. *Eur J Cancer Clin Oncol.* In Press.
  22. Hofland LJ, van Koetsveld LJ, Verleun TM, Lamberts SWJ. Glycoprotein hormone alpha-subunit and prolactin release by cultured pituitary adenoma cells from acromegalic patients. *Clin Endocrinol (Oxf).* 1989;30:601-11.
  23. Reubi JC, Heitz PU, Landolt AM. Visualization of somatostatin receptors and correlation with immunoreactive GH and PRL in human pituitary adenomas. Evidence for different tumor subclasses. *J Clin Endocrinol Metab.* 1987;65:65-73.
  24. Reubi JC. New specific radioligand for one subpopulation of brain somatostatin receptors. *Life Sci.* 1985;36:1829-36.
  25. Reubi JC, Landolt AM. High density of somatostatin receptors in pituitary tumors from acromegalic patients. *J Clin Endocrinol Metab.* 1984;59:1148-51.
  26. Reubi JC, Cortes R, Maurer R, Probst A, Palacios JM. Distribution of somatostatin receptors in the human brain: an autoradiographic study. *Neuroscience.* 1986;18:329-46.
  27. Hainsworth JD, Johnson DH, Creco FA. Poorly differentiated neuroendocrine carcinoma of unknown primary site. *Ann Intern Med.* 1988;109:364-71.
  28. Reubi J-C, Horibarger U, Essed CE, Jeekel J, Klijn JGM, Lamberts SWJ. Absence of somatostatin receptors in human exocrine pancreatic adenocarcinomas. *Gastroenterology.* 1988;95:760-3.



## SOMATOSTATIN-RECEPTOR IMAGING IN THE LOCALIZATION OF ENDOCRINE TUMORS

S.W.J. LAMBERTS, W.H. BAKKER, J.-C. REUBI, AND E.P. KRENNING

**Abstract Background and Methods.** A number of different tumors have receptors for somatostatin. We evaluated the efficacy of scanning with  $^{123}\text{I}$ -labeled Tyr<sup>3</sup>-octreotide, a somatostatin analogue, for tumor localization in 42 patients with carcinoid tumors, pancreatic endocrine tumors, or paragangliomas. We then evaluated the response to octreotide therapy in some of these patients.

**Results.** Primary tumors or metastases, often previously unrecognized, were visualized in 12 of 13 patients with carcinoid tumors and in 7 of 9 patients with pancreatic endocrine tumors. The endocrine symptoms of these pa-

tients responded well to therapy with octreotide. Among 20 patients with paragangliomas, 8 of whom had more than one tumor, 10 temporal (tympanic or jugular), 9 carotid, and 10 vagal tumors could be visualized. One small tympanic tumor and one small carotid tumor were not seen on the scan.

**Conclusions.** The  $^{123}\text{I}$ -labeled Tyr<sup>3</sup>-octreotide scanning technique is a rapid and safe procedure for the visualization of some tumors with somatostatin receptors. A positive scan may predict the ability of octreotide therapy to control symptoms of hormonal hypersecretion. (*N Engl J Med* 1990; 323:1246-9.)

**L**ARGE numbers of high-affinity somatostatin binding sites have been found on most pancreatic endocrine tumors and carcinoid tumors.<sup>1-4</sup> In the majority of patients with such tumors, long-term therapy with octreotide successfully controls clinical symptoms, apparently through the somatostatin receptor-mediated inhibition of hormone release.<sup>5-7</sup>

We recently described the visualization of such tumors in vivo after the intravenous administration of a somatostatin analogue labeled with iodine-123.<sup>8</sup> In this study we describe the results of this scanning procedure in 42 patients with known endocrine tumors.

## METHODS

## Patients

We studied 13 patients with metastatic carcinoid disease (9 men and 4 women; mean age, 61 years [range, 24 to 78]). All 13 patients had histologically confirmed metastatic carcinoid disease. In seven patients the primary carcinoid tumor, which was in the gut in all seven, had been removed. The results of the scanning procedure in one of these patients have been described elsewhere.<sup>8</sup> In addition, we studied nine patients with pancreatic endocrine tumors (four men and five women; mean age, 62 years [range, 45 to 81]). In all nine patients the diagnosis was histologically confirmed after the removal of the primary tumor; in seven of them preoperative hormonal examinations suggested the presence of the tumor. In both the patients with metastatic carcinoid disease and those with pancreatic endocrine tumors, the spread of the disease had been investigated by CT scanning of the abdomen and ultrasonography. In five of the patients the results of scanning with  $^{123}\text{I}$ -labeled Tyr<sup>3</sup>-octreotide have been described elsewhere.<sup>8,9</sup> Twenty patients with paragangliomas (10 men and 10 women; mean age, 51 years [range, 16 to 83]) were also studied. In all of them the presence of at least one paraganglioma was suspected, because of earlier arteriography. All the patients gave informed consent to participate in the study, which was approved by the ethics committee of our hospital.

## Materials

The somatostatin analogues octreotide (Sandostatin, SMS 201-995) and Tyr<sup>3</sup>-octreotide (204-090) were obtained from Sandoz (Ba-

sel, Switzerland). The Tyr<sup>3</sup>-octreotide was labeled with  $^{123}\text{I}$  with use of chloramine-T.<sup>10</sup> As a final preparatory step the radiopharmaceutical agent was passed through a low protein-binding 0.22- $\mu\text{m}$  Millex-GV filter (Millipore, Milford, Mass.) in order to sterilize it. Depending on the results of the labeling procedure, the interval between injection and scintigraphy, and whether single-photon-emission CT (SPECT) was also performed, the doses of  $^{123}\text{I}$ -labeled Tyr<sup>3</sup>-octreotide ranged from 37 to 555 MBq, given as a bolus intravenous injection.<sup>8</sup> There were no side effects of the administration of  $^{123}\text{I}$ -labeled Tyr<sup>3</sup>-octreotide.

## Scanning

Planar and SPECT images were obtained with a large-field-of-view gamma camera (Counterbalance 3700, Siemens Gammasonics, Erlangen, Germany) equipped with a 190-KeV parallel-hole collimator. Generally, the field of view when the Tyr<sup>3</sup>-octreotide was injected covered the abdomen and some of the thorax. Starting at the time of the injection, digital images were recorded with a Gamma-II computer (Nuclear Diagnostics, Uppsala, Sweden) every 3 seconds for 2 minutes, then every 60 seconds for 28 minutes. In this 30-minute period analogue images were also obtained regularly. Thirty minutes after the injection, the patients underwent anterior and posterior whole-body static scintigraphy and, if indicated, SPECT. Static images, both analogue and digital, were obtained about 30 minutes and 2, 4, 24, and sometimes 48 hours after injection. Subtraction scintigraphy with albumin microcolloid labeled with technetium-99m (56 MBq; Albu-Res, Solco, Birsfelden, Switzerland) was performed in normal liver tissue.

We used a simple yes-or-no system to define the tumors as visualized during this scanning procedure, but always at a time when the surrounding organs were virtually devoid of radioactivity. Depending on the type and location of the tumor we chose different standard times and techniques of visualization. The best time for obtaining optimal gamma-camera pictures, as well as SPECT scans, is discussed below.

## RESULTS

## Patients with Carcinoid Tumors

Among the patients with metastatic carcinoid disease, 10 had undergone surgery and in 7 the primary carcinoid tumor had been removed. In the six whose primary carcinoid tumors had not been removed, the tumor was visualized; in all six the primary tumor was located in the small intestine. In 11 of the 13 patients liver metastases were detected; in 1 patient only peritoneal metastases were visualized, and in 1 no uptake of  $^{123}\text{I}$ -labeled Tyr<sup>3</sup>-octreotide was seen. The best gamma-camera pictures showing the metastases were obtained within 2 minutes after the injection of the

From the Departments of Medicine (S.W.J.L., E.P.K.) and Nuclear Medicine (W.H.B., E.P.K.), Erasmus University, Rotterdam, the Netherlands; and Sandoz Research Institute, Bern, Switzerland (J.-C.R.). Address reprint requests to Dr. Lambert, at the Department of Medicine, University Hospital Dijkzigt, 40 Molewaterplein, 3015 GD Rotterdam, the Netherlands.

Supported by grants from the Dutch Cancer Foundation and a special grant from the University Hospital Dijkzigt, Rotterdam.

isotope (when normal liver tissue had not yet been fully visualized) or after 24 to 48 hours (when the normal liver, gallbladder, and bile ducts no longer contained appreciable amounts of radioactivity). The  $^{123}\text{I}$ -labeled Tyr<sup>3</sup>-octreotide liver scan and the  $^{99\text{m}}\text{Tc}$ -labeled colloid scan of one of these patients are shown in Figures 1A and 1B. The tumor tissue visualized in the Tyr<sup>3</sup>-octreotide scan was localized mainly in the right lobe of the liver (Fig. 1A), whereas the  $^{99\text{m}}\text{Tc}$ -labeled colloid was localized mainly in the left lobe (Fig. 1B). The two scans show a greatly enlarged liver. Extrahepatic metastases (Fig. 1C) were found in lymph nodes on the left side of the neck in seven patients, and in bone (ribs, vertebrae, skull, or pelvis) in eight; in five there was evidence of peritoneal or intraabdominal metastases (or both). None of the 13 patients were known on the basis of symptoms, physical examination, or other imaging studies to have such extensive disease. In particular, the lymph nodes containing tumor in the left side of the neck had been detected on physical examination in only two of the patients who had abnormal scans in this region, but they were palpated in three other patients after the results of the Tyr<sup>3</sup>-octreotide scan were known. In the first four patients studied, the presence of carcinoid-tumor tissue in the lymph nodes in the neck, liver, or both and in the peritoneum was confirmed by needle biopsy. The one patient with no abnormality on the Tyr<sup>3</sup>-octreotide scan had extensive carcinoid tumor in the liver, abdomen, and thorax.

All 13 patients were subsequently treated with octreotide, given subcutaneously in divided doses varying from 150 to 600  $\mu\text{g}$  per day. In 10 of the 11 patients who had episodes of flushing, the number per

day decreased by 50 percent or more; in 8 of the 9 who had diarrhea, it decreased by 50 percent or more; and in all 4 with abdominal or bone pain (or both) the pain virtually disappeared. After three days of octreotide therapy, urinary excretion of 5-hydroxyindoleacetic acid decreased by 22 to 85 percent (mean, 36) in the six patients in whom it was measured. The patient whose carcinoid tumor was not visualized with  $^{123}\text{I}$ -labeled Tyr<sup>3</sup>-octreotide had no decrease in flushing episodes and diarrhea during two weeks of therapy with octreotide in doses of up to 1500  $\mu\text{g}$  per day.

#### Patients with Pancreatic Endocrine Tumors

In seven patients with pancreatic endocrine tumors, the primary tumors were visualized after the injection of  $^{123}\text{I}$ -labeled Tyr<sup>3</sup>-octreotide. Three patients had gastrinomas, two insulinomas, one a somatostatinoma, and one an undifferentiated endocrine pancreatic tumor. The size of the primary tumors in these patients ranged from 2 to 14 cm in diameter. Metastases were visualized in four of the seven patients. In none of these four patients had the metastases (in lymph nodes in the neck in two, bone in one, and liver in two) been detected earlier. In five patients a single subcutaneous dose of 50  $\mu\text{g}$  of octreotide substantially decreased the secretion of hormone by the tumor from two to six hours after administration. In the patient with an undifferentiated endocrine pancreatic tumor in whom no hormonal hypersecretion was detected, long-term therapy with octreotide (300  $\mu\text{g}$  a day for six months) resulted in a decrease in upper abdominal pain, but no change in tumor size as evaluated by CT scanning. In four of the patients with positive scans, *in vitro* autoradiography confirmed the presence of large numbers of high-affinity  $^{123}\text{I}$ -labeled

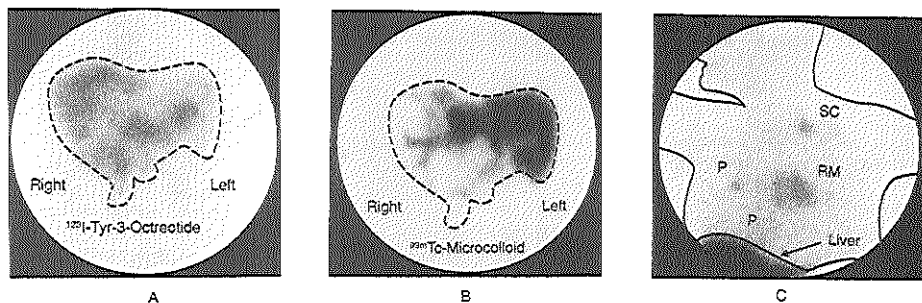


Figure 1. Primary Tumor and Metastases in a Patient with Metastatic Carcinoid Disease.

Panel A shows a gamma-camera picture of the liver 24 hours after the administration of  $^{123}\text{I}$ -labeled Tyr<sup>3</sup>-octreotide. Note the tumor deposits positive for somatostatin receptors, mainly in the right lobe of the liver. Panel B shows a  $^{99\text{m}}\text{Tc}$ -labeled colloid scan of the liver in the same patient 20 minutes after injection. Most of the left lobe appears intact, whereas the liver tissue containing tumor is not visualized. Note the enlargement of the liver in both scans. Panel C shows carcinoid metastases in a supraclavicular lymph node on the left side (SC), in the retroperitoneum (RM), and in the pleura (P) 30 minutes after the administration of  $^{123}\text{I}$ -labeled Tyr<sup>3</sup>-octreotide (anterior view) ( $\times 2$ ).

Tyr<sup>3</sup>-octreotide binding sites. In two patients the tumors were not visualized after the administration of Tyr<sup>3</sup>-octreotide. Both patients had an insulinoma, and neither tumor bound any <sup>123</sup>I-labeled Tyr<sup>3</sup>-octreotide *in vitro*.

#### Patients with Paragangliomas

In all 20 patients with paragangliomas, the tumors were visualized after the administration of <sup>123</sup>I-labeled Tyr<sup>3</sup>-octreotide. Ten of the 11 temporal tumors (tympanic or jugular), 9 of the 10 carotid tumors, and all 10 vagal tumors were visualized (Fig. 2). Two tumors were not visualized in these 20 patients; one patient had a small (less than 5 mm) tympanic-nerve paraganglioma, and another patient had a small (3 mm) carotid tumor. Eight patients had more than one tumor deposit. The smallest tumors visualized were about 1 cm in diameter. The specificity of our findings was confirmed by pathological examination of the tumors in 15 patients and by arteriography, CT, or both in the other 5.

#### DISCUSSION

Octreotide is currently used to treat patients with metastatic carcinoid and pancreatic endocrine tumors.<sup>5-7</sup> Its administration results in a remarkable improvement in the clinical condition of most patients, mainly through the suppression of hormonal hypersecretion. We have previously found that most such tumors, especially those in patients with a good response to octreotide therapy, contain large numbers of octreotide receptors.<sup>1,4</sup> The relative affinity of the so-

matostatin receptors on most human tumors for natural somatostatin-14, its precursor somatostatin-28, and Tyr<sup>3</sup>-octreotide varies; in most instances the affinity for Tyr<sup>3</sup>-octreotide is slightly higher than that for somatostatin-14 or somatostatin-28.<sup>1,3</sup>

In 12 of 13 patients with metastatic carcinoid disease and in 7 of 9 patients with pancreatic endocrine tumors, the *in vivo* imaging procedure using <sup>123</sup>I-labeled Tyr<sup>3</sup>-octreotide provided information concerning the localization of the primary tumors, the secondary spread of the disease, or both. Virtually all the patients had previously undetected metastases. The identification of tumor tissue in lymph nodes on the left side of the neck in seven patients with carcinoid tumors and two with endocrine pancreatic tumors underlines the value of a thorough examination in such patients. In one patient with carcinoid disease in whom the scan was negative, long-term octreotide therapy had no beneficial clinical effect, suggesting that the patient's tumor had no receptors. Similarly, no receptors could be detected on the insulinoma tissue of the two patients in whom the *in vivo* scan was negative.

The <sup>123</sup>I-labeled Tyr<sup>3</sup>-octreotide imaging technique was also used successfully in the localization of paragangliomas. Such tumors are often difficult to localize, and in most patients arteriography is necessary to confirm the diagnosis.<sup>11,12</sup> Of considerable importance was the localization of multiple paragangliomas in eight patients.

We found that tumors in the abdomen were well visualized within 30 minutes after the administration of the isotope, before the surrounding background activity in the liver, biliary tract, and gastrointestinal tract was so considerable that it became difficult to distinguish between tumor and physiologic uptake. Additional scans were possible 24 hours later, when the organs again contained little radioactivity. SPECT proved to be of great value in localizing the site of Tyr<sup>3</sup>-octreotide uptake in tumors, especially when the tumors were located close to sites with physiologic uptake of radioactivity. Tumors positive for somatostatin receptors in the chest, neck, and skull, however, can be readily visualized at any time 30 to 240 minutes after the administration of the isotope because the background level of radioactivity is very low by that time.

We did not correlate the degree of radionuclide uptake in these tumors with the extent of the biochemical response or the clinical responsiveness to short-term or long-term octreotide. Uptake of <sup>123</sup>I-labeled Tyr<sup>3</sup>-octreotide was found, however, in all tumors with a clinical or biochemical response to a single dose of octreotide or to long-term administration. Thus, <sup>123</sup>I-labeled Tyr<sup>3</sup>-octreotide imaging may be useful in predicting responsiveness to octreotide therapy.

We conclude that <sup>123</sup>I-labeled Tyr<sup>3</sup>-octreotide imaging is a quick and safe way to identify tumors that have somatostatin receptors, and tumors as small as 1 cm in diameter (e.g., paragangliomas) can be detected. We

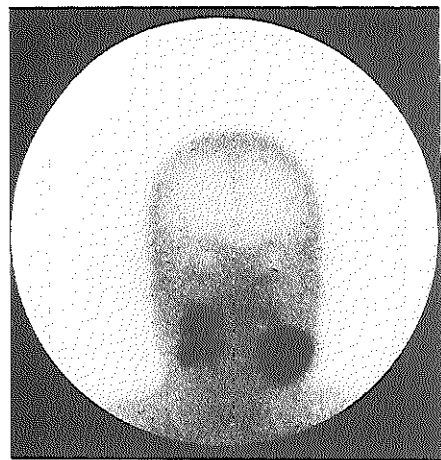


Figure 2. Gamma-Camera Picture Four Hours after the Administration of <sup>123</sup>I-Labeled Tyr<sup>3</sup>-Octreotide in a Patient with Multiple Paragangliomas, Showing Bilateral Carotid Paragangliomas and One Vagal Paraganglioma (Anterior View).

found this technique to be valuable in locating not only primary but also secondary deposits of these tumors, which may be very difficult to localize with current diagnostic techniques. Although these results are encouraging, the sensitivity and specificity of this scanning procedure in the localization of such tumors must be confirmed by studies of larger numbers of patients.

# REFERENCES

1. Reubi J-C, Hackl WH, Lamberts SW. Hormone-producing gastrointestinal tumors contain a high density of somatostatin receptors. *J Clin Endocrinol Metab* 1987; 65:1127-34.
2. Reubi J-C, Maurer R, von Werder K, Torhorst J, Klijn JG, Lamberts SW. Somatostatin receptors in human endocrine tumors. *Cancer Res* 1987; 47:551-8.
3. Reubi J-C, Lang W, Maurer R, Koper JW, Lamberts SW. Distribution and biochemical characterization of somatostatin receptors in tumors of the human central nervous system. *Cancer Res* 1987; 47:5758-64.
4. Kvols LK, Reubi J-C. Treatment of metastatic carcinoid tumors with somatostatin analogue (octreotide) and correlation of response with presence of somatostatin receptors. Presented at the International Symposium on Somatostatin, Montreal, 1989. abstract.
5. Kvols LK, Moertel CG, O'Connell MJ, Schutt AJ, Rubin J, Hahn RG. Treatment of the malignant carcinoid syndrome: evaluation of a long-acting somatostatin analogue. *N Engl J Med* 1986; 315:663-6.
6. Kvols LK, Buck M, Moertel CG, et al. Treatment of metastatic islet cell carcinoma with a somatostatin analogue (SMS 201-995). *Ann Intern Med* 1987; 107:162-8.
7. O'Donoghie TM, ed. Neuroendocrine disorders of the gastroenteropancreatic system: clinical applications of the somatostatin analogue SMS 201-995. *Am J Med* 1986; 81:Suppl 6B:1-101.
8. Krenning EP, Bakker WH, Breeman WAP, et al. Localization of endocrine-related tumours with radioiodinated analogue of somatostatin. *Lancet* 1989; 1:242-4.
9. Lamberts SWJ, Hofland LJ, van Koetsveld PM, et al. Parallel in vivo and in vitro detection of functional somatostatin receptors in human endocrine pancreatic tumors: consequences with regard to diagnosis, localization, and therapy. *J Clin Endocrinol Metab* 1990; 71:566-74.
10. Bakker WH, Krenning EP, Breeman WA, et al. Receptor scintigraphy with a radio iodinated somatostatin analogue: radiolabeling, purification, biological activity and in vivo application in animals. *J Nucl Med* 1990; 31:1501-9.
11. Glenner G, Grimbley P. Tumors of the extra adrenal paraganglion system. *Annals of tumor pathology. Series 2, Fascicle 9*. Washington, D.C.: Armed Forces Institute of Pathology, 1974.
12. Pauw KH, Krenning EP, van Urk H, et al. Scintigraphy of glomus tumors with <sup>123</sup>I-labeled Tyr<sup>3</sup>-octreotide, a synthetic somatostatin analogue. Presented at the Politzer Society of Otolaryngology, Las Palmas, Spain, 1989. abstract.

© Copyright, 1990, by the Massachusetts Medical Society  
Printed in the U.S.A.



## Treatment With Sandostatin and In Vivo Localization of Tumors With Radiolabeled Somatostatin Analogs

Steven W.J. Lamberts, Willem H. Bakker, Jean-Claude Reubi, and Erik P. Krenning

The presence of high numbers of somatostatin receptors seems to be the basis for the successful control by Sandostatin<sup>®</sup> of hormonal hypersecretion by most growth hormone-secreting pituitary adenomas, endocrine pancreatic tumors, and carcinoids. In this report, we present preliminary data on in vivo somatostatin receptor imaging with a <sup>123</sup>I-coupled somatostatin analog (204-090) in patients with these types of tumors.

© 1990 by W.B. Saunders Company.

SOMATOSTATIN is a regulatory hormone or tissue factor that plays an inhibitory role in the normal regulation of several organ systems, including the central nervous system, the hypothalamus and the pituitary gland, the gastrointestinal tract, and the exocrine and endocrine pancreas.<sup>1-3</sup> Recently, Sandostatin became available for routine clinical use: it is a somatostatin analog that has several characteristics different from native somatostatin: (1) it inhibits growth hormone (GH) preferentially over insulin; (2) it has a longer half-life in the circulation, causing a prolonged inhibitory effect in target organs of somatostatin; (3) it is active after subcutaneous administration; and (4) administration of Sandostatin is not followed by rebound hypersecretion of hormones (see ref 4).

Somatostatin receptors remain present on a variety of tumors that arise in tissues that also contain these receptors in the normal state. High numbers of somatostatin receptors have been found on GH-secreting pituitary tumors and on most metastatic endocrine pancreatic tumors and carcinoids.<sup>5-7</sup> Sandostatin treatment normalizes clinical symptomatology in most acromegalic patients, while GH hypersecretion and elevated circulating insulin-like growth factor type 1 (IGF-1) levels are well controlled.<sup>8</sup> Hormonal hypersecretion from endocrine pancreatic tumors and carcinoids is also suppressed during Sandostatin therapy in most patients.<sup>9,10</sup> This results in rapid improvement in the quality of life, while preliminary evidence of control of tumor growth has been presented (see ref 4).

It was remarkable that in vitro autoradiographic studies of these tumors virtually always revealed very high densities of somatostatin binding sites, which contrasted relatively sharply to those found on the surrounding "normal" tissue.<sup>6,7</sup> The presence of higher numbers of somatostatin receptors on many of these tumors was also reflected by the observation

that one single subcutaneous administration of 50 to 100 µg Sandostatin suppressed tumorous hormone secretion (ie, in acromegalic or gastrinoma patients) much longer than normal hormone secretion.<sup>8</sup>

These considerations led us to explore whether it might be possible to detect somatostatin receptor positive tumors in vivo by the administration of a radioactive iodine-labeled analog.<sup>11</sup> 204-090 is a Sandostatin analog with tyrosine in position 3, substituting for phenylalanine. The biological activities of Sandostatin and 204-090 are similar. <sup>123</sup>I-bound 204-090 (37-555 mBq) was injected intravenously (IV) in patients who were suspected to have somatostatin-receptor positive tumors, and planar or emission computed tomography (ECT) images were made with a gamma camera. After the bolus injection of radioiodinated 204-090, rapid accumulation of radioactivity was seen in the liver. Approximately 50% of the activity was cleared from the bloodpool within 2 minutes after IV injection. Localization of the primary tumors and their (previously often unknown) metastases with radioiodinated 204-090 was possible in five of six endocrine pancreatic tumors (the sixth patient had a 204-090 receptor-negative insulinoma) and in 12 of 12 patients with metastatic carcinoid disease. The detection of metastases in lymph nodes, bone, and liver points toward the powerful discriminating ability of this technique. It also confirms previous in vitro observations that showed that metastases of somatostatin receptor-positive tumors remain receptor-positive.<sup>6</sup> The observed accumulation of radionuclide at the site of the tumor after IV injection appears to be instantaneous and prolonged, in contrast to the bloodpool activity, which rapidly decreases.

In Figs 1A-D, the dynamics of this in vivo somatostatin receptor imaging technique in one of our patients with a metastatic carcinoid can be clearly seen. In Fig 1A, both the heart (top) and the liver are visualized 2 minutes after isotope administration, while a dense metastasis is visible in the lower margin of the liver. After 30 minutes (Fig 1B), radioactivity has disappeared from the heart, while more somatostatin receptor-positive metastases are visible now throughout the liver. In addition, the spleen is visualized. Note that the huge metastasis in the right upper part of the liver is not homogeneous; this is caused by central necrosis within this metastasis. In Fig 1C, the liver of this patient is just visible after 21 hours, while the somatostatin receptor-positive carcinoid

From the Departments of Medicine and Nuclear Medicine, Erasmus University, Rotterdam, The Netherlands; and Sandoz Research Institute, Berne, Switzerland.

Address reprint requests to Steven W.J. Lamberts, MD, Department of Medicine, University Hospital Dijkzigt, 60 Malewakerplein, 3015 GD Rotterdam, The Netherlands.

© 1990 by W.B. Saunders Company.  
0026-0495/90/3909-2040\$03.00/0

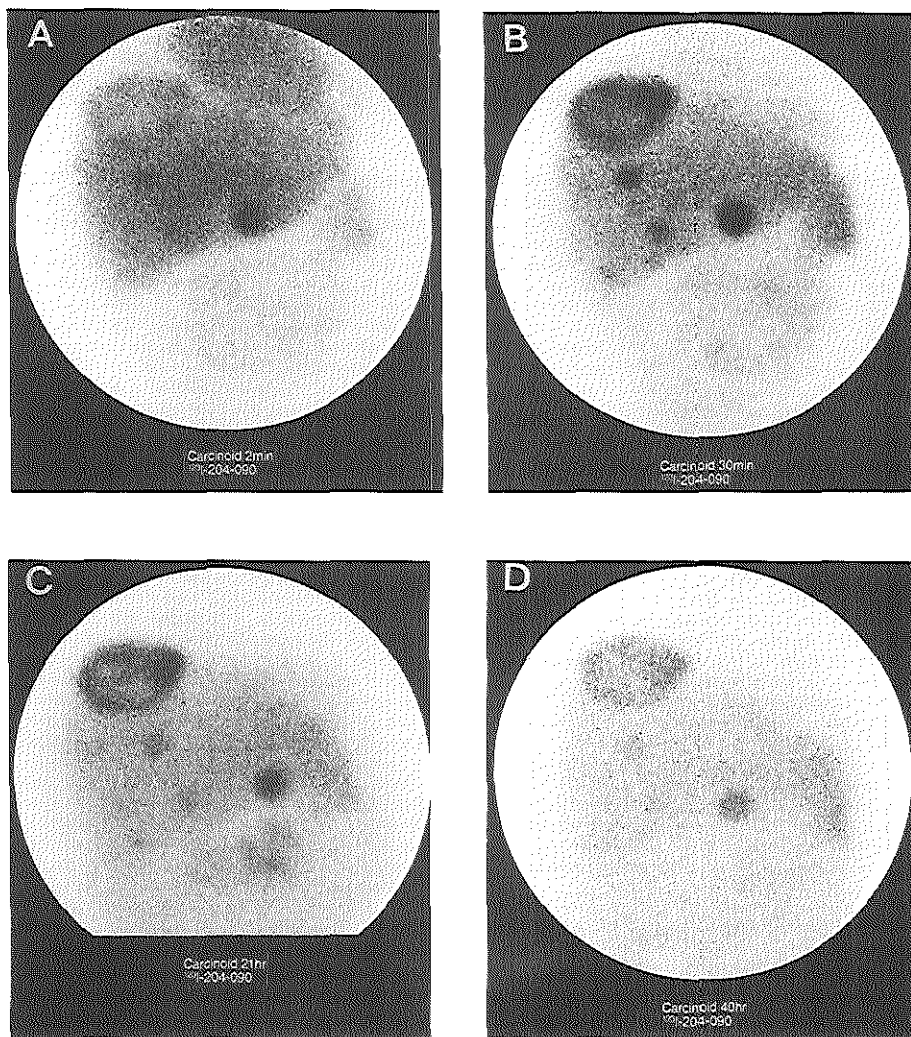


Fig 1. The dynamics of somatostatin receptor imaging in a patient with metastatic carcinoid syndrome. Gamma-camera pictures. (A) 2 minutes, (B) 30 minutes, (C) 21 hours, and (D) 40 hours after  $^{125}\text{I}$ -204-090 administration.

metastases remain positive even up till 40 hours after administration of the  $^{123}\text{I}$ -204-090 (Fig 1D). Whole-body scanning of this carcinoid patient also revealed a somatostatin receptor-positive metastasis in a lymph node on the left side of the neck (Fig 2).

Apart from endocrine pancreatic tumors and carcinoids, we extended our studies on the use of the somatostatin receptor imaging technique also to other tumors of the amine precursor uptake and decarboxylation (APUD)-cell system: in 18 of 18 patients with paragangliomas, the tumor could be visualized. In four of these patients previously unknown multiple tumor localizations were detected. All three small-cell lung cancers, as well as one neuroblastoma, but only one of four pheochromocytomas and one of five medullary thyroid carcinomas could be visualized. So, virtually all APUD cell tumors are somatostatin receptor-positive. However, in those tumors, which are known in general to synthesize and/or secrete somatostatin, the tumors can often not be visualized *in vivo*, probably because of desensitization of the somatostatin receptors on these tumors.

The *in vivo* receptor imaging technique can also be applied to patients with pituitary tumors. In all three acromegalic patients, in two patients with thyrotropin (TSH) secreting pituitary tumors, as well as in three patients with "nonfunctioning" pituitary tumors, the application of this technique successfully visualized the somatostatin receptor-positive tumors. Figure 3 shows an example of a suprasellarly extending GH-secreting pituitary tumor 24 hours after isotope administration.

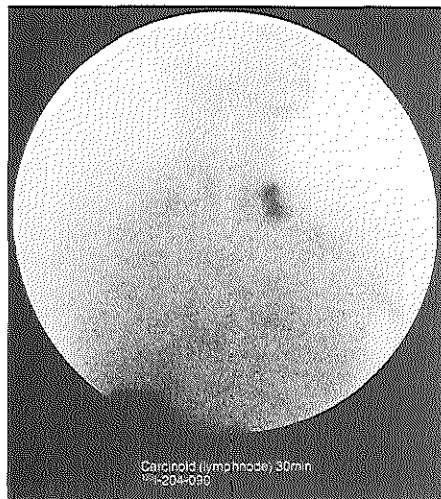


Fig 2. A somatostatin receptor-positive lymph node in the left part of the neck, 30 minutes after  $^{123}\text{I}$ -204-090 administration in a patient with metastatic carcinoid syndrome.

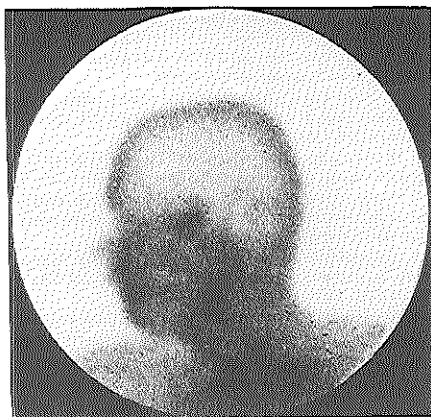


Fig 3. The 24-hour  $^{123}\text{I}$ -204-090 scan in a patient with a suprasellar GH-secreting pituitary adenoma.

Most well-differentiated human brain tumors, like meningiomas and low-grade astrocytomas, contain somatostatin receptors, while undifferentiated brain tumors mainly contain epidermal growth factor (EGF) receptors.<sup>12-14</sup> All five meningiomas and three low-grade astrocytomas investigated so far could be visualized with the  $^{123}\text{I}$ -204-090 imaging technique.

In conclusion, we have described in this report the preliminary results of the use of a new imaging technique with  $^{123}\text{I}$  coupled to a somatostatin analog. This method for the first time opens the possibility of localization of primary somatostatin receptor-positive tumors and their metastases. Preliminary data have been obtained that a hormone-secreting tumor that can be visualized by this method will also respond to therapy with Sandostatin, with a suppression of hormone release. Theoretically, this somatostatin receptor imaging technique represents a new approach that might be extended to other receptor-containing tumors. Therefore, it can be considered as a new, powerful alternative to tumor localization performed with monoclonal antibody technology. Many of these tumors show still considerable accumulation of radioactivity at the tumor site after 24 to 48 hours. This occurs despite the half-life of  $^{123}\text{I}$  of approximately 13 hours. In principle, this opens the possibility that radiotherapy of these somatostatin receptor-positive tumors with  $\beta$ -emitting radionuclides labeled to somatostatin analogs will be feasible in the future.

#### REFERENCES

- Guillemin R: Peptides in the brain: the new endocrinology of the neuron. *Science* 202:390-402, 1978
- Reichlin S: Somatostatin (part 1). *N Engl J Med* 309:1495-1501, 1983

3. Reichlin S: Somatostatin (part 2). *N Engl J Med* 309:1556-1563, 1983
4. Lamberts SWJ: Therapeutic effects of somatostatin analogs. *ISI Atlas of Science: Pharmacol* 179-184, 1988
5. Reubi JC, Landolt AM: High density of somatostatin receptors in pituitary tumours from acromegalic patients. *J Clin Endocrinol Metab* 59:1148-1153, 1984
6. Reubi JC, Maurer R, von Werder K, et al: Somatostatin receptors in human endocrine tumors. *Cancer Res* 47:551-558, 1987
7. Reubi JC, Hackl WH, Lamberts SWJ: Hormone-producing gastrointestinal tumors contain high density of somatostatin receptors. *J Clin Endocrinol Metab* 65:1127-1134, 1987
8. Lamberts SWJ, Uitterlinden P, Verschoor L, et al: Long-term treatment of acromegaly with the somatostatin analogue SMS 201-995. *N Engl J Med* 313:1576-1580, 1985
9. Williams G, Anderson JV, Williams SJ, et al: Clinical evaluation of SMS 201-995: long-term treatment in gut neuroendocrine tumours, efficacy of oral administration, and possible use in non-tumoural inappropriate TSH hypersecretion. *Acta Endocrinol* 286:26-36, 1987
10. Kvols LK, Moertel CG, O'Connell MJ, et al: Treatment of the malignant carcinoid syndrome. Evaluation of a long-acting somatostatin analogue. *N Engl J Med* 315:663-666, 1986
11. Krenning EP, Bakker WH, Breeman WAP, et al: Localisation of endocrine-related tumours with radioiodinated analogue of somatostatin. *Lancet* i:242-244, 1989
12. Reubi JC, Maurer R, Klijn JGM, et al: High incidence of somatostatin receptors in human meningiomas: Biochemical characterization. *J Clin Endocrinol Metab* 63:433-438, 1986
13. Reubi JC, Lang W, Maurer R, et al: Distribution and biochemical characterization of somatostatin receptors in tumors of the human central nervous system. *Cancer Res* 47:5758-5764, 1987
14. Reubi JC, Horisberger U, Lang W, et al: Coincidence of EGF receptors and somatostatin receptors in meningiomas but inverse, differentiation-dependent relationship in glial tumors. *Am J Pathol* 134:337-344, 1989

## SUMMARY AND CONCLUSION

In this thesis the development and application are described of two radiopharmaceuticals, which act on the basis of specific binding that exists between the peptide hormone *somatostatin* and its receptor.

*Chapter 1* starts with a brief historic review of the research on radionuclides and corresponding kinds of radiation. The introduction of the "tracer"-concept in botany by Hevesy in 1923 has actually marked the start of what we at present call in vivo nuclear medicine diagnostics. In 1926 followed the first in vivo application in man: the measurement of blood flow by means of the naturally occurring radium-C. In the next decennia a large number of discoveries has been made in the field of nuclear physics. By means of nuclear reactors and cyclotrons artificial radionuclides were produced. A number of them were rapidly applied in in vivo nuclear medicine. Radioactive iodine ( $^{131}\text{I}$ ) was long the most important tracer for human in vivo applications. Later, this radionuclide was replaced by the much shorter living technetium ( $^{99\text{m}}\text{Tc}$ ), which gamma energy also appeared to be much more favourable for imaging. Finally, in the historic review the first in vivo applications of radionuclides to tumor diagnostics are described.

The second part of the chapter describes the general biochemical principles of scintigraphic imaging. Various types of radiopharmaceuticals are mentioned, such as radionuclides in ionic form or as element, coupled to particles and aerosols, and as part of dissolved compounds. The last group is divided in non-specifically acting (i.e. with inert behaviour) and specifically acting (e.g., with particular metabolic properties) radiopharmaceuticals. Finally, radiopharmaceuticals are introduced which actions are based on binding to receptors on tumor cells. Therefore, these tumors can be imaged scintigraphically.

In the last part of the chapter the peptide hormone *somatostatin* is introduced. Somatostatin inhibits the function of various, mostly endocrine glands. Also, in many endocrine-active tumors which contain large numbers of somatostatin receptors, hormone production is inhibited by somatostatin. Somatostatin itself however, is not suitable for therapy, because it is rapidly degraded in vivo. The 8 amino acids-containing somatostatin-analogue *octreotide* is more stable in vivo than somatostatin itself (with 14 amino acids) because of its smaller cyclic structure along with two D-amino acids. Octreotide is now frequently used in the treatment of patients with hormone-producing tumors. Because of the receptor-mediated

action of octreotide it is concluded that radiolabeled somatostatin analogues are potentially suitable to visualize somatostatin receptor-positive tumors by means of the gamma camera.

In *Chapter 2* is described that octreotide derivatives bind specifically to somatostatin receptors. Already in 1985 [Tyr<sup>3</sup>]-octreotide has been successfully applied in vitro to detect somatostatin receptors in tumors. For this purpose, [Tyr<sup>3</sup>]-octreotide is labeled with radioactive iodine (<sup>125</sup>I). The research described in this chapter was done in order to investigate whether radiolabeled [Tyr<sup>3</sup>]-octreotide would be suitable as radiopharmaceutical for in vivo detection and visualization of somatostatin receptor-positive tumors, that are otherwise difficult to trace. [Tyr<sup>3</sup>]-octreotide was labeled with <sup>125</sup>I by the chloramine-T method. HPLC-investigations showed that predominantly monoiodo-[Tyr<sup>3</sup>]-octreotide (with strong somatostatin receptor-binding properties) is formed. Diiodo-[Tyr<sup>3</sup>]-octreotide (with diminished somatostatin receptor-binding properties) is formed in a much smaller amount. In addition, it was demonstrated that [<sup>125</sup>I-Tyr<sup>3</sup>]-octreotide, [Tyr<sup>3</sup>]-octreotide, and somatostatin itself inhibited the secretion of growth hormone by rat pituitary cells in a similar way. In vivo experiments were performed with <sup>125</sup>I-labeled [Tyr<sup>3</sup>]-octreotide, which is suitable for scintigraphic imaging in contrast to [<sup>125</sup>I-Tyr<sup>3</sup>]-octreotide. The compound was administered intravenously to control rats and rats having somatostatin receptor-positive pancreatic tumors. The radiopharmaceutical is rapidly cleared from the circulation by the liver. This results in a rapidly decreasing background radioactivity in favour of the detection of somatostatin receptor-positive processes, already very shortly after administration. Above the somatostatin receptor-positive tumors an increasing radioactivity was measured, allowing their scintigraphic imaging. The specificity of this detection was demonstrated by the observation that in rats in which the somatostatin receptors were previously blocked with a large excess of octreotide, only decreasing blood background could be measured above the tumors. It was concluded that radiolabeled [Tyr<sup>3</sup>]-octreotide is a promising radiopharmaceutical for diagnosis in humans, because various human tumors possess large numbers of receptors with high affinity for somatostatin.

*Chapter 3* deals with the first human applications of [<sup>125</sup>I-Tyr<sup>3</sup>]-octreotide. The metabolism of this somatostatin-analogue in humans has been investigated. Similar to the rat [<sup>125</sup>I-Tyr<sup>3</sup>]-octreotide was cleared very rapidly from the blood circulation mainly by the liver (nearly 85 % of the dose within 10 minutes), and the radionuclide became visible directly afterwards in the gallbladder and subsequently in the intestines. Three hours after injection still 70 % of radioactivity in the circulation consisted of intact [<sup>125</sup>I-Tyr<sup>3</sup>]-octreotide. The radioactivity in the urine showed a similar pattern. Later, an increasing amount of free iodide was found, pointing to degradation of the radiopharmaceutical in vivo. On the basis of the radioactivity in blood and excreta and of gamma camera measurements of the liver

and the gallbladder as a function of time the radiation dose of the most important organs was calculated. Thus, an effective dose equivalent (0.021 mSv/MBq) was determined, similar to that of other  $^{123}\text{I}$ -radiopharmaceuticals. At the end of the chapter the tumor-seeking properties of [ $^{123}\text{I}$ -Tyr $^3$ ]-octreotide are described followed by some examples of successful scintigraphy of somatostatin receptor-positive tumors.

*Chapter 4* starts with an enumeration of important disadvantages of [ $^{123}\text{I}$ -Tyr $^3$ ]-octreotide: (a) the limited availability of the pure radionuclide, (b) the time-consuming labeling and purification procedure, (c) the physical half-life of  $^{123}\text{I}$  (13.2 hours), which is so short that scintigraphy later than 24 hours after administration is difficult, and (d) the interfering background radiation in the upper abdominal area, where somatostatin receptor-positive tumors often are located. Because of these disadvantages a DTPA-conjugated somatostatin analogue, i.e. [DTPA-D-Phe $^1$ ]-octreotide, was developed which can be labeled with radioactive indium ( $^{111}\text{In}$ ,  $t_{1/2} = 2.8$  days) in a simple one-step procedure. The labeling appeared to be performed with retention of the somatostatin-like properties. [ $^{111}\text{In}$ -DTPA-D-Phe $^1$ ]-octreotide bound specifically to somatostatin receptors in rat brain cortex membranes, although not as strongly as the iodinated compound. Besides, the specific somatostatin-like biologic effect was demonstrated by a dose-dependent inhibition of growth hormone production by rat pituitary cells. It was noted, that this indium-labeled somatostatin analogue is very suitable for a simple "kit"-preparation.

*Chapter 5* describes the first in vivo application of [ $^{111}\text{In}$ -DTPA-D-Phe $^1$ ]-octreotide in rats. The biodistribution of the radiopharmaceutical after intravenous injection was investigated in control rats and in rats with somatostatin receptor-positive pancreatic tumors. Similar to [ $^{123}\text{I}$ -Tyr $^3$ ]-octreotide, the indium-labeled compound was rapidly cleared from the blood circulation. But in contrast to the predominant hepatic clearance of [ $^{123}\text{I}$ -Tyr $^3$ ]-octreotide, [ $^{111}\text{In}$ -DTPA-D-Phe $^1$ ]-octreotide is largely cleared by the kidneys. The majority of the administered dose was excreted into the urine in the form of the intact radiolabeled peptide, without significant degradation. Specific accumulation was demonstrated by ex vivo autoradiography in the anterior pituitary gland which contains somatostatin receptors. In the adrenals of rats in which the somatostatin receptors were not previously blocked with excess octreotide, considerably more radioactivity was measured than in those of blocked animals, which is in agreement with the presence of somatostatin receptors in this organ. The same held for the radioactivity measured in the tumors. The tumors were clearly detected with the gamma camera in the untreated rats but not in those treated with excess octreotide. Since [ $^{111}\text{In}$ -DTPA-D-Phe $^1$ ]-octreotide has a longer residence in the blood circulation as compared to [ $^{123}\text{I}$ -Tyr $^3$ ]-octreotide, the exposure of the tumor to the radiopharmaceutical is longer, although this results in higher background on the day of

injection. However, 24 hours after administration of [ $^{111}\text{In}$ -DTPA-D-Phe $^1$ ]-octreotide more radionuclide is cleared from the body as compared to [ $^{125}\text{I}$ -Tyr $^3$ ]-octreotide, with a consequently lower background. Furthermore, the interference in the upper abdomen as seen with [ $^{125}\text{I}$ -Tyr $^3$ ]-octreotide is not present after administration of [ $^{111}\text{In}$ -DTPA-D-Phe $^1$ ]-octreotide. Finally, the imaging of tumors 24 hours and later will be favoured by the longer physical half-life of  $^{111}\text{In}$ . In conclusion [ $^{111}\text{In}$ -DTPA-D-Phe $^1$ ]-octreotide was named a promising radiopharmaceutical for routine imaging of somatostatin receptor-positive tumors.

The scintigraphic application of [ $^{111}\text{In}$ -DTPA-D-Phe $^1$ ]-octreotide in man is introduced in *Chapter 6*. As in the animal model, the radiopharmaceutical was rapidly cleared from the blood and predominantly excreted via the kidneys. HPLC-investigations of urine demonstrated that [ $^{111}\text{In}$ -DTPA-D-Phe $^1$ ]-octreotide was excreted mainly in the intact form. Intestinal excretion amounted to only a few percent of the administered radionuclide. Based on the radioactivity-time courses in blood, excreta, kidneys, spleen and liver the radiation doses of the most important organs were determined. The calculated effective dose equivalent is 0.08 mSv/MBq, which is similar to other  $^{111}\text{In}$ -labeled radiopharmaceuticals. Scintigraphy by means of [ $^{111}\text{In}$ -DTPA-D-Phe $^1$ ]-octreotide was best performed 24 hours after administration of the radiopharmaceutical, when circulating background has considerably decreased. The sensitivity of the detection of somatostatin receptor-positive tumors appeared to be similar to that of [ $^{125}\text{I}$ -Tyr $^3$ ]-octreotide, with the exception of the upper part of the abdomen, where somatostatin receptor-positive tumors are frequently localized and where [ $^{111}\text{In}$ -DTPA-D-Phe $^1$ ]-octreotide shows much less background radiation.

Because the liver is an important organ in the degradation of many bioactive peptides, the hepatic metabolism of both radiolabeled somatostatin analogues was investigated. *Chapter 7* describes the use of the isolated rat liver perfusion system, in which the circulating medium as well as the excreted bile were radiochemically analyzed. Similar to in vivo studies, radioiodinated [Tyr $^3$ ]-octreotide appeared to be rapidly cleared from the circulating medium. Radioactivity was rapidly excreted into the bile as intact [ $^{125}\text{I}$ -Tyr $^3$ ]-octreotide. In contrast to [ $^{125}\text{I}$ -Tyr $^3$ ]-octreotide, [ $^{111}\text{In}$ -DTPA-D-Phe $^1$ ]-octreotide was hardly cleared by the liver: the amount of radioactivity in the medium remained almost constant during the study, whereas little radioactivity was found in the bile. These results show, that whereas [ $^{125}\text{I}$ -Tyr $^3$ ]-octreotide is rapidly cleared by the liver and is excreted in intact form into the bile, [ $^{111}\text{In}$ -DTPA-D-Phe $^1$ ]-octreotide is hardly handled by the liver. The results of the liver perfusion studies are in full agreement with the human and rat findings. The isolated rat liver perfusion system appears to be a convenient method for the study of the hepatic metabolism of potential radiopharmaceuticals. The results obtained with this system may be used to predict the in vivo metabolism of such compounds, although additional information about renal clearance is required.



The first more extensive clinical results of scintigraphy with radiolabeled somatostatin derivatives are described in the *Appendix-papers*. *Appendix I* deals with the first application of [ $^{125}\text{I}$ -Tyr $^3$ ]-octreotide to the localization of various endocrine somato-statin receptor-positive tumors. In *Appendix II* the agreement between in vitro study of the presence of somatostatin receptors, octreotide therapy, and in vivo scintigraphy, is described. It was concluded, that positive scintigraphy with [ $^{125}\text{I}$ -Tyr $^3$ ]-octreotide predicts an effective suppression by octreotide of hormone hypersecretion by these tumors. This conclusion was also drawn from the studies described in *Appendices III & IV*, in which patients with hormone-producing carcinoid tumors, endocrine pancreatic tumors, or pituitary adenomas, and patients with paragangliomas were investigated scintigraphically using [ $^{125}\text{I}$ -Tyr $^3$ ]-octreotide.

## CONCLUSION

During the past 10 years favourable results are obtained with specifically acting radiopharmaceuticals. It is remarkable, that this is especially the case with small molecules. The successful positron emission tomography (PET) of the brain, using small positron-emitting compounds, is well known. Unfortunately, application of PET-radiopharmaceuticals is limited for economic reasons, and mainly useful for diagnosis of brain and heart pathology. A broader indication field exists for radiolabeled monoclonal antibodies and their fragments: various tumors and infections may be traced because of the specific binding to antigens present on these processes. However, monoclonal antibody scintigraphy is frequently hindered by (a) slow clearance from the circulation, (b) minor accumulation in processes, and (c) high non-specific binding to various (non-target) tissues. Compared to the antibodies and their fragments (> 70 kD), much smaller compounds (< 2 kD) have two advantages: (1) the much more rapid clearance results in a low background, which favours scintigraphic imaging and, (2) diffusion into the extravascular space occurs more easily. The radioiodinated MIBG which is used for imaging pheochromocytoma and neuroblastoma, has gained importance in this group of low-molecular weight radiopharmaceuticals.

As small native bioactive peptides have been used in characterization of pathology *in vitro* already for a long period of time, it was decided to use derivatives of such compounds *in vivo* in order to image tumors on the basis of binding to native peptide receptors. *Octreotide* is an octapeptide, which has a bioactive site like that of the 14 amino acids-containing native peptide hormone *somatostatin*, a peptide with hormone release-inhibiting properties. Because of its larger stability as compared to the native peptide, octreotide is frequently used for therapy in patients with hormone-producing tumors. The action of octreotide is a receptor-mediated process. Like octreotide, [ $^{125}\text{I}$ -Tyr $^3$ ]-octreotide was known to bind in vitro to somatostatin receptors, present on cells of various tumors. In the

described studies, [ $^{123}\text{I-Tyr}^3$ ]-octreotide appeared to accumulate *in vivo* also in somatostatin receptor-positive tumor tissue after intravenous injection. By consequence, these tumors were imaged with the gamma camera. However, major drawbacks such as the strong background interference in the upper abdomen (where somatostatin receptor-positive tumors often are located) and the cumbersome preparation procedure led us to a second octreotide derivative with somatostatin receptor-binding properties: [DTPA-D-Phe $^1$ ]-octreotide. This peptide was radiolabeled with  $^{111}\text{In}$  in a simple one-step procedure without the need for further purification. *In vitro* indium-labeled [DTPA-D-Phe $^1$ ]-octreotide, like iodinated [ $^{123}\text{I-Tyr}^3$ ]-octreotide, showed somatostatin receptor-binding properties and somatostatin-like hormone release inhibition. However, *in vivo* the indium-labeled somatostatin analogue showed a metabolic behaviour, completely different from [ $^{123}\text{I-Tyr}^3$ ]-octreotide: in contrast to the hepatobiliary clearance and consequent intestinal degradation of [ $^{123}\text{I-Tyr}^3$ ]-octreotide, [ $^{111}\text{In-DTPA-D-Phe}^1$ ]-octreotide was cleared from the circulation by the kidneys without distinct degradation. The very fast disappearance of [ $^{123}\text{I-Tyr}^3$ ]-octreotide from the blood circulation was considered as an *advantage* for tumor scintigraphy because of the low background already shortly after administration (Chapter 2), while the much slower disappearance of [ $^{111}\text{In-DTPA-D-Phe}^1$ ]-octreotide was *also* regarded as a benefit (Chapter 5) because of a longer exposure to the tumor. This is understandable, considering that the advantage of [ $^{123}\text{I-Tyr}^3$ ]-octreotide only holds for the first hours after administration while the benefit of [ $^{111}\text{In-DTPA-D-Phe}^1$ ]-octreotide holds for 24 hours and later due to its much better excretion without degradation. Despite its somewhat lower receptor-binding properties [ $^{111}\text{In-DTPA-D-Phe}^1$ ]-octreotide turned out to be a better alternative for [ $^{123}\text{I-Tyr}^3$ ]-octreotide for imaging of somatostatin receptor-positive tumors, because of its more suitable metabolism, the longer half-life of the radionuclide, and its ready availability.

It has been demonstrated with [ $^{123}\text{I-Tyr}^3$ ]-octreotide and [ $^{111}\text{In-DTPA-D-Phe}^1$ ]-octreotide that it is possible to image somatostatin receptor-positive tumors (which are often difficult to localize with other techniques) with derivatives of a native peptide hormone by scintigraphy. Besides, if such tumor is endocrine-active, i.e. hormone-producing, a positive scintigraphy can predict efficient therapy with octreotide. Furthermore, it is likely that also *radiotherapy* with similar compounds, labeled with suitable, e.g.,  $\beta$ -emitting radionuclides, will be possible. Concerning the number of bioactive native peptides known, the two described radiopharmaceuticals will probably be followed by other small radiolabeled peptides for specific tumor targeting in the near future.

## SAMENVATTING EN CONCLUSIE

In dit proefschrift worden de ontwikkeling en de toepassing beschreven van twee radiofarmaca, waarvan de werking berust op de specifieke binding die bestaat tussen het peptidehormoon *somatostatine* en zijn receptor.

*Hoofdstuk 1* begint met een kort historisch overzicht van het wetenschappelijk onderzoek op het gebied van de radionucliden en de bijbehorende stralingssoorten. De introductie van het "tracer"-concept in de plantkunde door Hevesy in 1923 is feitelijk het startsein geweest voor wat we tegenwoordig de nucleair geneeskundige in vivo diagnostiek noemen. Al snel daarna (in 1926) volgde de eerste in vivo toepassing van een radionuclide bij de mens: de meting van de snelheid van de bloedsomloop met behulp van het in de natuur voorkomende radium-C. In de daarop volgende decennia werd een groot aantal ontdekkingen gedaan op het gebied van de kernfysica. Met behulp van kernreactoren en cyclotrons werden kunstmatige radionucliden geproduceerd, waarvan er een aantal snel hun toepassing vonden in de in vivo nucleaire geneeskunde. Nadat radioactief jodium ( $^{131}\text{I}$ ) aanvankelijk lange tijd de belangrijkste tracer was voor in vivo applicaties bij de mens, werd dit radionuclide van de eerste plaats verdrongen door het veel korter levende technetium ( $^{99\text{m}}\text{Tc}$ ), waarvan de gammastralingsenergie bovendien veel gunstiger bleek voor de beeldvormende diagnostiek. Het historisch overzicht vermeldt tenslotte de eerste in vivo toepassingen van radionucliden op het gebied van de tumordiagnostiek.

Het tweede gedeelte van het hoofdstuk beschrijft de algemene biochemische grondbeginselen, waarop scintigrafische beeldvorming berust. Aan de orde komen de verschillende typen radiofarmaca (met voorbeelden), zoals radionucliden in ionvorm of als element, gekoppeld aan deeltjes en aerosolen en als onderdeel van opgeloste verbindingen. In de laatstgenoemde categorie wordt onderscheid gemaakt tussen niet-specifiek (d.w.z. met een inert gedrag) en specifiek werkende radiofarmaca (d.w.z. met bijzondere metabole eigenschappen). Tenslotte wordt in dit gedeelte het accent gelegd op radiofarmaca, waarvan de werking berust op binding aan receptoren, die op tumoren aanwezig zijn. Als gevolg hiervan kunnen deze tumoren scintigrafisch in beeld gebracht worden.

In het laatste deel van het hoofdstuk wordt het peptidehormoon *somatostatine* geïntroduceerd. Somatostatine heeft een remmende werking op de functie van verschillende, meestal endocriene klieren. Veel endocrien actieve tumoren worden,

omdat zij grote aantallen receptoren voor somatostatine bevatten, in hun hormoonproductie geremd door somatostatine. Somatostatine zelf is echter niet geschikt voor therapie, omdat het in vivo snel wordt afgebroken. Het 8 aminozuren bevattende somatostatine-analoon *octreotide* heeft een biologisch actieve kern, die lijkt op die van somatostatine (met 14 aminozuren), en een grotere stabiliteit in vivo vanwege zijn kleinere cyclische structuur waarin zich bovendien twee D-aminozuren bevinden. Vanwege deze eigenschappen wordt octreotide nu frequent gebruikt bij de behandeling van patiënten met hormoon-producerende tumoren. Omdat de therapeutische werking van octreotide berust op de aanwezigheid van receptoren voor somatostatine, wordt geconcludeerd dat radioactief gemerkte somatostatine-analoga potentieel geschikt zijn om somatostatinereceptor-positieve tumoren met behulp van de gammacamera zichtbaar te maken.

In *Hoofdstuk 2* wordt beschreven dat octreotidederivaten, die een met somatostatine vergelijkbare biologisch actieve structuur hebben, specifiek binden aan de somatostatinereceptoren. Al sedert 1985 wordt de van octreotide afgeleide verbinding [Tyr<sup>3</sup>]-octreotide met succes toegepast om in vitro het bestaan van receptoren voor somatostatine in tumoren aan te tonen. Daartoe wordt dit peptide met radioactief jodium (<sup>125</sup>I) gemerkt. Het in dit hoofdstuk beschreven onderzoek had als doel na te gaan of radioactief gemerkt [Tyr<sup>3</sup>]-octreotide geschikt zou zijn als radiofarmacon voor het in vivo detecteren en zichtbaar maken van somatostatinereceptor-positieve tumoren, die vaak anderszins moeilijk zijn op te sporen. [Tyr<sup>3</sup>]-octreotide werd gemerkt met <sup>125</sup>I met behulp van de chloramine-T methode. HPLC-onderzoek wees uit dat hoofdzakelijk monojodo-[<sup>125</sup>I-Tyr<sup>3</sup>]-octreotide (met sterke somatostatinereceptor-bindende eigenschappen) wordt gevormd. Van di-jodo-[<sup>125</sup>I-Tyr<sup>3</sup>]-octreotide (met minder sterke somatostatinereceptor-bindende eigenschappen) wordt veel minder gevormd. Bovendien werd aangetoond, dat [<sup>125</sup>I-Tyr<sup>3</sup>]-octreotide de secretie van groeihormoon door rattehypofysecellen in gelijke mate afremt als het ongemerkte [Tyr<sup>3</sup>]-octreotide en somatostatine zelf. In vivo experimenten werden uitgevoerd met het voor scintigrafie geschikte <sup>123</sup>I gebonden aan [Tyr<sup>3</sup>]-octreotide. De verbinding werd intraveneus toegediend aan controleratten en ratten, die somatostatinereceptor-positieve pancreastumoren hadden. Het radiofarmacon wordt snel door de lever geklaard, waardoor de achtergrondactiviteit navenant daalt ten gunste van de vroegtijdige detectie van somatostatinereceptor-positieve processen, al zeer kort na de toediening. Ter plaatse van de somatostatinereceptor-positieve tumoren werd een stijgend activiteitsverloop gemeten, waardoor de tumoren scintigrafisch in beeld konden worden gebracht. De specificiteit van deze detectie werd aangetoond door de waarneming, dat in ratten waarin de somatostatinereceptoren tevoren door een grote overmaat octreotide geblokkeerd waren, ter plaatse van de tumor slechts een dalende bloedachtergrond werd gemeten. Geconcludeerd werd dat radioactief gelabeld [Tyr<sup>3</sup>]-octreotide een veelbelovend radiofarmacon voor de mens zou kunnen zijn, gezien het feit dat verschillende humane tumoren grote aantallen receptoren met een hoge affiniteit

voor somatostatine bezitten.

*Hoofdstuk 3* behandelt de eerste humane toepassingen van [ $^{123}\text{I}$ -Tyr $^3$ ]-octreotide. Het onderzoek naar het humane metabolisme van dit somatostatine-analoon wordt beschreven. Evenals bij de rat werd [ $^{123}\text{I}$ -Tyr $^3$ ]-octreotide zeer snel uit de bloedbaan geklaard door de lever (bijna 85 % van de dosis binnen 10 minuten), terwijl direct daarna het radionuclide zichtbaar werd in de galblaas en daarna in de darmen. Drie uur na injectie bestond nog 70 % van de nog aanwezige radioactiviteit in de circulatie uit intact [ $^{123}\text{I}$ -Tyr $^3$ ]-octreotide. De radioactiviteit in de urine vertoonde hetzelfde beeld. Later na injectie werd in toenemende mate vrij jodide gevonden, hetgeen wijst op afbraak van het radiofarmacon in vivo. Op basis van het activiteitsverloop in bloed en excreta en van gammacamerametingen van de lever en de galblaas als functie van de tijd werden de stralingsdoses van de belangrijkste organen bepaald. Zo werd een effectief dosisequivalent (0,021 mSv/MBq) berekend, vergelijkbaar met dat van andere  $^{123}\text{I}$ -radiofarmaca. Tenslotte worden de tumorzoekende eigenschappen van [ $^{123}\text{I}$ -Tyr $^3$ ]-octreotide beschreven aan de hand van enige voorbeelden van succesvolle scintigrafie van somatostatinerceptor-positieve tumoren.

*Hoofdstuk 4* begint met een opsomming van gebleken belangrijke nadelen van [ $^{123}\text{I}$ -Tyr $^3$ ]-octreotide: (a) de beperkte beschikbaarheid van het voor labeling vereiste ultrazuivere radionuclide, (b) de tijdrovende labelings- en zuiveringsprocedure, (c) de korte fysische halfwaardetijd van  $^{123}\text{I}$  (13,2 uur), die scintigrafisch onderzoek na meer dan 24 uur bemoeilijkt en (d) de storende achtergrondstraling ten gevolge van de lever-gal klaring in het bovenste deel van de buik, waar somatostatinerceptor-positieve tumoren zich vaak bevinden. Voor het ondervangen van de genoemde nadelen werd een DTPA-geconjugeerd somatostatine-analoon, t.w. [DTPA-D-Phe $^1$ ]-octreotide, ontwikkeld, dat op een eenvoudige één-staps manier met radioactief indium ( $^{111}\text{In}$ ,  $t_{1/2} = 2,8$  dagen) gemerkt kan worden. De labeling bleek te kunnen worden uitgevoerd met behoud van de eigenschappen van somatostatine. [ $^{111}\text{In}$ -DTPA-D-Phe $^1$ ]-octreotide bond specifiek aan somatostatinerceptoren in rattehersencortexmembranen, hoewel niet zo sterk als de geïodeerde verbinding. Bovendien werd het specifieke, op dat van somatostatine gelijkende, biologisch effect aangetoond door een dosis-afhankelijke remming van de groeihormoon-synthese in rattehypofysecellen. Opgemerkt wordt dat [ $^{111}\text{In}$ -DTPA-D-Phe $^1$ ]-octreotide zeer geschikt is voor een eenvoudige "kit"-bereiding.

*Hoofdstuk 5* beschrijft de eerste in vivo toepassing van [ $^{111}\text{In}$ -DTPA-D-Phe $^1$ ]-octreotide in ratten. De biodistributie van het radiofarmacon na intraveneuze injectie werd onderzocht in normale ratten en in ratten met somatostatinerceptor-positieve pancreastumoren. Evenals [ $^{123}\text{I}$ -Tyr $^3$ ]-octreotide werd [ $^{111}\text{In}$ -DTPA-D-Phe $^1$ ]-octreotide snel uit de bloedcirculatie geklaard, in dit geval niet door de lever, maar door de nieren. Het overgrote deel van de toegediende dosis werd in de vorm

van intact [ $^{111}\text{In-DTPA-D-Phe}^1$ ]-octreotide in de urine uitgescheiden, zonder noemenswaardige afbraak. Specifieke stapeling werd met behulp van ex vivo autoradiografie aangetoond in de hypofysevoorkwab, waarin zich somatostatinerceptoren bevinden. In de bijniere van ratten, waarvan de somatostatinerceptoren niet vooraf geblokkeerd waren met octreotide werd een aanmerkelijk hogere radioactiviteit gemeten dan in die van geblokkeerde dieren, hetgeen in overeenstemming is met de aanwezigheid van somatostatinerceptoren in dit orgaan. Hetzelfde gold voor de in de tumoren gemeten radioactiviteit. Met de gammacamera bleek het mogelijk ter plaatse van de ongeblokkeerde tumoren een in de tijd toenemende radioactiviteit te meten, terwijl de tumoren ook scintigrafisch in beeld konden worden gebracht. Omdat [ $^{111}\text{In-DTPA-D-Phe}^1$ ]-octreotide langer dan [ $^{125}\text{I-Tyr}^3$ ]-octreotide in de bloedsomloop blijft, is de blootstelling van de tumor aan het radiofarmacum groter, hoewel daardoor de achtergrondstraling op de dag van injectie hoger is. Echter, 24 uur na toediening van [ $^{111}\text{In-DTPA-D-Phe}^1$ ]-octreotide is meer radionuclide geklaard uit het lichaam vergeleken met [ $^{125}\text{I-Tyr}^3$ ]-octreotide, met als gevolg een lagere achtergrondstraling. Verder is de - bij [ $^{125}\text{I-Tyr}^3$ ]-octreotide gebruikelijke - storende achtergrondstraling in de bovenbuik bij [ $^{111}\text{In-DTPA-D-Phe}^1$ ]-octreotide niet aanwezig. Tenslotte zal het zichtbaar maken van tumoren na 24 uur en later door de langere fysische halfwaardetijd sterk worden begunstigd. In de conclusie wordt [ $^{111}\text{In-DTPA-D-Phe}^1$ ]-octreotide een veelbelovend radiofarmacum voor routine scintigrafie van somatostatinerceptor-positieve tumoren genoemd.

De scintigrafische toepassing van [ $^{111}\text{In-DTPA-D-Phe}^1$ ]-octreotide bij de mens wordt in *Hoofdstuk 6* geïntroduceerd. Evenals in het diersysteem werd het radiofarmacum snel geklaard uit de bloedsomloop en hoofdzakelijk via de nieren uitgescheiden. HPLC-onderzoek van urine wees uit, dat [ $^{111}\text{In-DTPA-D-Phe}^1$ ]-octreotide hoofdzakelijk in intacte vorm wordt uitgescheiden. Via de darmen werden slechts enkele procenten van het toegediende radionuclide uitgescheiden. Op basis van het activiteitsverloop in bloed en excreta en van gammacamerametingen van de nieren, milt en lever als functie van de tijd werden de stralingsdoses van de belangrijkste organen bepaald. Het effectieve dosis equivalent werd berekend op 0,08 mSv/MBq, vergelijkbaar met waarden gevonden voor andere  $^{111}\text{In}$ -radiofarmaca. Scintigrafie met behulp van [ $^{111}\text{In-DTPA-D-Phe}^1$ ]-octreotide bleek het beste te kunnen worden uitgevoerd 24 uur na toediening van het radiofarmacum, wanneer de circulerende achtergrond belangrijk is afgenomen. Scintigrafie van het bovenste gedeelte van de buik, waar somatostatinerceptor-positieve tumoren frequent voorkomen bleek met [ $^{111}\text{In-DTPA-D-Phe}^1$ ]-octreotide beter mogelijk omdat dit radiofarmacum daar juist minder hinderlijke achtergrondstraling geeft. Overigens bleek de gevoeligheid waarmee somatostatinerceptor-positieve tumoren elders in het lichaam konden worden aangetoond vergelijkbaar met die van [ $^{125}\text{I-Tyr}^3$ ]-octreotide.

Omdat de lever een belangrijk orgaan is voor de afbraak van veel biologisch actieve peptiden, werd het metabolisme van beide in de vorige hoofdstukken beschreven radioactief gemerkte somatostatine analoga in dit orgaan onderzocht. In dit, in *Hoofdstuk 7* beschreven, onderzoek werd gebruik gemaakt van een geïsoleerd ratteleverperfusiesysteem, waarin zowel het circulerende medium als de uitgescheiden gal radiochemisch werden onderzocht. [ $^{125}\text{I}$ -Tyr $^3$ ]-octreotide bleek snel uit het circulerende medium geklaard te worden, evenals in vivo het [ $^{125}\text{I}$ -Tyr $^3$ ]-octreotide uit de bloedbaan. Bovendien werd de radioactiviteit snel in de gal uitgescheiden, terwijl HPLC-onderzoek uitwees, dat het intact [ $^{125}\text{I}$ -Tyr $^3$ ]-octreotide betrof. In tegenstelling tot [ $^{125}\text{I}$ -Tyr $^3$ ]-octreotide werd [ $^{111}\text{In}$ -DTPA-D-Phe $^1$ ]-octreotide vrijwel niet door de lever geklaard: de radioactiviteit in het medium bleef nagenoeg gelijk tijdens het onderzoek, terwijl weinig radioactiviteit in de gal werd aangetroffen. Deze resultaten tonen aan, dat, terwijl [ $^{125}\text{I}$ -Tyr $^3$ ]-octreotide snel wordt geklaard door de lever en intact wordt uitgescheiden in de gal, [ $^{111}\text{In}$ -DTPA-D-Phe $^1$ ]-octreotide nauwelijks in de lever wordt verwerkt. De resultaten van de leverperfusiemetingen stemmen volledig overeen met de in vivo bevindingen bij de rat en bij de mens. Het geïsoleerde ratteleverperfusiesysteem blijkt een geschikte methode te zijn om het levermetabolisme van potentiële radiofarmaca te onderzoeken. De resultaten die met dit systeem verkregen worden, zouden kunnen worden gebruikt om het in vivo metabolisme van zulke verbindingen te voorspellen, hoewel aanvullende informatie over nierklaring vereist is.

In de *Appendix-artikelen* worden de eerste uitgebreidere klinische resultaten van scintigrafie met radioactief gelabelde somatostatine analoga beschreven. *Appendix I* behandelt de eerste toepassing van [ $^{125}\text{I}$ -Tyr $^3$ ]-octreotide bij de lokalisatie van verschillende endocriene somatostatinerceptor-positieve tumoren. In *Appendix II* wordt de gevonden overeenkomst tussen in vitro onderzoek (naar de aanwezigheid van somatostatinerceptoren), octreotidetherapie en in vivo scintigrafie beschreven. Geconcludeerd wordt dat positieve scintigrafie met behulp van [ $^{125}\text{I}$ -Tyr $^3$ ]-octreotide een effectieve onderdrukking (door octreotide) van de verhoogde hormoonsecretie in deze tumoren voorspelt. Deze gevolgtrekking wordt ook gemaakt uit het in *Appendices III & IV* beschreven onderzoek, waarin patiënten met hormoonproducerende carcinoid tumoren, endocriene pancreas tumoren of hypofyse adenomen en patiënten met paragangliomen met [ $^{125}\text{I}$ -Tyr $^3$ ]-octreotide scintigrafisch onderzocht zijn.

## CONCLUSIE

Gedurende de afgelopen 10 jaar zijn gunstige resultaten verkregen met specifiek werkende radiofarmaca. Het valt op, dat dit meer het geval is naarmate de molecuulgrootte afneemt. Bekend is de succesvolle positron emissie tomografie(PET)-scintigrafie van de hersenen met behulp van kleine positron-

emitterende verbindingen. Helaas kunnen deze PET-radiofarmaca hoofdzakelijk om economische redenen nog maar beperkt worden gebruikt, terwijl bovendien de toepassing vrijwel alleen tot de hersenen en het hart beperkt blijft. Een ruimer indicatiegebied leek te zijn gevonden voor de toepassing van radioactief gemerkte monoclonale antilichamen en fragmenten daarvan: allerlei tumoren en ontstekingen zouden ermee kunnen worden opgespoord door specifieke binding aan antigenen, die op deze processen voorkomen. Vaak bleek echter scintigrafie met monoclonale antilichamen in belangrijke mate gehinderd te worden door (a) trage klaring uit de bloedsomloop, (b) geringe stapeling in de ziekteprocessen en (c) hoge aspecifieke stapeling in allerlei weefsels. Vergeleken met de grote antilichamen c.q. fragmenten daarvan ( $> 70$  kD) hebben veel kleinere verbindingen ( $< 2$  kD) twee voordelen, die het in beeld brengen van ziekteprocessen gunstig beïnvloeden: (1) door een veel snellere klaring ontstaat al snel een lage achtergrondstraling en (2) zij difunderen beter naar de extravasculaire ruimte. Onder meer het MIBG (voor het in beeld brengen van het feochromocytoom en het neuroblastoom) heeft in deze groep van laag-moleculaire radiofarmaca een vaste plaats gevonden.

Omdat kleine natuurlijke biologisch actieve peptiden al lang gebruikt werden bij het *in vitro* karakteriseren van ziekten, werd besloten derivaten van zulke verbindingen *in vivo* te gebruiken om tumoren zichtbaar te maken op basis van binding aan natuurlijke peptidereceptoren. *Octreotide* is een octapeptide met een biologisch actieve kern vergelijkbaar met die van het 14 aminozuren bevattende natuurlijke peptidehormoon *somatostatine*, een peptide met remmende eigenschappen op hormoonproductie. Vanwege zijn grotere stabiliteit vergeleken met het natuurlijke peptide, wordt octreotide vaak gebruikt voor therapie bij patiënten met hormoonproducerende tumoren. De werking van octreotide verloopt via receptoren. Evenals octreotide bindt [ $^{125}\text{I}$ -Tyr $^3$ ]-octreotide *in vitro* aan somatostatinerceptoren op cellen van verschillende tumoren. In het beschreven onderzoek bleek [ $^{125}\text{I}$ -Tyr $^3$ ]-octreotide *in vivo* ook in somatostatinerceptor-positief tumorweefsel te stapelen na intraveneuze toediening. Daardoor werden deze tumoren met de gammacamera in beeld gebracht. Belangrijke nadelen, zoals de sterke achtergrondstoring in het bovenste deel van de buik (waar somatostatinerceptor-positieve tumoren zich vaak bevinden) en de omslachtige bereidingsprocedure, brachten ons op een tweede octreotide derivaat met somatostatinerceptor-bindende eigenschappen: [DTPA-D-Phe $^1$ ]-octreotide. Dit peptide werd radioactief gelabeld met  $^{111}\text{In}$  door middel van een eenvoudige éénstaps-procedure, waarna verdere zuivering niet noodzakelijk bleek. *In vitro* vertoonde indium-gelabeld [DTPA-D-Phe $^1$ ]-octreotide (evenals geïodiseerd [Tyr $^3$ ]-octreotide) somatostatinerceptor-bindende en hormoonproductieremmende eigenschappen. *In vivo* gedraagt [ $^{111}\text{In}$ -DTPA-D-Phe $^1$ ]-octreotide zich echter geheel anders dan [ $^{125}\text{I}$ -Tyr $^3$ ]-octreotide: in tegenstelling tot de lever-gal klaring en daarop volgende afbraak in de darmen, wordt [ $^{111}\text{In}$ -DTPA-D-Phe $^1$ ]-octreotide door de nieren uit de bloedsomloop geklaard zonder duidelijke afbraak. De zeer snelle verdwijning van [ $^{125}\text{I}$ -Tyr $^3$ ]-octreotide uit de bloedsomloop werd als *voordeel* voor tumorscintigrafie beschouwd vanwege de lage achtergrond al kort na



toediening (Hoofdstuk 2), terwijl de veel tragere verdwijning van [ $^{111}\text{In}$ -DTPA-D-Phe $^1$ ]-octreotide *eveneens* een voordeel werd genoemd (Hoofdstuk 5) vanwege de langere blootstelling aan de tumor. Dit kan echter gemakkelijk worden ingezien, als in aanmerking genomen wordt, dat het voordeel van [ $^{123}\text{I}$ -Tyr $^3$ ]-octreotide alleen geldt gedurende de eerste uren na toediening, terwijl het voordeel van [ $^{111}\text{In}$ -DTPA-D-Phe $^1$ ]-octreotide geldt voor 24 uur en later vanwege de veel betere excretie zonder afbraak. Zo bleek ondanks wat lagere receptor-bindende eigenschappen [ $^{111}\text{In}$ -DTPA-D-Phe $^1$ ]-octreotide een beter alternatief te zijn voor [ $^{123}\text{I}$ -Tyr $^3$ ]-octreotide voor de scintigrafie van somatostatinerceptor-positieve tumoren, juist vanwege het geschiktere metabolisme, de langere halfwaardetijd van het radionuclide en de gemakkelijke beschikbaarheid.

Met behulp van twee in dit proefschrift beschreven peptiden, [ $^{123}\text{I}$ -Tyr $^3$ ]-octreotide en [ $^{111}\text{In}$ -DTPA-D-Phe $^1$ ]-octreotide, is nu aangetoond dat het mogelijk is somatostatinerceptor-positieve tumoren scintigrafisch in beeld te brengen met derivaten van een natuurlijk peptidehormoon (lokalisatie met andere technieken is vaak moeilijk). Bovendien, als zo'n tumor endocrien-actief (d.w.z. hormoonproducerend) is, kan positieve scintigrafie effectieve therapie met octreotide voorspellen. Verder lijkt het waarschijnlijk, dat ook *radiotherapie* met vergelijkbare verbindingen, gelabeld met geschikte, b.v.  $\beta$ -emitterende radionucliden, mogelijk zal zijn. Gezien het aantal bekende biologisch actieve natuurlijke peptiden, zullen de twee in dit proefschrift beschreven radiofarmaca waarschijnlijk door andere kleine radioactief gelabelde peptiden voor specifieke tumorbinding gevolgd worden in de nabije toekomst.



## NAWOORD

Velen hebben bijgedragen aan het gereed komen van dit proefschrift. Aan hen allen ben ik veel dank verschuldigd.

In de eerste plaats dank ik mijn ouders, die mij na enige omzwervingen in een ander - mijn vader bekend - vakgebied voor een tweede maal in staat stelden, een universitaire studie aan te vangen en deze af te ronden.

Joan, Marjolein en Maarten hebben mij de laatste tijd meestal alleen via de huistelefoon gesproken en dan ging het over de fouragering of andere huishoudelijke zaken. Door de veelheid van (door Joan gestimuleerde) activiteiten in ons gezin is dat overigens niet al te zeer opgevallen. Het valt gelukkig te verwachten, dat het beschreven communicatiepatroon nu enige verandering zal ondergaan.

Toen Eric Krenning in 1983 Jorg Hennemann opvolgde als Hoofd van de afdeling Nucleaire Geneeskunde van het Academisch Ziekenhuis Rotterdam Dijkzigt wisten we dat we met hem een medicus met een (van huis uit ontwikkeld) gevoel voor techniek binnenhaalden. De aanwezigheid van een arts met technisch inzicht is immers essentieel voor de Nucleaire Geneeskunde. Eric bleek daarnaast een klinicus te zijn, die dankzij zijn werk in de afdeling Inwendige Geneeskunde III veel ervaring met het laboratoriumresearch had opgedaan. Hij legde in ons ziekenhuis de basis voor de brug tussen het laboratorium onderzoek en de in-vivo nucleaire geneeskunde, een essentiële voorwaarde, waaraan voldaan moet worden voor snelle en doeltreffende vernieuwingen. In-vitro biologisch werkzame stoffen moesten naar zijn vaste overtuiging ook in-vivo bij de mens kunnen worden toegepast. Voor zijn voortdurende stimulans (wèl eens lastig...) en niet aflatend enthousiasme ben ik hem buitengewoon erkentelijk.

In de periode, dat de beschreven artikelen en dit proefschrift zelf tot stand kwamen, heeft Theo Visser vele malen zijn waardevolle redactionele bijdragen geleverd. Met plezier denk ik terug aan de opbouwende sfeer van de gesprekken, die ik met hem voerde bij de samenstelling van de manuscripten mede namens alle andere auteurs. Vooral zijn compacte, duidelijke en zuivere weergave van het geschreven woord, was voor ons allen van onschatbare waarde.

Wout Breeman dank ik voor zijn belangrijke bijdragen aan het onderzoek. Zijn opgeruimde karakter, hulpvaardigheid, pragmatische aanpak, diplomatie en veelzijdigheid, zijn van grote waarde geweest. Ik stel het op hoge prijs, dat Wout bij de

promotie als paranimf wil optreden.

Steven Lamberts en Jean-Claude Reubi zijn reeds lange tijd werkzaam in het gebied van de endocriene tumoren. Jean-Claude legde ongeveer 10 jaar geleden al de basis voor het in dit proefschrift beschreven onderzoek door het aantonen van de binding van het somatostatine analogon [ $^{125}\text{I}$ -Tyr $^3$ ]-octreotide aan membranen van dit soort tumoren. Steven en Jean-Claude brachten mij de noodzakelijke kennis op dit gebied bij.

Rainer Albert, Leo Hofland, Jan-Willem Koper en Christian Bruns hebben vooral belangrijk ondersteunend onderzoek verricht in de fase, die voorafging aan de humane toepassing van de twee beschreven nieuwe radiofarmaca. Zij voerden nauwgezet de synthese van het DTPA-octreotide (RA), de proeven met betrekking tot de biologische respons (LH) en de in-vitro bindingsproeven (JWK & CB) uit.

Peter Kooij verrichtte de tijdrovende berekeningen, die vereist zijn voor de schatting van de stralingsdoses, die patiënten oplopen nadat aan hen de beschreven nieuwe radiofarmaca zijn toegediend.

Halverwege het onderzoek kwam Marion de Jong bij onze afdeling. Haar ervaring met leverperfusiemetingen in het schildklierlaboratorium kwam voor ons zeer goed van pas bij dit basale onderzoek, waarmee de onderling verschillende (lever)metabolismen van de twee radioactief gelabelde peptiden werd bevestigd. Haar hulpvaardige instelling en vooral haar optreden als klankbord zullen mij bij blijven.

Buddy Setyono-Han zorgde steeds zeer nauwgezet voor het in vivo tumormodel, waaraan we de beide radiofarmaca met succes getoetst hebben.

Ik dank ook Marcel van der Pluijm, die samen met de stageaires van het Van 't Hoff Instituut zorgvuldig de kwaliteit van de nieuwe radiofarmaca bewaakte onder meer met behulp van meer dan 1000 HPLC-runs!

De leden van ons in vivo team (onder leiding van Ina Loeve) wil ik zeker niet onvermeld laten: zij hebben tussen het gewone werk door en vaak buiten de normale werkuren de gammacamerametingen uitgevoerd.

Paula van Sintmaartensdijk-Schuijff en haar staf in de afdeling Endocrinologie ben ik zeer erkentelijk voor hun altijd bereidwillig gegeven verpleegkundige steun.

De medewerkers van het Audio Visueel Centrum dank ik voor de zorgvuldige uitvoering van het fotowerk.

Tot slot dank ik zeker ook alle anderen, die - op welke manier dan ook - mede de uitvoering van het "SMS"-onderzoek in onze afdeling mogelijk maakten.

## CURRICULUM VITAE

De schrijver van dit proefschrift werd op 23 oktober 1944 te 's-Gravenhage geboren. Het eindexamen gymnasium 8 werd in 1963 behaald aan het Tweede Vrijzinnig Christelijk Lyceum te 's-Gravenhage. Na in 1963 een korte periode aan de Technische Hogeschool Delft als student elektrotechniek ingeschreven te zijn geweest, volgde hij in de periode 1964/1965 het eerste jaar elektrotechniek aan de Hogere Technische School Wegastraat te 's-Gravenhage. In 1965 werd een begin gemaakt met de studie in de scheikunde aan de Rijksuniversiteit te Leiden. Het kandidaatsexamen (hoofdvak: scheikunde en bijvakken: wiskunde, natuurkunde en biologie) werd in mei 1969 behaald. In mei 1972 werd het doctoraal examen scheikunde afgelegd met hoofdvak organische chemie (radiochemie) en bijvakken neutronen-activeringsanalyse en fysisch-chemische scheidingsmethoden. Aansluitend volgde een dienstverband als doctoraal-assistent in de afdeling Röntgen- en Electronendiffractie van de Rijksuniversiteit te Leiden. In januari 1974 werd hij aangesteld als radiochemicus in de afdeling Nucleaire Geneeskunde van het Academisch Ziekenhuis Rotterdam Dijkzigt. In februari 1976 werd het "C"-diploma Deskundigheid Stralenbescherming behaald aan het J.A. Cohen Instituut, Interuniversitair Instituut voor Radiopathologie en Stralenbescherming, te Leiden. Op 1 november 1978 volgde de benoeming tot waarnemend hoofd van de afdeling Nucleaire Geneeskunde. Op 20 april 1985 werd hij als chemicus voor nucleaire geneeskunde ingeschreven in het A-register van de Nederlandse Vereniging voor Nucleaire Geneeskunde.

